STUDIES ON THE BEHAVIOUR OF PERVIOUS CONCRETE COLUMN IMPROVED GROUND SUBJECTED TO STATIC SHEAR AND SEISMIC LOAD

Thesis

Submitted in partial fulfillment of the requirements for the degree of
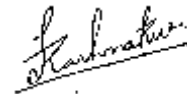
DOCTOR OF PHILOSOPHY

by

RASHMA R S V

DEPARTMENT OF CIVIL ENGINEERING

NATIONAL INSTITUTE OF TECHNOLOGY KARNATAKA

SURATHKAL, MANGALORE-575025

September 2021

DECLARATION

I hereby *declare* that the Research Thesis entitled "**Studies on the Behaviour of Pervious Concrete Column Improved Ground Subjected to Static Shear and Seismic Load"** which is being submitted to the **National Institute of Technology Karnataka, Surathkal** in partial fulfilment of the requirements for the award of the Degree of **Doctor of Philosophy** in **Civil Engineering**, is a *bonafide report of the research work carried out by me.* The material contained in this Research Thesis has not been submitted to any University or Institution for the award of any degree.

RASHMA R S V

(Register No: 177132CV501)

Department of Civil Engineering

Place: NITK Surathkal

Date: 28-09-2021

CERTIFICATE

This is to *certify* that the Research Thesis entitled **"Studies on the Behaviour of Pervious Concrete Column Improved Ground Subjected to Static Shear and Seismic Load"** submitted by **RASHMA R S V**, (Register Number: **177132CV501**) as the record of the research work carried out by her, is *accepted as the Research Thesis submission* in partial fulfilment of the requirements for the award of degree of **Doctor of Philosophy**.

Prof. B.R.Jayalekshmi

Research Guide
Professor
Department of Civil Engineering
NITK, Surathkal

4/10/2024

Prof. R. Shivashankar

Research Guide
Professor
Department of Civil Engineering
NITK, Surathkal

Prof. B.R.Jayalekshmi
Chairman-DRPC
Head of the Department
Department of Civil Engineering
NITK, Surathkal

Chairman (DRPC)
Department of Civil Engineering
National Institute of Technology Karnataka, Surathkal
Mangalore - 575 025, Karnataka, INDIA

Thank You Lord for Everything

Dedicated to My Family

ACKNOWLEDGEMENT

ABSTRACT

Granular piles or stone columns are extensively used across the globe for improving soft soils, especially for supporting embankments on soft grounds, because of its ease of construction and inherent advantages. Various modified stone columns and their behaviour under vertical loading are extensively reported in literature. However, the behaviour of improved ground under lateral loading conditions are limited. Additionally, among all the reported externally/internally improved stone columns, very few modified stone columns like encased stone columns, deep cement columns and rigid columns are generally used in practice. Therefore, present study considers modified stone column as pervious concrete column which is reported as an alternative to conventional stone column owing to its comparable permeability characteristics with stone column in addition to its higher vertical load carrying capacity. The behaviour of pervious concrete column improved ground under static shear and seismic loading conditions are carried out and compared with the performance of conventional stone column improved ground.

In the first part of the study, the behaviour of stone column and pervious concrete column under static shear loading conditions are investigated. The shearing resistances of pervious concrete column improved ground vis-à-vis ordinary stone column improved ground under static shear loading conditions are assessed. Numerical analyses were carried out by simulating direct shear test model and large shear test model, representing pervious concrete column improved ground using ABAQUS software. The single column modelled in the study represents the column placed beneath the toe of the embankment, where shear loading is predominant. Inclined direct shear tests are also analyzed by varying the slope (+/-) of potential failure surface with horizontal to represent the actual practical conditions. A total of 378 direct shear test models are analyzed to study the effect of normal pressure, effect of diameter, effect of reinforcement and effect of shear surface inclinations.

The ultimate shear strength of pervious concrete column improved ground is found to be higher than ordinary stone column improved ground. It is found that the pervious concrete column improved ground under zero normal pressure has significant

shear resistance than ordinary stone column improved ground and could be provided beneath the toe of the embankment for better shear performance.

In order to study the performance of improved ground with floating and end-bearing pervious concrete columns, large shear test tank model with increased depth is analyzed. The shear response of improved ground is quantified, and the parameters considered are depth of pervious concrete column/pile, floating and end bearing piles, diameter, single pile and two pile group and distance from the edge of loading area in the model. It is observed that the pervious concrete column improved ground exhibits better shear performance than ordinary stone column improved ground. It is found that the pervious concrete column undergoes very small lateral deflections. It is also observed that more number of pervious concrete columns, and closer they are to the loaded area, better is the shear performance. The end bearing pervious concrete column improved ground is found to have significantly higher shear resistance than floating pervious concrete column improved ground. Therefore, it is suggested to provide full depth of pervious concrete column up to the bearing strata for achieving better shear performance. Pervious concrete columns show significantly lesser lateral displacements compared to ordinary stone columns. Peak lateral displacements in case of pervious concrete column are at the surface and the deflected profile of the column is very much like that of a rigid pile with a free or unrestrained head condition.

Stone columns are highly recommended for mitigating liquefaction and the feasibility of pervious concrete column in preventing liquefaction is addressed in the second part of this study. Liquefaction induced lateral spreading causes catastrophic damages during and after earthquakes. Therefore, the effectiveness of pervious concrete column remediation in soil strata for mitigating liquefaction-induced lateral spreading is emphasized. The seismic performance of pervious concrete column improved ground is compared with conventional stone column improved ground. Three-dimensional finite element analysis using OpenSeesPL software is conducted to study the ground lateral deformation, excess pore water pressure generation and shear-strain behaviour of pervious concrete column improved ground on a mildly sloping soil strata of infinite extent under seismic loading. The parameters influencing the seismic performance of improved ground like area ratio, founding depth of columns, diameter of columns and hydraulic conductivity of columns are considered. The efficacy of pervious concrete

column on three types of soil strata in mitigating liquefaction along with parameters influencing ground lateral deformation such as thickness of sandwiched liquefiable soil layer, permeability of surrounding soil, ground surface inclination, peak ground acceleration and surcharge load are reported. The influence of earthquake characteristics such as frequency content, significant duration, time of peak ground acceleration and arias intensity on lateral displacement, excess pore pressure dissipation and shear stress-strain behaviour of modelled ground are also studied. Total stress analysis is also conducted and compared with effective stress analysis on maximum response profile along the depth of improved ground with column inclusions when subjected to earthquake loading conditions.

The stone column gets distorted during seismic loading due to shearing and causes dilation. The distorted gravel structure of stone column increases the length of the drainage path and retards the dissipation of excess pore water generated due to shaking. Whereas the pervious concrete column structure is not distorted due to seismic shaking and the pervious concrete column inclusion reduces drainage path for excess pore water to dissipate quickly. Therefore, the seismic shear strains developed in the surrounding soil is drastically reduced. The limited excess pore pressure generation and relatively higher effective confinement reduces the lateral displacement of pervious concrete column improved ground significantly.

It is found from various response parameters that the pervious concrete column improved ground has better seismic performance than conventional stone column improved ground. The lateral deformation profile of pervious concrete column is found to be similar to that of concrete pile, allowing excess pore water pressure to dissipate through the pores of pervious concrete column. Liquefaction-induced lateral deformation is found to be lesser in pervious concrete column improved ground in comparison with stone column improved ground. The lateral deformation of pervious concrete column remediated ground is found to be independent of surrounding soil permeability. The pervious concrete column inclusion is found to be a better alternative to stone column in mitigating liquefaction in susceptible soils like loose sand, medium-dense sand, sandwiched sand deposits and silt strata. It is also found that the pervious concrete column remediation is a better alternative than stone column in seismically active regions even with peak ground acceleration of 0.6g. It is found that the

generation of excess pore pressure reaches near zero values when the permeability of pervious concrete column is greater than 0.3 m/s irrespective of the characteristics of the earthquake events. From total stress analysis and effective stress analysis, it is observed that for column improved ground, in addition to pore pressure build-up, the maximum response profile is highly influenced by significant duration and frequency of seismic excitation. It is also concluded that pervious concrete columns could be used as an alternative to conventional stone columns to mitigate liquefaction to a larger extent.

Table of Contents

CHAPTER 8

CONLUSIONS

List of Figures

ix

List of Tables

Nomenclature

Abbreviations

AR	Area Ratio
ASTM	American Standard Testing Manual
DCM/DM	Deep Cement Mixing/Deep Mixing
DOF	Degrees of Freedom
ESA	Effective Stress Analysis
FBD	Free Body Diagram
FEM	Finite Element Modelling
FEMA	Federal Emergency Management
FOS	Factor of Safety
GLE	General Limit Equilibrium
IRC	Indian Road Congress
IS	Indian Standard
LE	Limit Equilibrium
OPENSEES	OPEN System for Earthquake Engineering Simulation
OSC/SC	Ordinary Stone Column/Stone Column
PCC	Pervious Concrete Column
PGA	Peak Ground Acceleration
TSA	Total Stress Analysis
VELACS	VErification of Liquefaction Analysis by Centrifuge Studies

Notations

P_{ac}	Active earth pressure of clay ground
P_{ae}	Active earth pressure of embankment
α	Adhesion factor
A_{sc}	Area of stone column
A_c	Area of surrounding clay
A	Area of unit cell
a_s	Area ratio

$\bar{c}$	Average cohesion along the interface of column-surrounding clay
N_c	Bearing capacity factor
B_r	Bulk modulus at reference pressure
S	Center to center spacing between columns
f_{ck}	Characteristic compressive strength of concrete
F_{rc}	Cohesive strength of clay along failure plane
z	Depth of shear failure plane
D	Diameter of column
D_e	Diameter of unit cell
Q_{u1}	End-bearing resistance of pervious concrete column base
r_u	Excess pore pressure ratio
$\emptyset_c$	Friction angle of cohesive soil
$\emptyset_e$	Friction angle of embankment fill
$\emptyset_{pcc}$	Friction angle of pervious concrete
$\emptyset_{sc}$	Friction angle of stone column
H_e	Height of the embankment
L	Improvement depth
β	Inclination of the shear surface with respect to the horizontal
σ_{v0}	Initial effective stress
σ_{r0}	Initial radial stress
k_0	Lateral earth pressure coefficient
L/D	Length to diameter ratio of columns
σ_v	Limiting axial stress in column
σ_{rl}	Limiting radial stress
Q_u	Load carrying capacity (geotechnical capacity) of rigid piles
G_{max}	Low strain shear modulus at reference pressure
ϕ_{TC}	Model friction angle, same as triaxial friction angle
M_w	Moment magnitude of earthquake
k_{pcol}	Passive earth pressure coefficient of column
P_{pc}	Passive earth pressure of clay ground
k	Permeability

k_s	Permeability of surrounding soil
ϕ_{PT}	Phase transformation angle
P_{ref}	Reference pressure for model calibration
QP1	Safe axial load on pervious concrete column
q_{safe}	Safe bearing pressure of soil
Q1	Safe load on column alone due to bulging,
Q2	Safe load on column alone due to surcharge
QP2	Safe load taken by intervening soil between pervious concrete columns
Q3	Safe load taken by intervening soil between stone columns
Qs1	safe structural capacity of pervious concrete column
FS	Safety factor
ρ	Saturated unit weight of soil
τ_{sc}	Shear strength in the stone column
τ_c	Shear strength of clay
F_{rf}	Shear strength of DM column along failure plane
F	Shear strength of improved ground
Vs	Shear wave velocity
$D_{5\text{-}95}$	Significant duration
Q_{u2}	Skin resistance developed between clay and pervious concrete column
N	Standard penetration test value
μ_c	Stress concentration factor for the clay
μ_{sc}	Stress concentration factor for the stone column
n	stress concentration ratio
σ	Stress due to embankment loading on the surface
σ_{sc}	Stress in the stone column
σ_c	stress in the surrounding cohesive soil
γ'_c	Submerged unit weight of clay
H_c	Thickness of clay ground
Load T	Total load on the ground
QP	Total safe load on pervious concrete column and tributary soil

Q	Total safe load on stone column and its tributary soil
$\overline{\sigma}_z^C$	Total vertical stress in the cohesive soil
q_u	Unconfined compressive strength of DM column
c_u	Undrained cohesion of clay
C_{u0}	Undrained shear strength at ground surface
k	Undrained shear strength increasing ratio with depth
τ_c	Undrained shear strength of cohesive soil
γ_c	Unit weight of cohesive soil
γ_e	Unit weight of embankment
γ_{sc}	Unit weight of the stone column
$\overline{\sigma}_z^{sc}$	Vertical effective stress acting on the sliding face of the stone column

CHAPTER 1

INTRODUCTION

This chapter introduces the topic and details the shear loading situations related to stone column improved ground. The research statement, research objectives and outline of thesis are also presented.

1.1 BACKGROUND

Stone columns are widely used to support low rise buildings, runways, highway facilities, storage tanks, embankments, bridge abutments and structures in which some settlements are acceptable. Due to the non-availability of strong soil, improvement of weak soil is increasing day by day. Even though, many ground improvement techniques like vacuum pre-consolidation, prefabricated vertical drains, lime treatment, cementation etc. are used, the most effective technique considered is use of granular piles/stone columns. Stone columns are extensively used for stabilizing weak soil. It increases the load bearing capacity and also reduces settlement. Granular piles also provide the shortest path to the excess pore water to discharge from highly permeable soil thereby mitigating liquefaction. It can speed up the process of consolidation and construction activities can be started without any delay, thereby managing time and cost of construction.

Stone columns are largely used to support embankments over weak soil. Thereby the load carrying capacity of weak soil is improved. Stone columns may fail by shear when it is subjected to horizontal load or movement. Columns withstand vertical loads, but when column supported embankments are huge, columns undergo shear failure. These columns can fail by bulging (long columns), or shear failure or by punching. The failure mode depends on many parameters such as strength, stiffness, length, diameter of column, reinforcement used, location, spacing, end condition, soft soil etc.

In a wide embankment constructed over a stone column improved ground, the soil beneath and adjacent to the toe of the embankment can move more laterally as shown in Fig.1.1 (Barksdale and Bachus 1983). This lateral movement is called lateral spreading and it reduces the support given to stone column and surrounding soil. They reported that the short end bearing stone columns fail in shear. They also reported that shear failure could occur for floating stone columns. In an embankment supported by

stone columns, the columns in the middle are mostly subjected to vertical loading. But the columns placed beneath the toe of the embankment is subjected to lateral loading. The failure of stone column supported embankment is as shown in Fig.1.1.
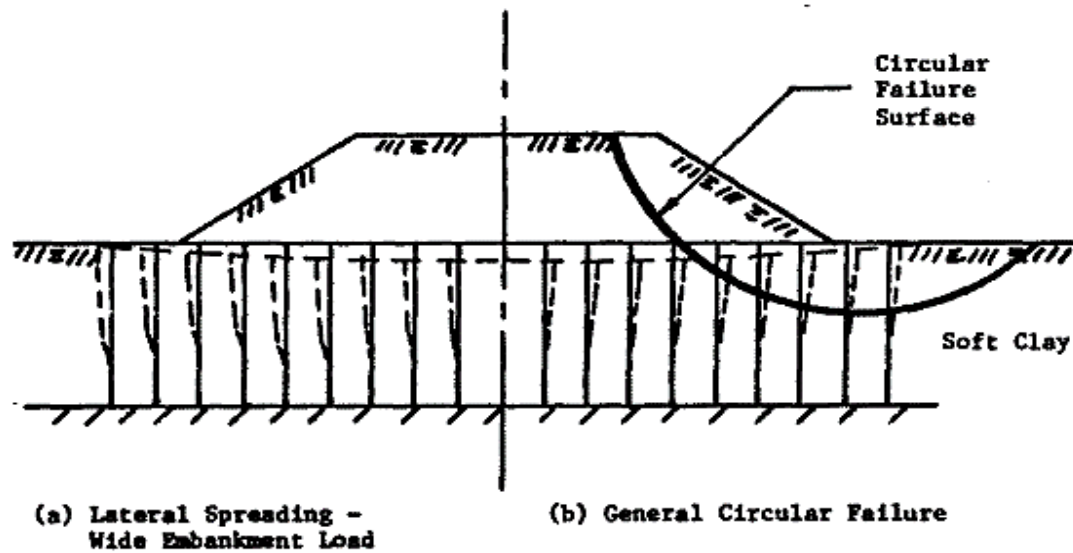
Figure 1.1 Failure of stone column supported embankment (Barksdale and Bachus 1983)

The composite ground representing an infinitely large, loaded area is modelled as a unit cell consisting of stone column and tributary surrounding soil. Figure 1.2 (a) represents a typical stone column arrangement and Fig. 1.2(b) shows the area per column considered as unit cell. Area replacement ratio (or Area ratio) is used to quantify the amount of soil replaced by stone column. The expression of area ratio (a_s) is as

follows: $a_s = \frac{A_{sc}}{A}$ (1.1)

where,

A : Total area of unit cell $= A_{sc} + A_c$

A_{sc} : Area of stone column

A_c : Area of surrounding soil

2
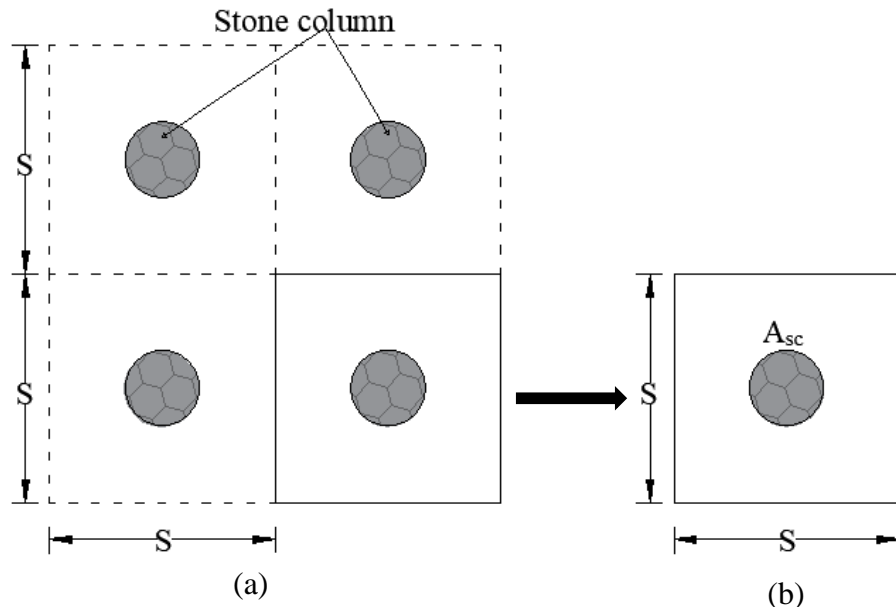
Figure 1.2 (a) Typical stone column arrangement (b) Unit cell

1.2 SHEAR STRENGTH OF STONE COLUMN IMPROVED GROUND

Shear strength of stone column improved ground on a sloping ground based on stability criteria was detailed by Barksdale and Bachus (1983) using unit cell concept. The stability of columns was analyzed by using average shear strength method. In this method the circular arc must pass through the stone column and the shear properties of entire material is weighted. A general stone column improved ground with stone column having friction angle alone and surrounding soil with both friction and cohesion was considered. The stress state within the selected stone column unit cell is as shown in Fig.1.3 at a depth where the circular arc intersects with the centerline of stone column.

The effective stress in the stone column due to the weight of the stone and applied stress due to embankment loading is given by:

$$\bar{\sigma}_z^{sc} = \gamma_{sc}\, z + \sigma \mu_{sc} \tag{1.2}$$

Where

$\bar{\sigma}_z^s$	:	Vertical effective stress acting on the sliding face of the stone column
γ_{sc}	:	Unit weight of stone (Saturated unit weight if below water table)
z	:	Depth below ground surface
σ	:	Stress due to embankment loading on the surface

μ_{sc} :   Stress concentration factor for the stone column given by

$$\mu_{sc} = \frac{n}{[1+(n-1)a_s]}$$

(Where

n   :   stress concentration ratio $n = \frac{\sigma_{sc}}{\sigma_c}$

σ_{sc} :   Stress in the stone column

σ_c :   stress in the surrounding cohesive soil)

The shear strength of the stone column (neglecting cohesion) is expressed as

$$\tau_{sc} = (\bar{\sigma}_z^{sc} \cos^2 \beta) \tan \emptyset_{sc} \tag{1.3}$$

Where

τ_{sc} :   shear strength in the stone column

β :   Inclination of the shear surface with respect to the horizontal

$\emptyset_{sc}$:   Angle of internal friction of the stone column
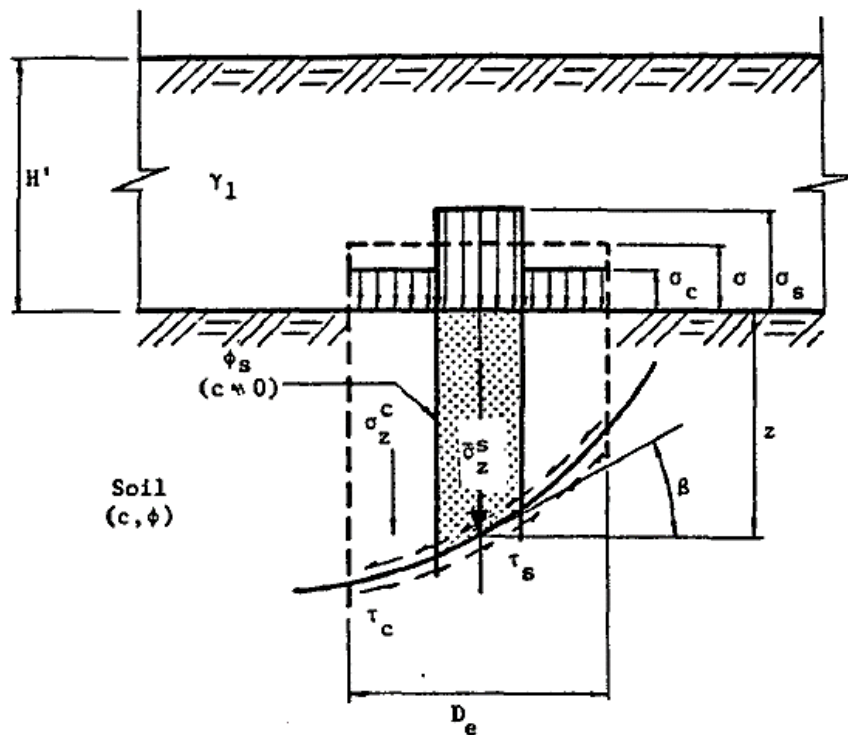
Figure 1.3 Shear strength of improved ground with stone columns (Barksdale and Bachus 1983)

The total stress in the cohesive soil considering stress concentration becomes,

4

$$\bar{\sigma}_z^C = \gamma_c z + \sigma \mu_c \tag{1.4}$$

Where

$\bar{\sigma}_z^C$:   Total vertical stress in the cohesive soil

γ_c :   Unit weight of cohesive soil

μ_c :   Stress concentration factor for the clay given by

$$\mu_c = \frac{1}{[1+(n-1)a_s]}$$

Therefore, the shear strength of cohesive soil is given by,

$$\tau_c = c_u + (\bar{\sigma}_z^c \cos^2 \beta) \tan \emptyset_c$$

(1.5)

Where

τ_c :   Undrained shear strength of cohesive soil

c_u :   Undrained cohesion of cohesive soil

$\emptyset_c$:   Angle of friction of cohesive soil

The average weighted shear strength τ within the tributary area to the stone column is

$$\tau = (1 - a_s)\tau_c + a_s \tau_{sc} \tag{1.6}$$

Theoretical shear resistance (F) of stone column improved soft ground is given by,

$$F = A_c \tau_c + A_{sc} \tau_{sc} \tag{1.7}$$

F :   Shear strength of improved ground

A_c :   Area of surrounding clay

τ_c :   Shear strength of clay

A_{sc} :   Area of stone column

τ_{sc} :   Shear strength of stone column

Murugesan and Rajagopal (2009) introduced a correction factor, $\acute{\alpha}$ to the shear strength equation to account for the loss of shear strength of stone aggregates, assuming full mobilization of the shear resistance of surrounding clay. The values of $\acute{\alpha}$ varies from 1 to 0.4 is based on the normal pressures applied. At higher normal pressures, the value

of ά is 0.4-0.5 and at low normal pressures, the value of ά is nearly equal to 1. The corrected shear strength equation is as follows:

$$F = A_c \tau_c + ά A_{sc} \tau_{sc} \tag{1.8}$$

Kitazume and Maruyama (2007) and Han (2014) reported horizontal shear as one of the possible column failure mode under embankment and is shown in Fig.1.4.
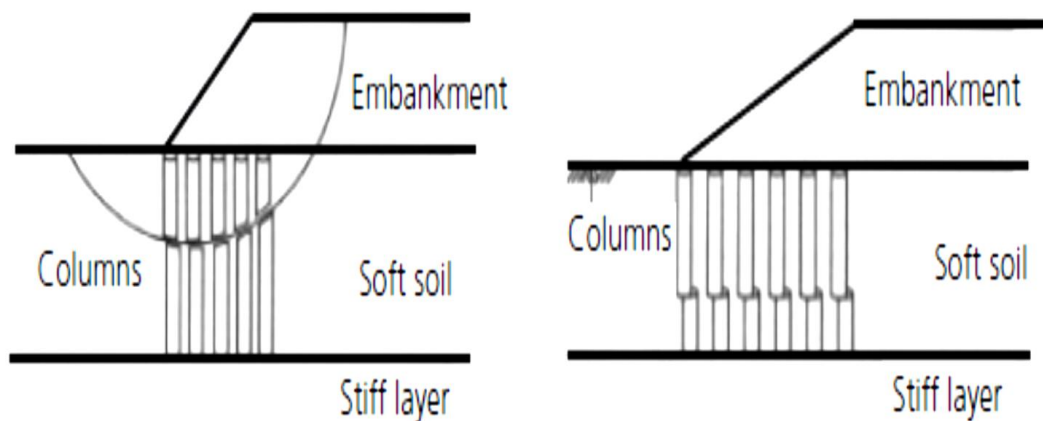
Figure 1.4 Possible circular and horizontal shear failure modes of columns under embankments (Han 2014)

1.3 SHEAR FAILURE OF IMPROVED GROUND

Kitazume and Maruyama (2007) evaluated the internal stability of Deep Cement Mixing (DCM) column improved ground using Rankine's theory of active and passive earth pressures. Assumed shear failure mode is as shown in the Fig.1.5
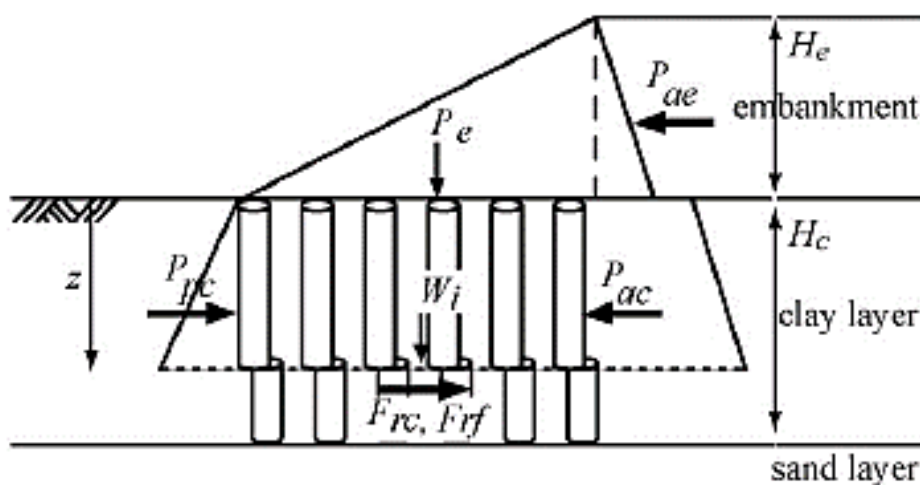
Figure 1.5 Assumed shear failure mode (Kitazume and Maruyama 2007)

Full mobilization of column shear strength is assumed for calculation. Shear failure plane is assumed at a depth z. Factor of safety is given as follows:

$$FS = \frac{P_{pc} + F_{rf} + F_{rc}}{P_{ae} + P_{ac}} \tag{1.9}$$

$$P_{ae} = \gamma_e . H_e . tan^2 \left(\frac{\pi}{4} - \frac{\emptyset_e}{2}\right) . \frac{H_e}{2} \tag{1.10}$$

$$P_{ac} = (2 . \gamma_e . H_e - 2 . (2 . C_{u0} + k . z) + \gamma_c z) . \frac{z}{2} \tag{1.11}$$

$$P_{pc} = \left(\gamma_c . z + 2 . (2 . C_{u0} + k . z)\right) . \frac{z}{2} \tag{1.12}$$

$$F_{rf} = \frac{q_u}{2} . a_s . L \tag{1.13}$$

$$F_{rc} = (C_{u0} + k . z) . (1 - a_s) . L \tag{1.14}$$

Where

F_{rc}	:	Cohesive strength of clay along failure plane (kN/m²)
F_{rf}	:	Shear strength of DM column along failure plane (kN/m²)
FS	:	Factor of safety
P_{ac}	:	Active earth pressure of clay ground (kN/m²)
P_{ae}	:	Active earth pressure of embankment (kN/m²)
P_{pc}	:	Passive earth pressure of clay ground (kN/m²)
a_s	:	Improvement area ratio
C_{u0}	:	Undrained shear strength at ground surface (kN/m²)
H_c	:	Thickness of clay ground (m)
H_e	:	Height of the embankment (m)
q_u	:	Unconfined compressive strength of DM column (kN/m²)
z	:	Assumed depth of shear failure plane(m)
k	:	Undrained shear strength increasing ratio with depth (kN/m³)
γ_c	:	Unit weight of clay ground (kN/m³)
γ_e	:	Unit weight of embankment (kN/m³)
$\emptyset_e$	:	Internal friction angle of embankment fill (degree)
L	:	Improvement Depth (m)

Kitazume and Maruyama (2007) and Shrestha et al. (2015) reported that the current design methods consider the shear failure of DCM columns for internal stability as shown in Fig.1.6 and stated that this kind of shear failure mechanism has not been verified experimentally and numerically.
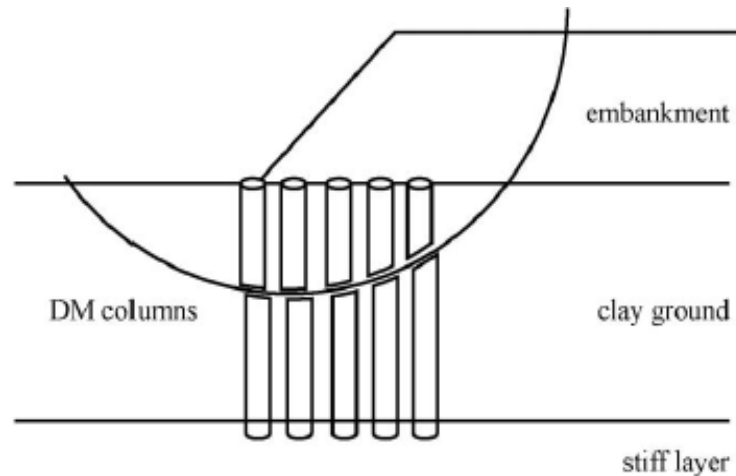
Figure 1.6 Shear failure of DCM columns (Kitazume and Maruyama 2007)

1.4 STONE COLUMN IMPROVED GROUND UNDER EARTHQUAKES

Noorzad et al. (2007) demonstrated the reinforcement effect of partially penetrating stone columns during an earthquake and proposed a numerical model representing improved ground by a unit cell with stone column at the center. The model considered the following assumptions. The permeability of stone column is free draining to ensure that there is no build-up of excess pore water pressure within the stone column during earthquakes. The horizontal component of displacement, velocity and acceleration of water and soil particles are equal during ground shaking. The stone column carries the major load imposed by the structure and minor load is shared by the soil. This load remains constant during shaking. It is also assumed that there is perfect bonding between soil and column.

Consider the dynamic equilibrium of the block containing the volume above the depth, *z*, as shown in Fig.1.7 which demonstrates the free body diagram (FBD) of the system above the depth, *z*.
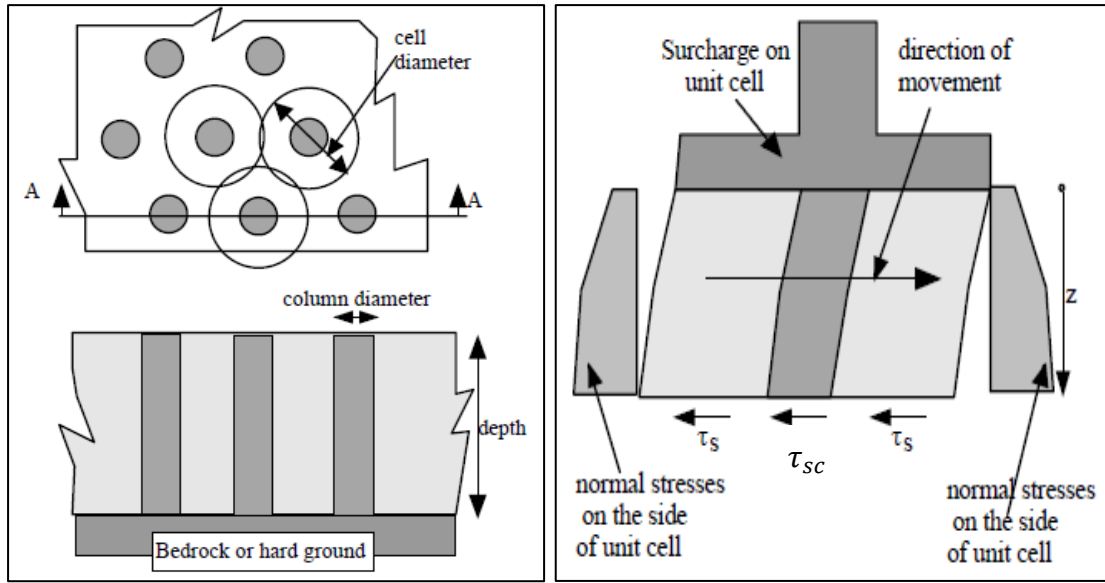
Figure 1.7 Stone column arrangement and FBD of unit cell block (Noorzad et al. 2007)

If W is the "weight" of the surcharge, γ_s the unit weight of the sand and γ_{sc} the unit weight of the stone column then one may write:

$$\frac{W}{g}\ddot{u}_1 + \int_0^z \left(\frac{\gamma_s}{g}A_s + \frac{\gamma_{sc}}{g}A_{sc}\right)\ddot{u}_\xi d\xi = A_s\tau_s + A_{sc}\tau_{sc} \tag{1.15}$$

where $\ddot{u}_1, A_s, A_{sc}$ and g stands respectively for horizontal surface acceleration, cross section area of sand (in the unit cell), cross section area of the column and the acceleration due to gravity and τ_s and τ_{sc} are the average shear stress components at depth z.

1.5 RIGID STONE COLUMNS

Barksdale and Bachus (1983) detailed the use of rigid stone columns (cement added to compacted column forming concrete rigid columns). It is reported that the rigid column is less dependent on the confinement provided by surrounding soil. Therefore, rigid columns can be used in very soft soils with high load carrying capacity than conventional stone columns.

Rigid columns can be also used to strengthen an intermediate weak layer where stone columns cannot be used. The intermediate weak layer can be stabilized with rigid column and load would be transmitted to underlying stone column through rigid column. The load-deformation response of rigid stone column is similar to that of a conventional pile and ultimate load carrying capacity is higher than stone columns (Barksdale and Bachus 1983). It can be also used for stabilizing stone column in weak

9

zones and also for improving stability of slopes. The construction of rigid stone column is carried out by vibro-displacement method and a bottom feed unit for adding cement is used. The cost of rigid stone column is also comparable with conventional stone column due to faster construction time (Barksdale and Bachus 1983).

Pervious concrete is generally used in pavement applications. The suitability of using pervious concrete material as a ground improvement method is proposed by Suleiman et al. (2014) and Ni et al. (2016). Pervious concrete is made from single sized aggregate mix with lower quantity of fine aggregate. The mix proportion used in their study was 1:0.5:4 with a water/cement ratio of 0.21. The permeability values of pervious concrete primarily depend on the mix used. However, the permeability coefficient of the pervious concrete is reported as ranging from 1.0 to 2.4 cm/s. The pervious concrete mixes prepared had porosity ranging from 6-23%, with the 28-day compressive strength varying from 10.4-34.0 MPa. The pervious concrete considered in their study had an average porosity of 12.5% and an average permeability of 1.21 cm/s. The average 28-day compressive strength of pervious concrete was reported as 22.2 MPa with an elastic modulus of 15.4 GPa. Based on these references, the average values of permeability is taken as 0.01 m/s, elastic modulus of 15.4 GPa and 28-day compressive strength of 22.2 MPa is considered in this study. A typical sample of pervious concrete, installation of pervious concrete in the field and core drilling samples are shown in Fig.1.8.

1.6 STATEMENT OF THE PROBLEM

Stone columns are practiced all over the world for improving the vertical load carrying capacity and reducing settlement of soft soils and silty sands. Researchers across the world have proposed various methods to improve vertical load carrying capacity of stone columns, but the behaviour under lateral loading is not well understood.

Stone columns are subjected to lateral loading when it is placed below huge embankments and adjacent to retaining walls. More research has to be carried out on stone columns under lateral loading to get an insight to the behaviour of improved ground. The friction angle and elastic modulus of stone column ranges between 35°to 36° and 30 MPa to 70 MPa respectively (Mitchell 1981; Barksdale and Bachus 1983). The hydraulic conductivity of stone columns is stated to be ranging from 0.09 cm/s to 2 cm/s (Baez 1995). Recent research suggested various reinforcements for ordinary stone columns in the form of providing geo-synthetic encasements, geogrid

encasements, vertical circumferential nails, horizontal strip, pervious concrete columns etc. However, some of the modified stone columns such as encased stone columns and deep cement mixing columns are mostly used in practice. Present study is aimed to study the behaviour of pervious concrete column (PCC) improved ground under static shear and seismic loading conditions. Pervious concrete column is selected because of its higher vertical load carrying capacity and comparable permeability similar to that of stone columns. Additionally, pervious concrete is made with less quantity of fine aggregate which makes it an environmentally sustainable material. Furthermore, the behaviour of floating pervious concrete column under shear loading as well as seismic loading is studied. The idea of this research is to give an insight into the performance of end-bearing and floating pervious concrete columns in lieu of conventional stone columns in improving shear resistance of weak ground.

Figure 1.8 Pervious concrete (a) Sample (b) Installation of pervious concrete column (c) Core drilling samples after 28 days

Pervious concrete columns provide an easy way for water to escape through the pores of highly permeable concrete similar to that of ordinary stone columns. However, clogging can occur to pervious concrete columns just like stone columns. Since single size aggregate is used in pervious concrete mix, clogging can be prevented to some extent. However, research is being carried out in pavement application to counter the clogging of pervious concrete (Eg: Kia et al.). In ground improvement scenario, a filter material can be provided around the circumference of pervious concrete column to prevent the intrusion of soil particles to the column. Therefore, the seismic performance evaluation of pervious concrete column improved ground is also carried out. The seismic performance along with liquefaction mitigation potential of pervious concrete column improved ground in comparison with stone column improved ground is also investigated.

1.7 RESEARCH OBJECTIVES

The research objectives of present study are as follows:

(i) To quantify the behaviour of pervious concrete column improved ground subjected to shear loading in comparison to stone column improved ground.

(ii) To study the mode of failure of end-bearing and floating pervious concrete column under shear.

(iii) To study the liquefaction mitigation potential of pervious concrete column improved ground and to compare with the seismic performance of stone column improved ground under similar earthquake loading conditions.

(iv) To understand the performance of end-bearing and floating pervious concrete column improved ground subjected to seismic excitation and to identify various parameters influencing the seismic performance of improved ground with stone column as well as pervious concrete column inclusion.

(v) To assess the efficacy of pervious concrete column in seismically active areas, various homogeneous liquefiable soil deposits such as loose sand, medium-dense sand and silt stratum and sandwiched liquefiable soil strata in mitigating liquefaction induced lateral spreading.

1.8 OUTLINE OF THESIS

Thesis is divided into eight chapters and presented as follows:

Chapter 1   Introduces the topic and shear loading situations related to it. It also explains the objectives of the present study and outline of thesis.

Chapter 2   Reviews the literature referred for the study and sub divided into modified stone columns, stone column performance subjected to static shear and seismic loading conditions.

Chapter 3   Explains the methodology used for the study, detailing numerical analysis of direct shear test models, large shear test models and seismic modelling of improved ground.

Chapter 4   Describes the direct shear test and inclined direct shear test models of improved ground with stone column and pervious concrete column inclusions. The effect of normal pressure, effect of diameter, effect of shear surface inclination, deformation of columns, are studied and presented.

Chapter 5   Details the large shear test models of floating and end-bearing column improved ground. The effect of depth of plugging, effect of diameter, effect of number of columns, deformation of columns, heave profile etc. are studied and results are presented.

Chapter 6   Investigates seismic analysis and liquefaction mitigation potential of pervious concrete column improved ground and stone column improved ground along with various influencing parameters like area ratio, diameter, depth of column inclusions, column and surrounding soil permeability, liquefiable soil thickness, ground surface inclination, surface load and earthquake characteristics.

Chapter 7   Presents design example and slope stability analysis of column supported embankment system

Chapter 8   Summarizes conclusions based on static shear analysis and seismic analysis of improved ground with pervious concrete column and stone column inclusions. The suggestions for future research are also added.

CHAPTER 2
LITERATURE REVIEW

Review of literature is divided into three sections. The first section describes the review of modified stone columns proposed for improving weak soils. In the second section, lateral (shear) load tests reported on improved ground with column inclusion is presented. Seismic analysis of stone column improved ground reported in the literature is discussed in the third section.

2.1 MODIFIED STONE COLUMNS

Malarvizhi and Ilamparuthi (2004) performed load tests on soft clay bed stabilized with single stone column and encased stone column having various slenderness ratios and using different type of encasing material. The settlement in encased stone column is found to be lesser than the stone column and the settlement decreased with the increasing stiffness of the encasing material. For smaller loads, the settlement reduction ratio is less in stone columns but for higher loads it is less in geogrid encased stone column. Encasing the stone column with geogrids resulted in an increase of load carrying capacity irrespective of whether the column is end-bearing or floating. In case of floating columns, the l/d ratio has less influence on the capacity of column for the lengths studied in their investigation. The ultimate load carrying capacity of the reinforced column increased with the stiffness of the reinforcement. They performed finite element analysis of a geogrid encased stone column to simulate the experimental conditions. The geogrid was modeled using the geogrid element, which can take only tensile force. They reported that the performance of encased stone column is better than the conventional stone column for all the diameters studied. For a particular settlement, the load intensity of the stabilized bed with smaller diameter columns is higher than the larger diameter columns. The stresses were higher in the smaller diameter columns. The hoop stress generated in the geogrid was responsible for the increase in load capacity of the encased stone columns. The stiffer the geogrid is, the hoop stresses developed is more and consequently, higher is the load carrying capacity. The dilatancy of the stones in the encasement reduces, but the composite effect of the stones and the geogrid contributes to the higher stress concentration ratio of the columns.

Murugesan and Rajagopal (2006) concluded that the load capacity and stiffness of the stone column can be increased by all-round encasement by geosynthetic. By geosynthetic encasement, it is found that the stone columns are confined, and the lateral bulging is minimized. The confining pressures generated in the stone columns are higher for stiffer encasements. The hoop tension forces developed in the encasement are significant within a depth equal to approximately twice the diameter of the stone column. The performance of encased stone columns of smaller diameters is superior to that of larger diameter stone columns because of mobilization of higher confining stresses in larger stone column. The higher confining stresses in the column leads to higher stiffness of smaller diameter encased columns. The confinement at the top portion of the stone column (where predominant bulging occurs) is sufficient for the improved performance of the stone column. It is adequate to encase the stone column up to a depth equal to two times the diameter of stone column to substantially increase its load carrying capacity. The load capacity of encased columns is not as sensitive to the shear strength of the surrounding soils as compared to ordinary stone columns. This is especially true for higher stiffness values of the encasement. The magnitude of loads transferred into the encased stone columns from the embankments can be increased by using stiffer encasement.

Black et al. (2007) presented the performance of small-scale stone columns that were enhanced by jacketing with tubular wire mesh, a bridging rod, and a concrete plug (Cement grout prepared at a 2:1 cement/water ratio was injected into the stone column to form a solid concrete plug in the peat region of the soil bed). From their experimental work, it was concluded that the load-carrying capacity and the settlement performance represented by the modulus subgrade reaction of a loaded plate supported on stone columns in peat can be improved by considering any of the above methods proposed.
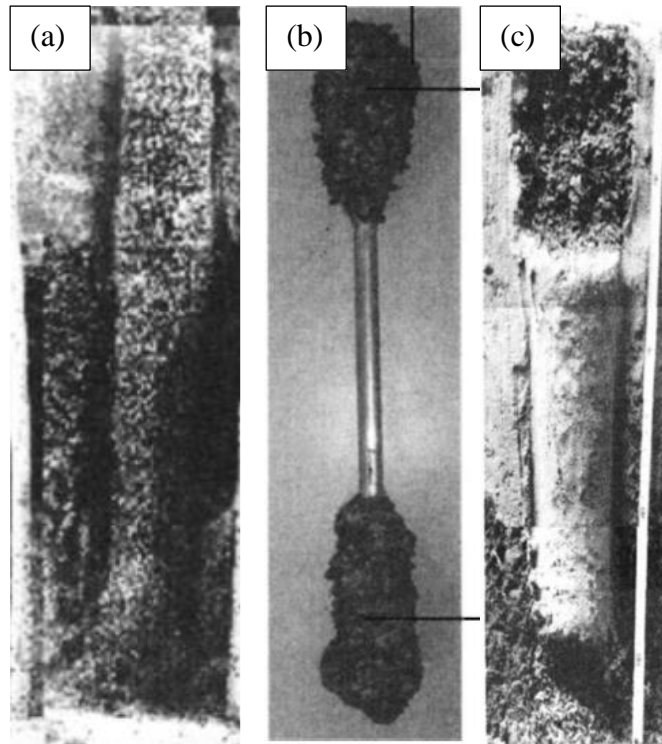
Figure 2.1 Modified stone column using (a) tubular wire mesh (b) a bridging rod and (c) concrete plug (Black et al. 2007)

Wu and Hong (2007) reported that slippage occurs for columns reinforced with stiffer inclusions. The stiffer the reinforcement, the lower is the axial strain at which slippage occurs. Slippage results in a flatter stress–strain curve, and lower axial strength than that for columns reinforced with less stiff inclusion. While granular material and the reinforcing sheet are bonded, column with smaller spacing produces stiffer behaviour for the same radius/spacing ratio. When slippage occurs, reinforced columns with the same radius/spacing ratio follow the same stress–strain curve except for the low-strain section. Under greater chamber pressure, both materials are bonded to greater axial strain, which results in an upward convex stress–strain curve at high axial strain. Embedding a reinforced granular column in soil increases the granular column strength compared to an unreinforced column subjected to constant confining pressure. The higher the strain, the greater is the axial stress discrepancy between columns subjected to constant and varying confining pressures.

Gniel and Bouazza (2009) focused on studying the effect of varying the length of encasement and investigating whether a column that was partially encased with geogrid would behave similarly to a fully encased column. In addition, isolated column

behaviour was compared to group column behaviour. The constrained conditions provided by unit-cell loading provided additional lateral confinement to the encased columns, preventing radial column failure, and enabling encasement mesh to be loaded to tensile capacity. Isolated columns failed by radial expansion below the level of encasement. For group columns, increasing the length of encasement acted to increase column stiffness and steadily reduce vertical strain. Fully encased columns reduced vertical strain by about 80% when compared to clay behaviour alone. For isolated columns, increasing the length of encasement acted to increase column capacity, although the strain at failure remained quite consistent. A large increase in capacity was observed for the fully encased column. Significant radial column bulging occurred directly below the base of the encasement for partially encased group columns.

Samadhiya et al. (2008) reported that, due to the inclusion of random fiber into the granular pile, load-settlement behaviour becomes ductile and the load carrying capacity increases and the granular pile behaves to more elastic manner than an unreinforced granular pile. Due to random fiber, the bulging diameter reduces, and the depth of maximum bulging diameter also decreases. But total length of bulging increases due to random fiber.

Wu et al. (2009) concluded that the improvement on the clay can be further enhanced by encapsulating the column with a flexible sleeve. Encapsulating the granular column in a flexible sleeve increases the stiffness and strength of the plain granular column and stiffness of the sleeve governs the column behaviour for the reinforced column loaded to a relatively lower axial strain. The adequate length that a sleeve can prevent a granular column from bulging depends on the characteristics of the in-situ soil and the stiffness and yield strength of the sleeve.

Shivashankar et al. (2010) suggested an alternative and effective method of enhancing the performance stone columns installed in soft soils by encasing the individual stone column with vertical circumferential nails from a series of laboratory plate load tests carried out in unit cell tanks. They concluded that the stone columns reinforced with vertical circumferential nails exhibit a stiffer and stronger response compared to that of conventional stone columns installed in soft soil, for all the diameters and area ratios studied. A schematic representation of test arrangement of stone column with vertical circumferential nails is presented in Fig.2.2. The performance is significantly enhanced

by increasing the number of nails and diameter of nails. Stone column reinforced with vertical circumferential nails over a depth thrice the diameter (3D) exhibits much higher stiffness and ultimate load capacity than stone column for all the diameters studied. Studies have shown that the confinement is needed only where bulging takes place. The benefit of vertical circumferential nails decreases with increase in the diameter of stone columns, for the same number of nails of specific diameter. The nails are found to be more effective for smaller area ratios. Bulge diameter and bulge length are decreased substantially for a stone column reinforced with vertical circumferential nails compared to that of stone column for all the diameters and area ratios studied.
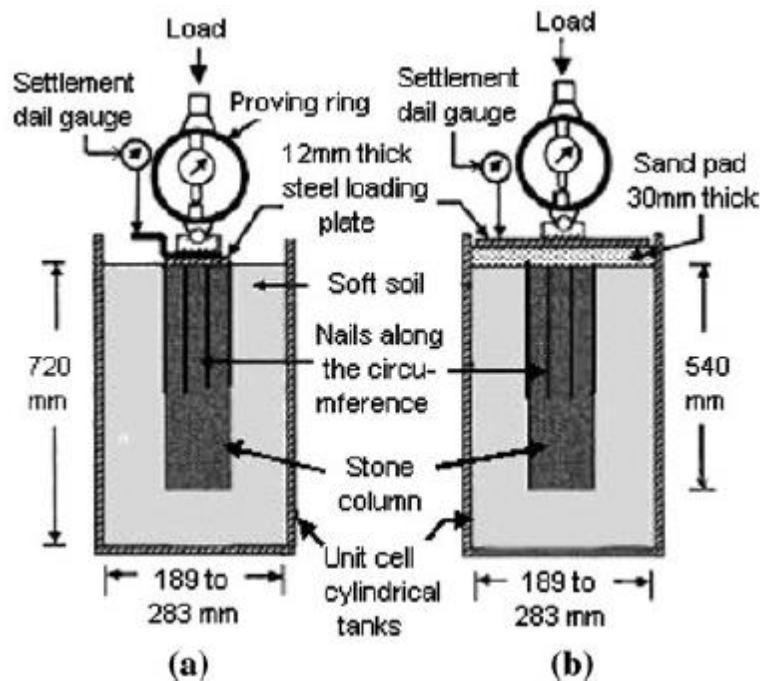
Figure.2.2 Test arrangement of stone column with vertical circumferential nails (Shivashankar et al. (2010)

Fattah and Majeed (2012) carried out numerical modelling on encased floating stone columns. The area replacement ratio has great effect on bearing improvement ratio for soft soil improved by stone column. The undrained shear strength (Cu) of the surrounding soil has a significant effect on bearing improvement ratio and settlement reduction. When the undrained shear strength (Cu) of the surrounding soil is decreased, the bearing improvement ratio is increased, and the settlement is decreased. The geogrid encasement of stone column greatly decreases the lateral displacement compared with ordinary stone column. The use of geogrid encasement gives better results when C_u is

18

higher and increasing the value of C_u plays important role in ordinary stone column. The important increase in strength of stone column occurs when it is encased by geogrid for L/d = 8 while in case of L/d = 4, a slight increase in (q/C_u) at the early stages of applying the load is obtained and then the value of (q/C_u) for both ordinary and encased stone columns is the same. The bearing improvement ratio (q treated / q untreated) increases with increase in the area replacement ratio (as) for both ordinary and encased stone columns, the increase in area ratio (a$_s$) is more efficient for encased stone column than ordinary stone column especially when area ratio (as) is more than 0.25.

Marto et al. (2013) analyzed geogrid encased stone columns and reported that the load capacity of stone column is increased by the increase of diameter of encased stone columns and load capacity and stiffness of stone column can be increased by providing geogrid encasement to full depth.

Ali et al. (2014) conducted tests on stone columns reinforced with lateral circular discs of geotextile in the column. Experiments were conducted on end bearing as well as floating stone columns and the reinforcement was found to be effective for both stone columns.

New method of using pervious concrete pile in place of stone column was proposed by **Suleiman et al. (2014)** and **Ni et al. (2016).** The authors conducted tests on isolated column tests and reported that the use of pervious concrete piles increased the vertical carrying capacity 4.4 times than that of plain stone columns. The pervious concrete considered in their study had an average porosity of 12.5% and an average permeability of 1.21 cm/s. The 28-day compressive strength of pervious concrete was reported as 22.2 MPa with an elastic modulus of 15.4 GPa. It was reported that the strength and stiffness of pervious concrete column is independent of the surrounding soil confinement in addition to its permeability characteristic similar to that of stone columns. The mode of failure of granular column and pervious concrete pile was found to be of by bulging and punching failure as shown in Fig.2.3. Therefore, they concluded that the pervious concrete column can be used for very soft clays and silts, organic and peat soils similar to piles. They also conducted fully instrumental lateral load test at the

SSI facility and reported that the behaviour was similar to that of a long concrete or steel pile when a rebar along the length was provided.
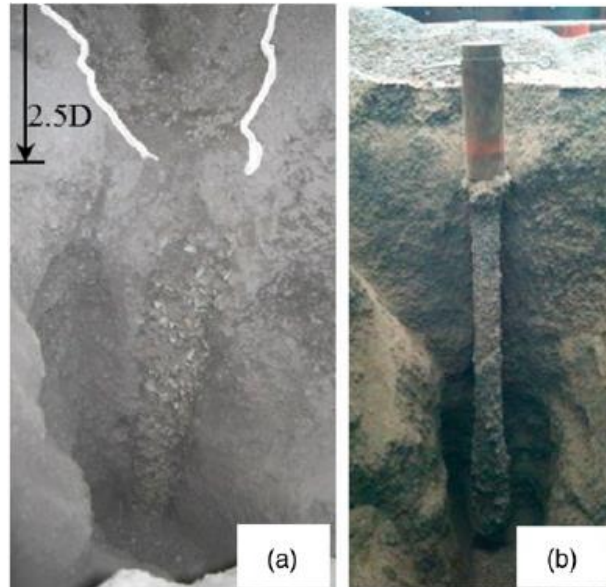
Figure 2.3 Mode of failure of columns (a) Bulging failure of granular columns (b) Punching failure of pervious concrete pile (Suleiman et al. (2014)

Castro (2017) studied the performance of groups of encased stone column beneath rigid footing. It is reported that the column arrangement has less influence on the reduction in settlement. Based on this, a new simplified approach to study group of encased stone column is proposed, by considering all the columns below footing as a single column with an equivalent area and encasement stiffness. The critical length of fully encased and partially encased column is around 2B or 3B, where B is the width of the footing.

Hong et al. (2017) performed numerical analysis on single encased granular column embedded in soft soil and reported that the stiffness of encasement significantly affects the bulging length of an encased column.

2.2 STONE COLUMNS UNDER STATIC SHEAR LOADING

Murugesan and Rajagopal (2009) conducted series of direct shear tests on plain stone column and reinforced stone column with geosynthetic encasement to study the behaviour of shear deformations in stone columns. They reported that the added encasement made stone column to behave as a semi rigid pile and shear load capacity was significantly improved. They also performed lab tests by inducing lateral soil movements in stone column treated soil and developed experimental setup to overcome

the depth restriction in direct shear test. A schematic representation of large shear load test setup is shown in Fig.2.4. The schematic representation of failure surface observed in unreinforced clay, reinforced clay with stone column and encased stone column is shown in Fig.2.5. They reported that the failure surfaces of the unreinforced clay and stone column reinforced clay have coincided because of the shear movement of the aggregate in stone columns along with the surrounding soil. However, the encased stone columns obstructed the lateral soil movement and the clay heaved up through the intervening space between the loading plate and the encased stone column.

Strain controlled loading

Displacement dial gauges

← 300 mm →

Soil movement

Stone Column

Geosynthetic encasement

600 mm

Clay soil

1200 mm

(a) Sectional elevation of the test set up

Rigid loading plate (300×300 mm)

100 or 50 mm clear gap

300 mm

Stone columns (75 mm Ø, 150 mm c/c)

(b) Plan view of the test set up
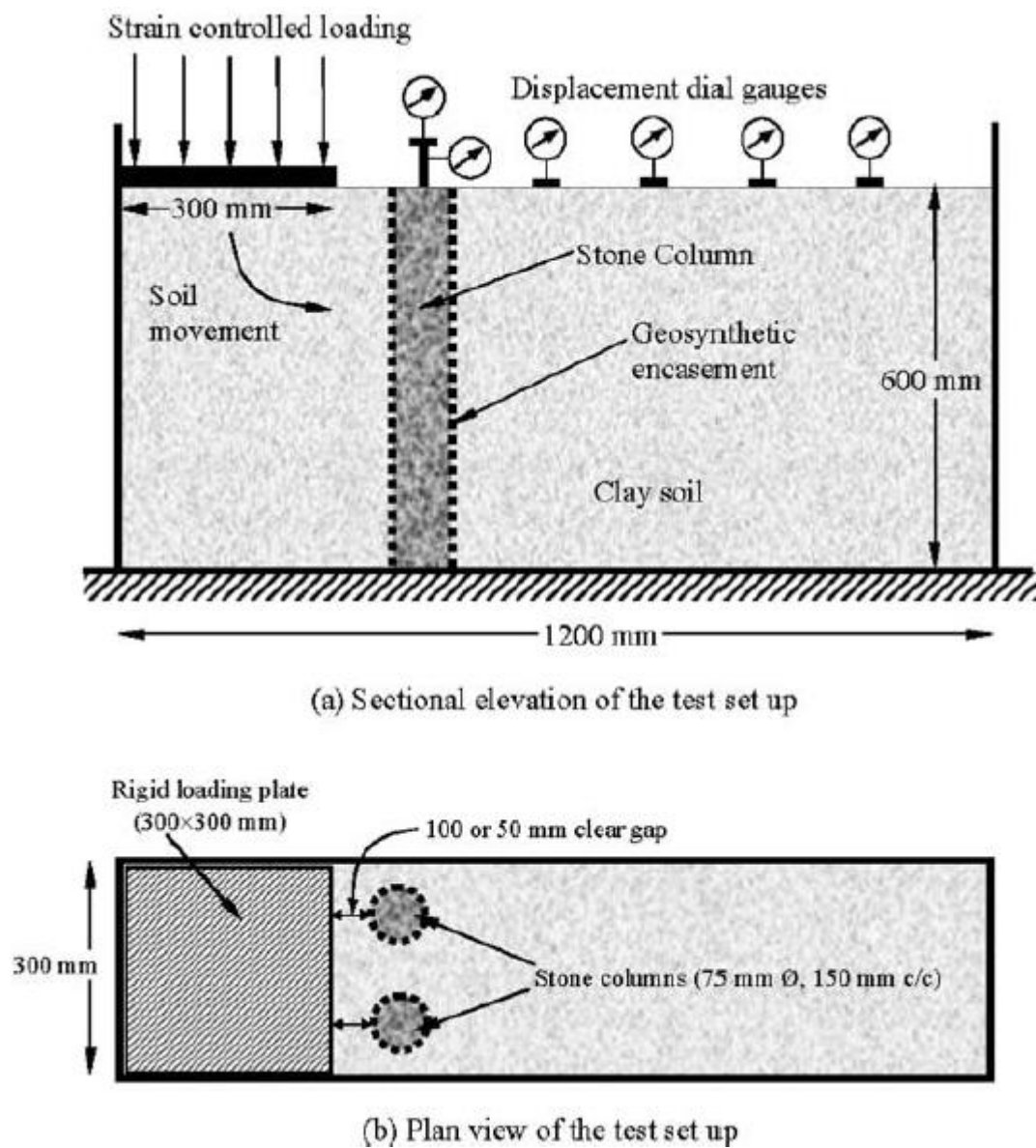
Figure 2.4 Large shear load test setup developed (Murugesan and Rajagopal, 2009)
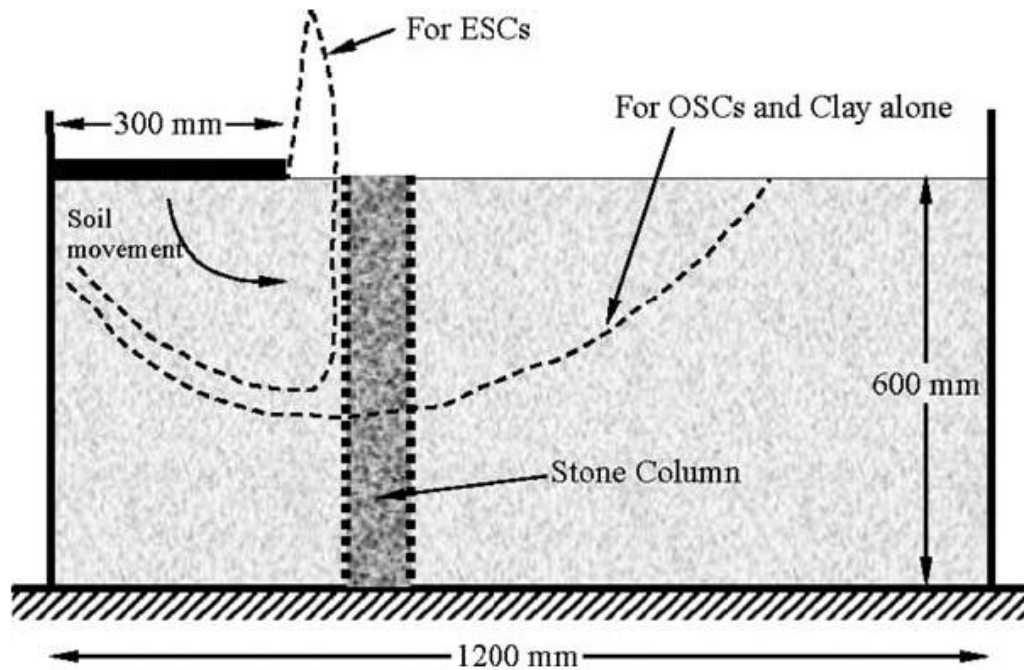
Figure 2.5 Failure surface observed in the clay, stone column and encased stone column reinforced clay (Murugesan and Rajagopal, 2009)

Bending failure mechanism of geosynthetic encased stone columns in soft soils was studied by **Jian et al. (2015)** by conducting indoor physical model test. They also conducted numerical studies and suggested one more row of columns may be required to provide higher lateral resistance in the soils beneath the toe of the embankment to improve its stability.

Mohapatra et al. (2016) conducted direct shear tests on plain and geosynthetic encased end bearing stone columns to study the behaviour under shear loading. They reported that the lateral load capacity of granular columns with encasement increased with the use of encasement layer, due to the mobilization of tensile forces in the layer. The shear strength was observed to be increased with increase in area ratio for encased stone columns. They also reported the strength reduction of encased stone column to that of plain stone column after the rupture of encasement. Tests were conducted on group arrangement and found to have higher shear resistance than single stone column. They conducted experiments in group of stone columns with square and triangular pattern. **Mohapatra et al. (2017)** performed three-dimensional modelling of ordinary and geosynthetic encased granular columns in direct shear test model using FLAC 3D and

mode of failure of encased stone column was presented as shown in Fig.2.6. 3D slope stability was also carried out to simulate field conditions.

(a) $\sigma_n = 15$ kPa

(b) $\sigma_n = 75$ kPa
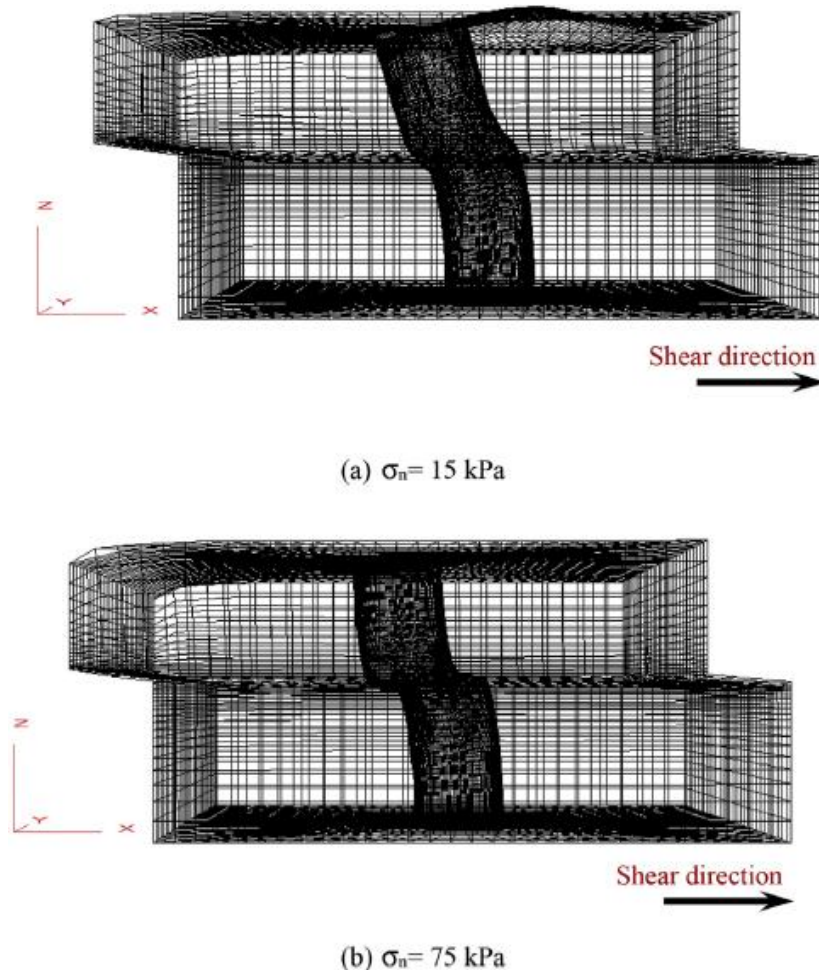
Figure 2.6 Failure modes of encased stone column (Mohapatra et al. 2017)

2.3 STONE COLUMNS UNDER SEISMIC LOADING

Seed and booker (1978) initially proposed the use of gravel drains in mitigating liquefaction. They developed one dimensional theory of pore water pressure generation and dissipation, extended to three dimensions and applied to the analysis of columnar gravel drains under a variety of earthquake conditions. Design charts were developed from those analyses for providing convenient basis for design considerations. It was reported that the dominant mechanism in the operation of a gravel drain system will be of pure horizontal drainage. It was also stated that the liquefaction of soil deposit can be reduced by installing a system of gravel or rock drains so that pore water pressures generated by cyclic loading may be dissipated almost as fast as they are generated.

23

Baez (1995) developed a mathematical model capable of modeling earthquake shear stress redistribution for evaluating improved drainage parameters and densification of liquefaction in soils ranging from clean sands to non-plastic silts. Design charts were developed for the cost-effective remediation using stone columns from SPT and CPT field tests for differing soil conditions. Based on densification mechanism, it was reported that the stone columns are more beneficial at close distances (3 ft) from the stone column.

Ashford et al. (2000) conducted full scale laterally loaded stone columns in liquefied soil. Controlled blasting was used to liquefy soil and assessed the performance before and after treatment with stone columns. Stone columns are found to improve stiffness of soil 2.5-3.5 times more than soil without stone column treatment. It was also found that the rate of excess pore pressure dissipation after blasting was significantly high due to the presence of stone columns.

Adalier et al. (2003) conducted centrifuge studies to assess liquefaction counter measure of densified non-plastic silty soils with stone columns. The focus of the study was on the overall stiffness of soil using stone columns rather than the drainage effectiveness of stone columns. The experiment was carried out on uniform silt ground, stone column treated ground with and without surcharge. It was reported that confinement is obtained with surcharge load and for stone column treated load with surcharge, lateral displacement reduced considerably.

Elgamal et al. (2009) conducted numerical modelling using OpenSeesPL on sand and silt strata with stone column and pile pinning remediation. Pile pinning was reported as effective for both sand as well as silt strata in mitigating liquefaction. However, stone column was found to be highly ineffective in silt strata. The ground surface displacement was reported to be less than 0.3 m using stone column remediation only when area ratio was from 20% to 30%. It was concluded that for achieving small scale deformation, area ratio greater than 40% is needed while using stone column remediation. Pile pinning with replacement ratio as low as 10% was found to provide very less lateral deformation.

Krishna (2011) reported the various mechanisms that contribute to the seismic performance of stone columns in mitigating liquefaction as drainage, storage, dilation and densification, and reinforcement. It was detailed that the stone columns tend to

dilate during earthquake event due to shearing. The seismic forces tend to develop positive pore pressure in the soil deposit causes an opposite effect of dilation in dense granular piles. Design charts reported by Seed and Booker 1971 were modified incorporating dilation and reinforcement effect of stone columns in mitigating liquefaction.

Yanmei and Xudong (2011) analyzed 3 D finite element model of group of stone columns with varying diameter, spacing and length of stone columns and reported the development of excess pore water pressure developed. It is reported that the stone column diameter, length and spacing influences liquefaction. The excess pore water pressure decreased with increase in stone column diameter and excess pore water pressure was more in the deeper layer than in the top layer.

Yashwant et al. (2011) conducted experimental studies on stone columns installed in marine clay under cyclic loads. Unit cell concept was adopted in their study and reported that the settlement is more when compared to static loading. The settlements were found to increase with number of cycles. They also reported that when the reinforced bed was given cyclic loads lower than failure loads, the stiffness and strength of the soil were enhanced.

Lu et al. (2012) conducted high performance seismic studies on remediated ground with OpenSeesPL software. They compared seismic performance of stone column and pile–pinning case and concluded that the highly viable remediation for cellular arrangement is by using pile pinning. For pile pinning remediation, the ground lateral displacement was found to be non-existent.

Liquefaction mitigation using stone column and pile pinning techniques on a liquefiable soil layer using OpenSeesPL software is studied by **Asgari et al. (2013).** Fully saturated sand and silt layers were considered as liquefiable layer in their study. The influence of soil and stone column permeability, ground slope inclination, diameter of column, area replacement ratio and earthquake characteristics on lateral displacement response is reported. They reported that the stone columns tend to dilate under earthquake loading. It is also stated that the presence of static shear stress component due to ground surface inclination increased lateral displacement for grounds with higher slope angle. This behaviour was due to the increase in final lateral displacement when the soil mass inclined to move downwards owing to high slope angle. It is also stated that the low

permeability of silt limited the drainage efficiency of stone column and suggested high stiffness pile pinning technique as an effective method for mitigating liquefaction in low permeability silt soils.

Raju et al. (2013) conducted cyclic plate load tests on black cotton soil, single stone column and group of stone columns and reported that the dynamic parameter called coefficient of elastic uniform compression, defined as the slope of load-elastic rebound graph increased with group and end bearing stone column than single and floating stone column.

Krishna et al. (2014) reviewed various aspects of ground improvement with granular columns of loose saturated sands. The seismic hazard mitigation using stone columns were presented and new charts were developed based on pore pressure generation and installation. The soil fabric evolution effect and densification effect in analyzing pore pressures were added and recommended the use of combined effect in the analysis and design of granular inclusions as seismic risk mitigating elements. They also reported that the granular inclusions are very effective in resisting the seismic loading in liquefiable soils.

Rayamajhi et al. (2014, 2016) conducted three-dimensional non-linear dynamic finite element simulations using OpenSeesPL software implementing incremental dynamic analysis. They studied shear reinforcement mechanism of dense granular column in reducing seismic shear stresses. The seismic shear stresses provided by dense granular columns are significantly lower than estimated based on shear strain compatibility assumption. They considered unit cell modelling approach and isolated shear reinforcement mechanism by considering hydraulic conductivity of granular column equal to that of surrounding soil. **Rayamajhi et al. (2016)** also reported that triggering of liquefaction was not prevented with the use of dense granular columns in sloping ground, but lateral displacements were reduced. The reduction in lateral displacement is attributed to the reinforcing and strengthening effects of granular column. The drainage effectiveness of dense granular columns subjected to earthquake shaking was found to be dependent on permeability of native soil as well as granular columns.

Zhan et al. (2014) conducted shake table tests on laminar shear box and reported the relation between excess pore water pressure and loading acceleration. At lower accelerations (0.030g, 0.097g and 0.161g), the excess pore water was less at different

depth of soil between piles. When the acceleration was 0.252g, the soil between piles liquefied, the pore pressure increased rapidly and reached its maximum value. It is also reported that when the loading acceleration was 0.325g, the excess pore water pressure was less than 0.252g. These results were due to the soil already been liquefied and the upper load taken by pile and soil distributed and the effective stress of soil between piles decreased.

Tang et al. (2015, 2016) conducted liquefaction studies on geo-synthetic encased stone columns using unit cell modelling approach. OpenSeesPL software was used in their liquefaction study. They reported that the lateral deformation reduced while using geo-synthetic encased stone columns than conventional stone columns as mitigation method. They also reported reduction in pore pressure generation while using geo-synthetic encasement. They studied the influence of encasement depth, stiffness of encasement, surface load and ground surface inclination.

Ferhat et al. (2017) conducted parametric studies on floating stone columns, under seismic loads with maximum east-west directional acceleration value of Van Muradiye earthquake. In their study, bearing capacity and load transfer mechanism was studied under earthquake effects and reported that the bearing capacity of the soil models with stone columns under earthquake force was 1.02-3.7 times compared to the bearing capacity of the soil models without stone column.

Geng et al. (2017) performed numerical study using OpenSeesPL to understand the seismic performance of encased stone column. Effectiveness of encased stone column on various types of sand strata, influence of encasement length, stiffness of encasement was addressed. Relatively high and better seismic performance of encased stone column is reported. The optimum encasement length is found as 4 m. It is also reported that the effectiveness of encased stone column is dependent on the properties of sand strata.

Meshkinghalam et al. (2017) carried out series of analytical modelling in FLAC 3D software. A single stone column at the centre of a cubical soil mass of 10 m was modelled. Boundary conditions applied was free field in lateral parts so that the plane wave propagating upward did not have any distortion at the boundary. The modulus of elasticity of stone column was 40 times more than the surrounding soil. Interface elements were used for modelling contact between soil and stone column. Upper boundary of model and environmental boundary of stone column were defined as

permeable boundary, which allowed flow to permeate from internal or external environment. They also conducted analysis in stone column group with square and triangular arrangement. Analysis without drainage was also carried out to study the effectiveness of drainage performance. Stone column drainage performance is found to be effective at depths of about 3 m to 3.5 m from the ground surface. They reported that the increase of column's diameter causes the increase of drainage at distance about 1 to 1.5 m from the surface, after which the column diameter does not influence drainage. It has been reported that at final cycles, the increment rate in settlement is more than column less state. Excess pore water pressure rate increases with increase in s/d ratio. They also concluded that the column group has a better settlement reduction for center-to-center distance of 2.5 to 3.5 times column diameter.

Pal and Deb (2019) reported the performance of clogged stone column using mathematical model and suggested that the peak value of excess pore water pressure ratio can increase up to 50% due to clogging. The fine sand particles migrated by seepage water blocks the hydraulic functioning of stone columns. The rate of dissipation of pore water is affected during earthquake due to clogging.

2.4 SUMMARY

The literature review carried out on modified stone columns, stone columns under shear and earthquake loading is summarized in Table 2.1. The load carrying capacity of foundation soil with ordinary stone columns can be improved by providing rigid and semi-rigid inclusions such as geosynthetic encasements (Murugesan and Rajagopal 2006; Wu and Hong 2007; Gniel and Bouazza 2009; Fattah and Majeed 2012; Hong et al. 2017), geogrid encasements (Malarvizhi and Ilamparuthi 2004; Marto et al. 2013), vertical circumferential nails (Shivashankar et al.2010), random fibre horizontal strip (Ali et al. 2014), pervious concrete piles (Suleiman et al. 2014) etc. Only geosyntheic encased columns and deep cement columns are used in construction sites and more detailed study needs to be done regarding the failure mechanism of above-mentioned other modified stone columns.

Table 2.1 Summary of literature review

Modified stone columns	
Major Contribution	Author(s)
1. Encased stone columns 2. concrete plug 3. random fibre 4. Circumferential nails 5. Pervious concrete piles	1. Malarvizhi and Ilamparuthi (2004); Murugesan and Rajagopal (2006); Wu and Hong (2007); Gniel and Bouazza (2009); Marto et al. (2013); Fattah and Majeed (2012); Hong et al. (2017) 2. Black et al. (2007) 3. Samadhiya et al. (2008) 4. Shivashankar et al. (2010) 5. Suleiman et al. (2014)

Stone columns under static shear loading	
Major Contribution	Author(s)
1. Direct shear tests and large shear tests on clay 2. Direct shear tests on sand	1. Murugesan and Rajagopal (2009) 2. Mohapatra et al. (2016)

Stone columns under seismic loading	
Major Contribution	Author(s)
1. Full scale field study 2. Centrifuge study 3. Shake table tests 4. Cyclic plate load tests 5. Analytical studies 6. Numerical modelling 7. Geo-synthetic encased stone columns-Seismic performance	1. Ashford et al. (2000) 2. Adalier et al. (2003), Yashwant et al. (2011) 3. Zhan et al. (2014) 4. Raju et al. (2013) 5. Seed and Booker (1987), Baez (1995), Krishna et al. (2011), Krishna (2014) 6. Elgamal et al. (2009), Lu et al. (2011), Yanmei and Xudong (2011), Asgari et al. (2013), Rayamajhi et al. (2016) 7. Tang et al. (2015), Geng et al. (2017)

Suleiman et al. (2014) and Ni et al. (2016) proposed a new alternative to conventional stone column system in the form of providing pervious concrete columns. The rigid behaviour of pervious concrete column and hydraulic conductivity similar to that of stone column makes pervious concrete column a better alternative to conventional stone column. Therefore, in this study pervious concrete column is considered.

Studies on the shear behaviour of stone column improved ground is limited. More research is needed to identify the parameters affecting shear failure of improved ground with stone columns as well as modified stone columns. From literature review, it can be observed that the shear performance of ground is evaluated using direct shear tests (Barksdale and Bachus 1983; Murugesan and Rajagopal 2009; Mohapatra et al. 2014) and large shear tests (Murugesan and Rajagopal 2009). Additionally, shear behaviour of modified stone columns other than encased stone column is limited. Therefore, it is required to address the shear behaviour of stone column improved ground and pervious concrete column improved ground.

Stone columns are widely used to mitigate liquefaction in seismic prone areas. Seismic performance of improved ground was reported from full scale field test (Ashford et al. 2000), centrifuge tests (Adalier et al. 2003; Yashwant et al. 2011), shake table tests (Zhan et al. 2014), cyclic plate load test (Raju et al. 2013), analytical modelling (Seed and Booker 1976, Baez 1995, Krishna et al. 2011, Krishna 2014) and numerical modelling (Elgamal et al. 2009, Lu et al. 2012, Yanmei and Xudong 2011, Asgari et al. 2013, Rayamajhi et al. 2016) to understand the liquefaction mitigation potential of stone columns. Numerical Studies conducted on single and group of stone columns and effect of column diameter on excess pore water pressures are reported. Recently, the seismic performance of encased stone column improved ground is reported as relatively better than stone column improved ground. However, studies on seismic behaviour of conventional stone column and modified stone column improved ground are also limited. Therefore, the seismic performance and influence of various parameters influencing liquefaction mitigation potential of stone column and pervious concrete column improved ground is undertaken.

CHAPTER 3

METHODOLOGY

Numerical simulations were performed using Finite element software ABAQUS to understand the behaviour of stone column and pervious concrete column improved ground under lateral loading conditions. Static loading conditions were simulated by modelling direct shear test and large shear tests and are discussed in Section 3.1. Further, seismic analyses of column improved ground were performed. Liquefaction mitigation study using stone column and pervious concrete column improved liquefiable soil strata was performed using three-dimensional finite element software OpenSeesPL and is detailed in Section 3.2.

3.1 STATIC SHEAR ANALYSIS OF IMPROVED GROUND

The potential failure surface of column improved ground under an embankment is shown in Fig.1.1. The columns placed beneath the toe of the embankment experiences significant shear loading. The shear performance of such an improved ground is evaluated by modelling direct shear test and large shear test. The methodology of static shear analysis of improved ground using numerical simulation of direct shear models and large shear models are discussed in Section 3.1.1 and Section 3.1.2 respectively.

3.1.1 Numerical modelling of direct shear test

Direct shear test is used to simulate static shear loading conditions of soil in the laboratory. The schematic representation of direct shear test setup is shown in Fig. 3.1. In direct shear test, one of the shear boxes is restrained from moving and the other box is given horizontal displacement to shear the soil while shearing along a plane. The large direct shear boxes of size 305×305 mm is used for modelling column placed beneath the toe of the embankment where shear load is predominant representing the column improved ground as per ASTM 3080 standards.

The plan and elevation of direct shear model used for numerical simulation is shown in Fig.3.2. The direct shear model has a plan area of 305×305 mm^2. The height of upper and lower shear box model was kept as 100 mm. Soft clay was modelled using Modified Cam Clay (MCC) model, which is used extensively by various researchers for modelling clay. Well established Mohr-Coulomb (MC) model was used for modelling

stone column properties and pervious concrete was modelled as linear elastic material. Eight noded brick elements were used to model clay and column inclusions. Coulomb frictional model was used to define the interaction between stone column-surrounding clay and pervious concrete column-surrounding clay surfaces. The interface friction coefficient used for stone column clay interface was 0.621, which is $\frac{2}{3}\tan\emptyset_{sc}$, where $\emptyset_{sc}$ is the angle of internal friction of stone column. As the behaviour of pervious concrete column was reported to be similar to that of a rigid pile, a value of 0.3 (which is $\tan\emptyset_c$, where $\emptyset_c$ is the angle of internal friction of surrounding clay) as frictional coefficient was considered. The soil box model, stone column and pervious concrete column were meshed individually, and the mesh was created automatically. The default values of control parameters in ABAQUS were kept as same (Shahu and Reddy 2011).
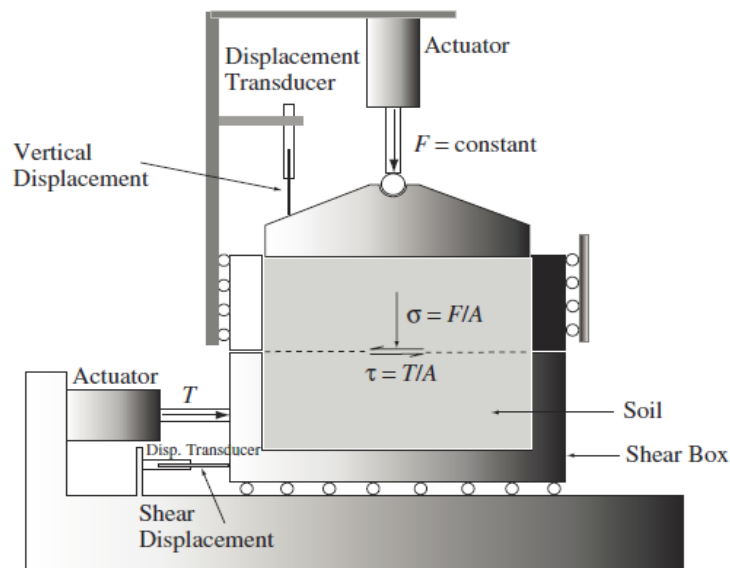
Figure 3.1 Direct shear test arrangement (Helwany 2007)

For the present study, stone column and pervious concrete column was positioned in the center of the direct shear model (Fig.3.2(a)) and shear performance of column improved ground was evaluated from the shear stress-horizontal displacement response of improved ground using finite element modelling. The performance of pervious concrete column improved ground under shear loading was compared with ordinary stone column improved ground.
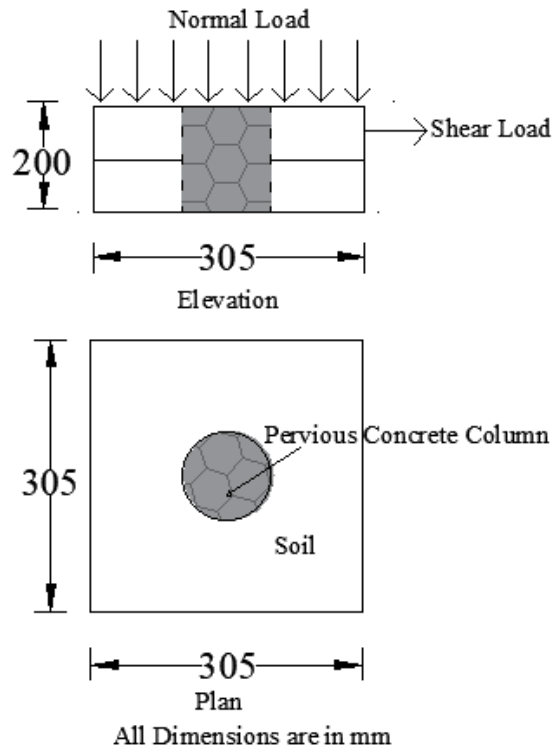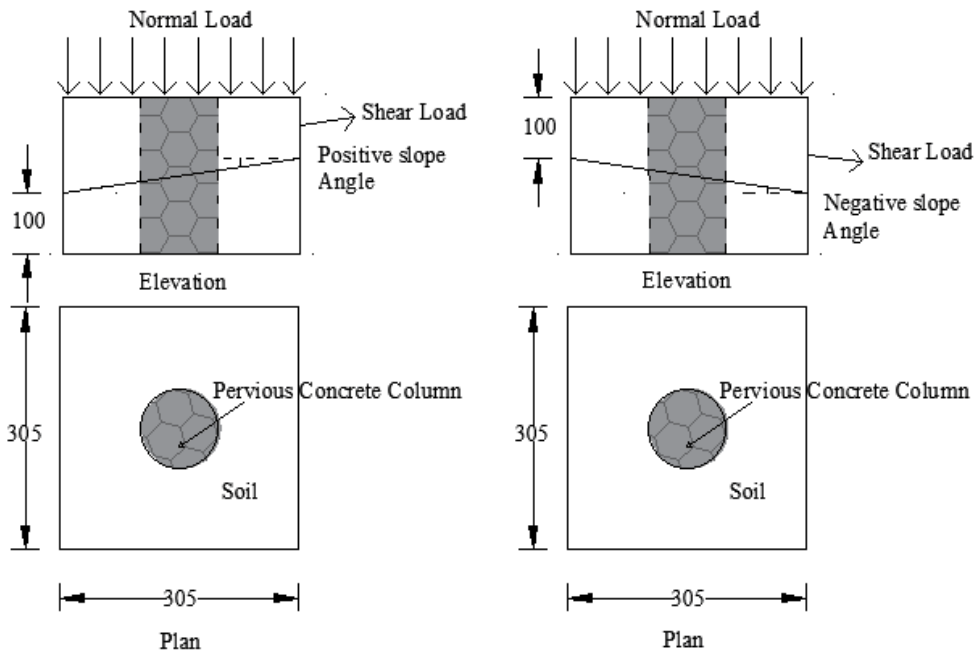
Figure 3.2 (a) Horizontal direct shear test (b) Inclined direct shear test model with pervious concrete column at the center

The ultimate shear resistance of improved ground using direct shear model simulation was carried out for three column diameters (50 mm, 70 mm and 90 mm). The parameters influencing shear performance of column improved ground such as diameter, normal pressure, effect of pervious concrete column and failure mode of columns under shear loading were addressed. The effect of inclination of potential shear failure surface with horizontal was also considered to evaluate the field conditions. Therefore, inclined direct shear tests as shown in (Fig.3.2(b)) with varying inclinations were also performed.

3.1.2 Numerical modelling of large shear test tank

The overall depth of direct shear box used by Murugesan and Rajagopal (2009) and Mohapatra et al. (2014, 2015, 2016) were 200 mm and 140 mm respectively. Large shear test setup was developed by Murugesan and Rajagopal (2009) with increased depth of 600 mm and strain-controlled loading was applied to the full width of the tank, thus inducing lateral soil movements in the soil within the tank. The shear test tank used by Murugesan and Rajagopal (2009) had a length of 1200 mm, width of 300 mm and depth of 600 mm. They applied strain-controlled loading along the full width of the shear test tank as equivalent to the embankment loading. The same size of experimental setup (Fig.3.3) and diameter of columns were chosen according to Murugesan and Rajagopal (2009) to simulate the large shear test model in FEM. Shear test tank model of size 1200 mm × 300 mm × 600 mm depth is larger in comparison with standard direct shear test dimensions of 305 mm × 305 mm × 200 mm depth. That's why the term 'large shear test tank' is used. Eight noded brick elements were used to model clay and column inclusions. Interaction between stone column and pervious concrete columns with surrounding soft clay was modelled using surface to surface contact formulation with Mohr-Coulomb failure criteria. An interface friction coefficient of 0.621 and 0.3 were used as frictional coefficient of stone column-surrounding clay and pervious concrete column-surrounding clay respectively. Original ground, stone column and pervious concrete columns were modelled using eight noded brick elements and the mesh was generated automatically. Default settings used in ABAQUS software were used as suggested in the user manual. The bottom face of the large shear test model was fixed along the three directions for all stages of simulation. Also, the vertical lateral

boundaries of shear test tank model were restrained from displacement perpendicular to the respective surfaces.

The pressure on the loading area (through a horizontally placed loading plate on the ground surface) is an indirect measure or indication of the shearing/ lateral resistance of the model ground. The loading plate as shown in Fig.3.3 was given a uniform vertical displacement of 50 mm and the lateral squeezing of unimproved ground, stone column improved ground and pervious concrete column improved ground were studied. The shear performance of improved ground was measured in terms of pressure-settlement response on the loading plate. In addition to end-bearing pervious concrete columns, floating pervious concrete columns were also considered. The effect of pervious concrete column in place of ordinary stone column, effect of diameter (considering 50 mm, 70 mm and 90 mm diameter columns), effect of floating pervious concrete columns with varying depths from 2D to 8D (D is the diameter of column considered) on shear resistance and lateral deformation of stone column and pervious concrete column were also investigated.
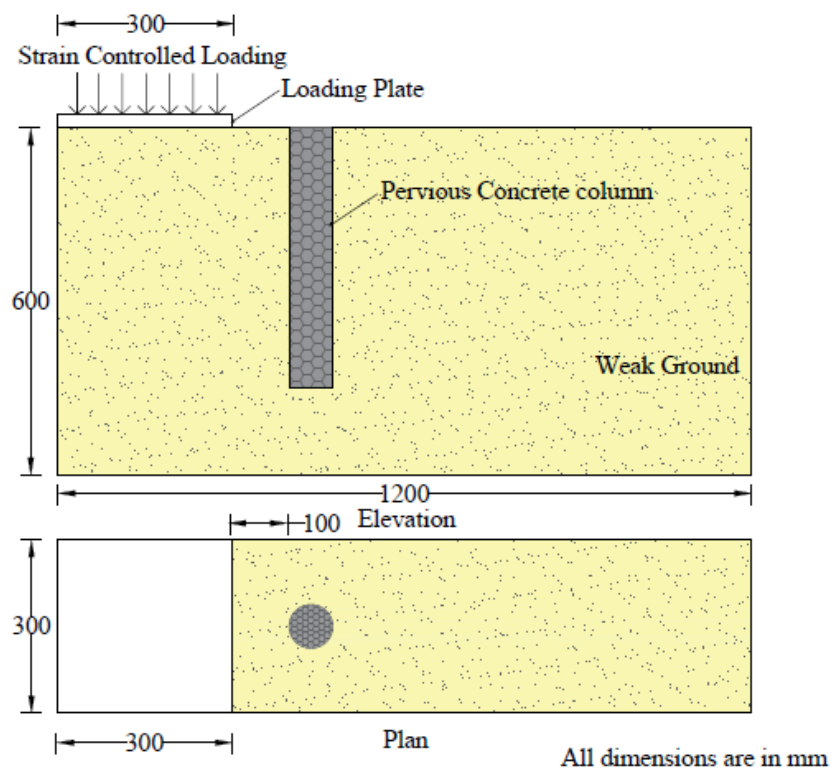
Figure 3.3 Large shear test tank with floating pervious concrete column

3.2 SEISMIC ANALYSIS OF IMPROVED GROUND

Stone columns are widely used to mitigate seismically induced liquefaction. Therefore, the liquefaction mitigation potential of improved ground while using pervious concrete columns were investigated. The seismic performance of pervious concrete column improved ground was compared with conventional stone column improved ground. Three-dimensional finite element analysis using OpenSeesPL was conducted to study the ground lateral deformation and excess pore water pressure generation of pervious concrete column improved ground on a mildly sloped soil stratum. The layout of pervious concrete column (PCC) arrangement is shown in Fig.3.4(a). The unit cell of remediated area is highlighted in the layout. Half of the unit cell is modelled because of symmetry. Similar unit-cell modelling approach has been used by many researchers (Elgamal et al. 2009; Rayamajhi et al. 2014; Tang et al. 2015; Geng et al. 2017). The depth of soil model is 10 m as shown in Fig.3.4(b). The center to center spacing of column were varied as 2D, 2.5D and 3D, which corresponds to area ratio of 20%, 13% and 9% respectively. The lower boundary of soil model was assumed as hard rock and seismic excitation along x-axis was given at the base of soil model. Periodic boundary conditions were applied at the left and right boundary of soil model as applied to group of piles subjected to earthquake loadings (Law and Lam 2001). Eight noded BRICKUP elements with u-p formulation were used to model column inclusions and soil strata.

The soil strata considered was fully saturated sand with an inclination of 4° infinite slope. The parameters influencing seismic performance of improved ground like area ratio, founding depth of columns, diameter of columns and hydraulic conductivity of columns were investigated. The efficacy of pervious concrete column on three types of soil strata in mitigating liquefaction along with parameters influencing ground lateral deformation such as thickness of sandwiched liquefiable soil layer, permeability of surrounding soil, ground surface inclination, peak ground acceleration and surcharge load were also studied.

The soil models were subjected to base excitation conforming to earthquake time history data of El-Centro 1940 earthquake along N-S direction and Loma Prieta 1989 earthquake along E-W direction scaled to 0.2g. The influence of earthquake characteristics on pervious concrete column improved ground was additionally

addressed. Total stress analyses were also performed, and the pressure build up was analyzed by comparing the seismic responses with effective stress analyses.

(a) Arrangement
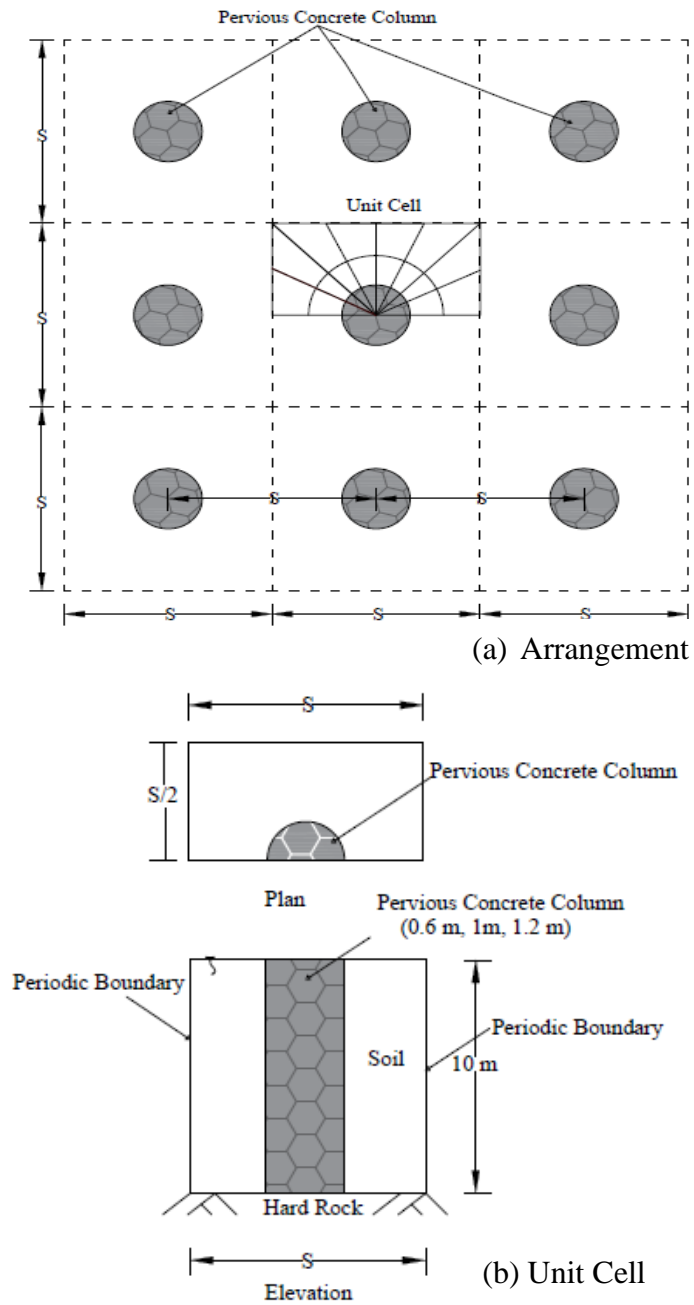
(b) Unit Cell

Figure 3.4 (a) Pervious concrete column (PCC) arrangement (b) Representative unit cell

3.3 SUMMARY

This chapter explains the methodology adopted to analyze the performance of improved ground under shear and seismic load. The columns placed beneath the toe of the embankment experiences significant shear loading. The shear performance of column improved ground is analyzed by modelling direct shear models and large shear models using ABAQUS. The liquefaction mitigation potential of pervious concrete column in place of stone column in liquefiable soil is performed using OpenSeesPL. The influencing parameters affecting the shear and seismic performance are required to develop design guidelines of pervious concrete column and therefore the soil models are analyzed by varying different parameters.

CHAPTER 4

SHEAR BEHAVIOUR OF PERVIOUS CONCRETE COLUMN IMPROVED GROUND USING DIRECT SHEAR TEST MODELS

In this chapter, the shear response of pervious concrete column improved ground is addressed and compared with stone column improved ground. Numerical modelling using ABAQUS software was used for analyzing improved ground. Direct shear tests and inclined direct shear tests were modelled, and details are mentioned in the subsequent sections.

4.1 DIRECT SHEAR TEST MODEL

The first step in the numerical modelling is to validate the present model by generating a similar model of already reported study from well accepted publications. Therefore, direct shear test model generated in ABAQUS software was validated using the data of experimental work done by Murugesan and Rajagopal (2009). Clay was used as unimproved ground in their study and properties are listed in Table 4.1. Therefore, for validation, direct shear test was modelled for the improved clay reinforced with stone column of diameter 100 mm under a normal pressure of 13.3 kPa. The dimensions of direct shear test box used was 300 mm × 300 mm × 200 mm. Displacement controlled loading was applied to the upper shear box although the displacement was given to lower shear box in their experimental setup. The results obtained from ABAQUS model and reference experimental data were found to be in good agreement and are following the pattern as shown in Fig.4.1.

The shear performance of stone column and pervious concrete column improved ground supporting the embankment was studied using numerical analyses of direct shear tests. The shear strength of ground with and without column inclusions were assessed. The direct shear test models of unimproved ground and stone column improved ground were analyzed and compared with pervious concrete column improved ground. The deformation patterns of column inclusions were also explored. The normal pressures considered on the top of direct shear model was varied from 0 kPa to 75 kPa which corresponds to 0 to 5 m of embankment height. The unit weight of embankment fill was considered as 15 kN/m^3. The normal pressure of 0 kPa and

15 - 75 kPa represents end column and center column respectively for the corresponding embankment heights.

The direct shear model dimensions were kept similar to that of large direct shear test i.e., 305 mm×305 mm and a depth of 200 mm as shown in Fig. 3.2(a) conforming to ASTM D3080. The upper part of direct shear model was moved relative to the lower part of model and the shear strength was calculated by summing up the respective horizontal forces divided by the plan area (305×305 mm^2). The horizontal displacement applied to the upper direct shear box model was 40 mm for all the cases studied.

Table 4.1 Validation of direct shear test model (Murugesan and Rajagopal, 2009)

Properties	Stone column	Clay
Constitutive Model	Mohr-Coulomb	Mohr-Coulomb
Unit weight(kN/m^3)	20	17
Elastic modulus(kPa)	45000	3000
Poisson's ratio	0.3	0.45
Cohesion(kPa)	1	20
Friction angle	42°	0
Dilation angle	10°	0
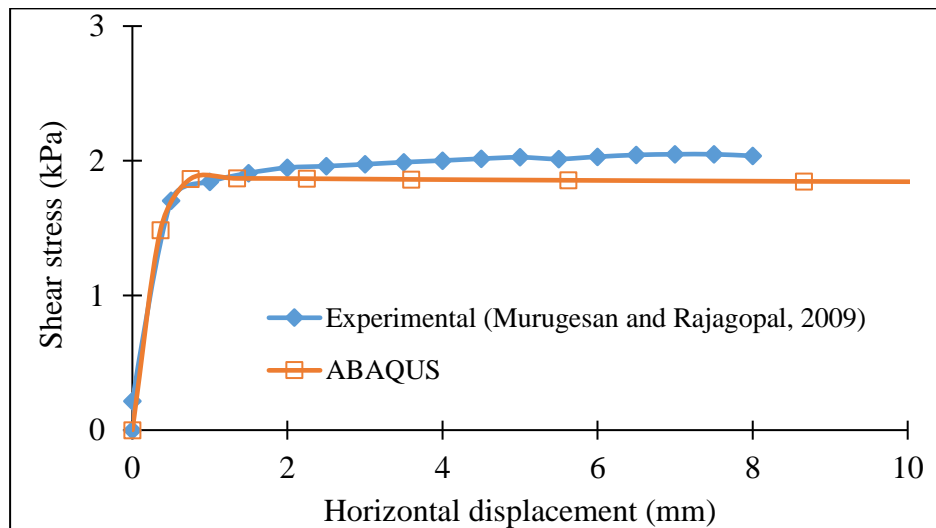
Figure 4.1 Validation of ABAQUS direct shear test model

The effect of pervious concrete column in place of stone columns, effect of diameter, effect of normal pressure, heave profile, mode of failure of columns under static shear load were carried out in direct shear tests. Pervious concrete column can be used for very soft clays and silts, organic and peat soils (Ni et al. 2016) whereas performance of stone columns are dependent on surrounding soil properties (Barksdale and Bachus 1983, Kempfert 2003). Therefore, very soft clay property is considered to compare pervious concrete column inclusion with stone column inclusion in weak ground. The properties used for modelling weak soil, stone column and pervious concrete column were taken from Shahu and Reddy (2011), Ambily and Gandhi (2007) and Ni et al. (2016) respectively and tabulated in Table 4.2. Soft clay was modelled using Modified Cam Clay (MCC) model, which is used extensively by various researchers for modelling clay. Well established Mohr-Coulomb (MC) model was used for modelling stone column properties and pervious concrete was modelled as linear elastic material. The soft clay, stone column and pervious concrete column was simulated using eight-noded brick elements with reduced integration. Coulomb frictional model was used to define the interaction between stone column-surrounding clay and pervious concrete column-surrounding clay surfaces. The interface friction coefficient used for stone column clay interface was 0.621, which is $\frac{2}{3}\tan\emptyset_{sc}$, where $\emptyset_{sc}$ is the angle of internal friction of stone column. As the behaviour of pervious concrete column was reported to be similar to that of a rigid pile, a value of 0.3 (which is $\tan\emptyset_c$, where $\emptyset_c$ is the angle of internal friction of surrounding clay) as frictional coefficient was considered. The soil box model, stone column and pervious concrete column were meshed individually, and the mesh was created automatically. As used by Shahu and Reddy (2011), default values of control parameters in ABAQUS were kept as same.

Two stages of loading were applied. In the initial stage, gravity loading was applied. In the second stage, normal pressure on the top of upper box was applied followed by a horizontal displacement of 40 mm to the upper box. The lower box was kept fixed during all stages of loading. The modelling of direct shear boxes was not carried out to simplify the model and to minimize the computation time. However, boundary conditions were applied to simulate the direct shear test setup as mentioned

in Potts (1987). The bottom face of the lower soil model was restrained in all three directions. The lateral vertical boundaries of upper and lower boxes were restrained from displacement perpendicular to the respective boundary surfaces during the geostatic step and normal pressure application. The lateral vertical boundaries of upper box were given a displacement of 40 mm along the prescribed direction for simulating the movement of upper box with respect to lower surface. The model geometry before and after subjected to shear displacement along with deformed shape of ordinary stone column and pervious concrete column is shown in Fig.4.2.

Table 4.2 Material properties used in finite element simulations

Clay	
Reference	Shahu and Reddy (2011)
Constitutive model	Modified Cam-Clay
Unit weight(kN/m^3)	17
Log Plastic modulus/Logarithmic Hardening constant for plasticity	0.11
Poisson's ratio	0.33
Bulk Modulus for Elastic behaviour	0.025
Critical State Stress ratio	0.703
Stones	
Reference	Ambily and Gandhi (2007)
Constitutive model	Mohr-Coulomb
Unit weight(kN/m^3)	16.62
Elastic modulus(kPa)	55000
Poisson's ratio	0.3
Cohesion(kPa)	0
Friction angle	43°
Dilation angle	10°
Pervious concrete	
Reference	Ni et al. (2016)
Constitutive model	Linear Elastic
Unit weight(kN/m^3)	16.5
Elastic modulus(GPa)	15.4
Poisson's ratio	0.3
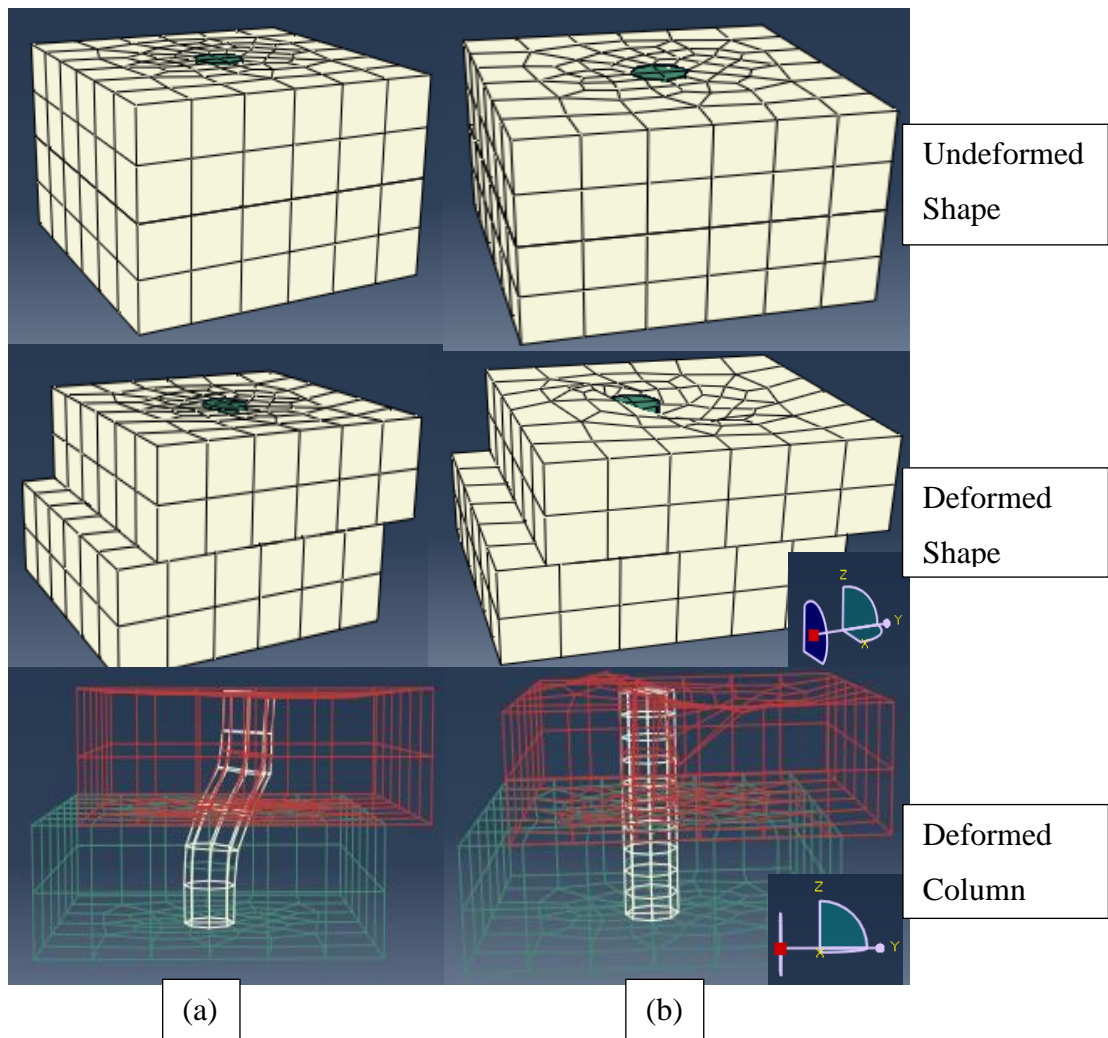
Figure 4.2 Direct shear model analysis of improved ground (a) with stone column (b) with pervious concrete column (50 mm diameter)

4.2 INCLINED DIRECT SHEAR TEST MODEL

To represent actual field cases, varying inclination (+/-) angles of the (planar) shear failure surface with the horizontal as shown in Fig.4.3 was considered. Therefore, inclined direct shear tests (Fig.3.2(b)) with slope angles $\pm 5°$, $\pm 10°$, $\pm 15°$ and $\pm 20°$ were performed. Material properties, numerical model used, and dimensions were kept same as horizontal direct shear test simulation except the inclination with horizontal. Simulation procedure was same as that of direct shear test analysis. The effect of difference in normal pressure acting on the inclined plane is to be considered in the analysis. Therefore, the shear strength of inclined direct shear model was calculated by summing up the secant component of horizontal forces divided by the respective plan area. The displacement loading for negative slopes are given in Table 4.3. Similarly,

the displacements along Y and Z directions are given accordingly for positive slopes (Table 4.4). The finite element programme for direct and inclined shear tests are listed in Table 4.5. A total of 378 analyses were carried out. The deformed model of pervious concrete column improved ground and stone column improved ground subjected to shear loading for positive slopes of 5°, 10°, 15°and 20° are shown in Fig.4.4 and Fig.4.5 respectively. Similarly, for negative slopes, Fig.4.6 and Fig.4.7 show the deformed model of pervious concrete column improved ground and stone column improved ground respectively under static shear.
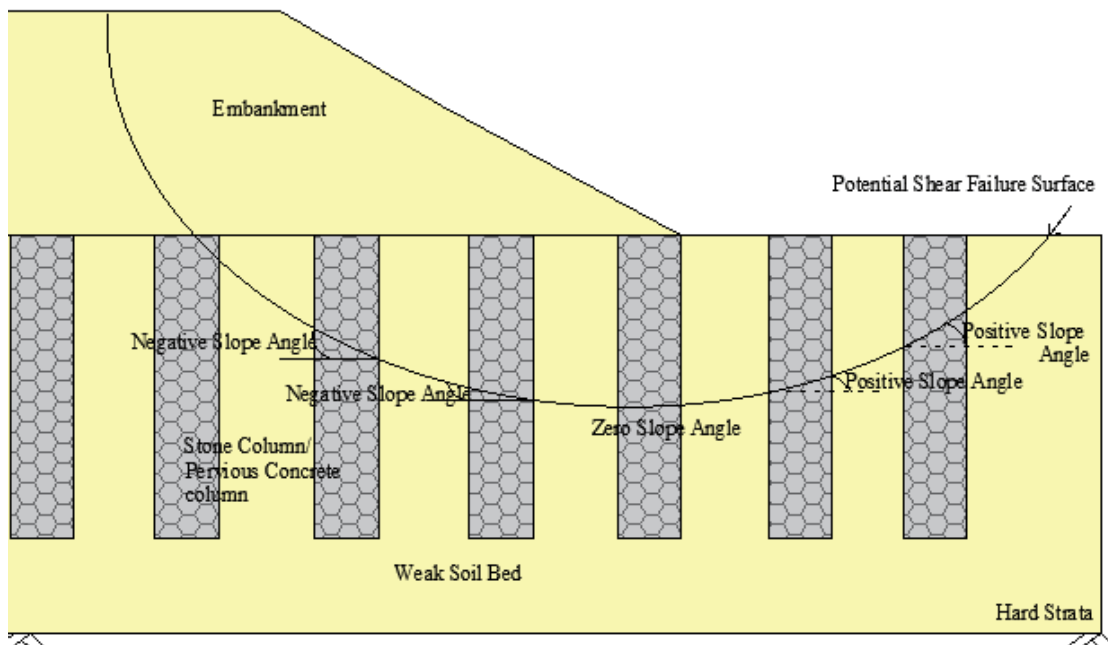
Figure 4.3 Potential shear failure surface in column supported embankment system

Table 4.3 Displacement applied for negative slopes

Displacement (m)	Slope angle				
	0°	-5°	-10°	-15°	-20°
Along X direction	0	0	0	0	0
Along Y direction	0.04	0.0398	0.03939	0.03863	0.03759
Along Z direction	0	-0.0034	-0.00694	-0.10347	-0.01367

Table 4.4 Displacement applied for positive slopes

Displacement (m)	Slope angle			
	+5°	+10°	+15°	+20°
Along X direction	0	0	0	0
Along Y direction	0.0398	0.03939	0.03863	0.03759
Along Z direction	0.0034	0.00694	0.10347	0.01367

Table 4.5 Finite element analysis matrix for direct shear tests

Description		Inclination of shear surface with horizontal					Number of Analyses
		0°	± 5°	± 10°	± 15°	± 20°	
Only Clay		✓	✓	✓	✓	✓	54
OSC	50 mm	✓	✓	✓	✓	✓	54
	70 mm	✓	✓	✓	✓	✓	54
	90 mm	✓	✓	✓	✓	✓	54
PCC	50 mm	✓	✓	✓	✓	✓	54
	70 mm	✓	✓	✓	✓	✓	54
	90 mm	✓	✓	✓	✓	✓	54
Total number of analyses done for various Normal Pressures(0,15,30,45,60,75kPa)							**378**
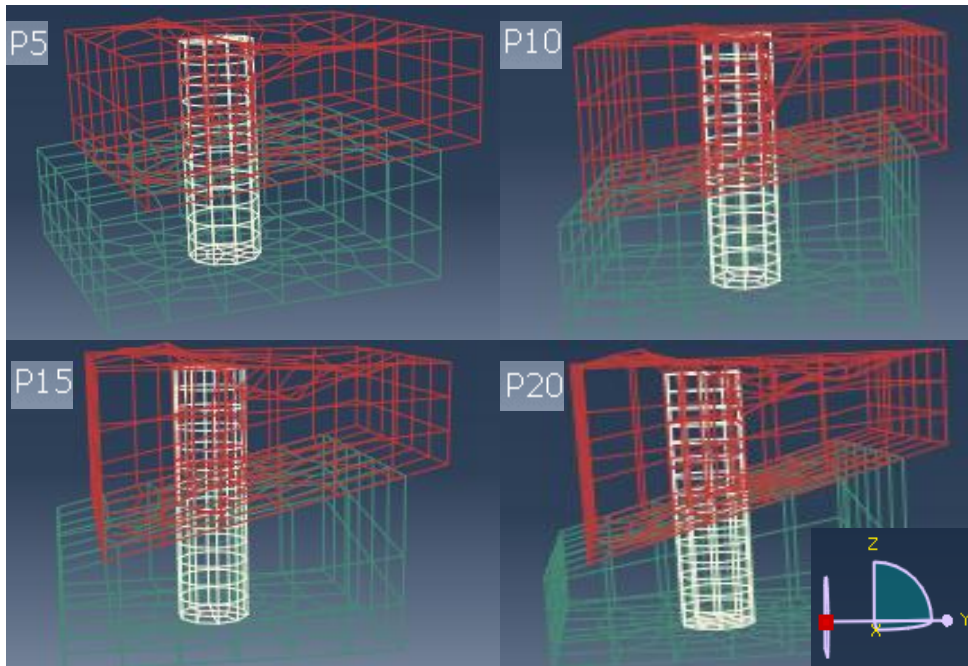
Figure 4.4 Deformed mesh of 70 mm diameter pervious concrete columns under 30kPa for positive slope failure surface with slope angles from 5° to 20°
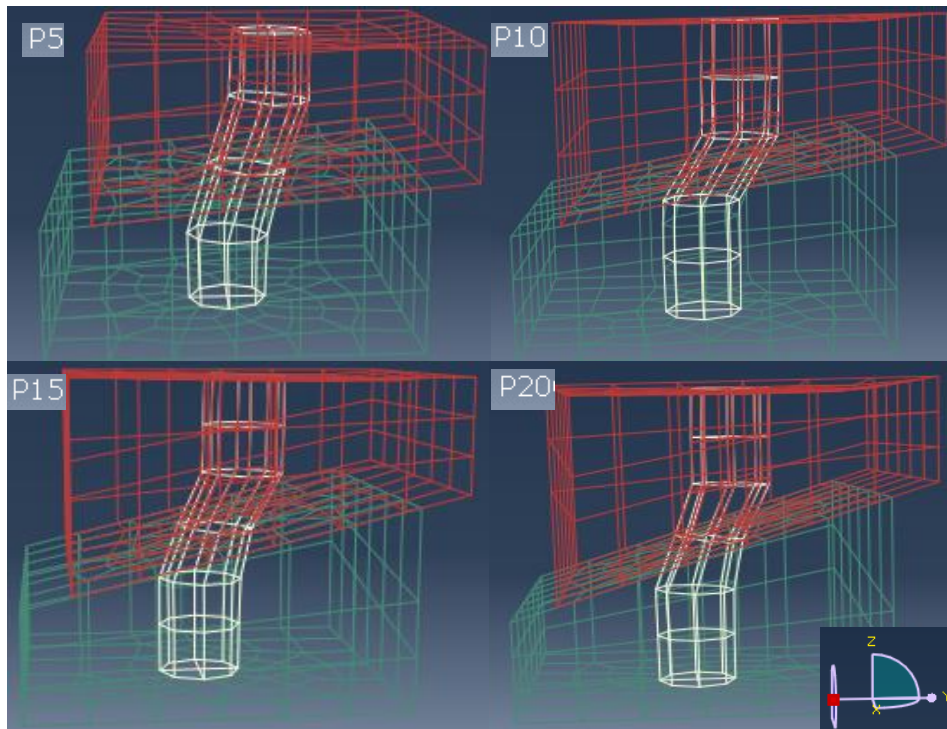
Figure 4.5 Deformed mesh of 70 mm diameter stone columns under 30kPa for positive slope failure surface with slope angles from 5° to 20°
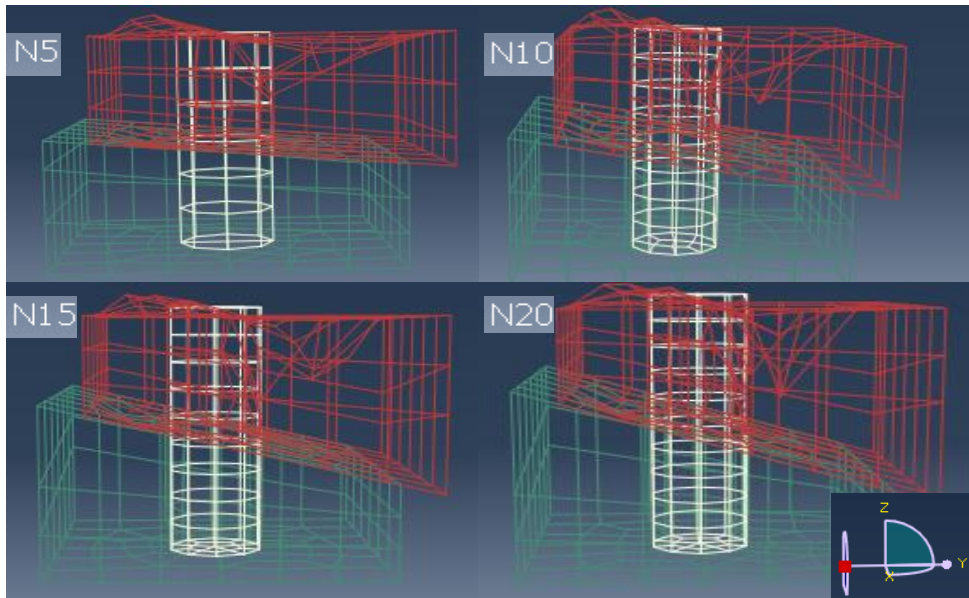
Figure 4.6 Deformed mesh of 90 mm diameter pervious concrete columns under 30kPa for negative slope failure surface with slope angles from 5° to 20°
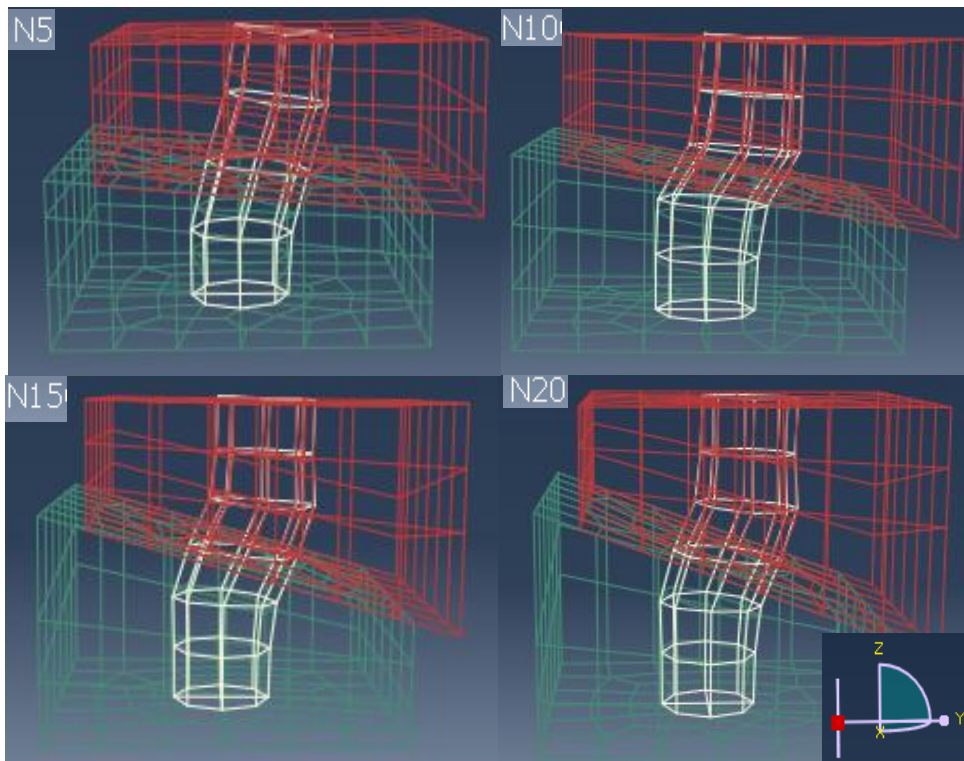
Figure 4.7 Deformed mesh of 90 mm diameter stone columns under 30kPa for negative slope failure surface with slope angles from 5° to 20°

4.3 RESULTS AND DISCUSSIONS

In the following graphs, the unimproved ground considered is represented as clay and improved ground with ordinary stone column and pervious concrete column are represented as OSC and PCC respectively.

4.3.1 Effect of normal pressure

Direct shear analysis of unimproved and improved ground was carried out by varying normal pressures ranging from 0 kPa to 75 kPa which corresponds to the embankment height from 0 m to 5 m for an embankment fill unit weight of 15 kN/m^3. The shear strength increased with increase in normal pressure for unimproved ground (clay), stone column improved ground and pervious concrete column improved ground as shown in Fig.4.8, Fig.4.9 and Fig.4.10 respectively.
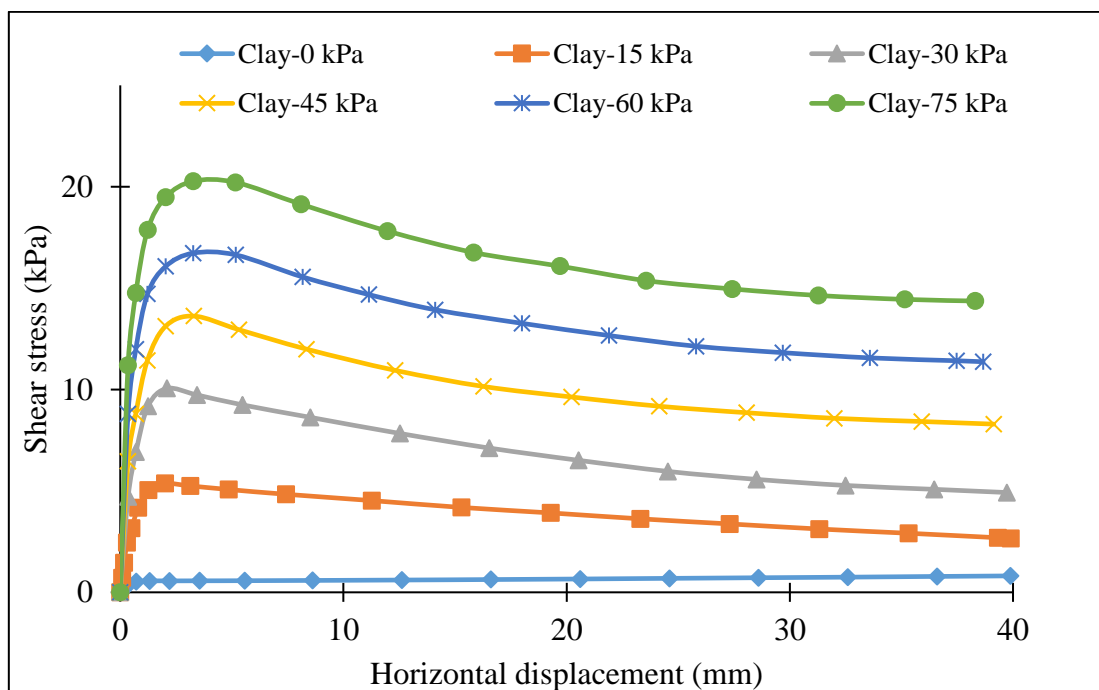
Figure 4.8 Effect of normal pressure on shear stress-displacement behaviour for unimproved ground
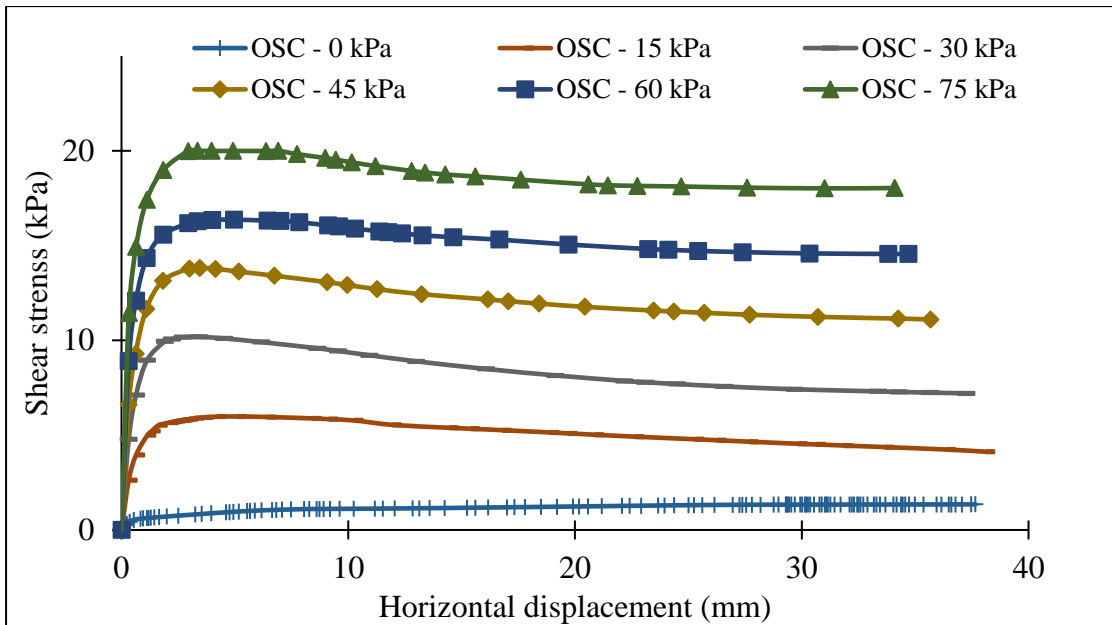
Figure 4.9 Effect of normal pressure on shear stress-displacement behaviour for stone column improved ground (OSC)
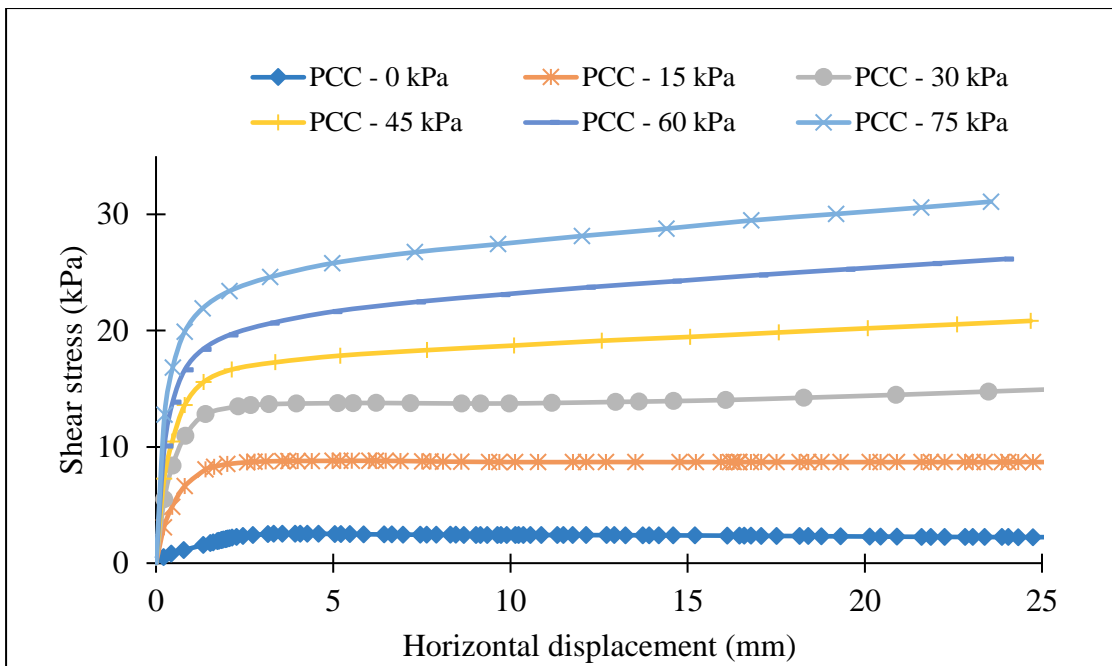
Figure 4.10 Effect of normal pressure on shear stress-displacement behaviour for pervious concrete column improved ground (PCC)

Figure 4.11 denotes shear stress-normal pressure variation of unimproved ground, ordinary stone column improved ground and pervious concrete column improved ground for 50 mm diameter column inclusion.
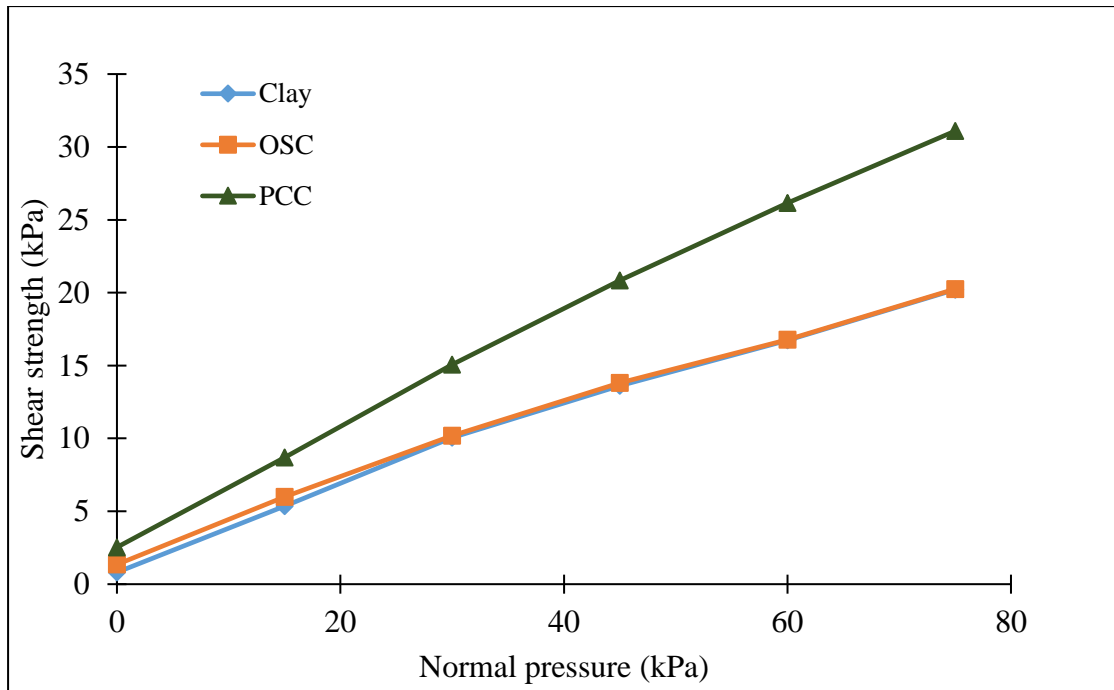
Figure 4.11 Effect of normal pressure on shear strength

Shear strength improvement at zero normal pressure for PCC is 87 % than OSC and this is significant for the columns placed beneath the toe of the embankment. The percentage of shear strength improvement for PCC are found to be 45%, 48%, 51%, 56% and 58% respectively for normal pressures ranging from 15 kPa to 75 kPa at an interval of 15 kPa. The increase of shear strength with normal stress is quite natural for soils, as the strength depends on the angle of internal friction through the normal stress. However, the pervious concrete mix similar to that of normal concrete with strength and stiffness has also contributed to the increase in shear strength of PCC improved ground. This study also indicates that the columns placed near the centerline of the embankment has a higher shear strength and the stone columns placed beneath the toe of embankment has less shear strength. The shear resistance beneath the toe of the embankment can be improved by providing pervious concrete columns.

4.3.2 Effect of reinforcement

Figure 4.12 and Fig.4.13 show the stress-strain behaviour of unimproved ground, ordinary stone column and pervious concrete column improved ground for normal pressures of 30 kPa and 75 kPa respectively. The diameter of column was 50 mm for both the respective analyses considered. The stone column improved ground has almost the same shear strength as that of clay alone as seen in Fig.4.12 and Fig.4.13. Therefore,

the ordinary stone column improved ground offers almost zero resistance as that of unimproved ground. The experimental results reported by Murugesan and Rajagopal (2009) also demonstrates this behaviour that the ordinary stone columns separated along the failure surface and moved along with the surrounding soil without offering any shear resistance.
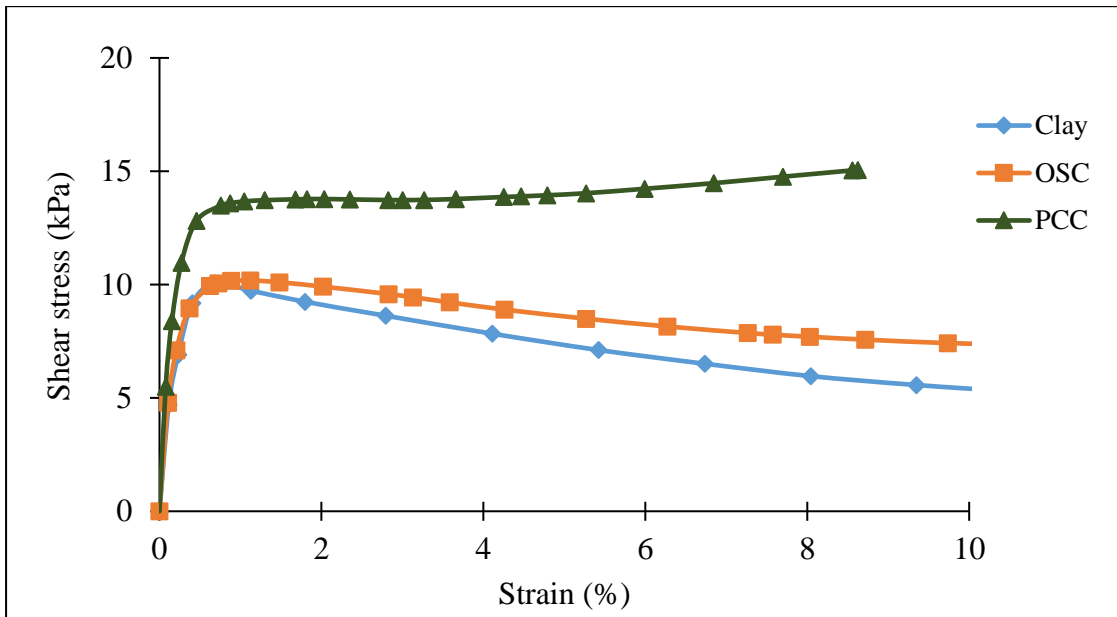
Figure 4.12 Effect of reinforcement (50 mm diameter columns under a normal pressure of 30 kPa)
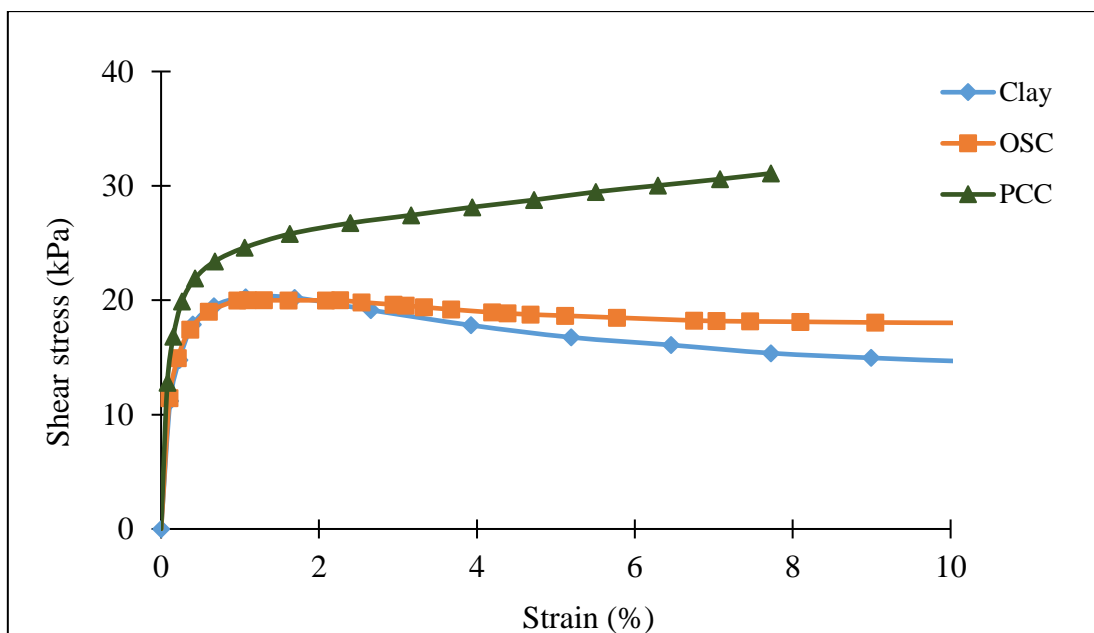
Figure 4.13 Effect of reinforcement (50 mm diameter columns under a normal pressure of 75 kPa)

The shear strength of pervious concrete column improved ground is 53% and 55 % more than unreinforced ground and stone column treated ground respectively for the normal pressure of 75 kPa. It is also observed that the shear resistance of pervious concrete improved ground linearly increases with increase in strain.

Figure 4.2 presents the undeformed and deformed mesh of stone column and pervious concrete improved ground respectively. The deformed mesh of stone column improved ground confirms the movement of stone column along the shear failure plane (Figure 4.2(a)), whereas the pervious concrete column has resisted the shear movement and behaviour of pervious concrete column is like a rigid pile (Figure 4.2(b)). This is attributed to the higher elastic modulus of pervious concrete material.

4.3.3 Effect of diameter

The effect of diameter of ordinary stone column and pervious concrete column was studied by varying column diameters as 50 mm, 70 mm and 90 mm. From Fig.4.14 and Fig.4.15, it can be noted that the shear strength of improved ground with ordinary stone column and pervious concrete column increased with increase in diameter. However, the shear strength improvement in ordinary stone column improved ground is only marginal as shown in the Fig.4.15 for normal pressure of 75 kPa. Generally, in higher diameter stone columns, bigger aggregate sizes are used. But this is not considered in the present study and this could be the reason for the marginal variation of shear strength in 50 mm, 70 mm and 90 mm diameter stone column reinforced ground.

In the case of pervious concrete improved ground, 90 mm column showed higher shear strength and has 15% and 34% improvement than 70 mm and 50 mm columns respectively under a normal pressure of 75 kPa. This improvement can be credited to the circumferential resistance offered by the rigid pervious concrete columns. It is also observed that the shear improvement with increase in diameter has an influence of normal pressure. The normal pressure below 45 kPa shows more improvement for larger diameter columns than with higher normal pressures for pervious concrete column improved ground. From Fig.4.16 and Fig.4.17, it is found that at low normal pressures, the shear stress ratio (defined as the ratio of maximum shear stress to applied normal pressure) increases with increase in diameter of stone column. However, at higher normal pressures, the increase of shear stress ratio is not observed and seems to be a marginal increase with increase in diameter. A smaller diameter pervious concrete

column could be provided beneath the toe of the embankment for improving the shear performance of stone column supporting embankment system.

The shear stress ratio values of 50 mm, 70 mm and 90 mm diameter column improved ground for varying normal pressures (0 kPa to 75 kPa) are given in Table AI-1, in Annexure.
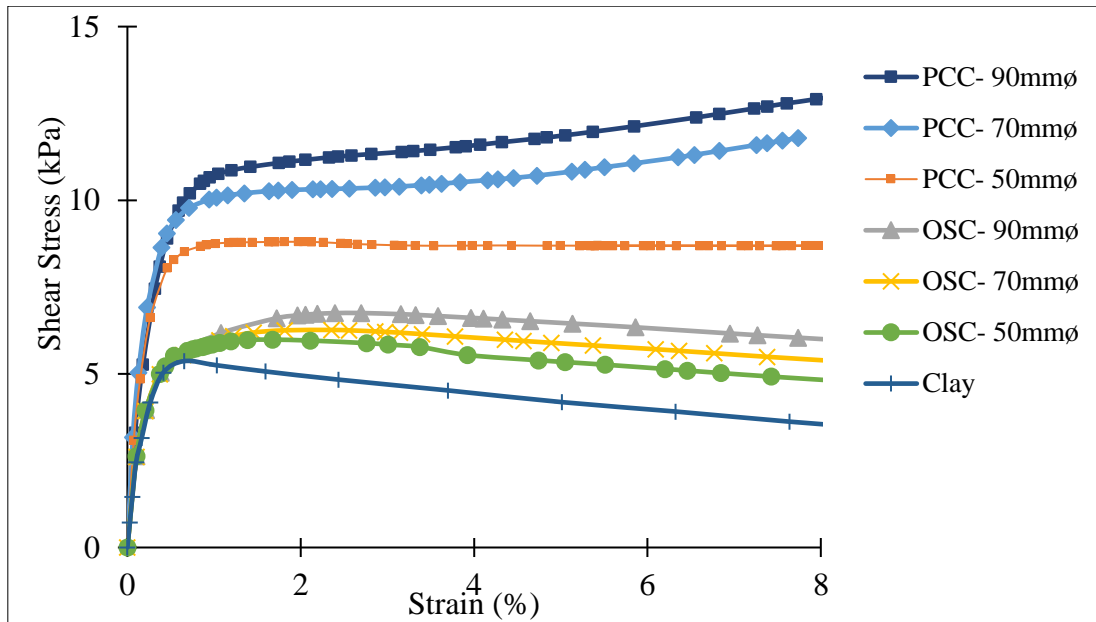
Figure 4.14 Effect of diameter of columns for a normal pressure of 15 kPa
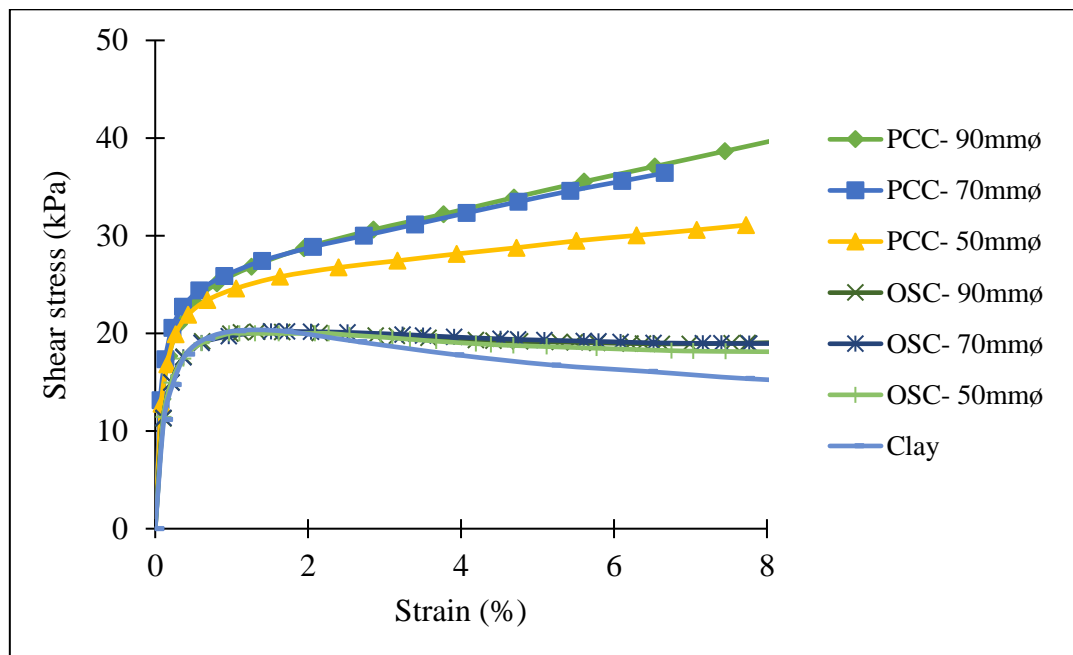
Figure 4.15 Effect of diameter of columns for a normal pressure of 75 kPa
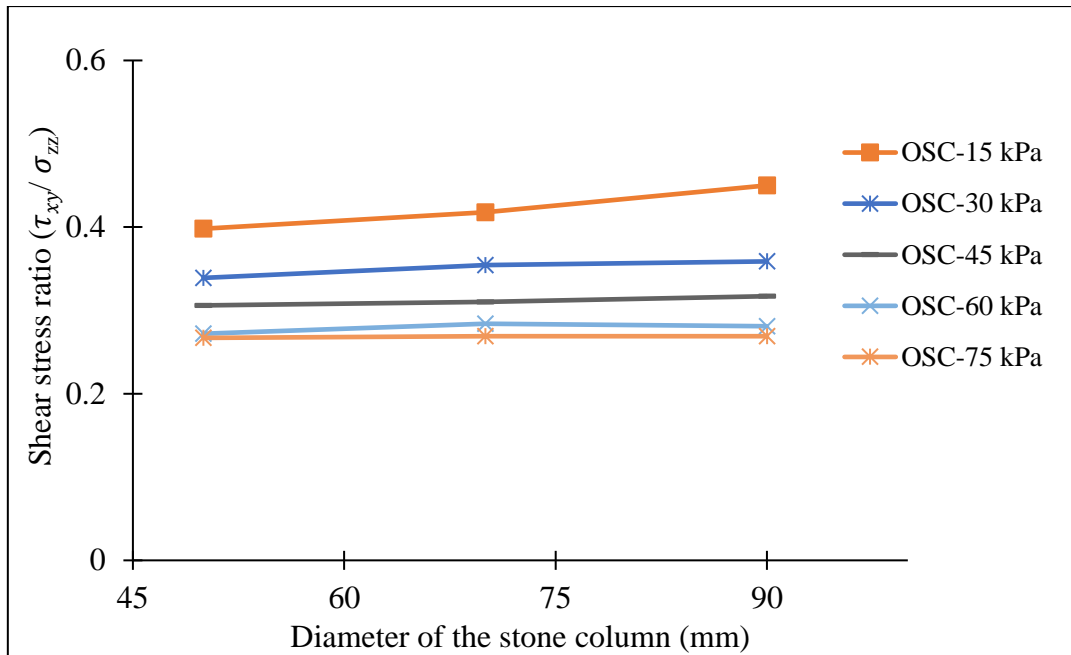
Figure 4.16 Effect of diameter of stone columns on shear stress ratio
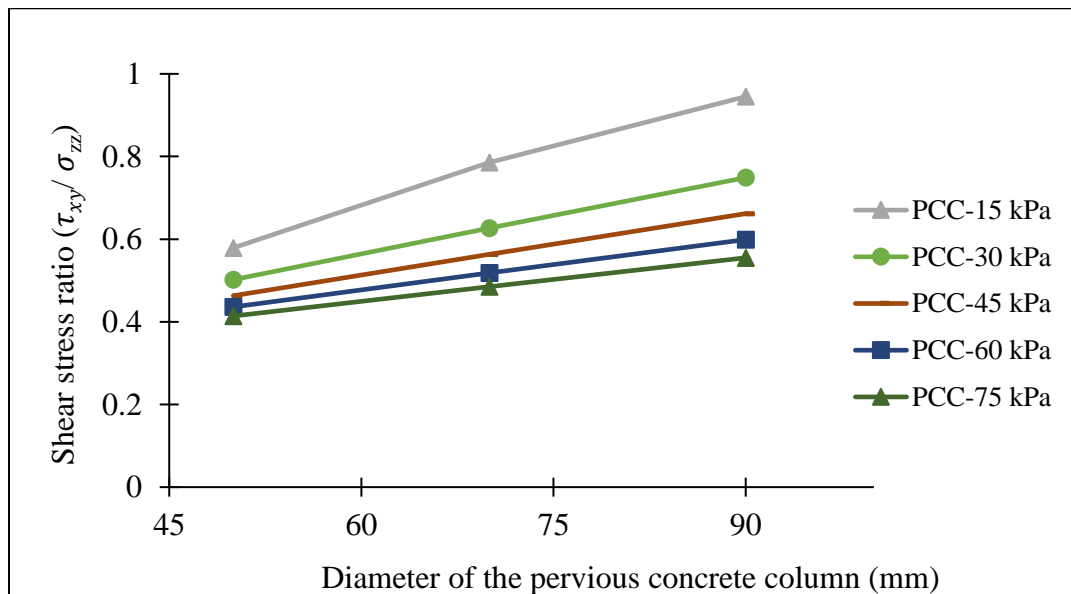
Figure 4.17 Effect of diameter of pervious concrete columns on shear stress ratio

4.3.4 Effect of inclination

To simulate the actual field situation, negative and positive inclinations of planar shear failure surface with horizontal was analyzed by varying the inclinations from 5° to 20°. The deformed model after analyses is as shown in Fig.4.4 and Fig.4.5 for positive inclinations for pervious concrete column improved ground and stone column improved

ground respectively. Figure 4.6 and Fig.4.7 show the deformed pervious concrete column and stone column for negative inclinations, respectively.

It is found that the shear strength of positive slope increased with increase in slope angle as shown in Fig.4.18, Fig.4.19 and Fig.4.20 which are representative graphs for unimproved ground, stone column improved ground and pervious concrete column improved ground. Figure 4.18, Fig.4.19 and Fig.4.20 also show the variation of negative slope and clearly indicates that the shear strength decreases with increase in slope angle. The above observation is found to be true for all the cases studied. The increase in shear strength for positive slope is due to the shear resistance offered by the soil slope itself i.e., shear resistance from within the ground slope. Whereas in negative slope, the shear resistance offered by the slope itself is less against movement and reduced shear strength is observed for all negative slopes. It can be established that the approximation made in the horizontal direct shear test has a demerit of predicting the actual shear strength with respect to positive and negative shear surface inclinations with horizontal. Also, it is noted that the shear strength of negative inclinations only in the case of pervious concrete column improved ground is almost same as that of with zero slope angle as shown in Fig.4.20. However, the shear performance of PCC improved ground is found to be better than SC improved ground for all the surface inclinations considered.
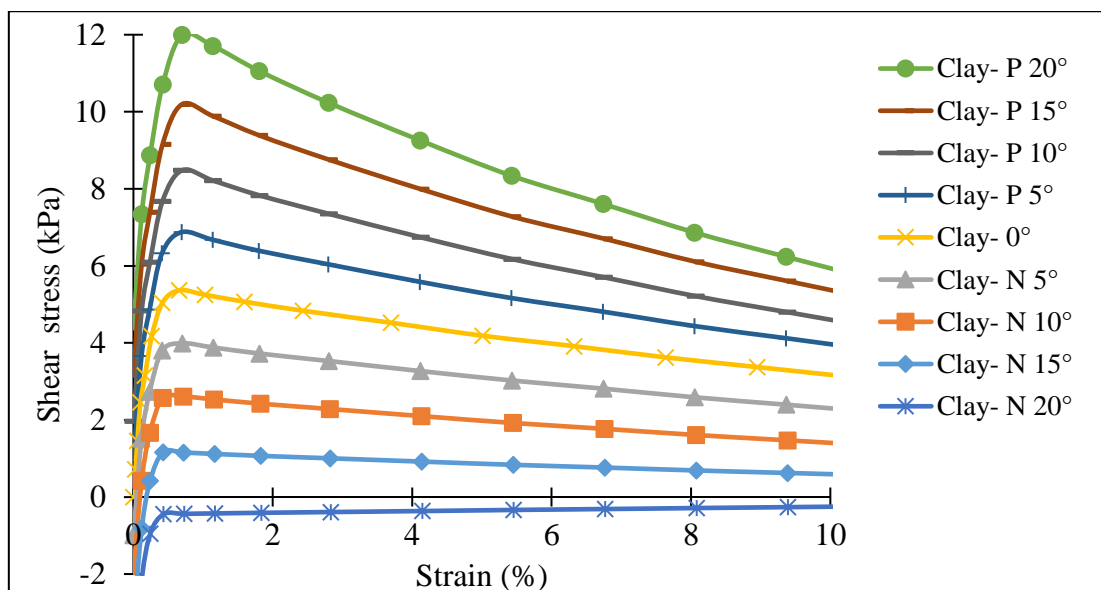
Figure 4.18 Effect of inclination of shear surface on unimproved ground for a normal pressure of 15 kPa
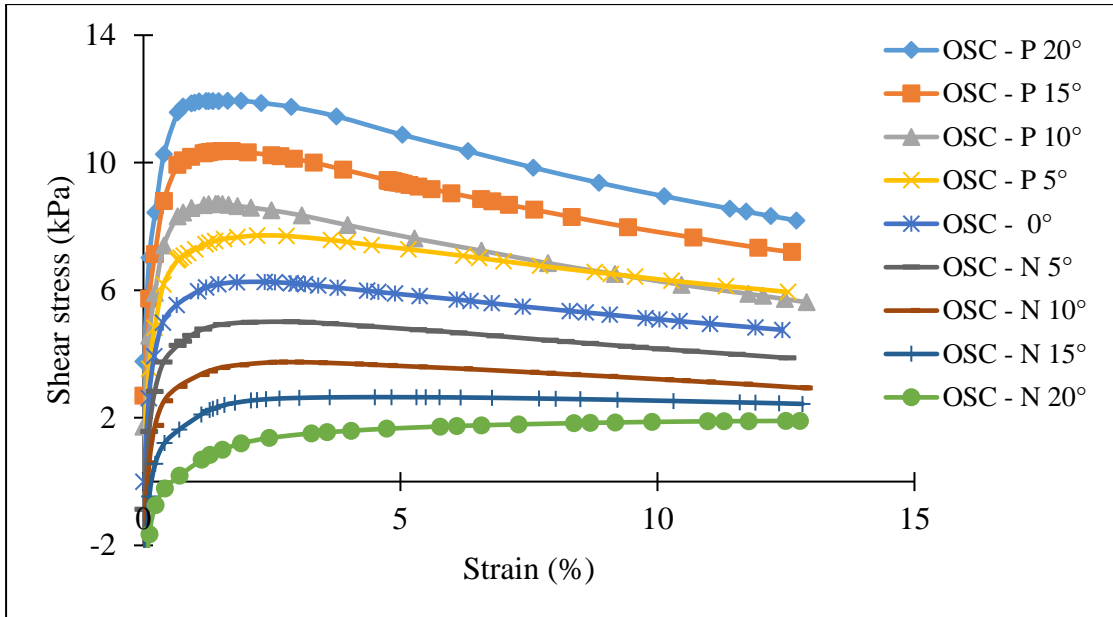
Figure 4.19 Effect of inclination of shear surface on ordinary stone column improved ground (70 mm diameter column and normal pressure of 15 kPa)
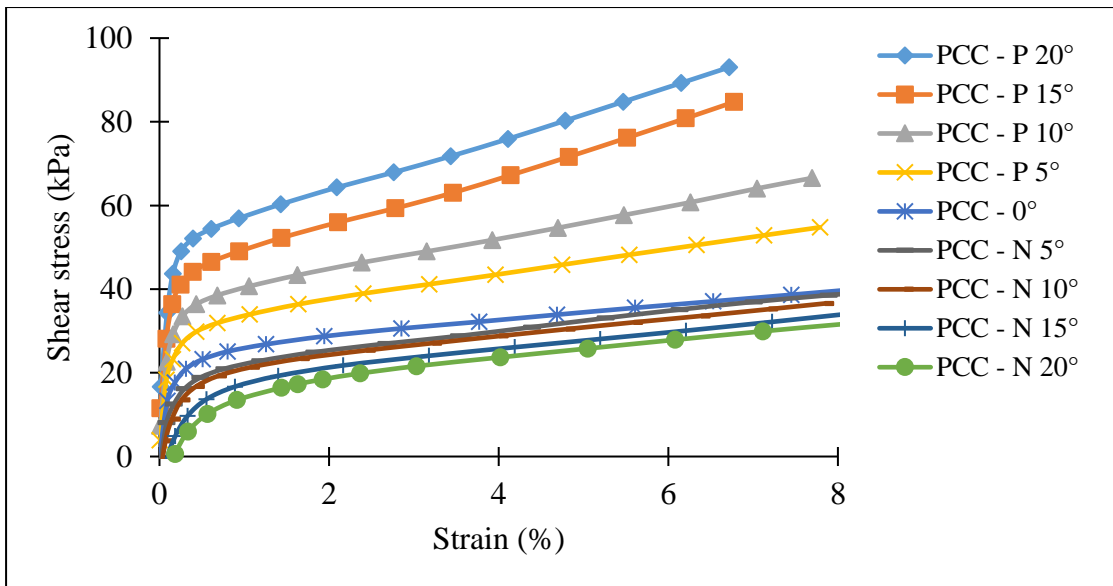
Figure 4.20 Effect of inclination of shear surface on pervious concrete column improved ground (90 mm diameter column and normal pressure of 15 kPa)

The variation of shear stress ratio with positive and negative inclination is almost linear for unimproved ground, stone column improved ground and pervious concrete column improved ground as depicted in Fig.4.21, Fig.4.22 and Fig.4.23 respectively. It is noticed that the slope of shear plane plays an important effect in the shear strength estimation and slope effect needs to be taken into account.
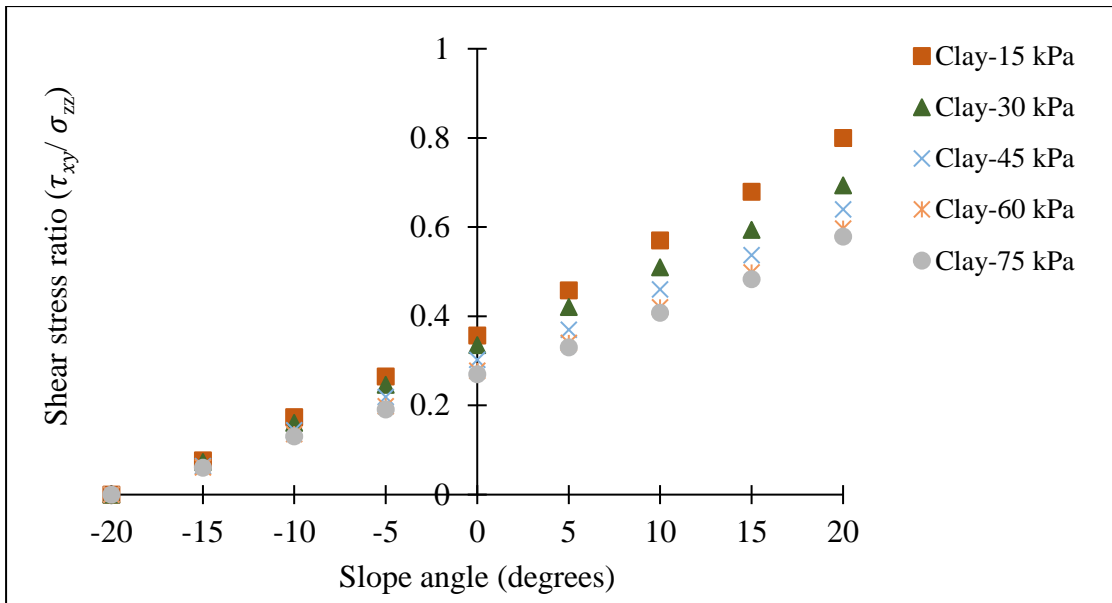
Figure 4.21 Effect of inclination of shear surface on shear stress ratio for unimproved ground
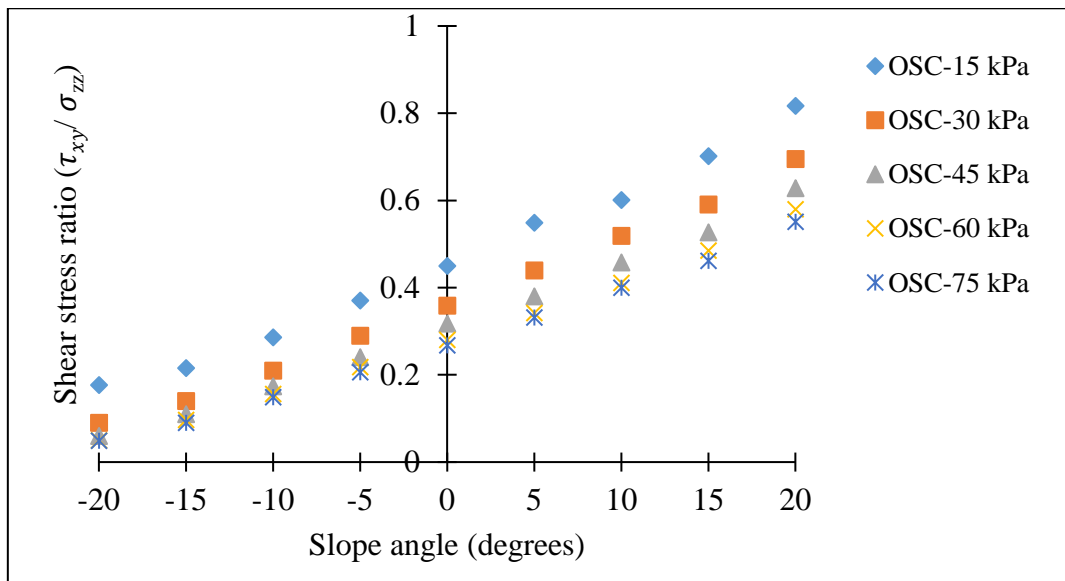
Figure 4.22 Effect of inclination of shear surface on shear stress ratio for stone column improved ground
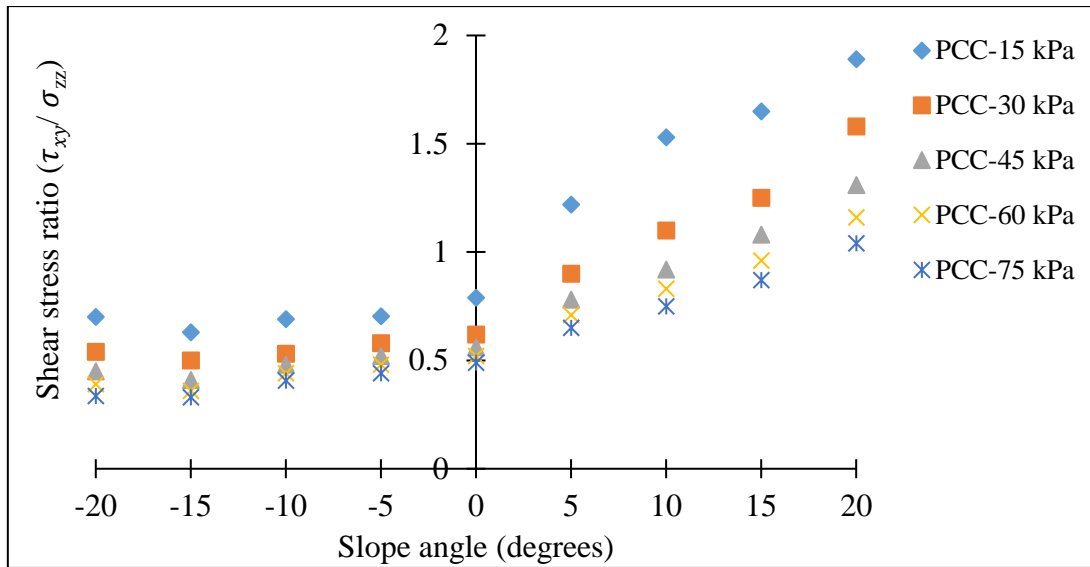
Figure 4.23 Effect of inclination of shear surface on shear stress ratio for pervious concrete column improved ground

The shear stress ratio values of 50 mm, 70 mm and 90 mm diameter column improved ground for varying inclination of shear surfaces ranging from P 20° to N 20° under normal pressures of 15 kPa to 75 kPa is tabulated in Table AI-1, 2, Table AI-3 and Table AI-4 respectively.

4.4 NON-LINEAR BEHAVIOUR OF PERVIOUS CONCRETE

In the direct shear model analysis, the pervious concrete material was modelled with linear elastic properties. In order to verify the direct shear analysis results of PCC improved ground modelled with the linear elastic model, Mohr-Coulomb constitutive model was selected as the non-linear model. The cohesion and angle of friction of PCC material were selected as 3000 kPa and 38° respectively. The interface friction coefficient used for PCC- clay interface was 0.521, which is $\frac{2}{3} \tan \emptyset_{pcc}$, where $\emptyset_{pcc}$ is the angle of internal friction of pervious concrete. An improved ground with PCC of diameter 50 mm under the normal pressure of 30 kPa was used to compare the shear stress-strain behaviour and deformation pattern. Figure.4.24 shows the shear stress-strain variation of PCC improved ground with linear and non-linear material models. It can be seen that there is similarity between the results with both of these material models. Also, the deformed shape of the PCC after the direct shear analysis was also found to be similar as shown in Fig.4.25. Therefore, the use of linear-elastic material model is justified.
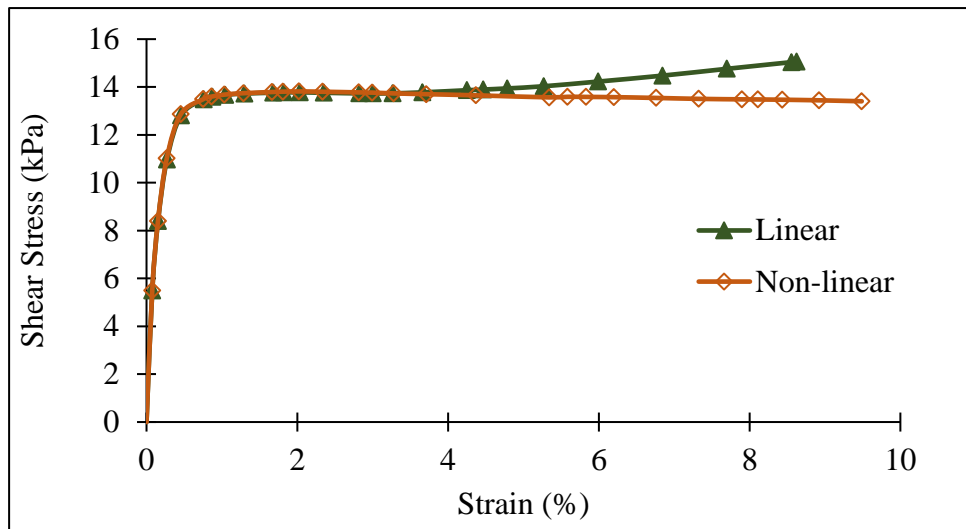
Figure 4.24 Shear stress-strain behaviour of PCC improved ground using linear-elastic and non-linear models

(a) Linear model   (b) Non-linear model
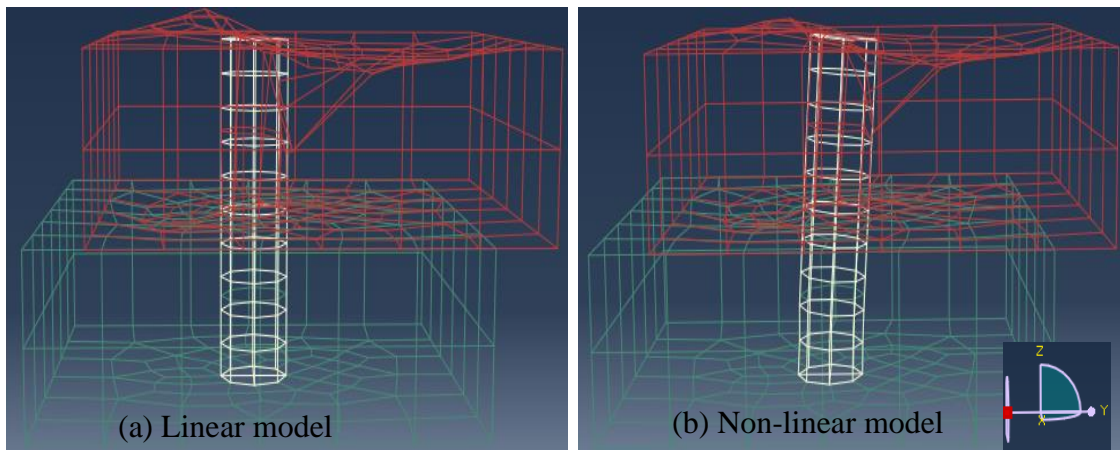
Figure 4.25 Deformed model of PCC improved ground using (a) Linear-elastic model (b)Non-linear model

4.5 SUMMARY

In this chapter, an attempt has been made to understand the shear behaviour of stone column and pervious concrete column improved ground. Following conclusions are made from numerical analysis of direct shear test models and inclined direct shear test models. The shear resistance of unimproved ground, stone column improved ground and pervious concrete column improved ground increases with increase in normal pressure. The shear strength of pervious concrete column improved ground with zero normal pressure is significant and could be implemented for a better shear performance

of stone column supported embankment system by placing pervious concrete columns beneath the toe of the embankment.

The pervious concrete column improved ground has higher shear strength than stone column improved ground for all the diameters considered. It is also observed that the shear resistance of ordinary stone column improved ground is almost zero. The shear resistance of pervious concrete column improved ground and stone column improved ground increased with increase in diameter.

Improved ground with positive slope angle has higher shear resistance than horizontal shear surface. The shear strength of positive slope increases with increase in slope angle, whereas for improved ground with negative slope, shear strength decreases with increase in slope angle. It is also recommended to consider the slope effect while determining shear strength.

CHAPTER 5

SHEAR BEHAVIOUR OF PERVIOUS CONCRETE COLUMN IMPROVED GROUND USING LARGE SHEAR TEST MODELS

In this chapter, the shear response of end-bearing and floating pervious concrete column improved ground is addressed and compared with stone column improved ground. Numerical modelling using ABAQUS software was used for analyzing improved ground with column inclusions. Large shear test models were analyzed, and details are mentioned in the subsequent sections.

5.1 LARGE SHEAR TEST MODEL

The depth of direct shear test model is 200 mm, and it cannot be used for studying the shear resistance of floating columns. Therefore, to overcome this depth limitation in the shear test model and to study the effect of depth of columns in shear performance, large shear test tank (with a depth of 600 mm) developed by Murugesan and Rajagopal (2009) was used. The experimental results carried out by Murugesan and Rajagopal (2009) using large shear test tank was used for validating the model generated in ABAQUS software. The large shear test selected for validation was of reinforced clay with ordinary stone column of diameter 75 mm placed at a clear gap of 50 mm from the edge of the loading plate (Fig 3.3). In the validation results as presented in Fig.5.1., experimental and numerical model results of original ground with stone column is shown in terms of pressure-settlement response and heave profile.

Strain controlled loading was applied to the full width of the tank, thus inducing lateral soil movements in the soil within the tank. The loading plate as shown in Fig.3.3 was given a uniform vertical displacement of 50 mm and the shear resistance of unimproved ground, stone column improved ground and pervious concrete column improved ground were studied. The shear performance of improved ground was measured in terms of pressure-settlement response on the loading plate. The study was extended to floating pervious concrete column for varying depths of 2D, 4D, 6D and 8D, where D is the diameter of column considered. The shear performance of floating columns was compared with end-bearing columns and conclusions are drawn. The analysis programme for large shear test is given in Table 5.1.
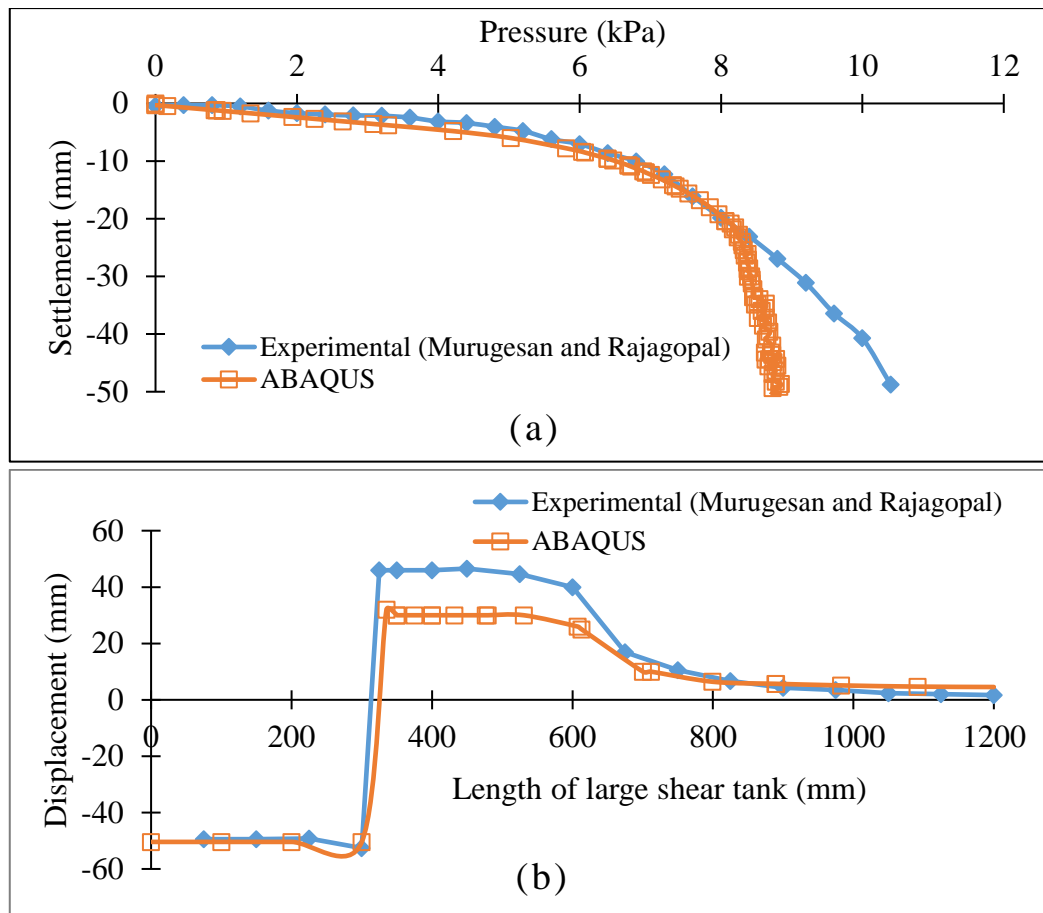
Figure 5.1 Validation of model (a) Pressure-settlement response of loading plate (b) Heave profile

Figure 5.2 and Fig.5.3 show the deformed models of pervious concrete column and stone column improved ground respectively under shear movement. The depth of column considered is 6D. Fig.5.4 and Fig.5.5 show the shear resistance of stone column and pervious concrete column improved ground with end-bearing condition respectively. It is very clear from Fig.5.5 that the end-bearing pervious concrete column has superior shear resistance than floating pervious concrete columns. The end-bearing stone column improved ground exhibits very little resistance and seemed to be moving along the shear direction as shown in Fig.5.4. However, the deformation of pervious concrete column is found to be similar to that of a rigid pile (Fig.5.5). The shear resistance of two pervious concrete column group arrangement is shown in Fig.5.6. It is seen that the two- pervious concrete column group has arrested the soil movements and the performance can be compared to that of a rigid pile.

62

Table 5.1 Analysis programme for large shear test

Description	Diameter (mm)	Clear gap between loading plate edge and column (mm)	No of columns	Depth of columns				
				End-bearing	Floating-8D	Floating-6D	Floating-4D	Floating-2D
Original ground								
Improved ground with stone columns	50	50	1	✓				
	70	50	1	✓				
	90	50	1	✓				
Improved ground with pervious concrete columns	50	50	1	✓	✓	✓	✓	✓
		50	2	✓				
	70	50	1	✓	✓	✓	✓	✓
		50	2	✓				
		100	1	✓	✓	✓	✓	✓
	90	50	1	✓		✓	✓	✓
		50	2	✓				

Figure 5.2 Deformed model of single pervious concrete column improved ground (Diameter (D) 70 mm and 6D depth)
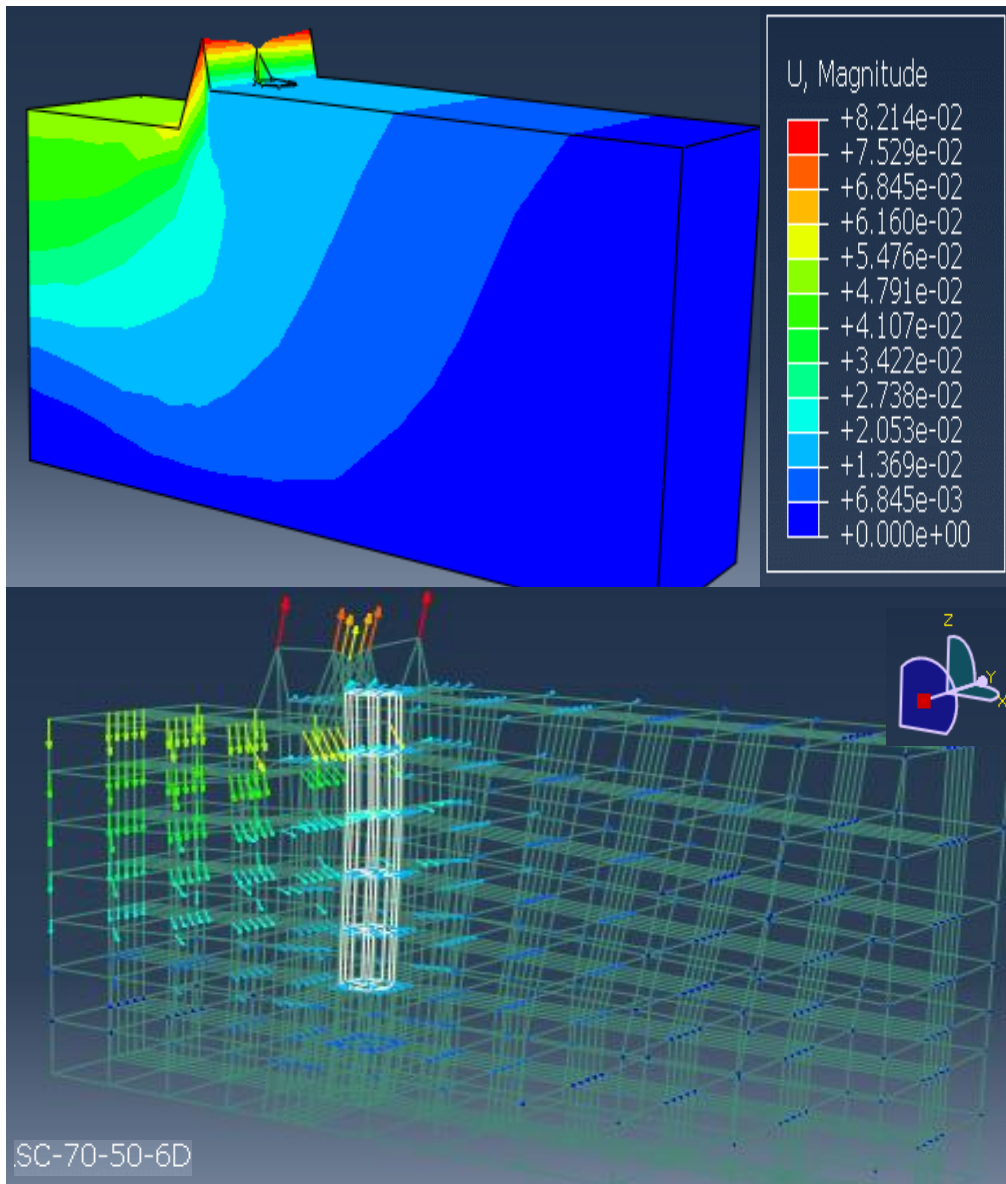
Figure 5.3 Deformed model of single stone column improved ground (Diameter (D) 70 mm and 6D depth)
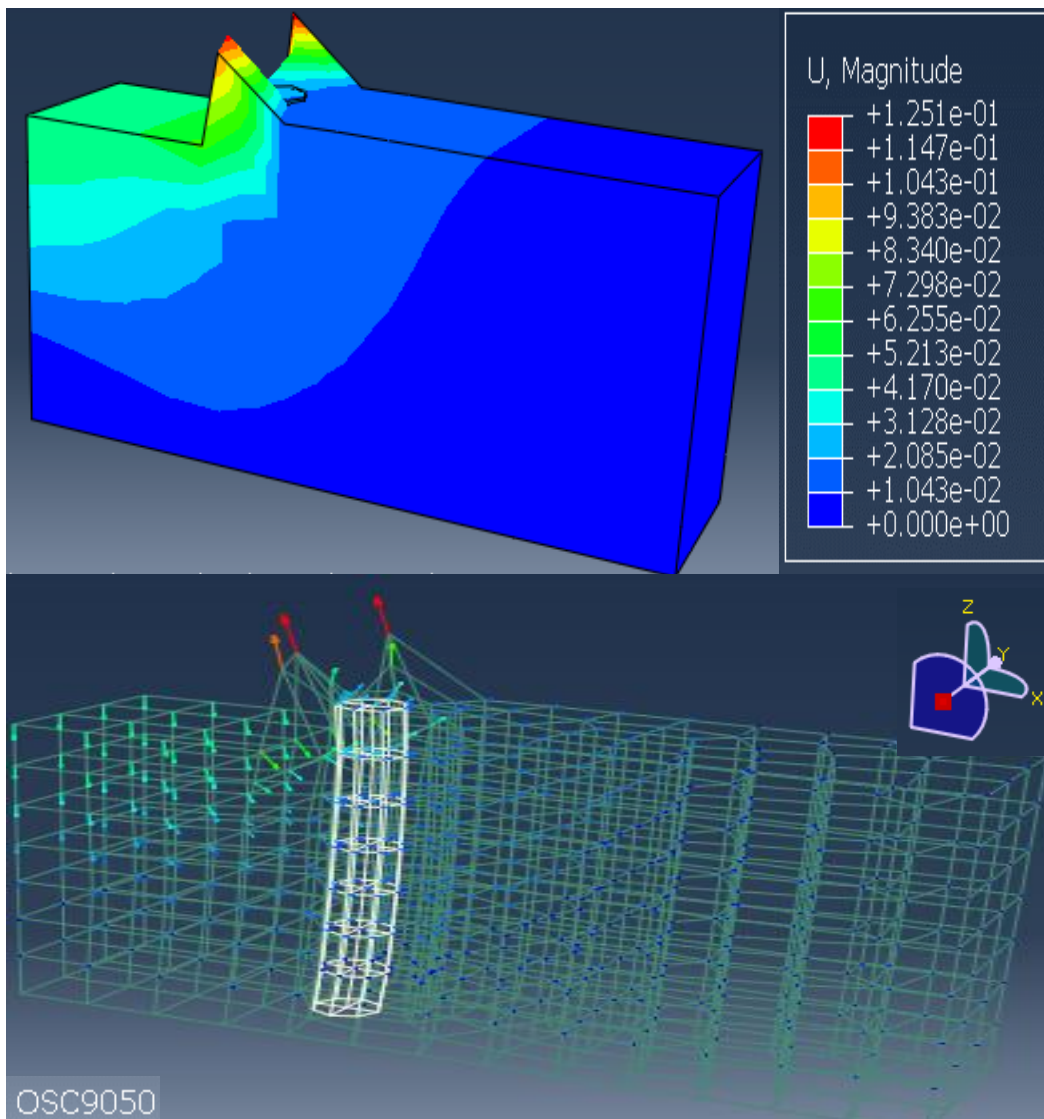
Figure 5.4 Deformed model of single stone column improved ground (Diameter 90 mm with end bearing condition)
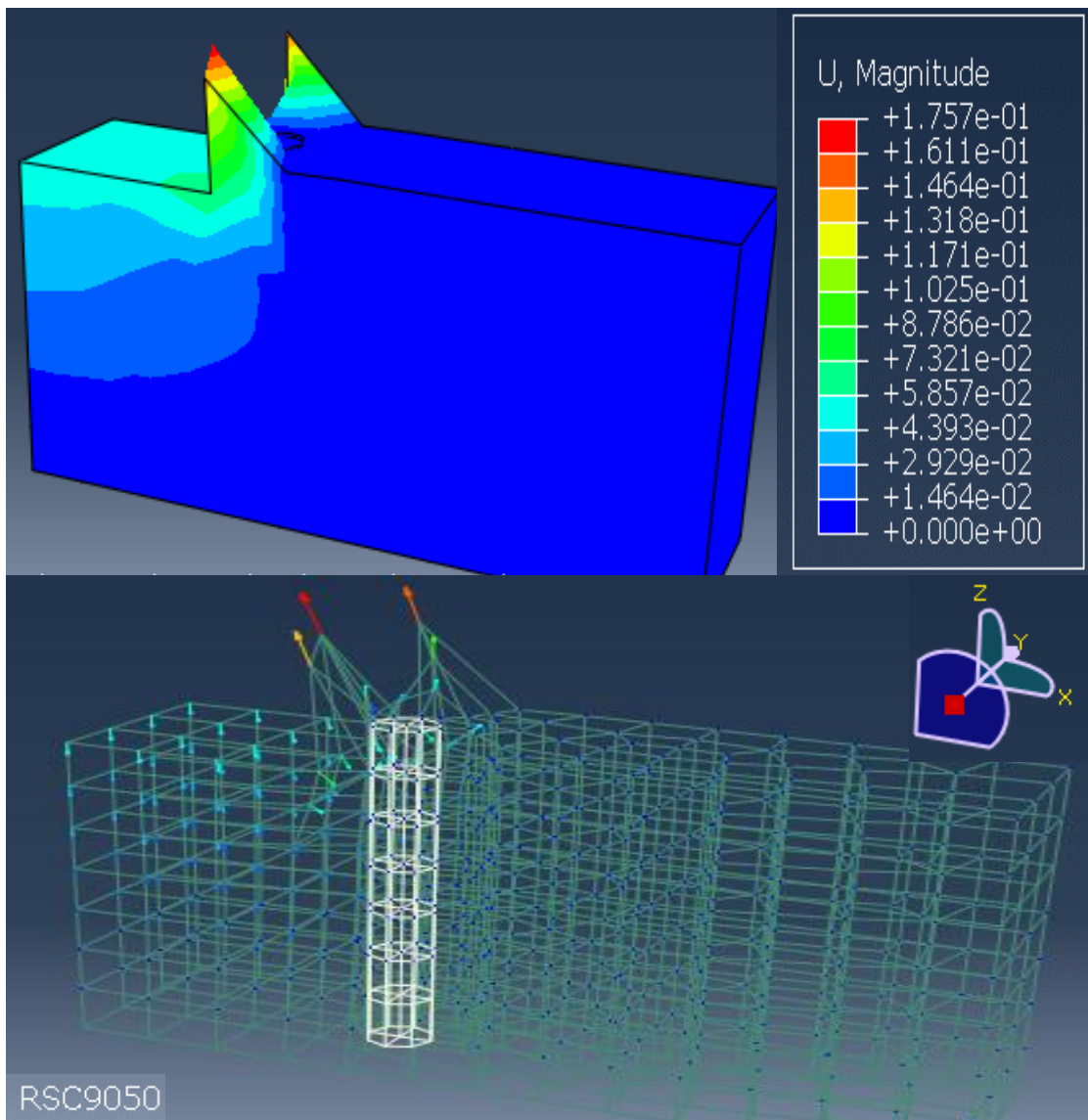
Figure 5.5 Deformed model of single pervious concrete column improved ground (Diameter 90 mm with end bearing condition)
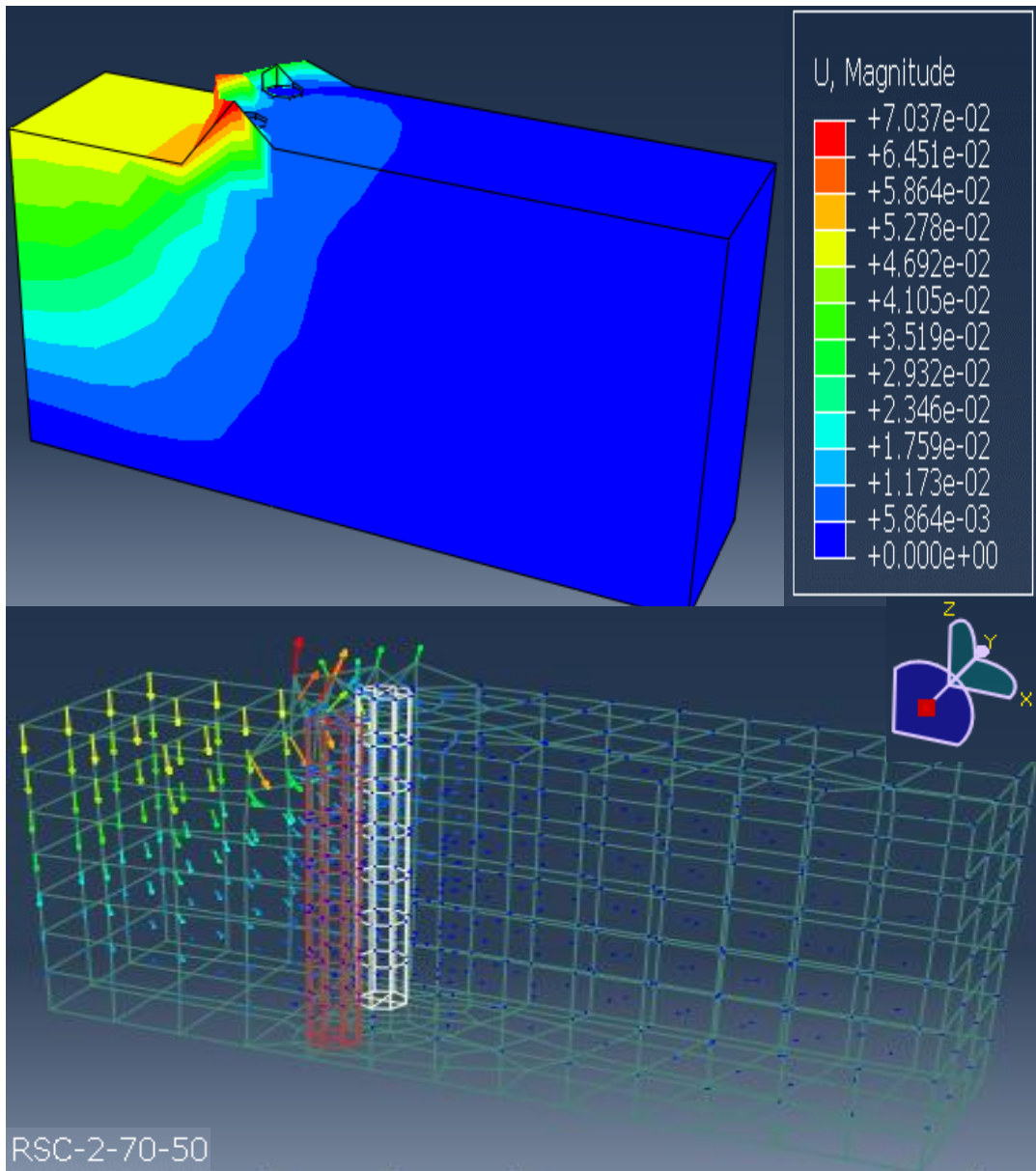
Figure 5.6 Deformed model of two pervious concrete column group improved ground (Diameter 70 mm with end bearing condition)

5.2 RESULTS AND DISCUSSIONS

The results of large shear test analyses are discussed in the following subsections.

5.2.1 Effect of pervious concrete column

The pressure-settlement (pressure on loaded plate) response of original ground, stone column improved ground and pervious concrete column improved ground were compared. Figure.5.7 shows the pressure-settlement response of original ground, ordinary stone column and pervious concrete column improved ground. The diameter of column considered was 90 mm. The end bearing columns were placed at a clear distance of 50 mm from the loading plate. From Fig.5.7, it is noted that the inclusion of pervious concrete column has increased the pressure on loading area when compared to conventional stone column. The pervious concrete column has higher modulus of elasticity and thereby the improved ground exhibits higher shear resistance than ordinary stone columns.
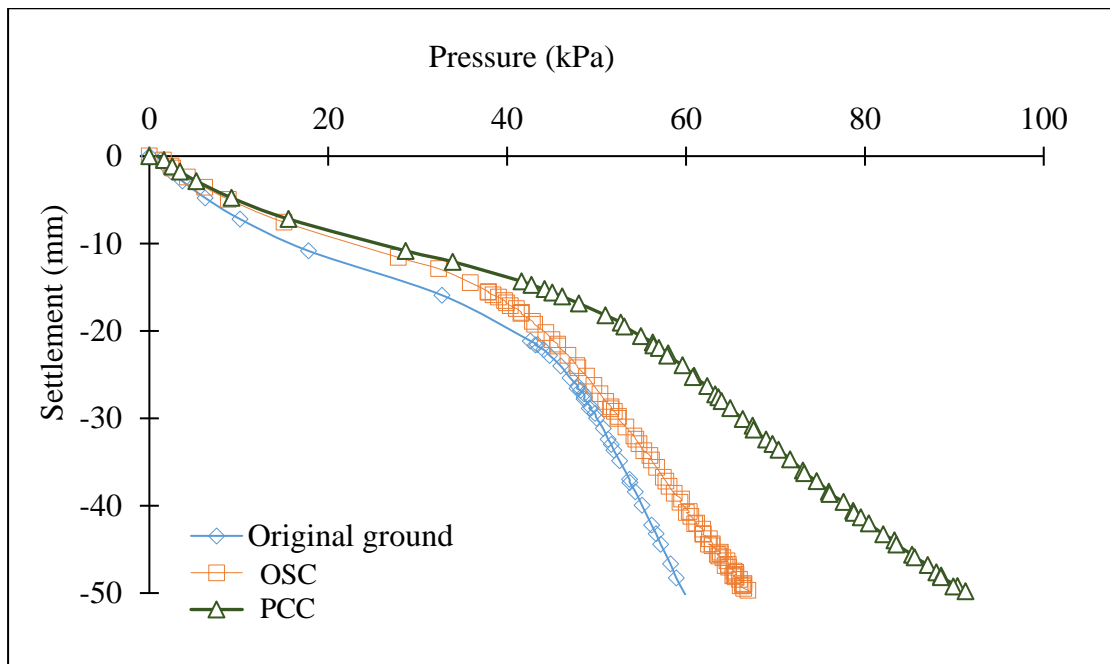
Figure 5.7 Effect of pervious concrete column using large shear test model

5.2.2 Effect of diameter

Figure 5.8 shows pressure-settlement response of original ground, stone column improved ground, pervious concrete column improved ground of column diameters 50 mm, 70 mm and 90 mm respectively. The columns were placed at a clear distance of 50 mm from the edge of the loading plate. The pressure-settlement response of stone column improved ground increased with increase in diameter of the columns, but the

variation is not significant. This could be attributed to the same aggregate property being used for 50 mm, 70 mm and 90 mm stone columns, even though in practical situations larger aggregate size is used for larger diameter columns.

The shear resistance of pervious concrete column improved ground has an improvement of 62%, 53% and 46% respectively for 90 mm, 70 mm and 50 mm diameter columns when compared to original ground. This clearly indicates that a larger diameter pervious concrete column improved ground exhibits better shear resistance than original ground.
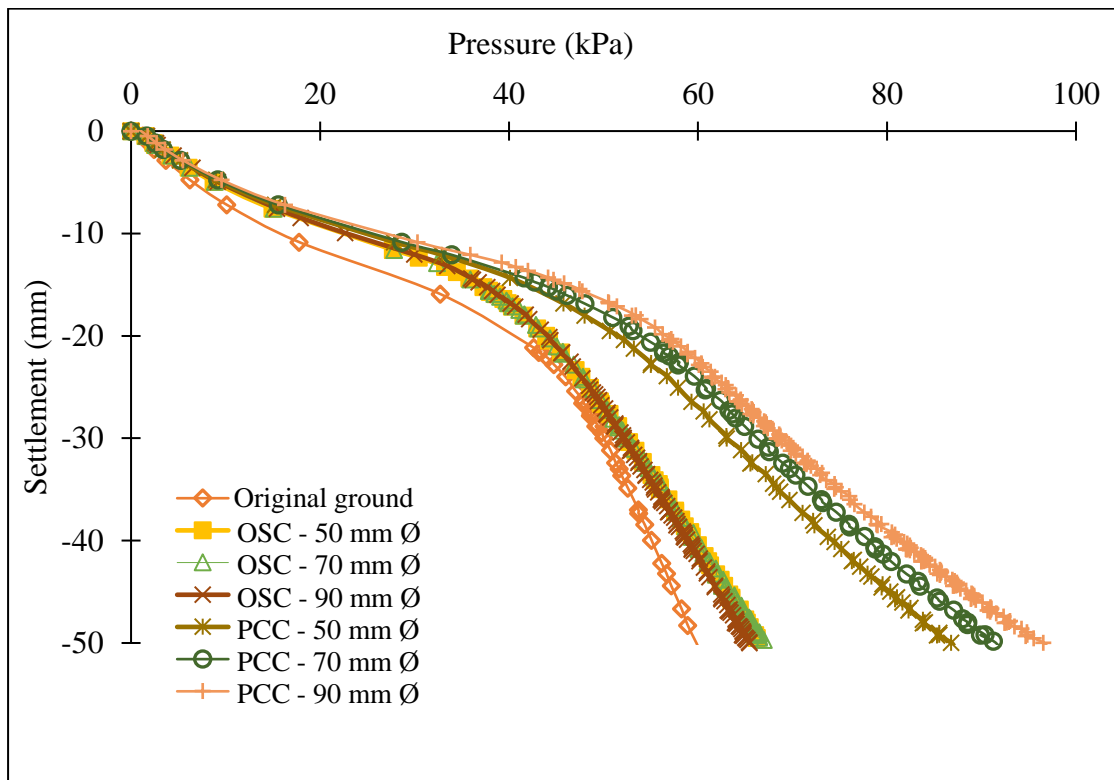
Figure 5.8 Effect of diameter of column

5.2.3 Effect of depth of column

To study the effect of depth of pervious concrete columns, the depth of column was varied as 2D, 4D, 6D, 8D for 70 mm diameter columns placed at 100 mm from the edge of loading area. End bearing pervious concrete columns placed at distances of 50 mm and 100 mm from the edge of loading area were also analyzed for comparison and results are presented in Fig.5.9. The pervious concrete column placed at a clear gap of 50 mm has shown better shear performance than the column placed at 100 mm clear gap. This is because of increased pressure on loading area due to the placement of column nearer to the loading area.

It is observed that the performance of improved ground with floating pervious concrete column of varying depth from 2D to 8D is such that there is no increase in pressure by increasing the length of pervious concrete floating column from 2D to 8D. The performance of end bearing pervious concrete column is found to be significantly higher than floating columns as shown in Fig.5.9 and, therefore, it is suggested to provide full depth of pervious concrete columns up to bearing strata for achieving better shear performance.
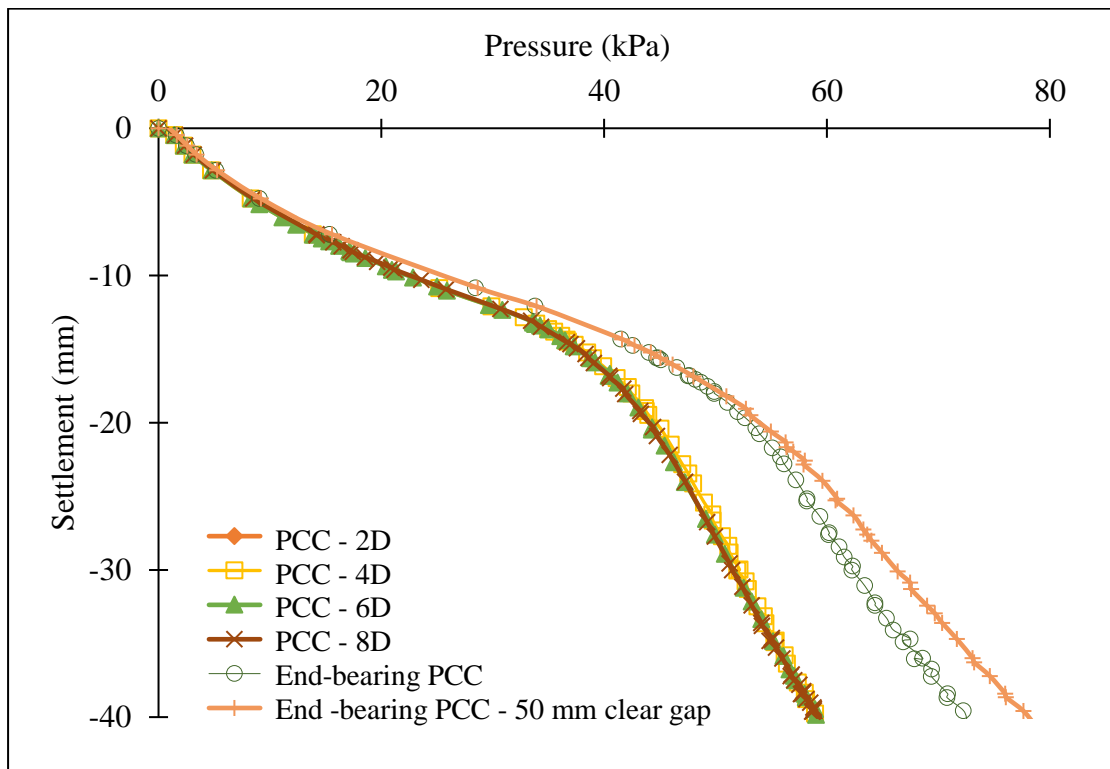
Figure 5.9 Effect of depth of pervious concrete columns

5.2.4 Effect of number of columns

The performance of two pervious concrete column group improved ground was compared with single pervious concrete column and ordinary stone column improved ground. The diameter of column considered was 70 mm and end bearing columns were analyzed. The results are presented in Fig.5.10. The improvement of weak ground with two pervious concrete column group, single pervious concrete column, and single stone column are 108%, 53% and 12% respectively. It is found that two pervious concrete column group has more shear resistance than single pervious concrete column improved ground.
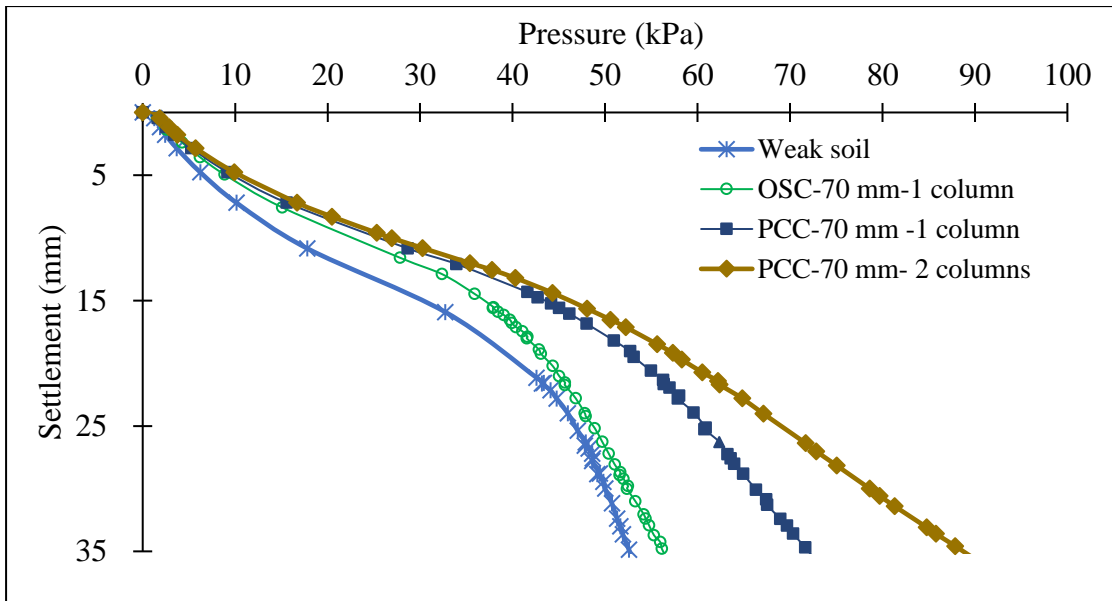
Figure 5.10 Effect of number of pervious concrete columns on shear resistance

5.2.5 Lateral deformation of columns

Figure 5.11 shows the lateral deflection of pervious concrete columns with that of ordinary stone columns. The lateral deflection at the top end of pervious concrete column is very less than that of stone column. The study was conducted for three diameters of 50 mm, 70 mm and 90 mm columns. The end-bearing columns were placed at a clear distance of 50 mm from the edge of loading plate.

The lateral defection at the top end of stone columns for all the three diameters have almost similar pattern. However, the lateral deflection of 90 mm pervious concrete column is lesser than that of 70 mm and 50 mm diameter columns.
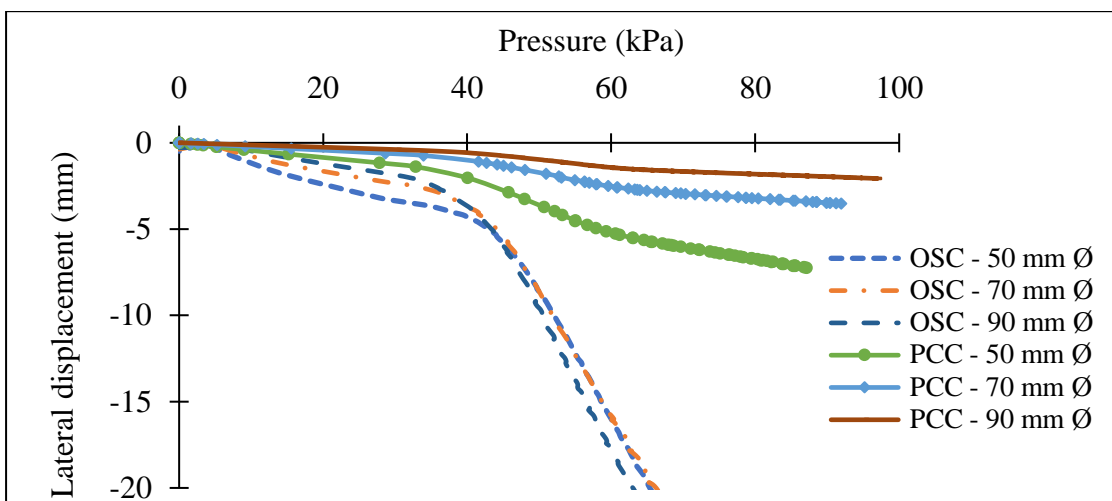
Figure 5.11 Pressure versus lateral deflection of the top end of stone columns

Figure 5.12 and Fig.5.13 represent the lateral deformation of stone column and pervious concrete column along the shorter and longer direction respectively. The lateral deformation of columns along the shorter direction represents the deflection of columns perpendicular to the direction of soil movement. Similarly, the lateral deformation of columns along the longer direction represents the deflection of columns along the direction of soil movement. It is evident that the pervious concrete columns behaved like a rigid pile with zero displacement for shorter direction and very less displacement along longer direction.

Along the shorter direction as shown in Fig.5.12, the stone columns have undergone shear failure and the stone column has seen moved more at the top of the column than the bottom end of the column. Along the longer direction, the stone columns of all diameters studied undergone maximum displacement at a depth of 200 mm, whereas pervious concrete columns undergone maximum displacement on the top end of column as shown in Fig.5.13. This clearly confirms the resistance offered by pervious concrete columns and its superior nature than ordinary stone columns under shear.
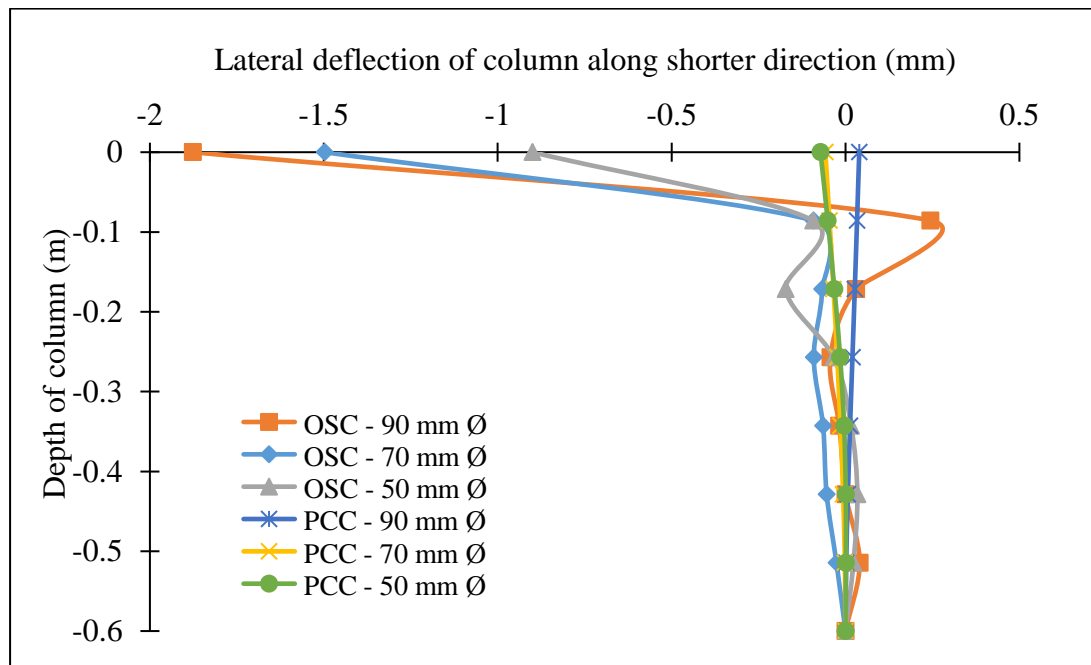
Figure 5.12 Lateral deformation of column along shorter direction
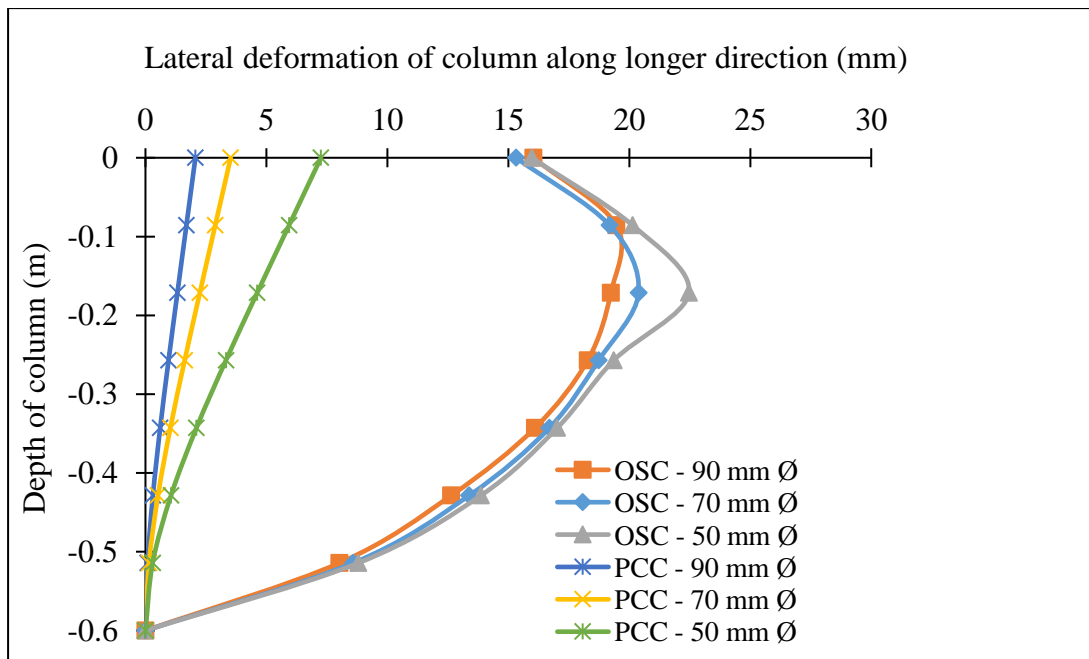
Figure 5.13 Lateral deformation of column along longer direction

Pervious concrete columns show significantly lesser lateral displacements compared to ordinary stone columns. Also, the profile of lateral displacements obtained with pervious concrete column and ordinary stone columns are entirely different. Peak lateral displacements in case of pervious concrete column are at the surface and the deflected profile of the column is very much like that of a rigid pile with a free or unrestrained head condition. In the case of ordinary stone columns, the peak lateral displacements occurred at some depth beneath the ground surface, very much like that of the lateral movements of the subsoil (in case of unimproved ground) beneath and beyond the edges of the embankment, that one would observe with inclinometer measurements at site (Bergado et al. 1991).

5.2.6 Heave profile

After numerical analysis, the heave profile of clay was assessed. The heave profile of clay is as shown in Fig.5.14. It is noticed that the pervious concrete column completely resisted the shear movements and the behaviour could be compared with rigid pile without undergoing any deformations. It is interesting to note that the soil movement beyond pervious concrete column is very less. Therefore, it can be concluded that

pervious concrete column improved ground has better shear resistance than conventional stone column improved ground.
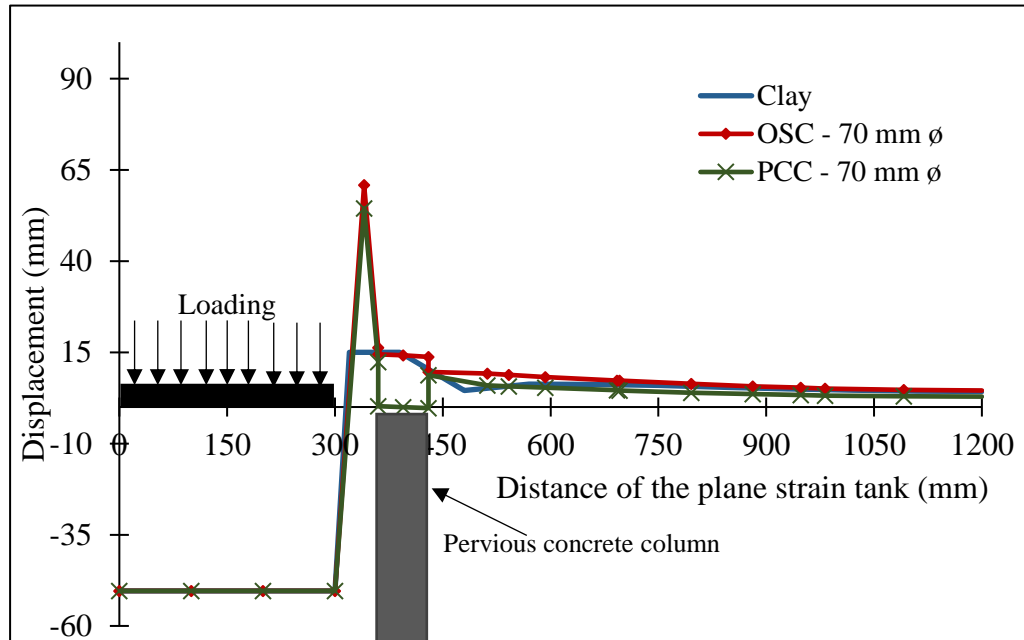
Figure 5.14 Heave profile observed for clay

5.3 NON-LINEAR BEHAVIOUR OF PERVIOUS CONCRETE

Linear elastic model was used to model pervious concrete material in large shear test tank models too. Hence, similar to the non-linear model mentioned in Section 4.5, a comparison of large shear test results with non-linear material model and linear elastic model was performed to verify the use of linear elastic model. Therefore, Mohr-Coulomb material model was selected in place of linear elastic model and an improved ground with PCC of diameter 90 mm placed at a clear spacing of 50 mm from the edge of the loading plate was taken to compare the pressure-settlement and heave profile results of linear-elastic and non-linear models. Figure 5.15 and Fig.5.16 show the pressure-settlement and heave profile of PCC improved ground. From these figures, it is observed that the results from both of these material models are identical. Therefore, the use of linear elastic model in the study is justified.
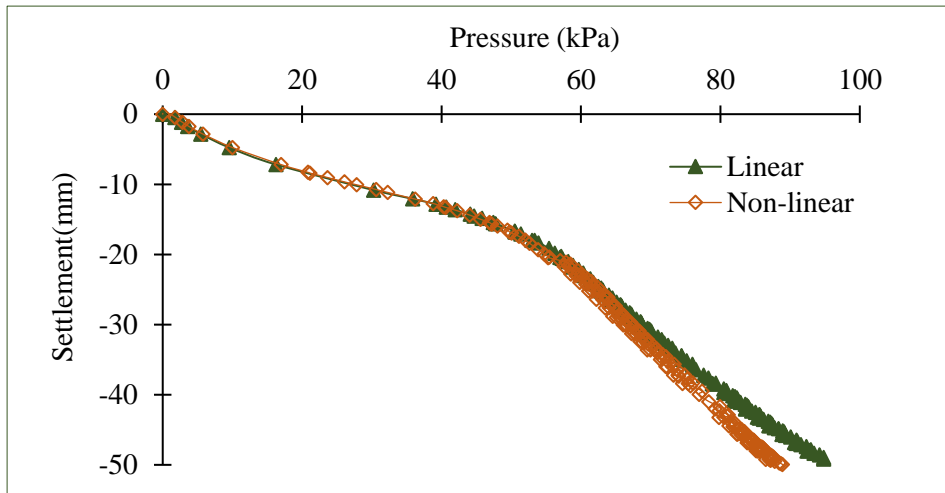
Figure 5.15 Pressure-settlement response of PCC improved ground using linear-elastic and non-linear models
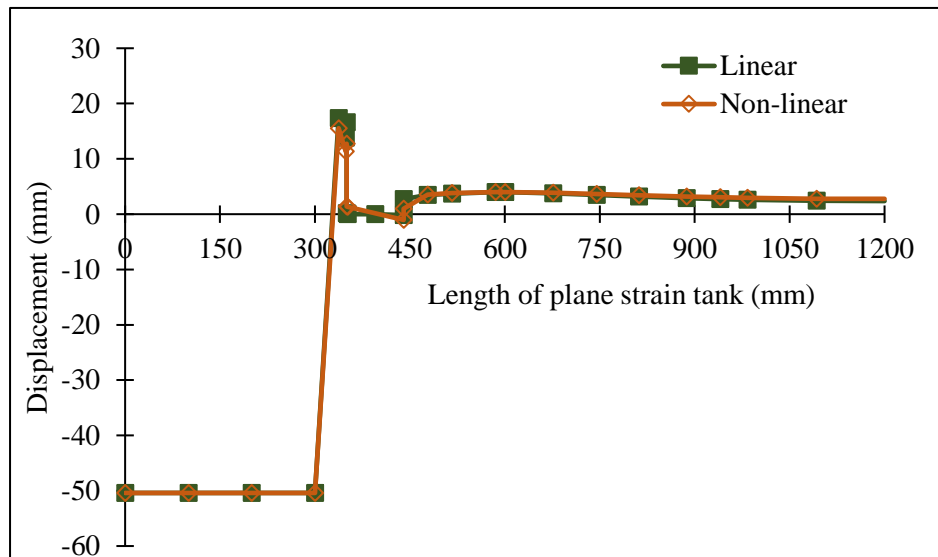
Figure 5.16 Heave Profile of PCC improved ground using linear-elastic and non-linear models

5.4 SUMMARY

In this chapter, shear performance of floating stone column and pervious concrete column improved ground are being reported using large shear test models. The column placed in large shear test tank model represents columns placed beneath the toe of the embankment and the vertical loading applied to the full width of model induces shear loading within the soil. The feasibility and shear performance of pervious concrete columns in lieu of conventional stone columns were considered and following conclusions are drawn.

The pervious concrete column in place of conventional stone column for improving weak ground is found to offer better shear resistance. The shear strength of improved ground increases with increase in diameter for pervious concrete column inclusions for all the cases considered. There is no appreciable improvement in pressures on the loading area due to increase in diameters of ordinary stone columns. It is also observed that two pervious concrete column group has higher shear resistance than a single pervious concrete column.

The pervious concrete column with end-bearing condition exhibits better shear resistance than floating conditions. Therefore, it is recommended to provide pervious concrete columns till hard strata for optimum shear performance. Pervious concrete columns show significantly lesser lateral displacements compared to ordinary stone columns. Also, the profile of lateral displacements obtained with pervious concrete column and ordinary stone column are entirely different. Peak lateral displacements in case of pervious concrete column are at the surface and the deflected profile of the column is very much like that of a rigid pile with a free or unrestrained head condition. In the case of ordinary stone columns, the peak lateral displacements occurred at some depth beneath the ground surface. Stone column placed beneath the toe of the embankment are liable to undergo shear failure and are seen to move along with the soil.

CHAPTER 6

SEISMIC RESPONSE OF PERVIOUS CONCRETE COLUMN IMPROVED GROUND

In this chapter, the seismic response of pervious concrete column improved ground is addressed and compared with stone column improved ground. Numerical modelling using OpenSeesPL software was used for analyzing improved ground. Unit cell modelling approach with periodic boundary conditions was used for modelling improved ground and details are mentioned in the subsequent sections.

6.1 LIQUEFACTION INDUCED LATERAL SPREADING

Liquefaction is a phenomenon in which saturated, or partially saturated sands and silts loses its shear strength when subjected to seismic vibrations and behaves like a liquid. The soil structure is distorted due to cyclic shear strains developed in saturated cohesionless soils due to seismic waves propagating through the soil layer. If there is no provision for the drainage of excess pore water to dissipate, the intergranular stress gets transferred to interstitial pore water. This causes soil to soften due to decreased intergranular stresses. When the intergranular stresses approach zero, that means the total soil stress is transferred to interstitial pore water, the soil behaves like liquid temporarily. This phenomenon of soil to transform from solid to liquid state is known as liquefaction.

Liquefaction generally occurs in loose saturated or partially saturated cohesionless soils. The liquefaction phenomenon induces ground deformations and associated ground failures. One of the ground failures due to horizontal displacement of ground is known as lateral spread. Lateral spread generally occurs in gentle slope or in a free face adjacent to water bodies. Lateral spread occurs due to combined response of gravitational and earthquake induced inertial forces acting on soil layer. The surface layers commonly break into large blocks as shown Fig.6.1 due to lateral spread. These surface blocks move down the gentle slope or free face due to seismic ground shaking. This causes zones of extension with open fissures (Youd 1984 and Youd 2018).
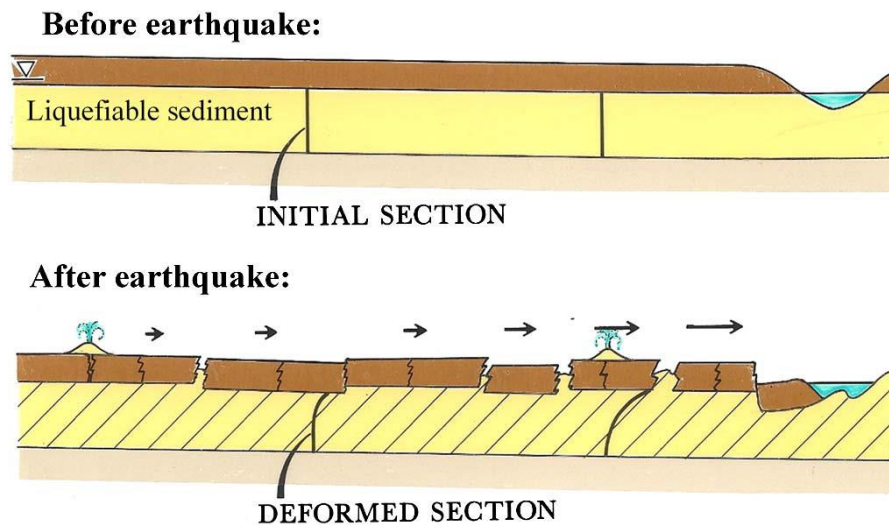
Figure 6.1 Lateral spread (Youd 1984)

The destructive effect of liquefaction is due to related lateral spreading damages. Therefore, the liquefication mitigation potential of improved ground emphasizing on lateral spreading is addressed. Stone columns are widely used to mitigate liquefaction to a greater extent by draining excess pore water through its pores present in the stone column. However, the pervious concrete column is reported to have vertical load carrying capacity which is four times more than ordinary stone column with comparable permeability characteristics and can be considered as an alternative to conventional stone column. Therefore, the seismic performance of pervious concrete column improved ground and stone column improved ground in mitigating liquefaction induced lateral spreading is focused.

6.2 PERIODIC BOUNDARY

Periodic boundary simulates infinite number of piles with same amount of displacements at both sides of the boundary. The deformations at the left and right boundary of the model would be identical and the stress field within the region enclosed by one periodic boundary is shown in Fig.6.2. This type of boundary condition is being used for simulating group of columns subjected to seismic loading conditions.

6.3 OpenSeesPL SOFTWARE

OpenSeesPL is a graphical user interface software used for analyzing three-dimensional ground and ground-structure response to earthquake loading. This software is developed by Lu et al. (2004). The software is primarily intended to be used for

conducting liquefaction studies using coupled solid-fluid analysis. This software is equipped for modelling ground modification using gravel drains and stone columns in mitigating liquefaction (OpenSeesPL user manual). The soil model for modelling cohesionless soil is developed with multi-yield surface plasticity. The material type used in OpenSeesPL for defining cohesionless soils are PDMY(PressureDependentMultiYield) models.
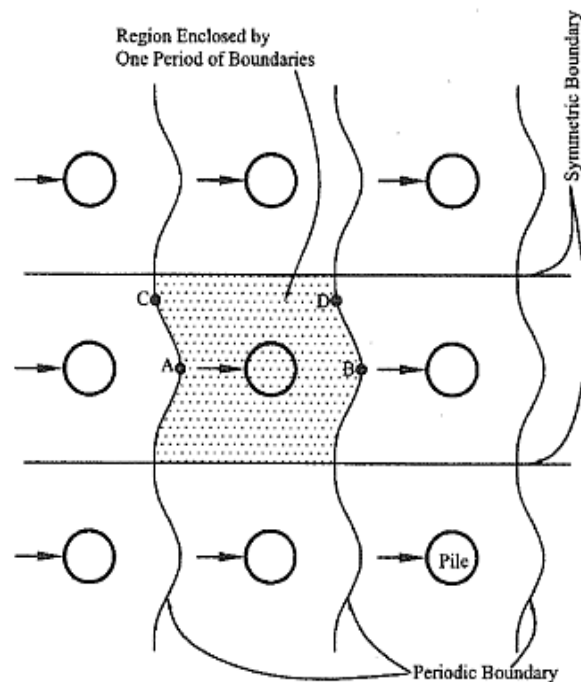
Figure 6.2 Periodic boundary for large pile group (Law and Lam 2001)

The element used is known as BRICKUP element, an eight-noded element with u-p formulation. Each node in BRICKUP element has 4 DOF. The DOF, 1 to 3 represents solid displacement (u) and DOF 4 represents fluid pressure (p). This element is used for analyzing dynamic response of fully coupled solid-fluid model based on Biot's theory of porous medium (OpenSeesPL user manual).

6.4 NUMERICAL MODELLING

The layout of pervious concrete column (PCC) arrangement is shown in Fig.3.4(a). The unit cell of remediated area is highlighted in the layout. Similar unit-cell modelling approach was used by various researchers (Elgamal et al. 2009; Asgari et al. 2013; Tang, et al. 2015, 2016; Rayamajhi et al. 2014, 2016). The center to center spacing of column were varied as 2D, 2.5D and 3D, which corresponds to area ratio of 20%, 13% and 9% respectively. Half of the unit cell normal to the direction of seismic excitation

was modelled because of symmetry. The depth of model is 10 m as shown in Fig.6.3(a). The 3D model generated in OpenSeesPL is as shown in Fig.6.3(b). A sample showing the plan of column improved unit cells for varying diameters by maintaining a constant area ratio is presented in Fig.6.3(c).

Fully saturated sand stratum with a mild infinite slope of 4° was considered as free-field case. The stone column and pervious concrete column as inclusions were used as improvement cases. Sand stratum was considered to have a relative density of 40%. The default values available in OpenSeesPL for cohesionless soil with 40% relative density was used to model free-field case. The stone column was considered as dense cohesionless material with gravel permeability (Lu 2006 ; Elgamal et al. 2009). The pervious concrete is reported to have a 28-day compressive strength of 22 MPa which is similar to that of normal concrete (Suleiman et al. 2014). Therefore, pervious concrete parameters were assumed as comparable to that of normal concrete. The cohesion of concrete is reported as varying from 2.94 MPa to 12.34 MPa for compressive strength range of 14.4 MPa to 47 MPa (Pul et al. 2017). Hence, the cohesion of pervious concrete was conveniently taken as 3 MPa. The friction angle of high modulus columns is reported as ranging from 37° to 40° (Fan et al. 2018). Therefore, 38° was selected as friction angle for pervious concrete.

The sand strata, stone column and pervious concrete were modelled with PressureDependMultiYield02 (PDMY02) constitutive model. The multiphase material model is defined with linear, non-linear, fluid and liquefaction parameters (Yang et al. 2008). The linear soil property includes saturated unit weight of soil, shear modulus and bulk modulus. Non-linear property is defined by cohesion and angle of internal friction. Fluid property is defined with combined bulk modulus, unit weight of water along with horizontal and vertical permeability. Phase transformation angle is used to define the liquefaction property of soil model with default contraction and dilation parameters. The parameters used are presented in Table 6.1.

Stone column was assumed to be fully bonded with sand for simplicity (Elgamal et al. 2009; Tang et al. 2015, 2016; Rayamajhi et al. 2014, 2016). The sand strata, stone column material and pervious concrete were discretized into 8 noded brick element with u-p formulation. The model was fully saturated up to ground level and seismic excitation was given at the base. The periodic boundary conditions were applied at the

left and right boundary of the model (Lu et al. 2004; Elgamal et al. 2009; Asgari et al. 2013; Tang et al. 2015, 2016; Rayamajhi et al., 2014, 2016). The base was assumed as rigid rock and zero pore-pressure boundary was assumed on ground surface. The soil model was analyzed in two stages. In the first stage, gravity loading due to mild inclination was applied. The mild inclination imposes a static driving shear stress component due to gravity and accumulated longitudinal downslope deformation is caused (Lu 2006; Lu et al. 2011). In the second stage, the base was excited with earthquake vibrations. Rayleigh damping of 2% was considered (Rayamajhi et al. 2014; Tang et al. 2015). The thickness of finite element mesh was selected in such a way that the frequency content which can pass through model is 30 Hz. The thickness used was 0.5 m. Smaller mesh thickness was selected to ensure correct prediction of liquefaction behaviour (Lu et al. 2011).

6.5 VALIDATION OF NUMERICAL MODEL

Validation of model generated in OpenSeesPL was carried out by simulating the prototype of well documented VELACS centrifuge model 02. Then, the experimental results of VELACS model 02 test conducted by Taboada and Dobry 1998 was compared with those obtained from the numerical model analyzed using OpenSeesPL in terms of ground lateral displacement and excess pore pressure values at points shown in Fig 6.4(a). The prototype model results of VELACS centrifuge model were also well documented (Ghasemi and Pak 2016).

The description of VELACS experiment is as follows: The inclined model test was intended to study the lateral spreading phenomenon on sloping grounds. The laminar box of prototype dimensions as shown in Fig.6.4(a) was filled with Nevada sand of approximately 40% relative density. The sand was fully saturated, and the model was inclined at an angle of 4° with horizontal in prototype scale. The experiment was conducted with 50g centrifugal acceleration and acceleration time history as shown in Fig.6.4(b) was applied at the base of the model. The plan of the validation model is 23 m × 23 m and half of the soil model is analyzed because of symmetry as shown in Fig.6.3. The depth of the soil model is 10 m and periodic boundary conditions were given for left and right boundaries of the soil model.

(a) Model details

(b) 3D model with seismic excitation applied at base

(c) Plan of soil models showing constant area of 13%
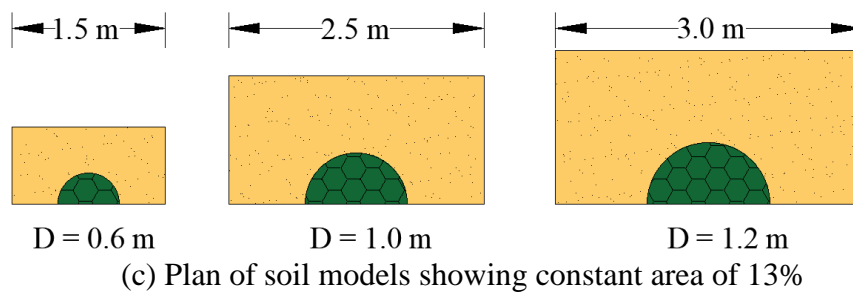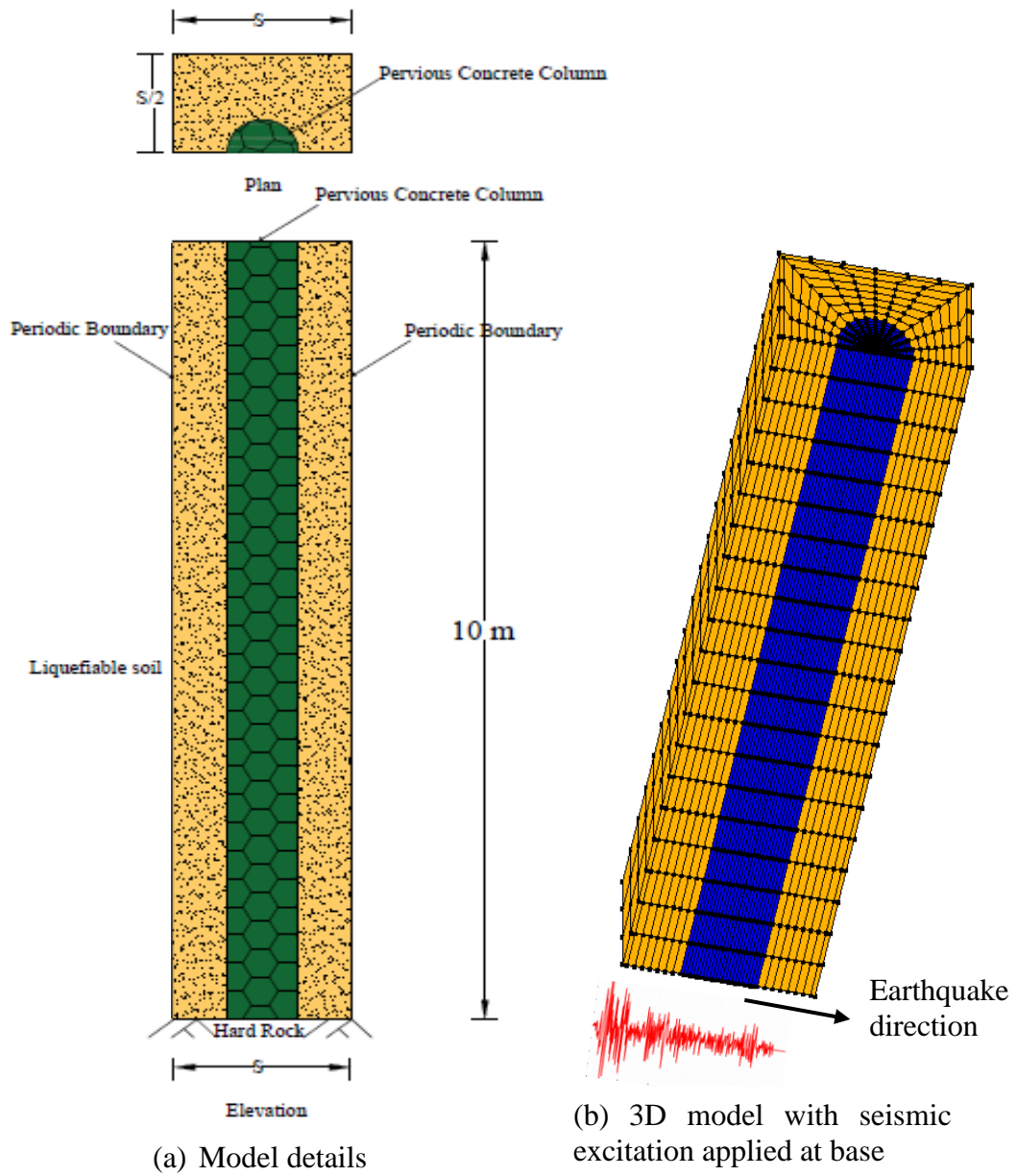
Figure 6.3 Soil model in OpenSeesPL (a) Remediated ground with pervious concrete column (PCC) (b) 3D model with seismic excitation applied at base (c) Plan of soil models showing constant area ratio of 13% for different diameter columns

The validated results were in very good agreement with experimental results as presented in Fig.6.5(a) and Fig.6.5(b) for excess pore water pressure-time histories at various depths and lateral displacement-time histories, respectively. The points where the results were compared are marked in Fig 6.4(a) as P5, P6, P7, P8 and LVDT1 to LVDT6. Figure 6.5(c) shows the ground settlement due to the shaking and demonstrates reasonable agreement with experimental results.

(a)

(b)
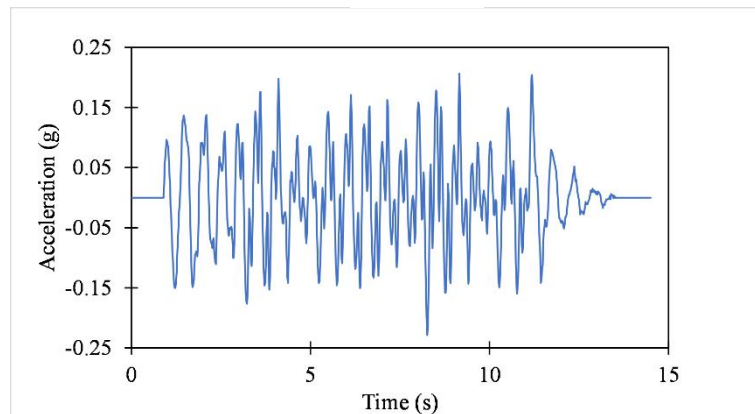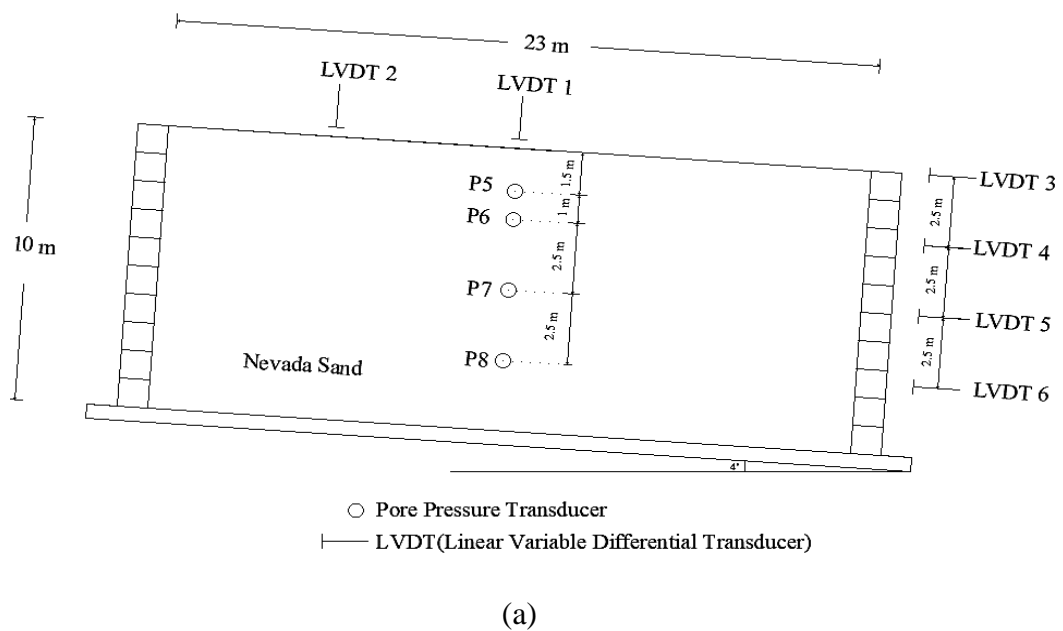
Figure 6.4(a) VELACS Experiment Model 2 (Prototype Scale) (b) Input acceleration at the base of laminar box ((Prototype Scale)
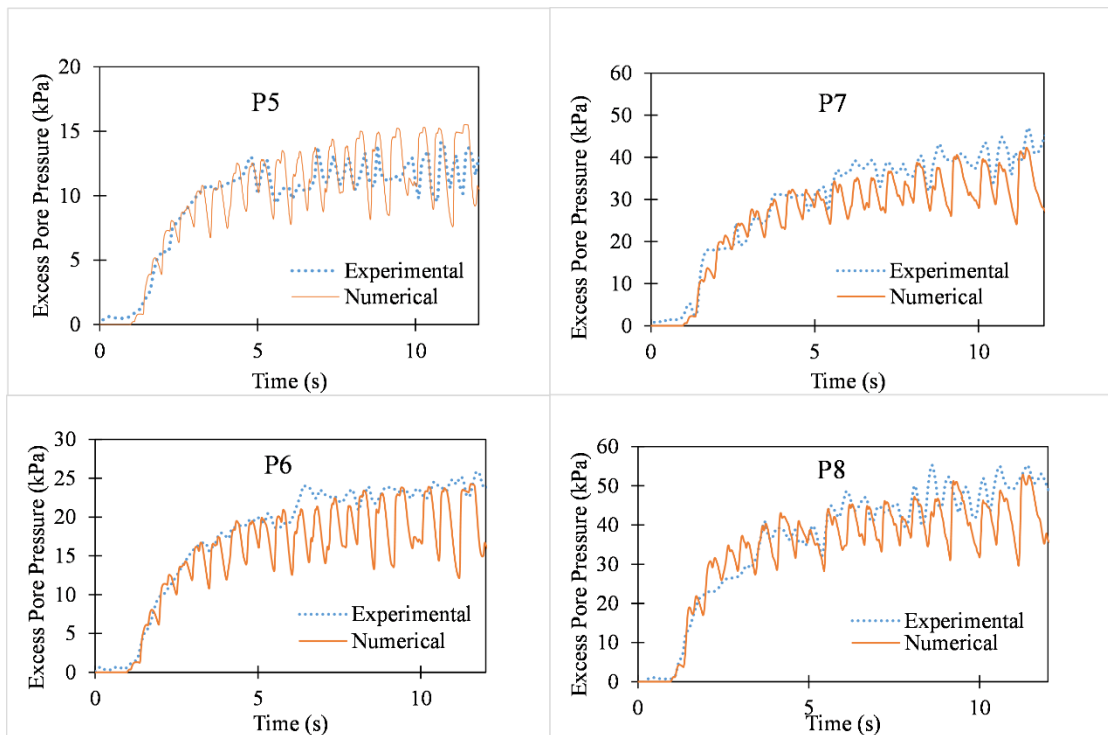
Figure 6.5(a) Validation of model (Excess pore pressure-time histories at points P5, P6, P7 and P8)
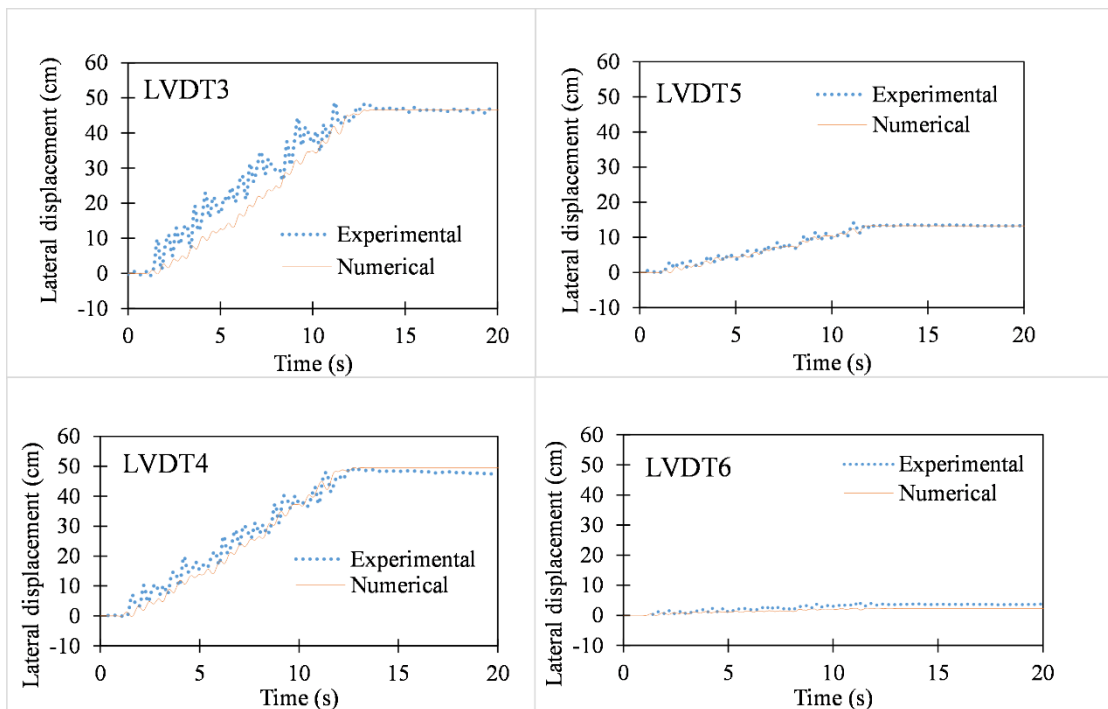
Figure 6.5(b) Validation of model (Lateral displacement-time histories at points LVDT3, LVDT4, LVDT5 and LVDT6)
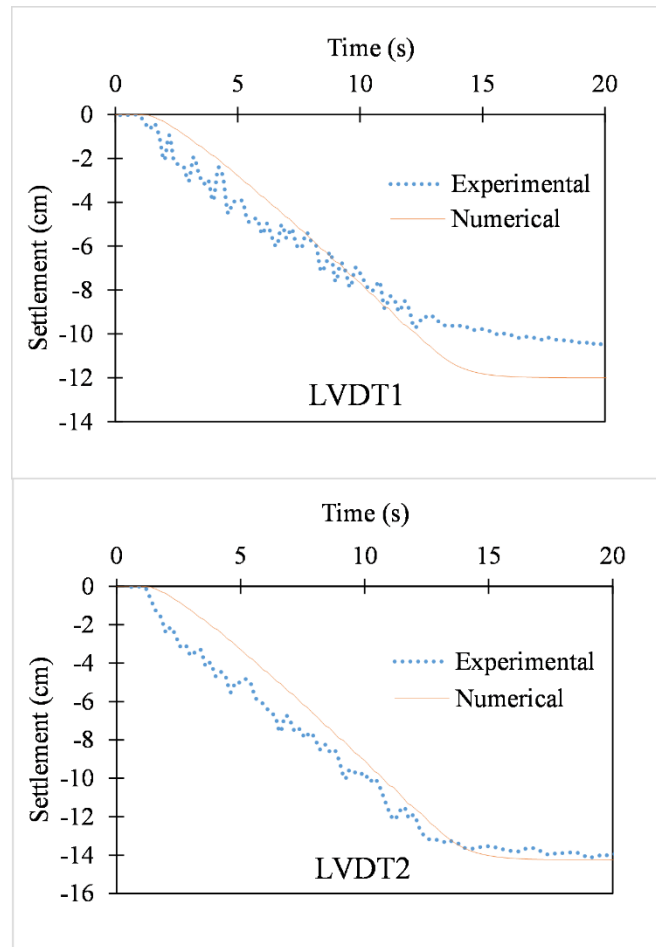
Figure 6.5(c) Validation of model (Ground settlement time-histories at points LVDT1 and LVDT2)

6.6 METHODOLOGY

The seismic performance of pervious concrete column improved ground in terms of ground lateral deformation, excess pore pressure generation and shear stress-strain behaviour was investigated initially. The diameter of pervious concrete column and stone column was taken as 0.6 m with an area ratio of 20%. Subsequently, the various factors influencing the seismic performance of column improved ground such as depth of PCC, area ratio, diameter of the column, permeability of PCC and surrounding soil, ground surface inclination, surface load, peak ground acceleration, ground motion characteristics, thickness of liquefiable soil and different soil strata were analyzed. The various parameters analyzed with range adopted are summarized in Table 6.2 along with parameters that remained constant for each study.

The effect of floating pervious concrete column was quantified by varying L/D (depth of column (L) to diameter of column (D) ratio) as 4, 6 and 8. The column

diameter of 1m was considered. The area ratio of floating pervious concrete columns was kept as 13% and seismic performance was compared with end bearing column improved ground. The effect of diameter of column inclusions on lateral deformation was studied by varying diameters (0.6 m, 1.0 m and 1.2 m) for a constant area ratio of 13%. The effect of area ratio was explored by varying the center to center spacing of 0.6 m diameter columns from 2D to 3D. The spacing of 2D to 3D corresponds to area ratio of 20% to 9%.

The influence of column permeability on the seismic performance of pervious concrete column was studied by varying hydraulic conductivity of pervious concrete column as 0.01 m/s, 0.1m/s and 1.0 m/s. The permeability of pervious concrete column was also kept same as that of sand strata to simulate the clogged condition considering hydraulic function alone, i.e., the pores of pervious concrete being filled with surrounding soil scenario. The seismic performance of clogged pervious concrete column was also compared with working stone column condition.

Since the aim of the study was to account for seismically induced lateral spreading, a fully saturated soil strata of 4° infinite extent was considered as free-field case. Sand deposits up to 20 m depth and sandwiched sand deposits of thickness 3 to 10 m were reported as the types of deposits in which liquefaction is expected (Ishihara 2007). For studying the influence of varying thickness of liquefiable soil on lateral spreading, sandwiched sand deposits of varying thickness from 2m to 8m were considered. The soil model used was remediated ground with SC and PCC of diameter 1m corresponding to an area ratio of 13%. The soil model with varying liquefiable soil thickness is shown in Fig.6.6. The liquefiable soil layer is overlaid by 1m thick non-liquefiable soil and underlain by non-liquefiable soil layer. The total depth of soil profile was kept equal to 12 m by increasing the depth of underlying non-liquefiable layer with varying liquefiable soil thickness from 2 m to 8m (Fig.6.6). The embedment depth of SC and PCC inclusion to underlying non-liquefiable layer was taken as 1 m. The non-liquefiable soil layer was considered as dense sand with a relative density of 87% (Rayamajhi et al. 2014, 2016).

To study the efficacy of PCC inclusion on various liquefiable soil strata, loose sand and medium-dense sand with shear wave velocity (V_s) of 153 m/s and 223 m/s respectively were investigated. The respective shear wave velocity of soil strata was

chosen based on site classification as per FEMA listed in Table 6.3. In addition to sand stratum, the performance of PCC on silt stratum was also considered. The properties of silt strata were considered similar to that of medium-dense sand strata with permeability range of silty soil (Yang & Elgamal 2002; Elgamal et al. 2009; Asgari, et al. 2013).

For understanding the influence of soil permeability on lateral deformation, the permeability of medium-dense sand strata was replaced with soil permeability ranging from 6.6×10^{-02} m/s to 6.6×10^{-04} m/s. The influence of ground surface inclination on lateral deformation was conducted by varying ground surface inclination angle from 0° to 8°. The surface load applied to remediated ground with SC and PCC was varied from 0 kPa to 200 kPa to understand the effect of surface load on lateral deformation. The influence of peak ground acceleration on lateral displacement was carried out by applying the scaled earthquake excitation (0.1g, 0.2g, 0.4g, 0.6g and 0.8g) at the base of the model. The influence of ground surface inclination and surface load was conducted on soil models with SC diameter of 1m and with an area ratio of 13% (center to center column spacing of 2.5D, D is the diameter of column) and was compared with PCC remediated ground. For understanding the influence of various types of soil strata, permeability of surrounding soil and peak ground acceleration, diameter of the column and area ratio considered were 0.6 m and 20% respectively, where 20% area ratio corresponds to center-to-center column spacing of 2D, D is the diameter of column.

To understand the seismic performance of remediated ground with SC and PCC, two different earthquake waveforms conforming to earthquake-time history data of El-Centro 1940 N-S component (Fig.6.7(a)) and Loma Prieta 1989 E-W component (Fig.6.7(b)) scaled to 0.2g were used. The characteristics of scaled earthquake data used for the analysis is detailed in Table.6.4.

The influence of earthquake parameters like significant duration, frequency content, arias intensity, on the performance of pervious concrete column improved ground were investigated. Two ground motion data recorded at two different places where intensive liquefaction damages were reported are selected as earthquake data for seismic analysis. The earthquake excitation was scaled to 0.2g and given as the input base excitation and frequency content of both earthquakes are 1.17 Hz and 1.63 Hz respectively as shown in Fig.6.7. The significant duration (D_{5-95}) and number of significant excitation cycles of scaled El-Centro earthquake are 23.84 s and 14.5 cycles

whereas for Loma Prieta earthquake, the significant duration ($D_{5\text{-}95}$) and number of significant excitation cycles are 4.4 s and 5.8 cycles respectively (Table 6.3). The center to center spacing between columns of diameter 0.6 m were considered with a wider spacing of 3D, (D being diameter of column) as per provisions in IS code of practice IS 15284. Area ratio corresponding to a spacing of 3D is 9%, calculated as the ratio of area of column inclusion to the total area of improvement. The permeability of both stone column and pervious concrete column inclusion were considered as equivalent to gravel permeability for the benchmark cases and these three benchmark cases were analyzed first. Then, the influence of pervious concrete column permeability on generation of excess pore pressure was addressed. The permeability of stone columns can be varied in the field. Therefore, the permeability of pervious concrete column was also varied to find the permeability for which the initiation of liquefaction could occur and also to find the optimum value of pervious concrete column permeability above which the excess pore pressure generation is nearly non-existent. The performance of pervious concrete column improved ground was also compared with stone column improved ground and unimproved ground subjected to above mentioned earthquake excitations.

To understand the pore pressure build-up in column improved ground, total stress analysis (TSA) and effective stress analysis (ESA) were performed. In total stress analysis, water table is ignored and therefore pore pressure generation is not possible. Whereas effective stress analysis uses coupled two-phase model and pore pressure generation is possible. Therefore, the maximum response profile of SC and PCC improved ground subjected to El Centro and Loma Prieta excitations from total and effective stress analysis were compared.

Table 6.1 Material model parameters

Soil model Parameters	Loose sand	Medium-dense sand	Silt	Stone column	Pervious Concrete
Saturated unit weight of soil (kN/m^3)	17	18	18	21	21.5
Reference pressure for model calibration P_{ref} (kPa)			101		
Low strain shear modulus at reference pressure G_{max} (MPa)	40	90	90	130	10580
Bulk Modulus at reference pressure B_r (MPa)	160	220	220	260	14460
Model friction angle, same as triaxial friction angle ϕ_{TC}	32°	36°	36°	42°	38°
Phase transformation angle ϕ_{PT}	26°	26°	26°	26°	26°
Shear strength at zero effective confining pressure (cohesion) (kPa)	0	0	0	0	3000
Permeability (m/s)	6.6 x10^{-5}	6.6 x10^{-5}	6.6 x10^{-7}	0.01	0.01

Table 6.2 Parameters influencing seismic performance and range of variation

Description	Parameter	Range adopted	Constant Parameters
Effect of pervious concrete column	Sand, SC, PCC	N/A	Column diameter: 0.6 m, AR: 20% End bearing columns
Effect of floating PCC	L/D ratio	4, 6, 8	Column diameter: 1.0 m, AR: 13%
Effect of area ratio	Area ratio (%)	20, 13, 9	Column diameter: 0.6 m End bearing columns
Effect of diameter	Diameter (m)	0.6 ,1.0, 1.2	AR: 13%, End bearing columns
Effect of permeability of PCC	PCC permeability (m/s)	0.01, 0.1, 1.0, 6.6×10^{-05}	Column diameter: 1.0 m, AR: 13% End bearing columns
Efficacy of pervious concrete column in various soil strata	Soil strata	Loose sand, Medium-dense sand, Silt strata	Column diameter: 0.6 m, AR: 20% End bearing columns
Influence of thickness of liquefiable soil	Liquefiable soil thickness (m)	2, 4, 6, 8	Column diameter: 1.0 m, AR: 13% End bearing columns
Influence of surrounding soil permeability	Surrounding soil permeability (m/s)	$6.6\times10^{-02} - 6.6\times10^{-04}$	Column diameter: 0.6 m, AR: 20% End bearing columns
Influence of ground surface inclination	Ground surface inclination (°)	0 – 8	Column diameter: 1 m, AR: 13% End bearing columns
Influence of surface load	Surface load (kPa)	0 – 200	Column diameter: 1 m, AR: 13% End bearing columns
Influence of peak ground acceleration	Peak ground acceleration	0.1g – 0.8g	Column diameter: 0.6 m, AR: 20% End bearing columns
Influence of earthquake characteristics	Ground motions with different characteristics (scaled to 0.2g)	El-Centro 1940 Loma Prieta 1989	Homogeneous liquefiable soil: Column diameter: 0.6 m, AR: 9 %
			Sandwiched soil deposits: Column diameter: 1.0 m, AR: 13%
Total stress analysis versus effective stress analysis	SC, PCC	N/A	Column diameter: 0.6 m, AR: 9 % End bearing columns
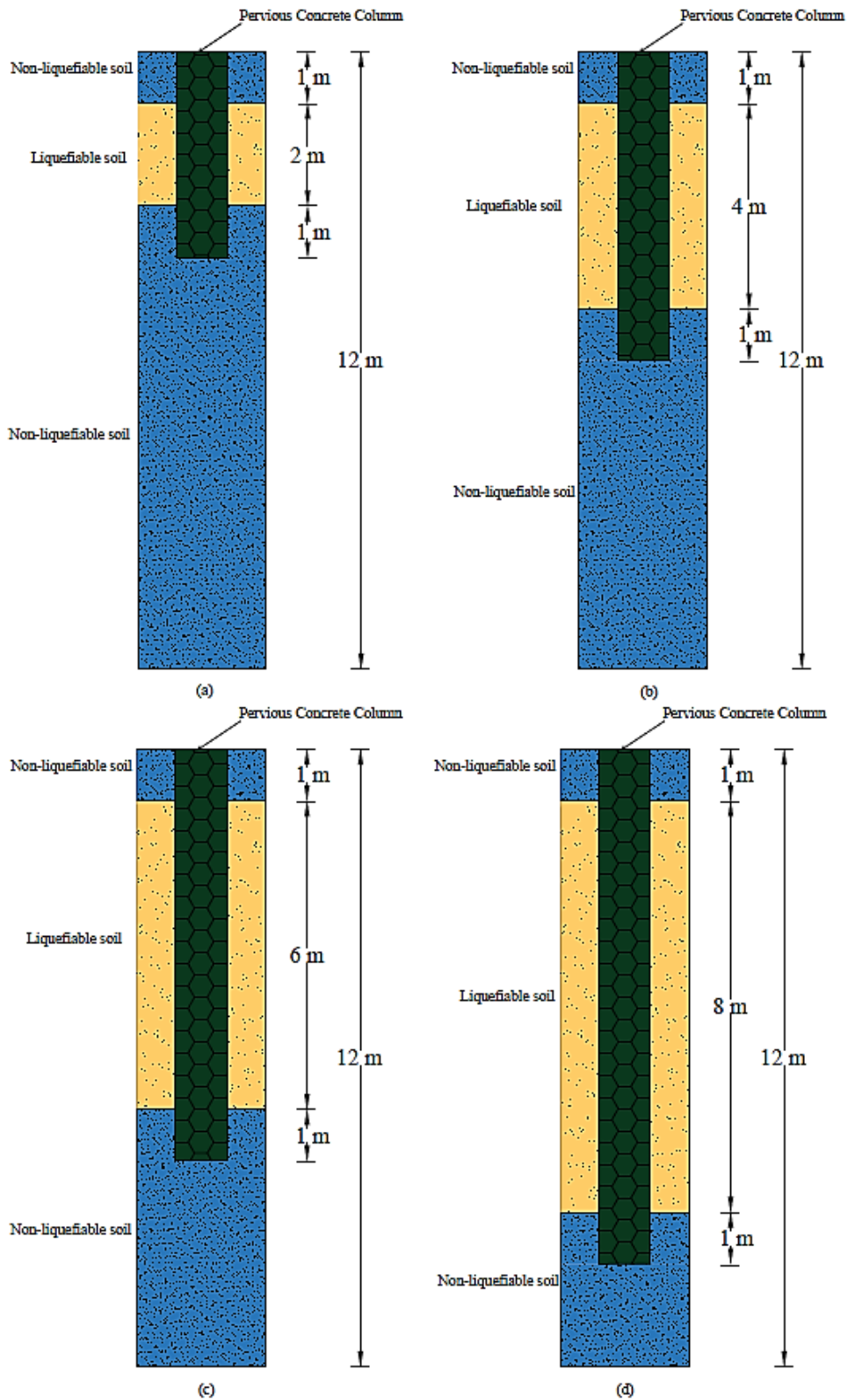
Figure 6.6 Sandwiched liquefiable soil with varying thickness of (a) 2m (b) 4m (c) 6m and (d) 8m

Table 6.3 Site classification as per FEMA

Site Class	Shear wave velocity, Vs (m/s)	SPT value N	Shear strength of soil (kPa)
E	< 180	< 15	< 50
D	180-360	15-50	50-100
C	360-760	> 50	> 100

Table 6.4 Earthquake characteristics

Earthquake Parameters	El-Centro 1940 N-S	Loma Prieta 1989 E-W
Date of Occurrence	18/05/1940	18/10/1989
Recorded Station	117 El Centro	Treasure Island
Moment Magnitude of earthquake, M_w	7.0	6.93
Maximum horizontal acceleration (g)	0.3188	0.1458
Predominant frequency (Hz)	1.17	1.63
Significant duration D_{5-95} (s)	23.84	4.4
Number of significant excitation cycles (Hz)	14.5	5.8
Arias intensity for PGA scaled to 0.2g (m/s)	0.686	0.564
Energy flux for PGA scaled to 0.2g ($J\,m^{-2}s^{-1}$)	805	1715
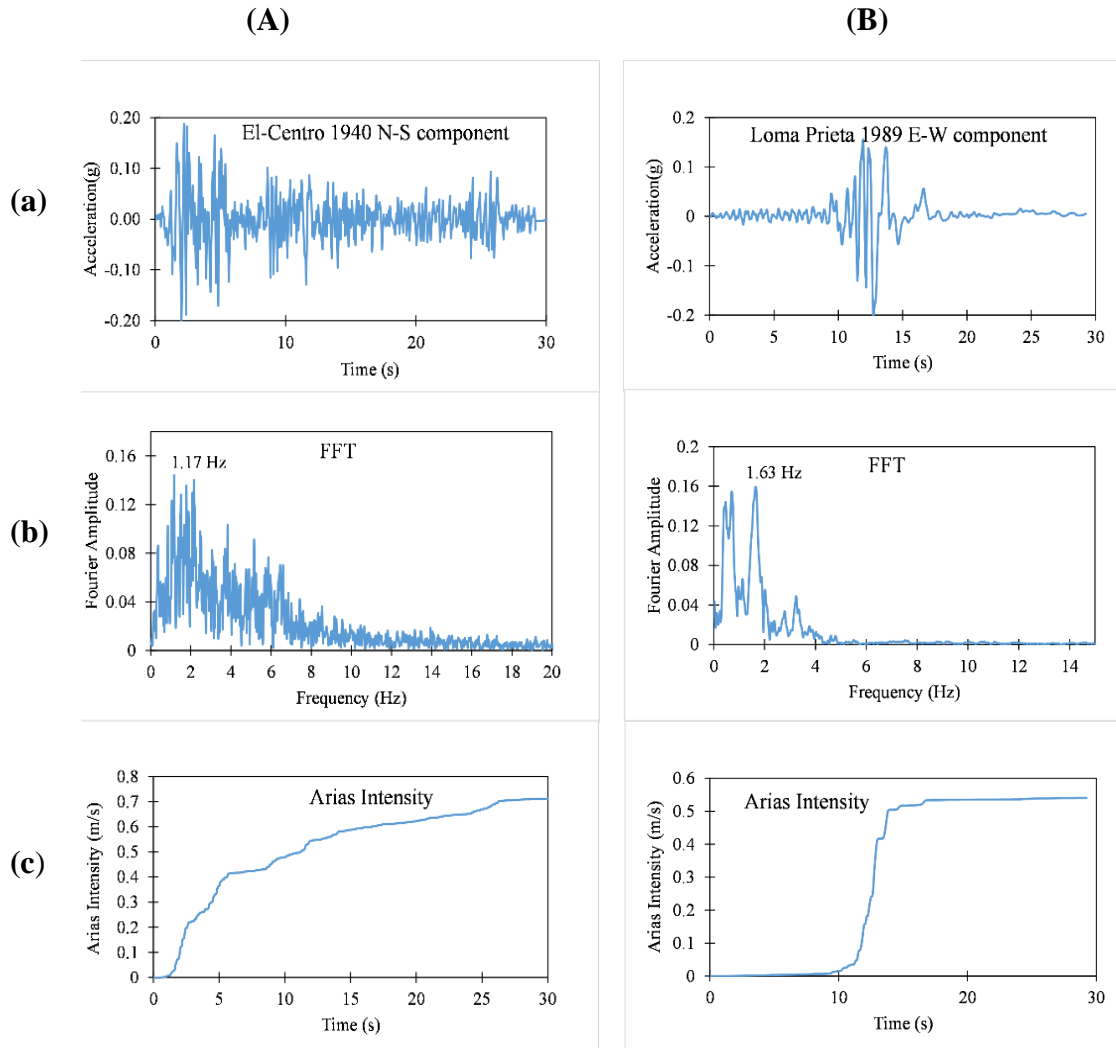
Figure 6.7 Earthquake data scaled to 0.2g (A) El-Centro 1940 (B) Loma Prieta 1989 (a) Time history of acceleration (b) FFT (c) Arias Intensity

6.7 RESULTS AND DISCUSSIONS

The results of seismic response of improved ground with stone column (SC) and pervious concrete column (PCC) inclusions are discussed in the following subsections.

6.7.1 Effect of pervious concrete column vis-à-vis stone column

The lateral displacement of pervious concrete column improved ground (PCC) was compared with stone column improved ground (SC). Figure 6.8 shows the ground lateral response at the centre of finite element mesh for column of diameter 0.6 m and for a constant area ratio of 20%. The response of PCC improved ground is 70 % better than that of stone column improved ground and 96 % higher than free-field case. Lateral displacement of improved ground using pile pinning is reported as non-existent and pile pinning is reported as a highly viable technique for cellular remediation (Lu et al. 2012 ; Asgari et al. 2013). The lateral displacement response of PCC is similar to that of pile

pinning case with almost zero displacement, along with hydraulic functionality, which makes it a better alternative to stone columns.
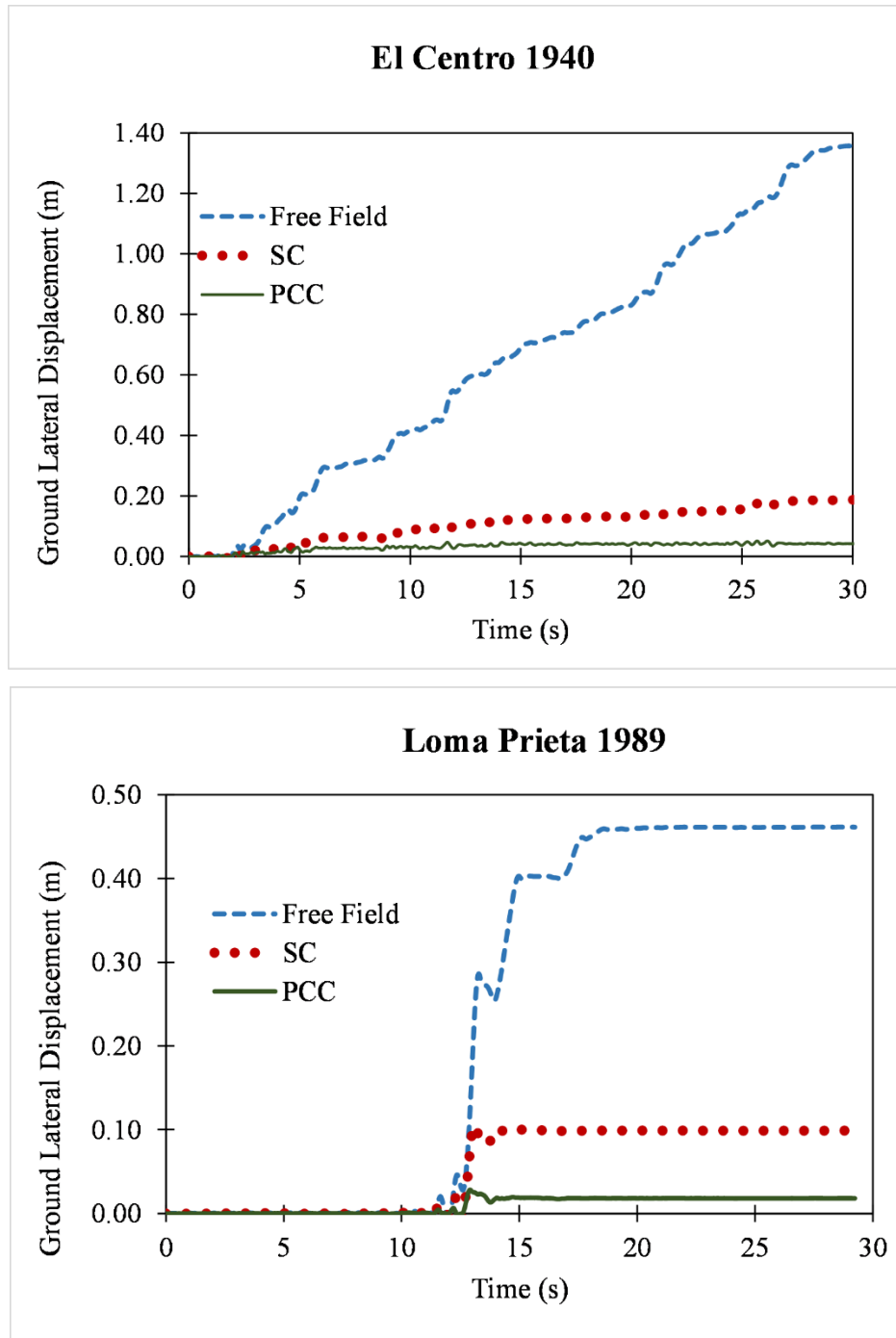
Figure 6.8 Effect of PCC on Ground lateral displacement (Diameter of column =0.6 m, AR =20%)

The deformed mesh of stone column and pervious concrete column improved ground at the end of seismic excitation along shaking direction is shown in Fig.6.9 for a scale

factor of 5. It is clearly seen that the pervious concrete column has undergone less lateral deformation when compared to stone column. The stone column is also seen to be moving along with surrounding soil as shown in Fig.6.9.
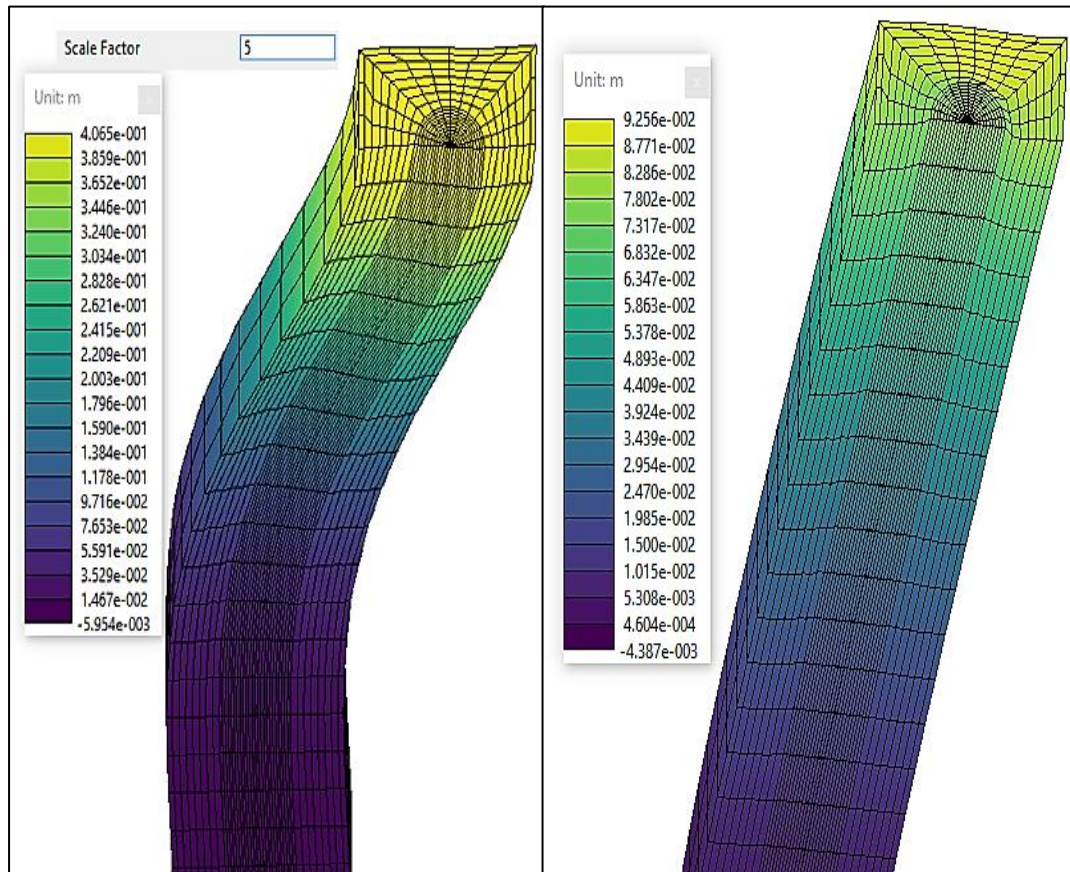
(a) Stone column   (b) Pervious concrete column

Figure 6.9 Deformed mesh at the end of seismic excitation along the direction of shaking for (a) Stone column improved ground (b) Pervious concrete column improved ground (Diameter of column =0.6 m, AR =13%)

The ground surface acceleration-time histories of unimproved ground, improved ground with SC and PCC are presented in Fig.6.10 along with seismic excitation at the base. The acceleration-time histories are obtained at the center of the soil model on the surface. The acceleration plots for all the cases display no asymmetric patterns and more negative spikes indicate the static driving forces imposed by gravity due to mild 4° inclination (Fig.6.10). For the free-field case, the peak surface acceleration is found to be 0.28g and 0.3g at the ground surface for El-Centro and Loma Prieta excitations respectively. With SC inclusion, the peak surface acceleration is observed as around

0.3 g for both the excitations. The peak surface acceleration due to PCC inclusion is found to be 0.4g and 0.3g at the ground surface for El-Centro and Loma Prieta excitations respectively. This is due to the presence of rigid PCC column. The similar increase in surface peak acceleration with stone column inclusion is well stated (Elgamal et al. 2009, Rayamajhi et al. 2016).
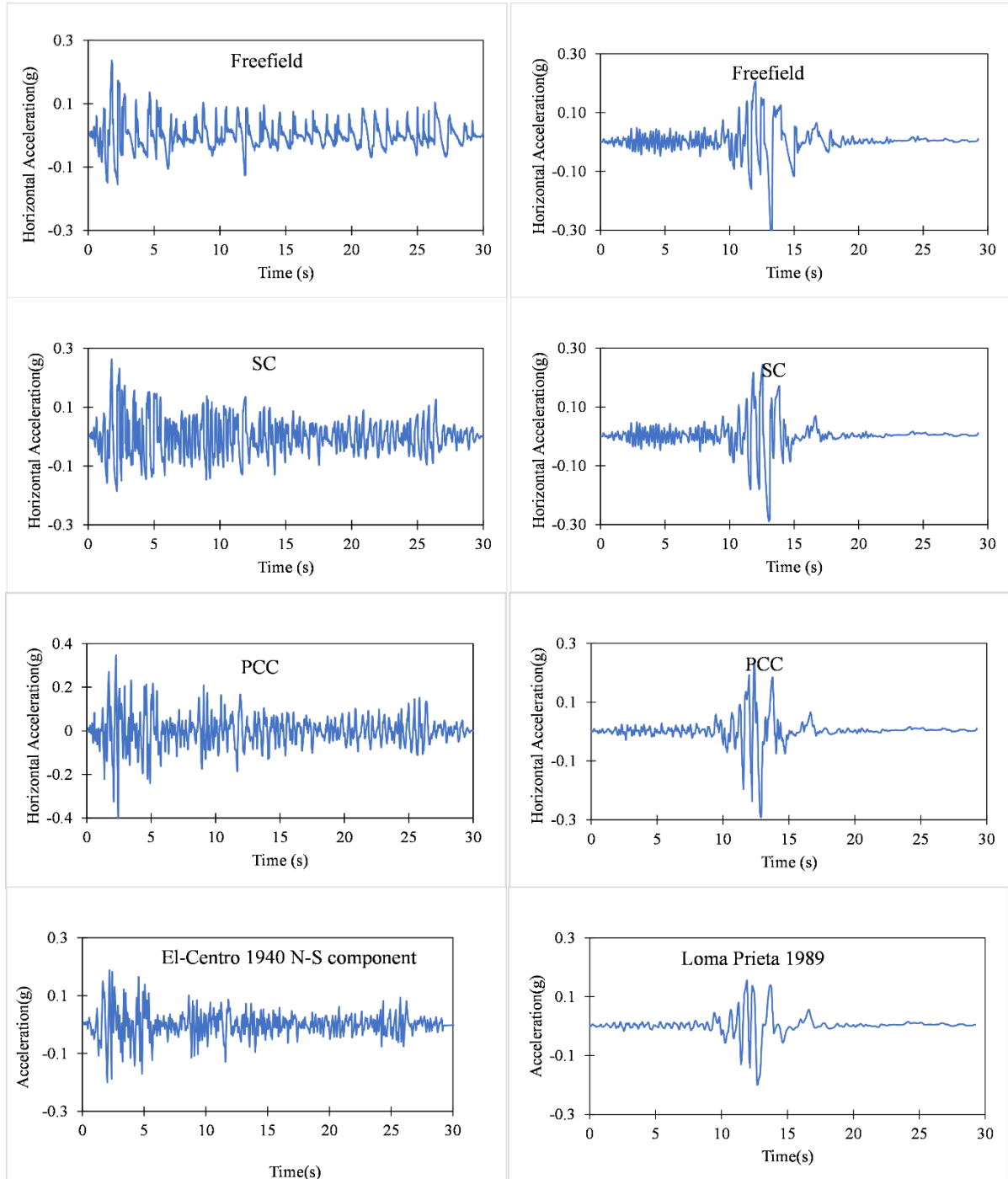
Figure 6.10 Acceleration-time history (a) Free-field case (b) SC case (c) PCC case (d) El-Centro 1940 and Loma Prieta 1989 as base excitation (Scaled to 0.2g)

Zhang et al. (2017) reported the acceleration response and excess pore water dissipation of pervious concrete pile composite foundation in comparison with gravel pile and low-grade concrete pile numerically using FLAC. The surface acceleration amplification is found to be less for pervious concrete pile composite foundation than granular pile and low-grade concrete pile. The reduction in foundation surface acceleration indicates that the upper construction resonance can be prevented using pervious concrete pile. They have also reported obvious pressure reduction effect of pervious concrete pile composite foundation. However, detailed study on surface acceleration response needs to be further investigated.

Figure 6.11 shows excess pore pressure generation of PCC case (at depths of 2 m, 4 m, 6 m and 8 m) in comparison with stone column case and free-field case. It is found that the excess pore pressure generated during earthquake shaking is very limited for pervious concrete column improved ground. The limited excess pore pressure generation (Fig.6.11) indicates that the pervious concrete column drained excess water though its pores to the surface than stone columns. This also indicates that the PCC can perform better in liquefaction scenario.

For 0.6 m diameter of column with an area ratio of 20%, excess pore water pressure - time histories at 2 m, 4 m, 6 m and 8 m depths from ground surface at the center of model (where PCC is placed) and edge of the model (surrounding sand) is analyzed as shown in Fig.6.12 (a). It reveals that the center of the model drains more water than the edge of the model as expected. This also represents that the excess pore pressure generation is very limited even at the edge of the model due to PCC inclusion (Fig.6.12 (a)). Thus, the PCC inclusion reduces the drainage path and therefore the developed excess pore water is dissipated almost as fast as it is generated during seismic shaking. This is attributed to the structure of PCC not being distorted due to seismic load. Fig.6.12 (b) shows the excess pore water pressure-time histories at 2 m, 4 m,6 m and 8 m depths from ground surface at the center of the model where SC is placed and edge of model. The SC drains more water than surrounding soil. However, the excess pore pressure generation at the surrounding soil with SC inclusion is not very limited as seen in the case of PCC. Thus, it can be concluded that both the SC and PCC dissipate water through it pores, but the better performance is seen in PCC than SC at the surrounding soil.

El Centro 1940
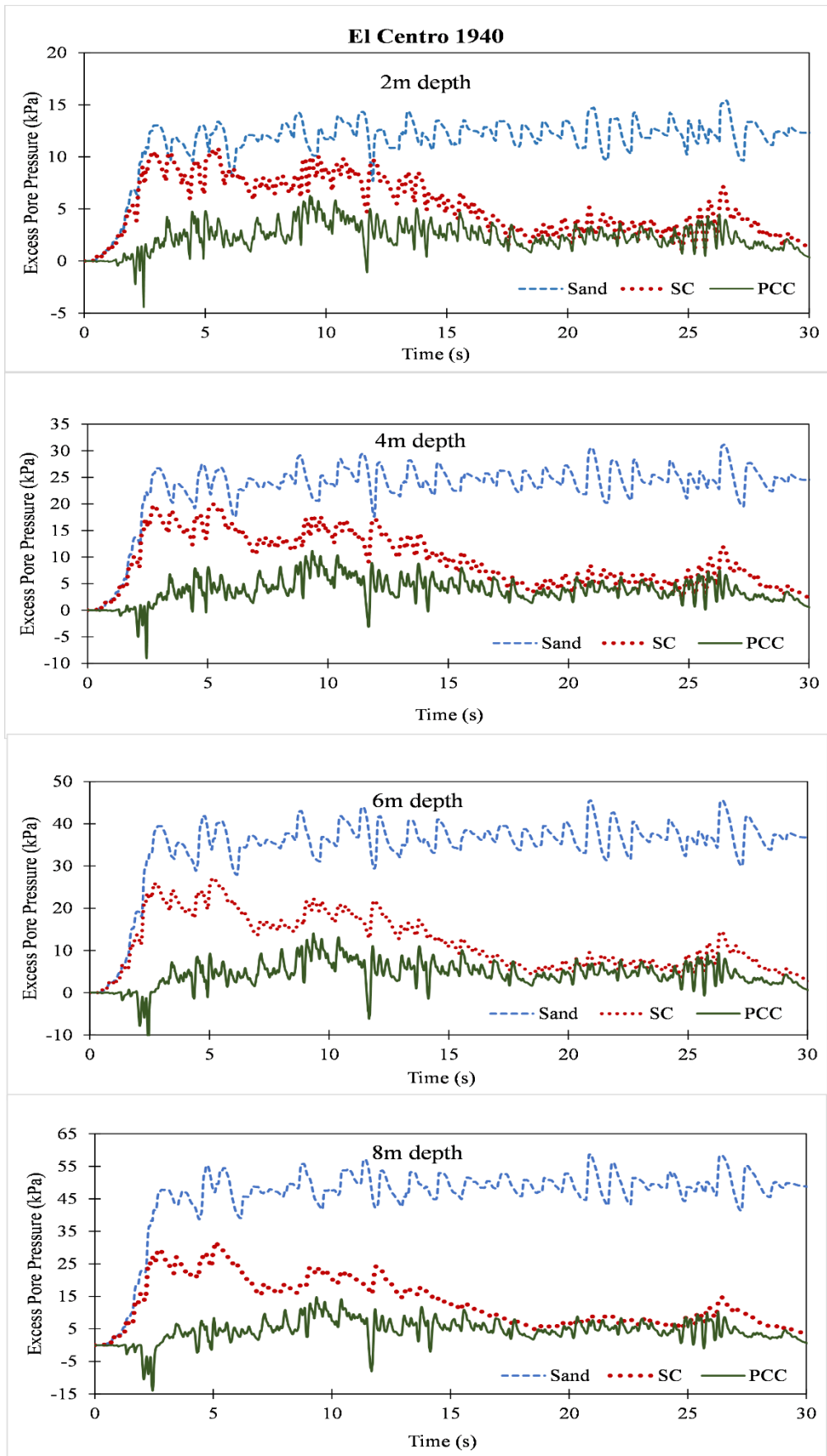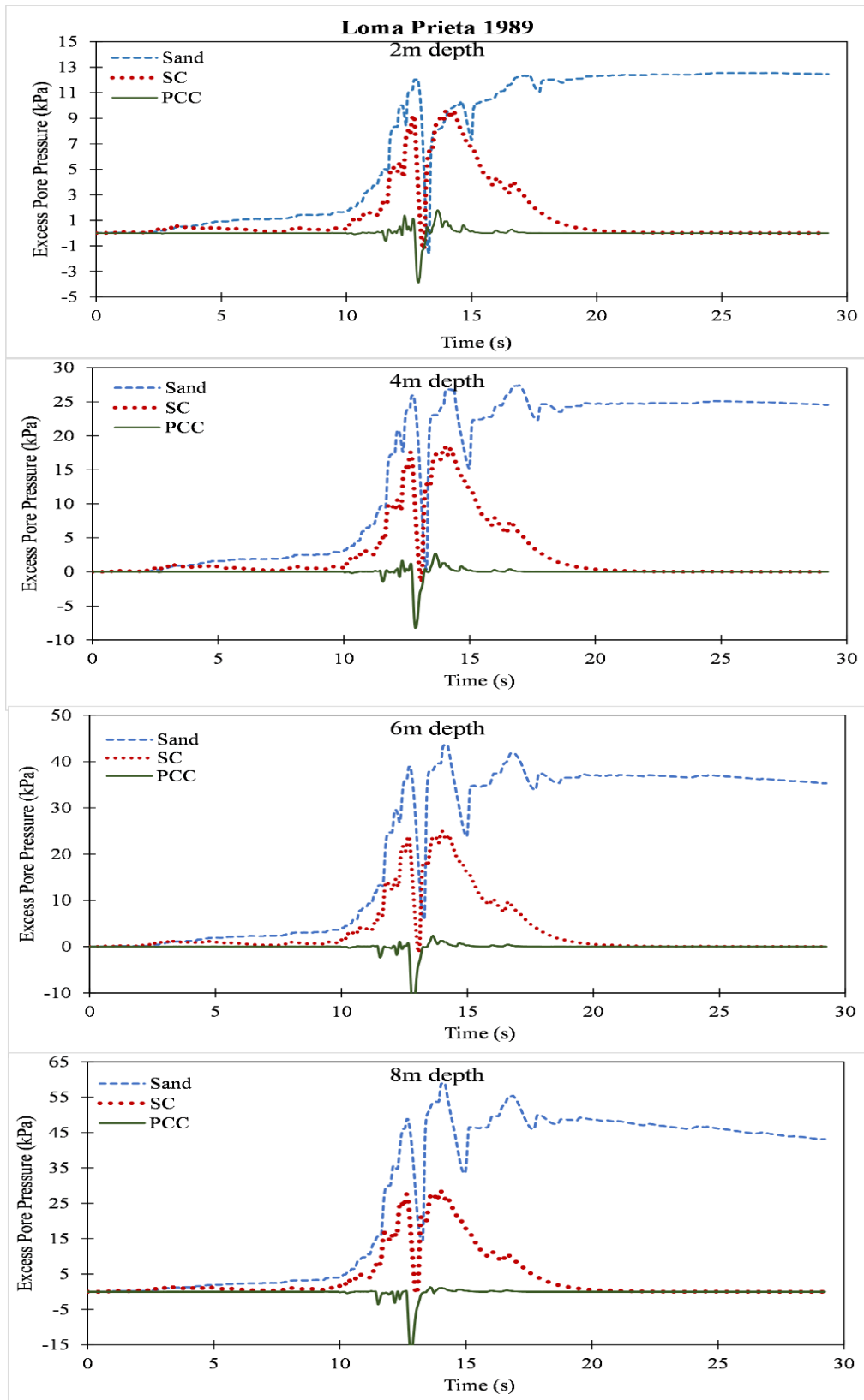
Figure 6.11 Excess pore water pressure-time histories at the center of the finite element mesh (a) at 2 m (b) at 4 m (c) at 6 m (d) at 8 m depths from ground surface.(Diameter of column =0.6 m, AR =20%)

100
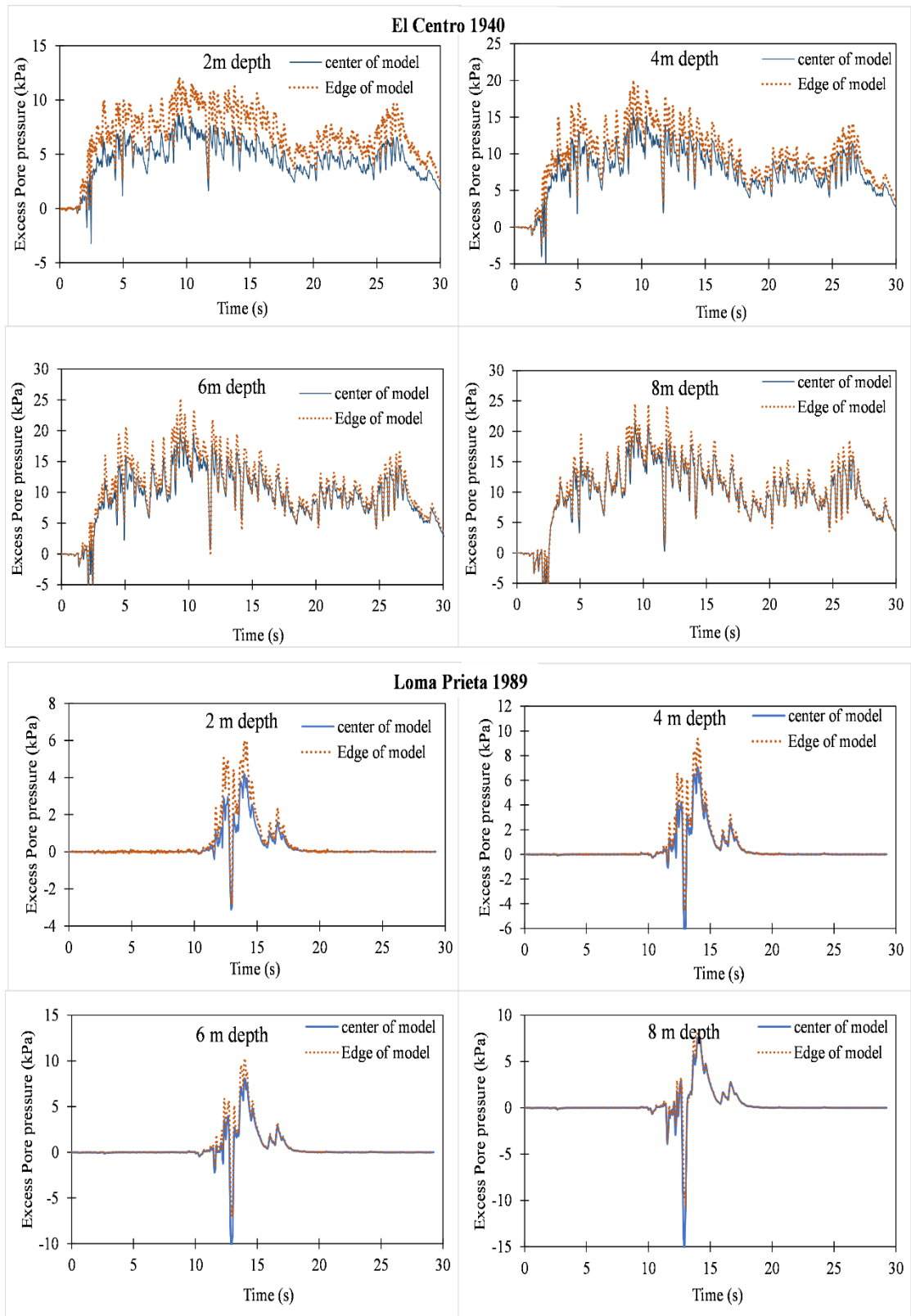
Figure 6.12 (a) Excess pore water pressure-time histories using PCC at 2 m, 4 m, 6 m and 8 m depths from ground surface at the center of the model (PCC) and edge of model (sand) (Diameter of column =0.6 m, AR =20%)
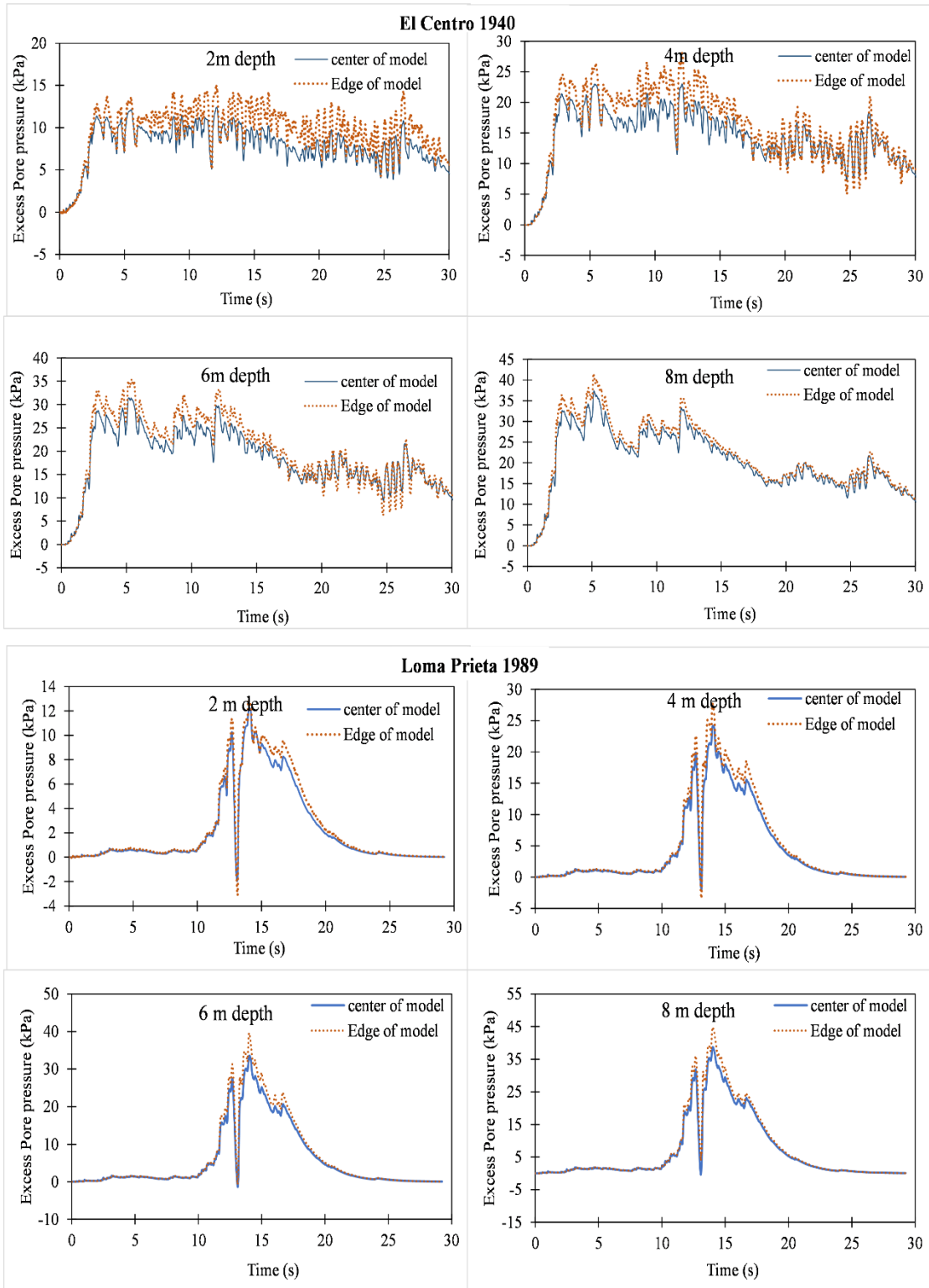
Figure 6.12 (b) Excess pore water pressure-time histories using SC at 2 m, 4 m,6 m and 8 m depths from ground surface at the center of the model (SC) and edge of model (sand) (Diameter of column =0.6 m, AR =20%)

Shear stress-strain behaviour and stress path of free-field (sand) case and improved cases with stone column (SC) and pervious concrete column (PCC) are compared. For comparison, a location is selected at a distance of 0.45 m from model center along the longitudinal direction for different depths. The selected point, 0.45 m represents the location of surrounding soil in the soil model. Figure 6.13 represents the lateral shear stress- strain plot for three cases at depths of 1.4 m, 3.4 m 5.4 m and 7.4 m from the ground surface level. It is evident that the shear stress-strain reduces sharply for PCC case than SC case (Fig.6.13). This reduction in shear stress-strain is attributed to the dissipation of excess pore pressure. The shear stress versus effective confinement stress plot is shown in Fig.6.14. Detailed stress path of three cases at a distance of 0.45 m from model center at 1.4 m, 3.4 m, 5.4 m and 7.4 m depth from the ground surface is shown in Appendix II. For the column improved ground shown in Appendix II, the diameter of column considered is 0.6 m for an area ratio of 20%. Relatively larger effective confinement stress is seen in PCC case when compared to SC case and free-field case and therefore higher shear resistance is generated.

For all the depths shown in Fig.6.14, the effective confinement stress of PCC is relatively higher than SC case. Also, the shear strain levels in PCC case are significantly lesser than SC case. However, it is noted that the shear strain amplitude of surrounding soil in the case of SC improved ground at the depth of 3.4 m (7.5%) is higher than the shear strain amplitude at 1.4 m and 5.4 m (4% and 1% respectively) (Fig.6.13). This indicates that the surrounding soil liquefied at 3.4 m for SC improved ground under El-Centro motion. The liquefaction of surrounding soil at the depth of 3.4 m increased the shear stress levels of SC improved ground at depths of 5.4 m and 7.4 m as shown in Fig.6.14. However, this type of liquefaction behaviour is not observed for SC improved ground under Loma Prieta excitation. And PCC improved ground has not shown any liquefaction behaviour under El-Centro as well as Loma Prieta excitations, indicating its better performance than SC.

Due to limited excess pore pressure generation of PCC improved ground (Fig.6.11), reduction in shear stress-strain behaviour (Fig.6.13) and stress path (Fig.6.14) confirms the higher liquefaction mitigation potential of pervious concrete columns.

Figure 6.15 illustrates the shear stress-time histories of soil element at a distance of 0.45 m from centre of finite element mesh for 1.4 m, 3.4 m, 5.4 m and 7.4 m depth

respectively from ground surface. The shear stress-time history plot at a distance of 0.45m from the model center represents the surrounding soil around improved SC and PCC case. The free field case, SC case and PCC case are compared for the diameter of end-bearing column 0.6 m with an area ratio of 20%. The shear stress-time history plot shows peak shear stress values at points where peak earthquake acceleration is observed (Fig.6.15) for all three cases considered.

The shear stress- time histories of soil element at the center of model for the depths of 1.4 m, 3.4 m, 5.4 m and 7.4 m from ground surface is shown in Fig.6.16. The shear stress-time history plot at the center represents the shear stress developed in the center of stone column as well as pervious concrete column. It is noted that that the shear stress-time response of PCC case started increasing at the time where peak earthquake acceleration occurred. Thereafter the shear stress remained high and constant till the end of shaking duration (Fig.6.16). Whereas for SC case, the shear stress at the center of model is found to be almost negligible when compared to PCC case. Increase in shear stress is observed with increase in depth considered for PCC case (Fig.6.16). This indicates the higher shear resistance offered by pervious concrete column in place of stone column.

From Fig.6.15 and Fig.6.16, it is clear that for free-field case SC and PCC case, the surrounding soil has reached near zero shear stress at the end of shaking duration whereas at the center of PCC, shear stress increased. It is also noted that the stone column center has shown less shear stress during earthquake shaking, indicating weak shear performance of stone column improved case.

In the case of SC improved ground, the dense gravel piles (stone column) get distorted during seismic loading due to shearing and causes dilation (increase in volume). The distorted gravel structure of stone column increases the length of the drainage path thereby retarding the dissipation of excess pore water generated due to shaking. This causes reduction in effective stress and results in more lateral displacement. The PCC inclusion shortens the drainage path for excess pore water to dissipate quickly as the PCC structure is not distorted due to seismic shaking. Therefore, the seismic shear strains developed in the soil is very less. The limited excess pore pressure generation and relatively higher effective confinement reduces the lateral displacement of PCC improved ground significantly.

104

The liquefaction mitigation potential of pervious concrete column improved ground is assessed using criteria based on excess pore pressure, shear strength criteria and shear strain or shear deformation criteria. The excess pore pressure generated in PCC improved ground is much lesser than that of SC improved ground as well as unimproved ground subjected to similar conditions. The reduction in excess pore pressure is seen at the times of peak input earthquake acceleration. It is also noted that, the shear stress of surrounding soil is found to be having non-zero value during the strong shaking. The reduction in excess pore pressure shows significant reduction in shear stress-strain behaviour and relatively higher effective confinement. Therefore, it can be concluded that pervious concrete column improved ground performs better than stone column improved ground under earthquakes.

El Centro 1940
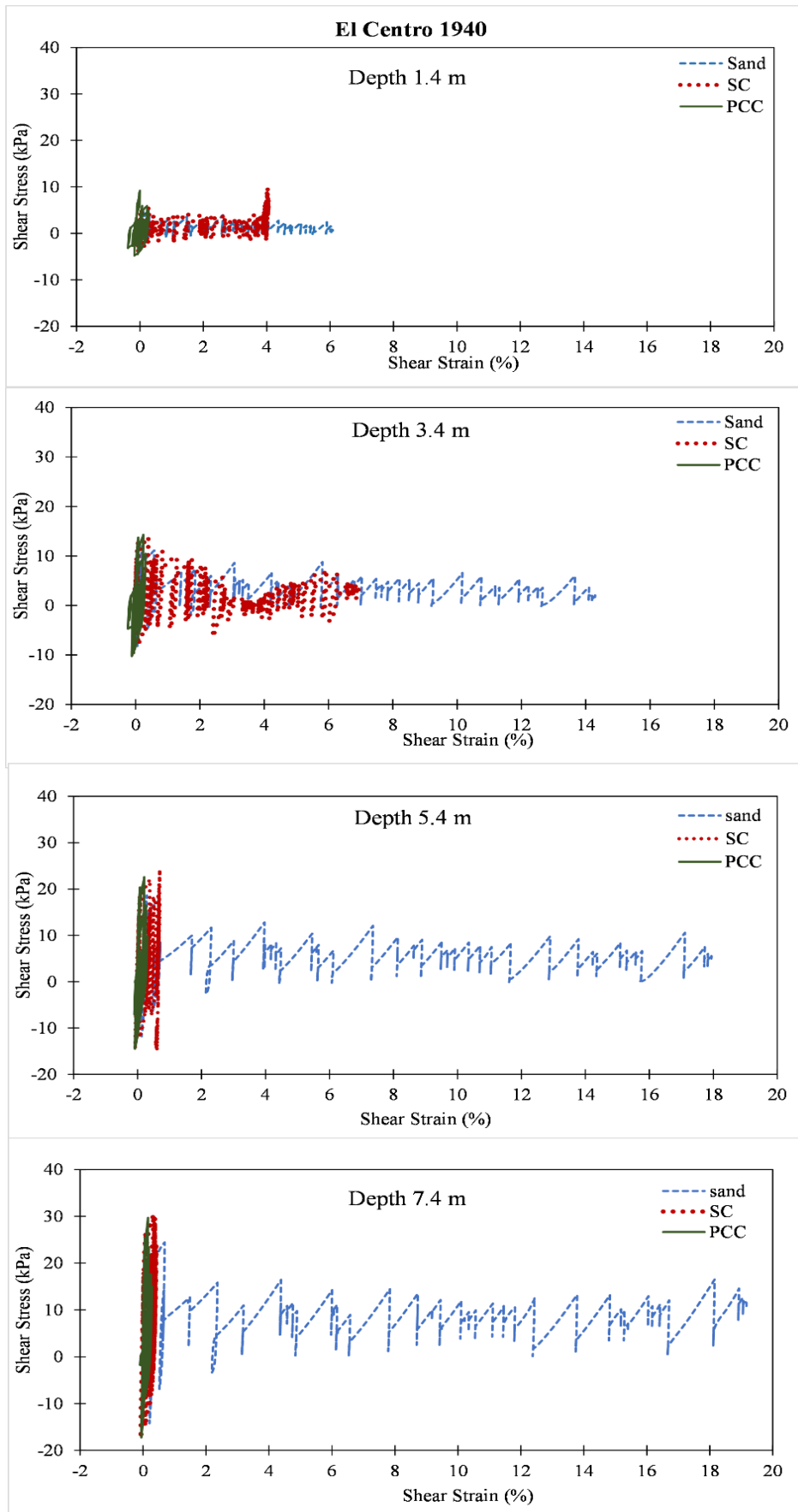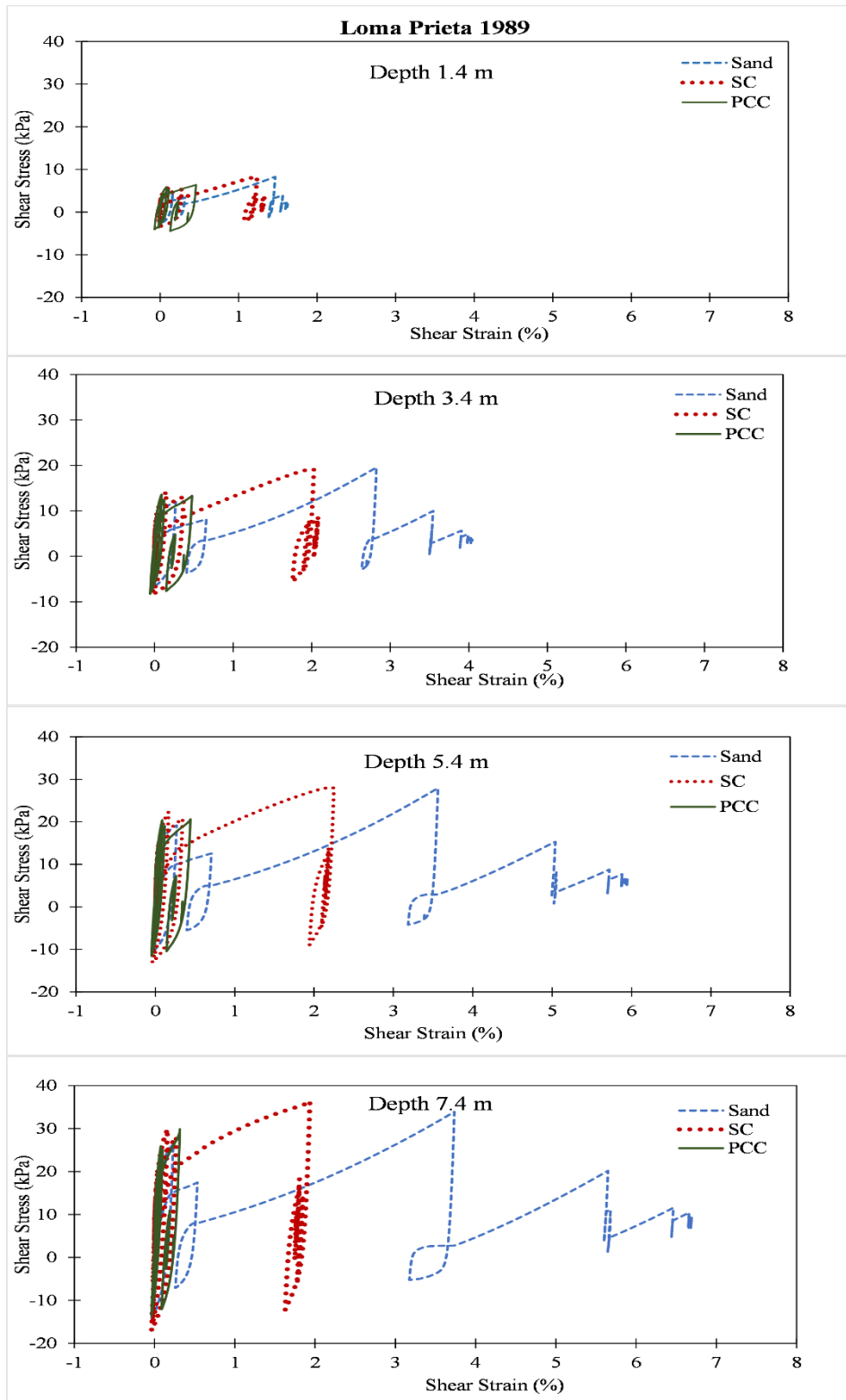
Figure 6.13 Shear stress versus shear strain responses under El-Centro and Loma Prieta ground motions at a distance of 0.45 m from model center at (a) 1.4 m (b) 3.4 m (c) 5.4 m (d) 7.4 m depth from ground surface (Diameter of column =0.6 m, AR =20%)

El Centro 1940
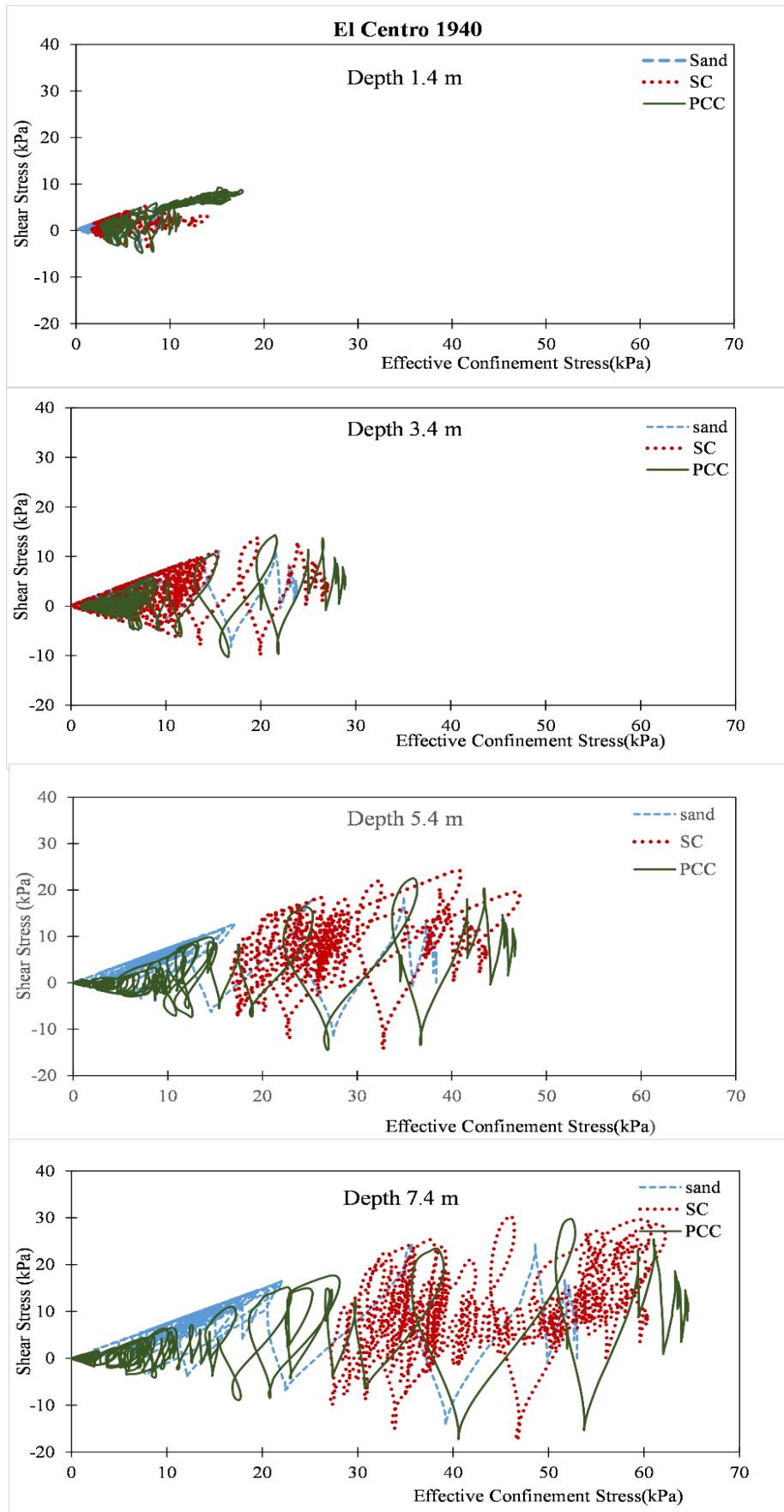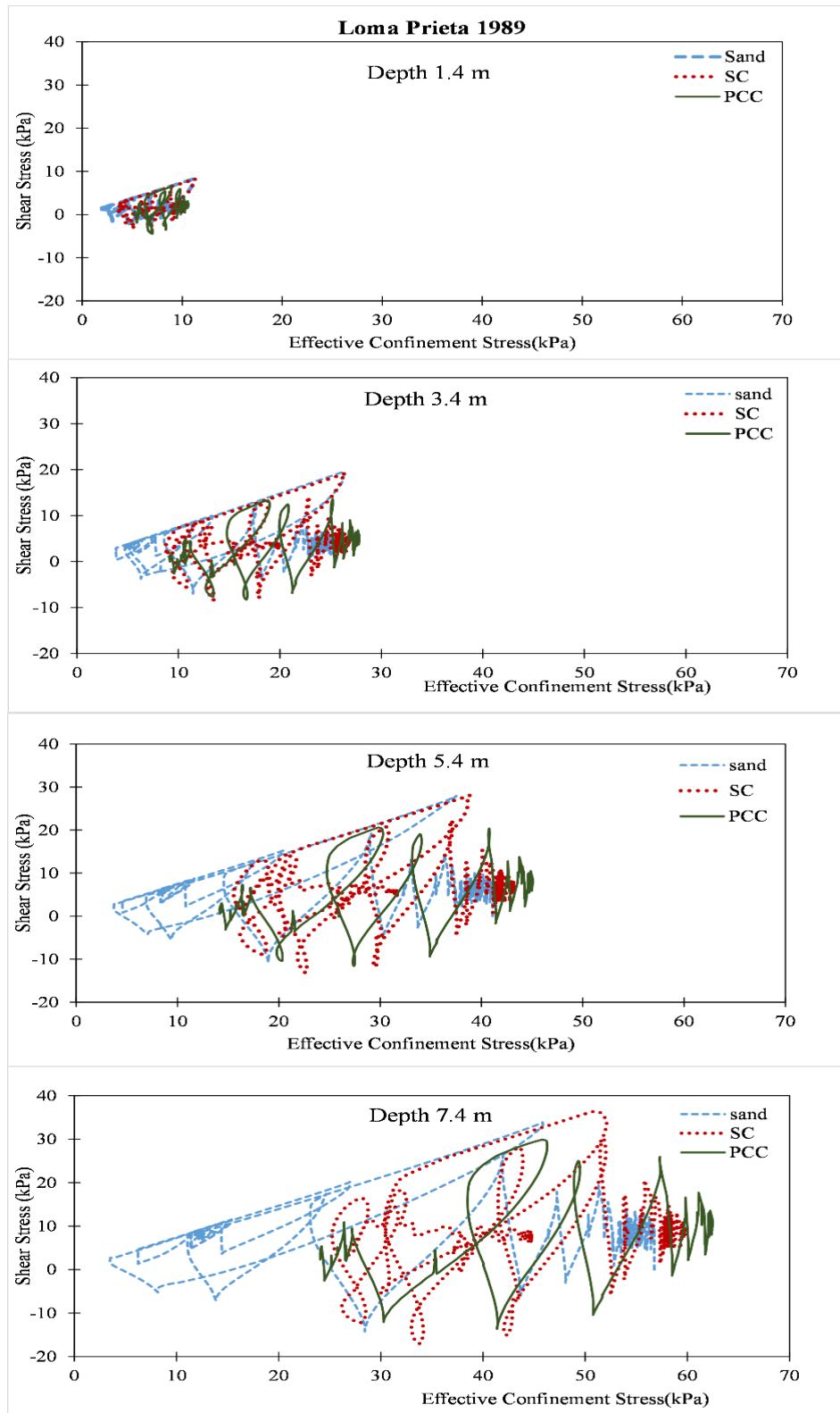
Figure 6.14 Shear stress versus Effective Confinement Stress of soil elements under El-Centro and Loma Prieta ground motions at a distance of 0.45 m from model center at (a) 1.4 m (b) 3.4 m (c) 5.4 m (d) 7.4 m depth from ground surface (Diameter of column =0.6 m, AR =20%)
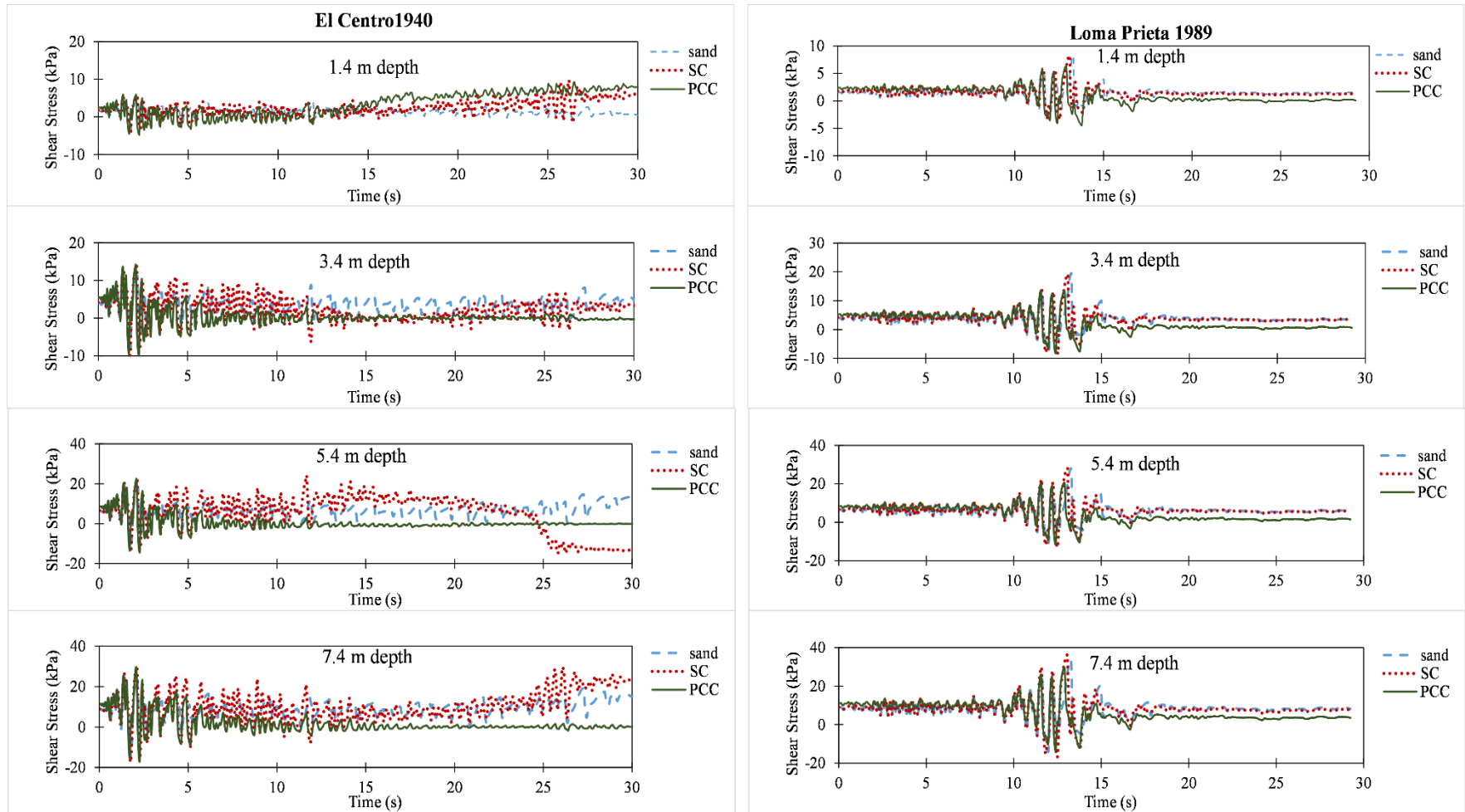
Figure 6.15 Shear stress- time histories of soil element at a distance of 0.45 m from centre of finite element mesh at (a) 1.4 m (b) 3.4 m (c) 5.4 m and (d) 7.4 m depth from ground surface (Diameter of column =0.6 m, AR =20%)
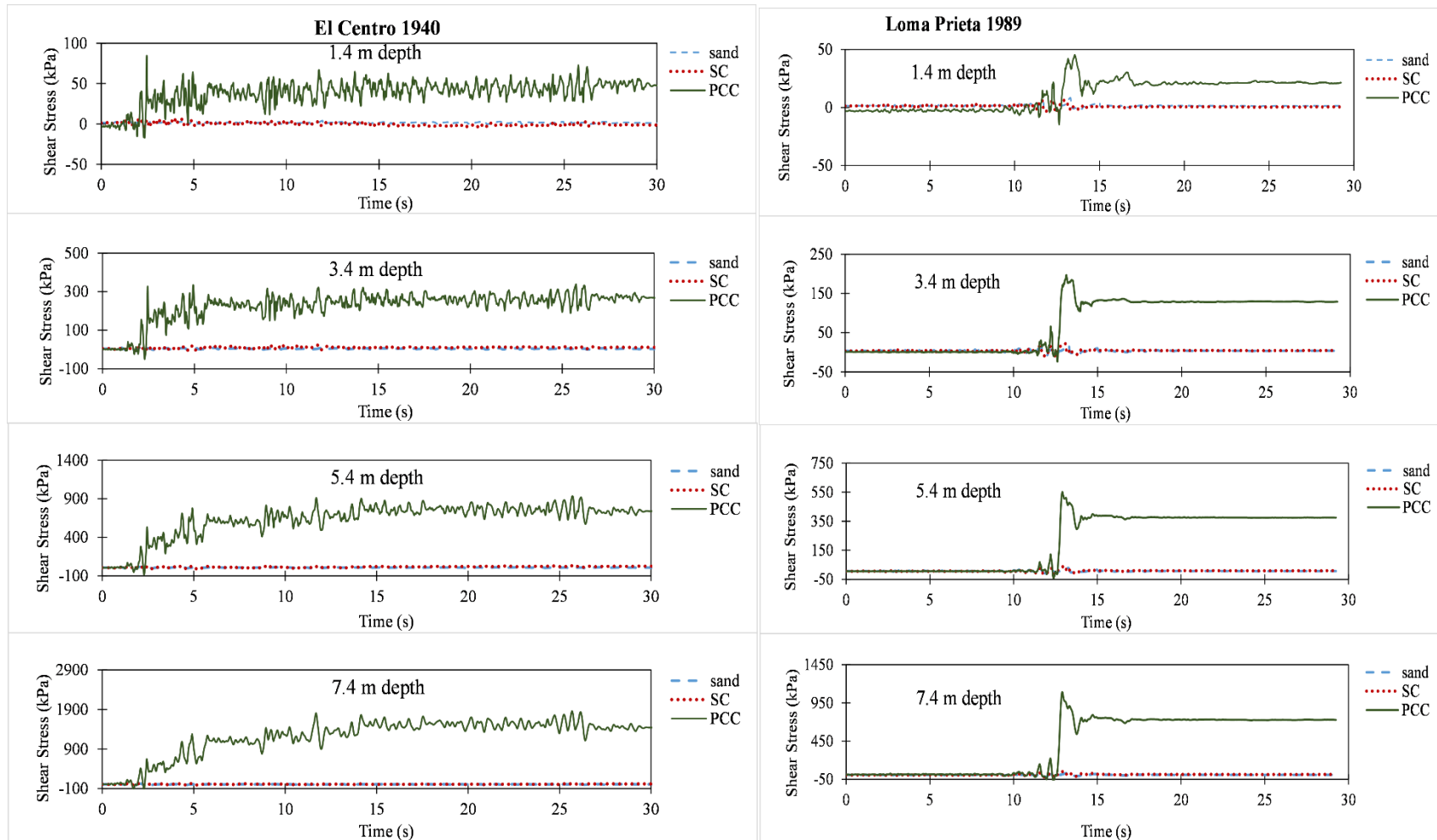
Figure 6.16 Shear stress- time histories at the centre of finite element mesh at (a) 1.4 m (b) 3.4 m (c) 5.4 m and (d) 7.4 m depth from ground surface (Diameter of column =0.6 m, AR =20%)

111

6.7.2 Effect of floating PCC vis-à-vis end bearing columns

The seismic performance was analyzed for floating columns with L/D ratio varying from 4 to 8. The performance was compared with end-bearing PCC and SC. The diameter of column and area ratio were kept constant as 1 m and 13% respectively. The lateral deformation at ground surface with floating PCC inclusion are found to be more than stone column with end bearing condition as shown in Fig 6.17. The lateral displacement profile along the depth of soil below ground level at the center of finite element mesh are as shown in Fig.6.18. It determines that the floating pervious concrete columns are found to move further along the floating depth than stone column with end bearing condition. Therefore, it is recommended to provide full depth of pervious concrete column for better and optimum performance. However, the end-bearing stone column has undergone more lateral displacement when compared to end-bearing pervious concrete column. The better seismic performance of end-bearing PCC improved ground is attributed to the rigidity of pervious concrete column material along with its founding depth.

The performance of pervious concrete column with L/D ratio of 8 is found to have similar lateral displacement as that of end bearing stone column (Fig.6.17). It is important to note that in the lateral displacement profile (Fig.6.18), the floating PCC with L/D ratio 8 has moved significantly more along the founding depth in between rigid rock (10m) and founding depth (8m). This is same for the three floating conditions considered and the lateral displacement of PCC column is found to be significantly more between hard strata and founding depth. Therefore, it is highly recommended to provide the pervious concrete column till the hard strata for minimizing lateral spreading during earthquakes.
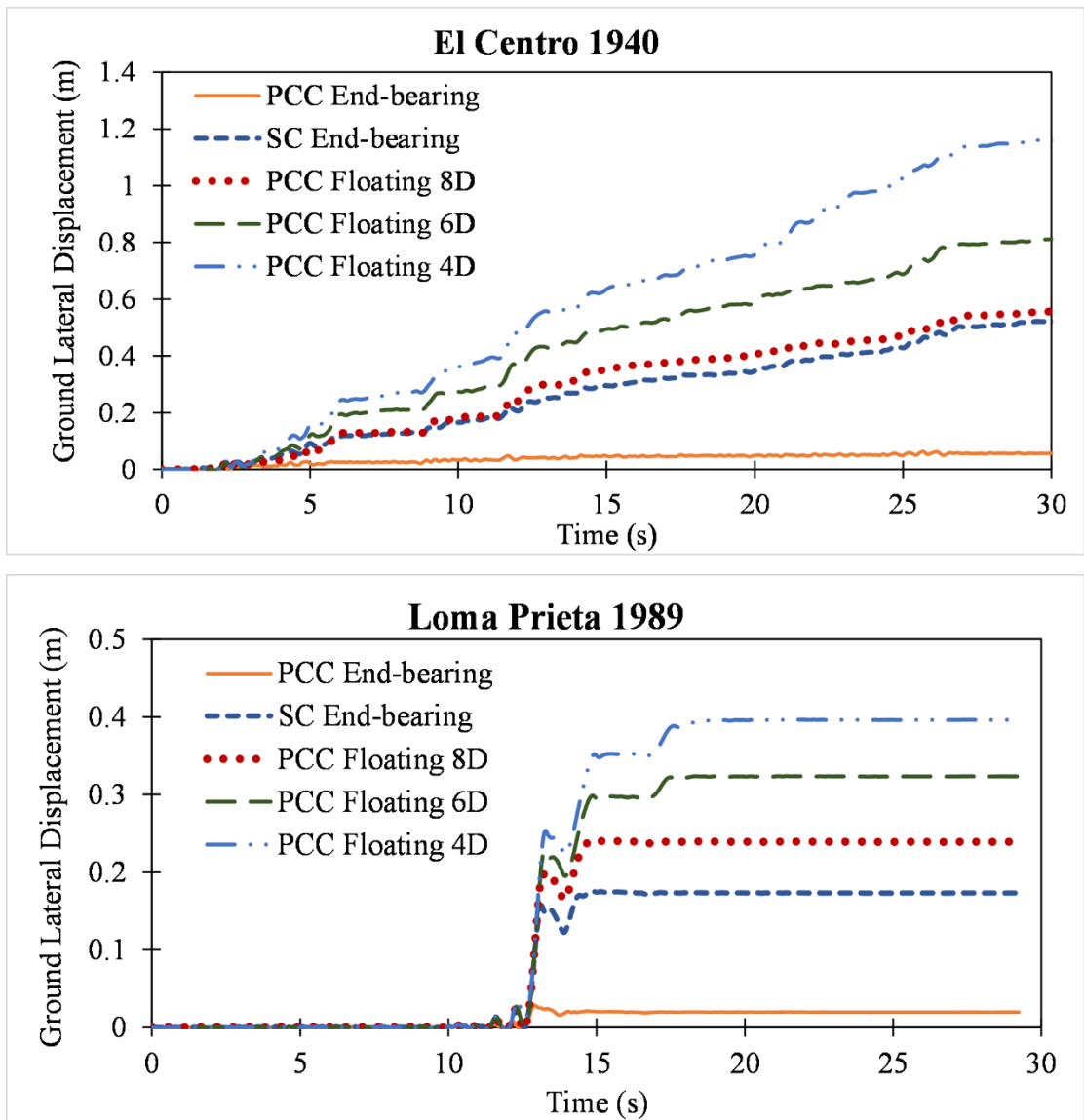
Figure 6.17 Effect of depth of PCC (Diameter of column =1.0 m, AR =13%)
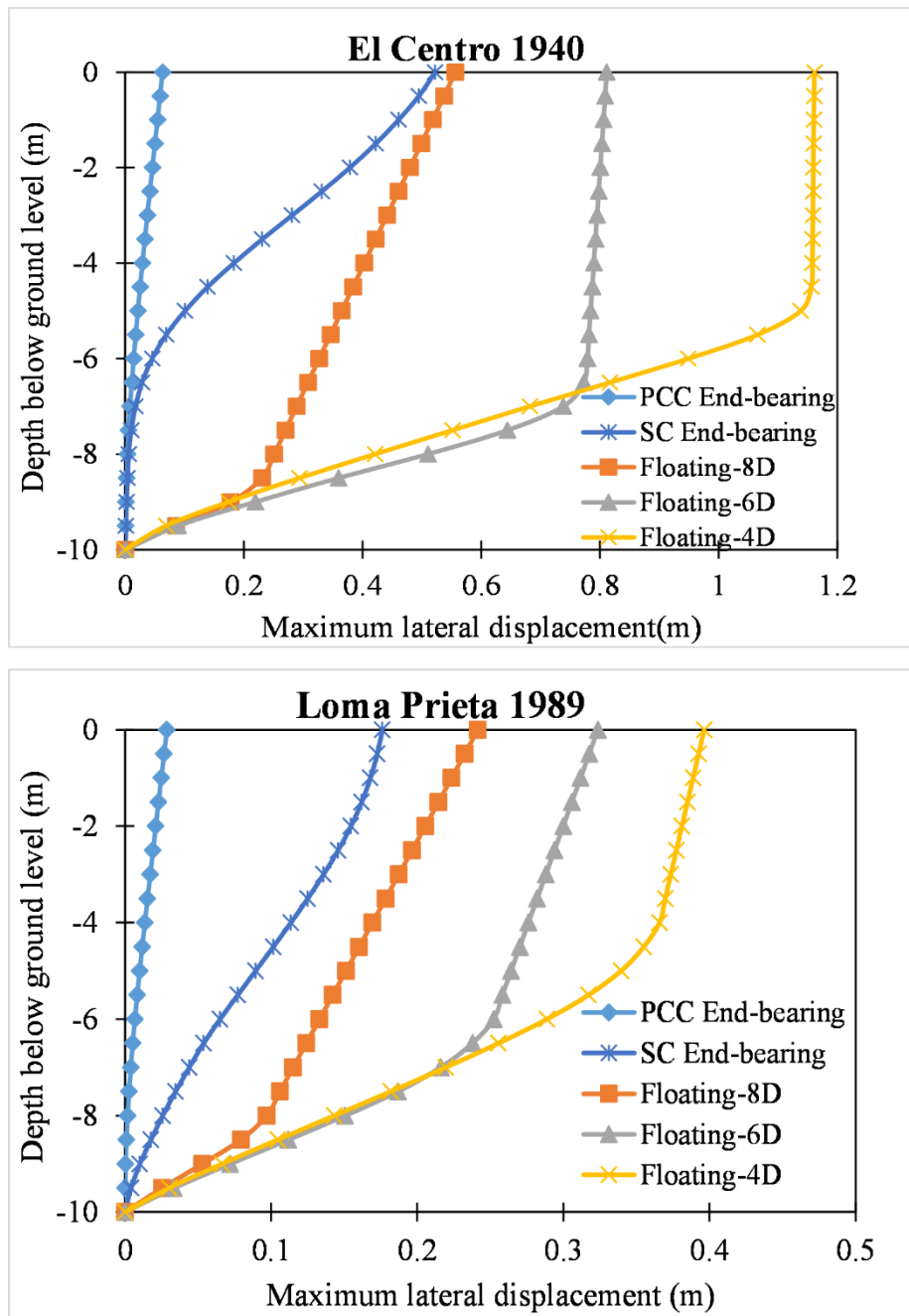
Figure 6.18 Maximum lateral displacement of PCC and SC at the center of finite element mesh (Diameter of column =1.0 m, AR =13%)

6.7.3 Effect of area ratio

In order to study the effect of area ratio, column of diameter 0.6 m with end bearing condition was analyzed with area ratios ranging from 20% to 9%. It is found that the performance of both SC and PCC improved ground improves with increase in area ratio (Fig.6.19). The ground lateral displacement assessed at the center of the improved soil model with PCC inclusion having an area ratio of 9% is found to be lesser than with

SC inclusion with an area ratio of 20%. Generally, it is difficult to achieve 20% area ratio in field due to proximity of columns. Hence it is economical and practically feasible to provide PCC with wider spacing instead of conventional SC at closer spacing.
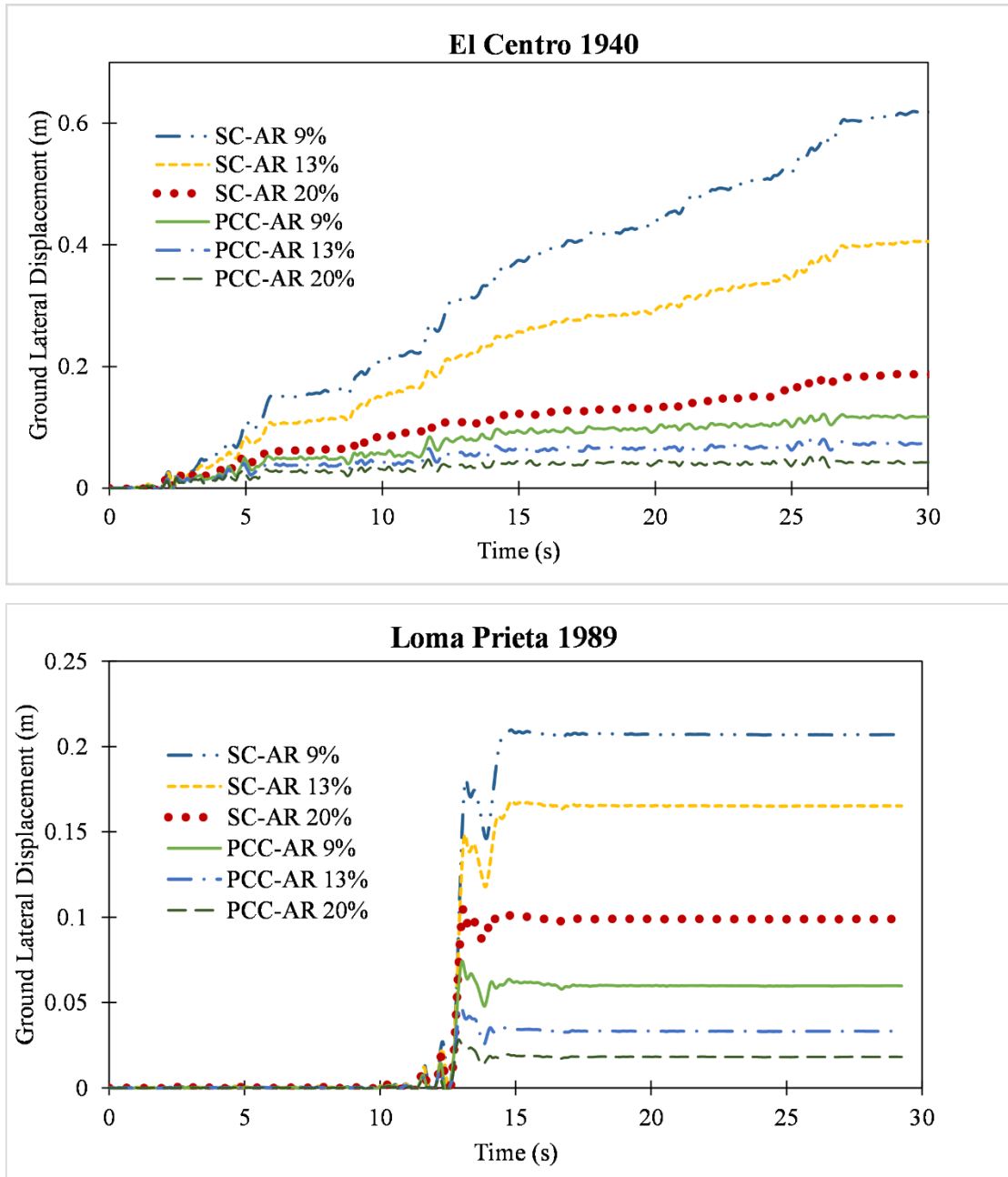
Figure 6.19 Effect of area ratio (Diameter of column =0.6 m, End-bearing condition)

6.7.4 Effect of diameter

The effect of diameter of PCC was studied by varying the diameter (0.6 m, 1.0 m and 1.2 m) respectively for a constant area ratio of 13% and with end bearing conditions. A plan showing constant area ratio of 13% for various diameter columns is presented in Fig.6.3(c). The end bearing condition was selected because of its enhanced performance compared to floating columns. It is seen that the lateral deformation decreased with increase in diameter for both stone column and PCC (Fig.6.20). This could be attributed to the stiffness of improved ground with larger diameter columns. The lateral displacement profile along the soil depth for pervious concrete column and stone column are as shown in Fig.6.21. It is found that the pervious concrete column behaves like rigid pile with very less lateral deformation similar to that of rigid concrete pile with free head conditions (Fig.6.21). The stone column has undergone more lateral displacement as compared to pervious concrete column. The better seismic performance of PCC improved ground is attributed to the rigidity of pervious concrete column material.
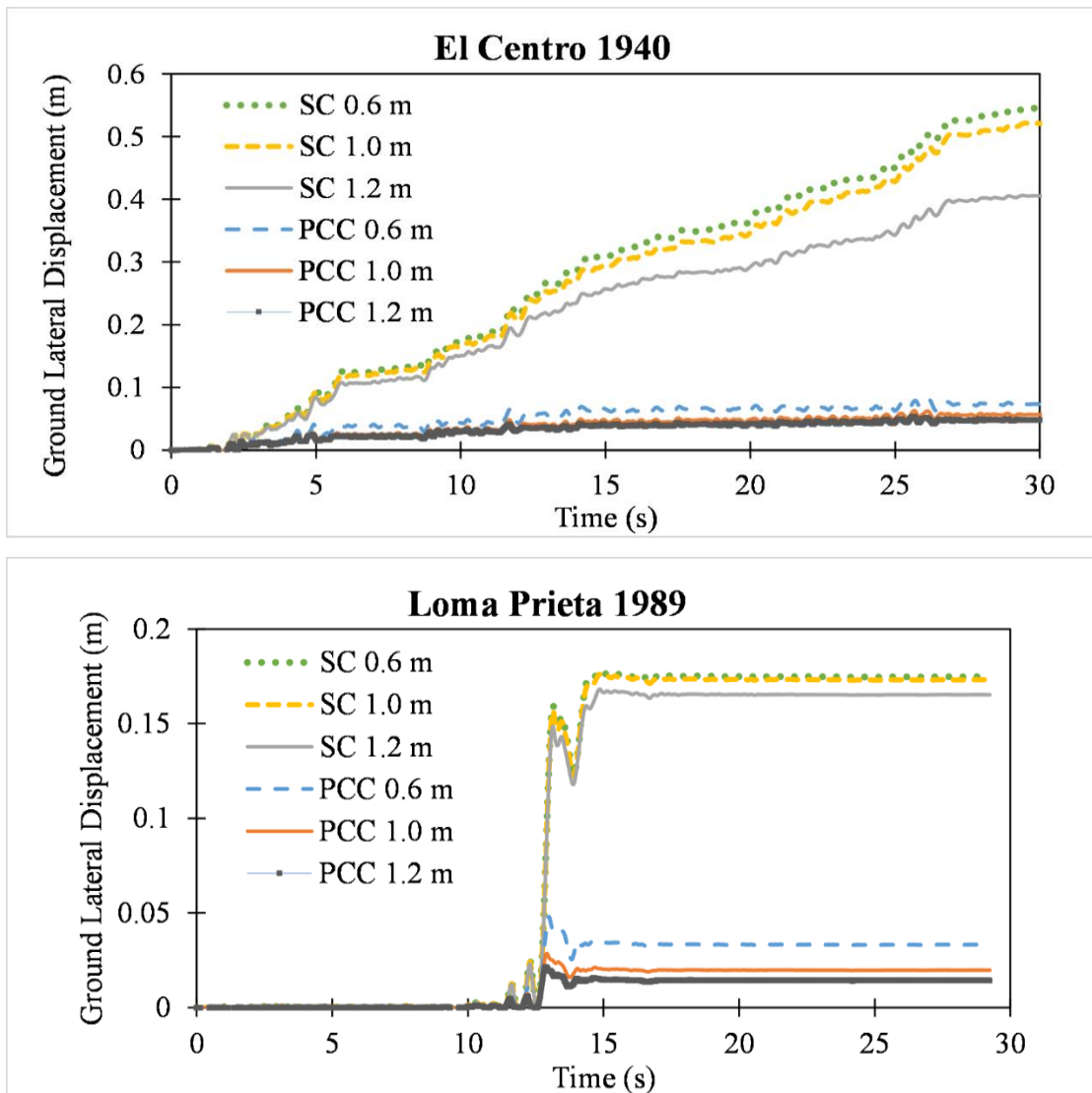
Figure 6.20 Effect of diameter of PCC on ground lateral displacement (AR=13%, End-bearing condition)
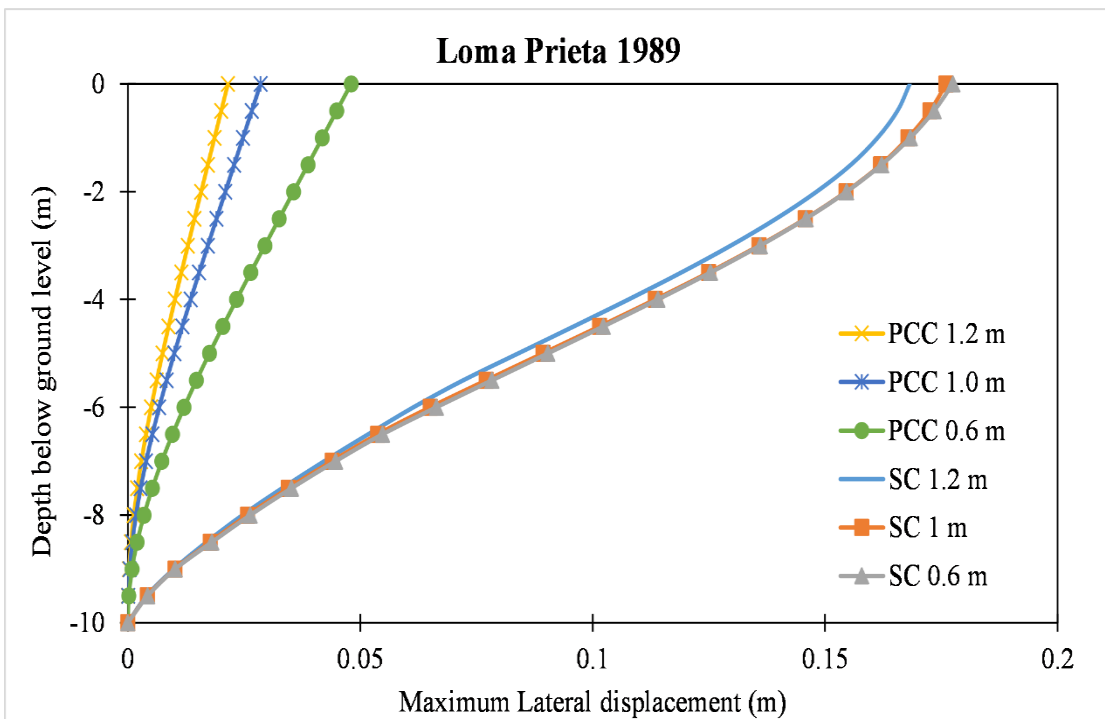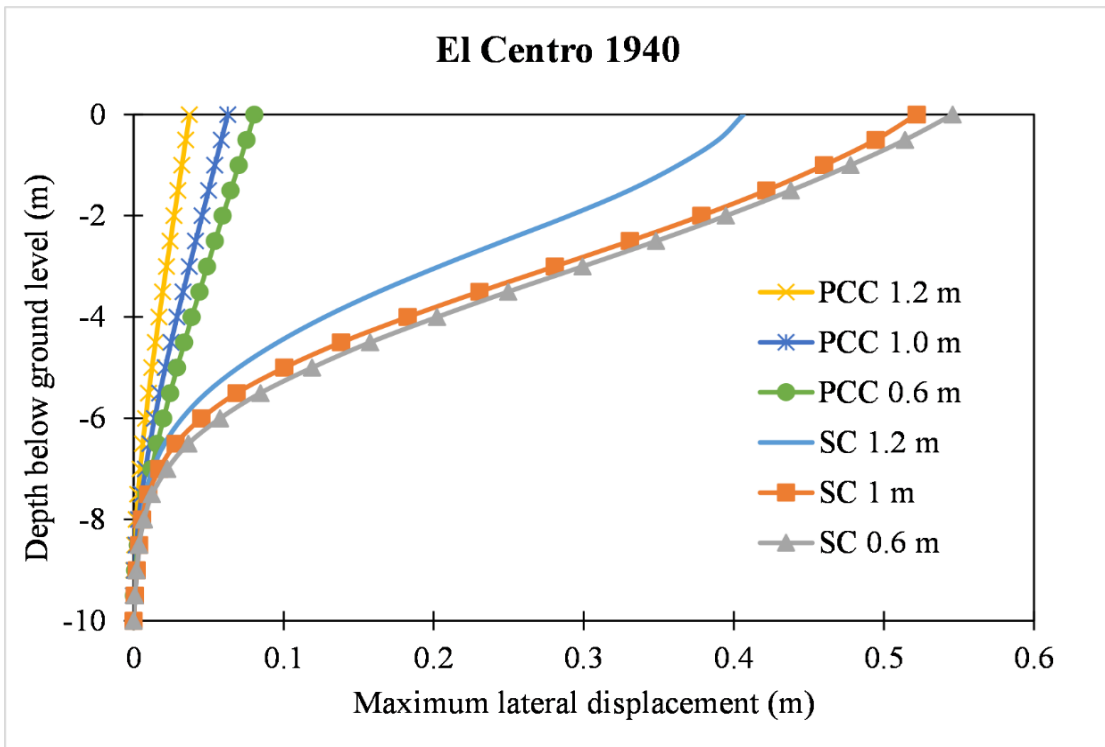
Figure 6.21 Maximum lateral displacement of PCC and SC at the center of FE mesh (AR=13%, End-bearing condition)

6.7.5 Effect of permeability of PCC

Effect of permeability of PCC was studied by varying permeability of pervious concrete material as 0.01 m/s, 0.1 m/s and 1.0 m/s for PCC of diameter 1m and with an area ratio of 13%. The columns with end bearing conditions were considered. Also, the clogged condition of PCC was analyzed by reflecting the hydraulic conductivity of pervious concrete the same as surrounding sand strata.

From Fig.6.22, it is found that the lateral deformation of improved ground is not significantly influenced by increase in permeability of pervious concrete column inclusion. Figure.6.23 represents the excess pore pressure ratio-time histories of PCC improved ground with varying permeability and is compared with SC improved ground. The excess pore pressure ratio is defined as the ratio of excess pore pressure to initial vertical stress. Liquefaction is initiated when excess pore pressure becomes equal to initial vertical stress, ie, r_u= 1.0. However, the value of excess pore pressure ratio r_u is considered as 0.6 (r_u< 1.0) for sloping strata (Jiaer et al. 2004). It is found that the excess pore pressure ratio (r_u) with all three varying pervious concrete permeability (0.01 m/s, 0.1 m/s and 1.0 m/s) is less than 0.6, which means that the improved ground is non-liquefied (Jiaer et al. 2004). Also, for PCC improved ground, r_u is found to be approximately 0.1 and zero for PCC permeability of 0.1 m/s and 1m/s respectively (Fig.6.23). The increase of pervious concrete permeability to 0.1 m/s can escalate the liquefaction mitigation using PCC improved ground significantly.

The excess pore pressure ratio, r_u for PCC improved ground is compared with clogged PCC as shown in Fig.6.24. The seismic performance of clogged PCC is found to be similar as stone column with normal unclogged hydraulic conductivity in terms of r_u ratio (Fig.6.24). The improved ground with clogged PCC and SC normal unclogged permeability has similar r_u ratio around 1.5. Thus, a clogged PCC is concluded to limit excess pore pressure generation similar to the working of unclogged stone column.
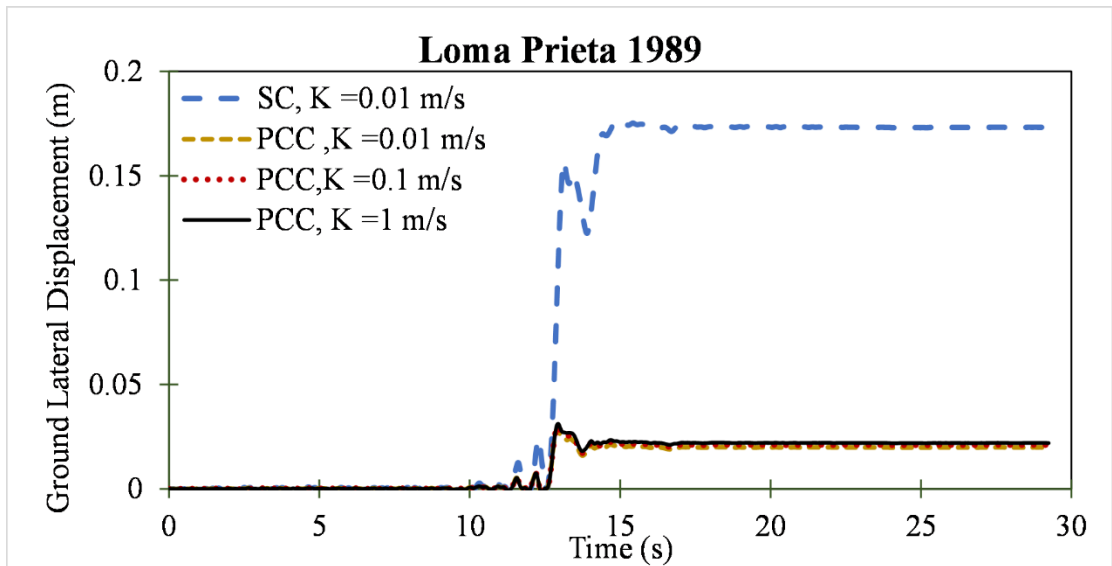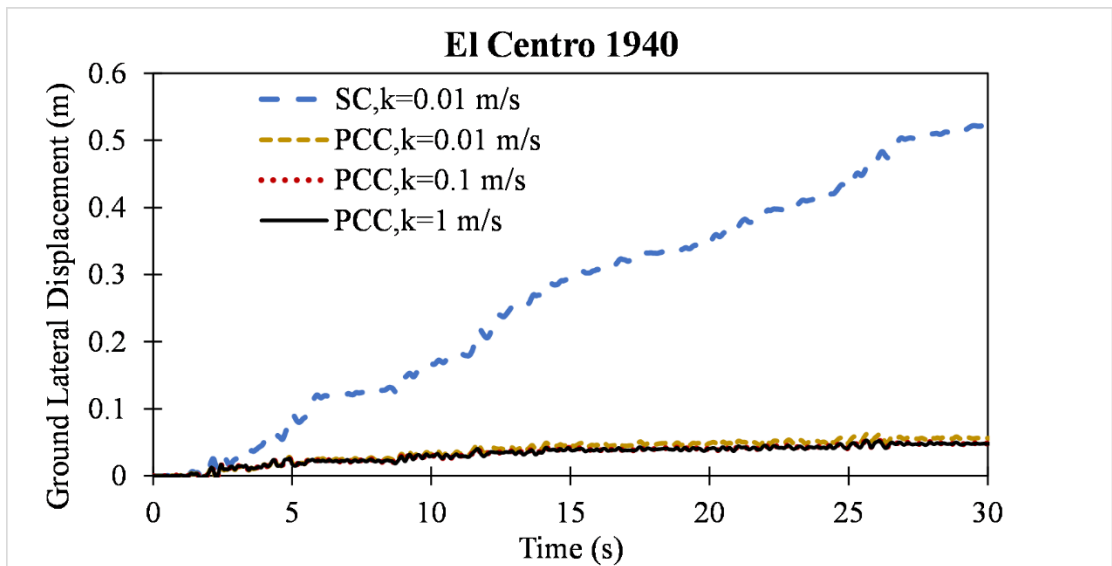
Figure 6.22 Effect of permeability of PCC on ground lateral displacement (Diameter of column =1.0 m, AR=13%, End-bearing condition)

El Centro 1940

121
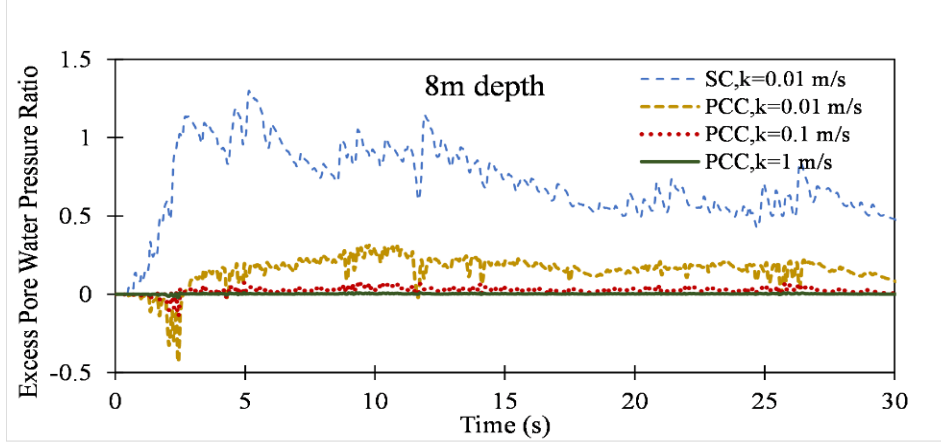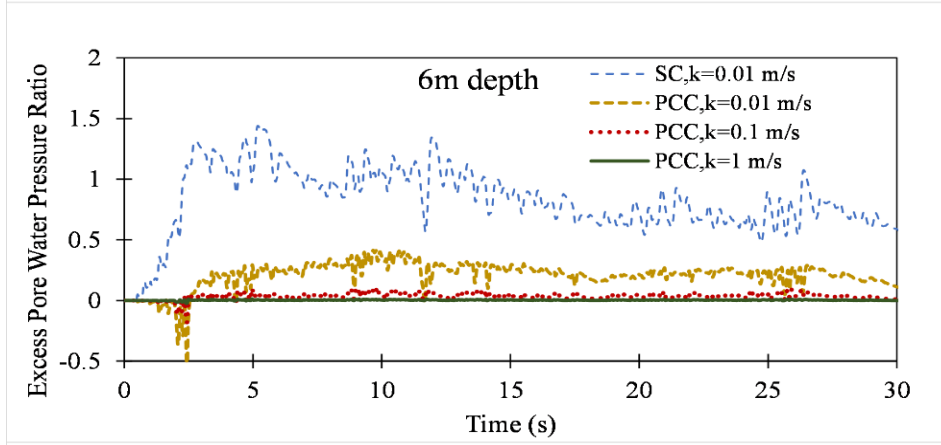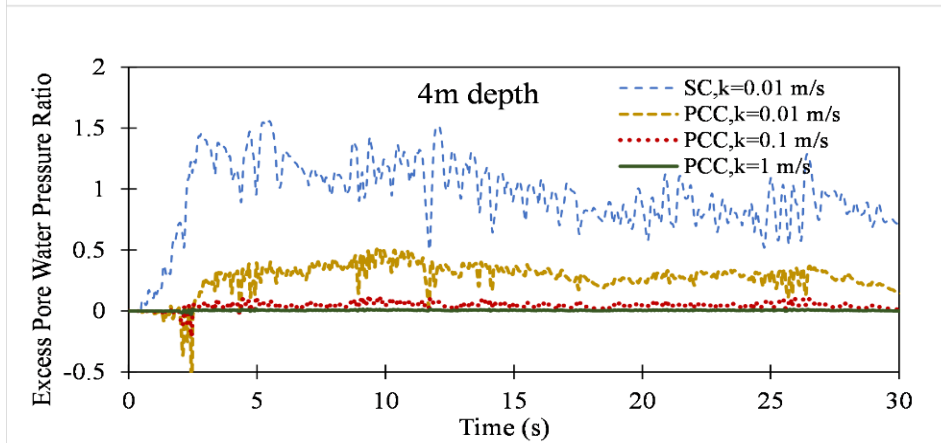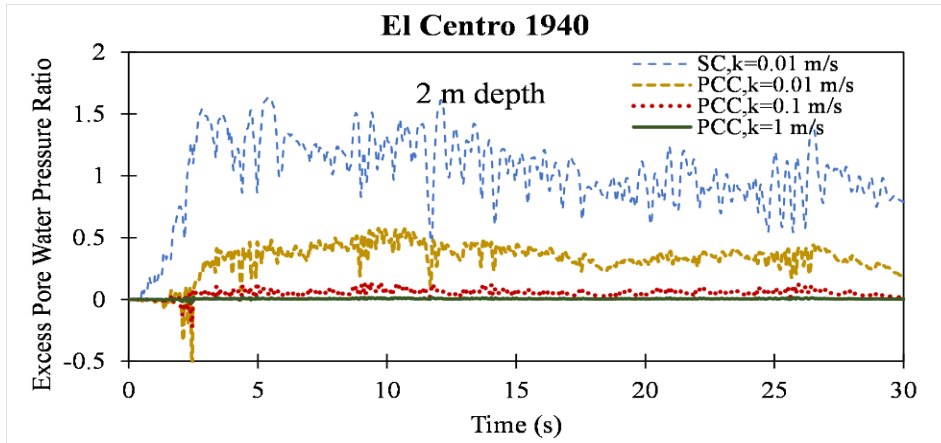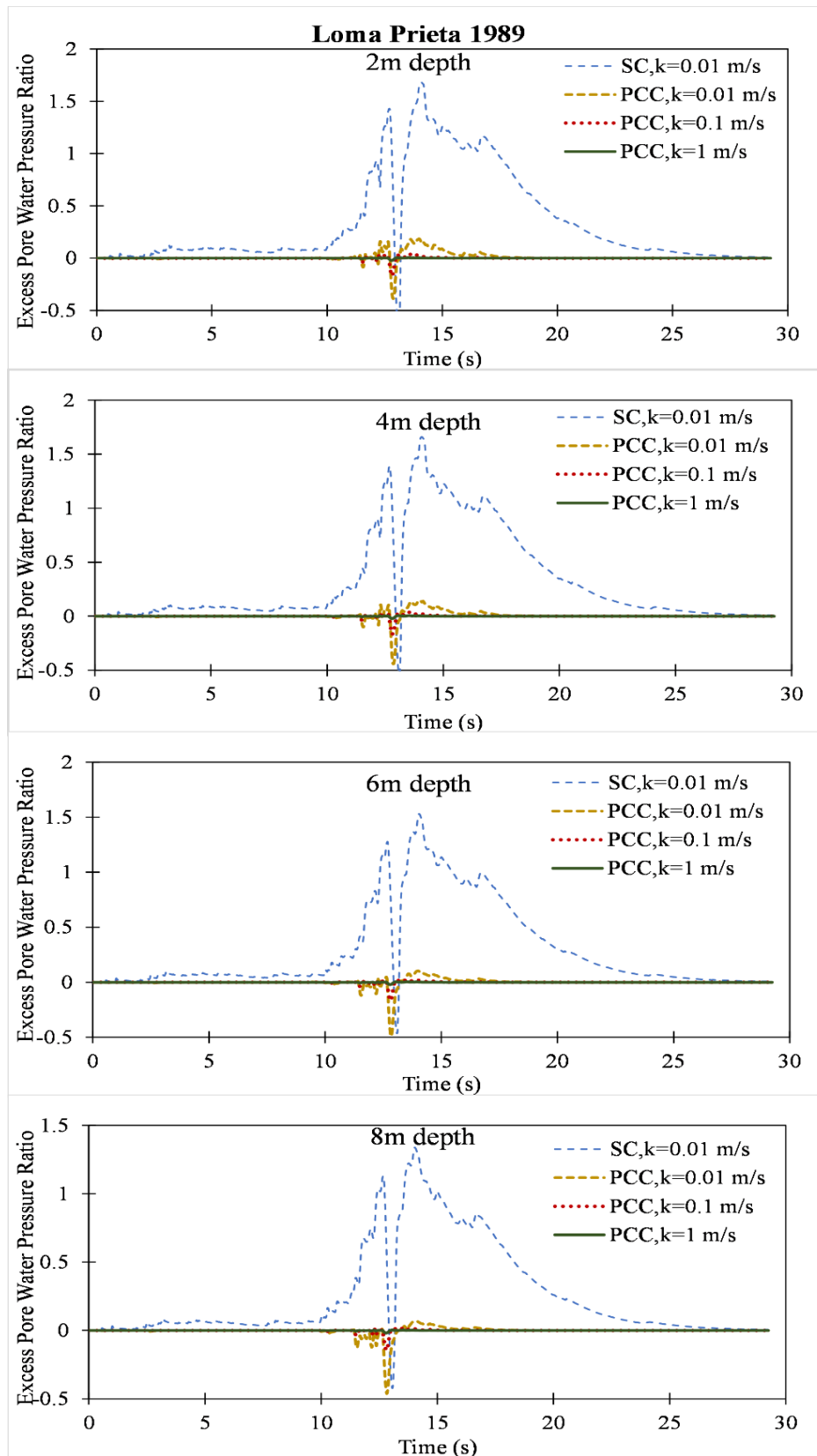
Figure 6.23 Effect of permeability of PCC on excess pore pressure ratio (Diameter of column =1.0 m, AR=13%, End-bearing condition)
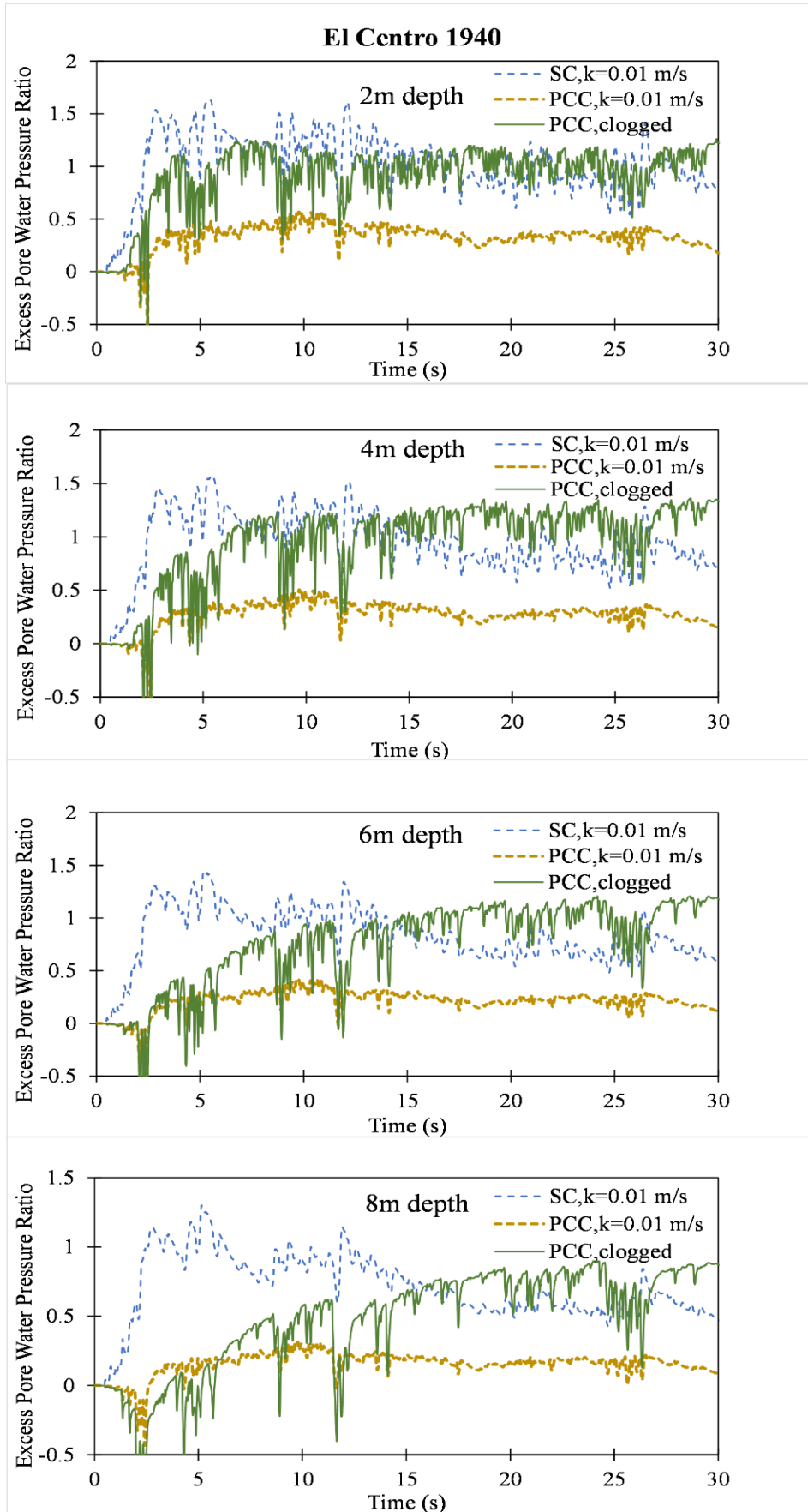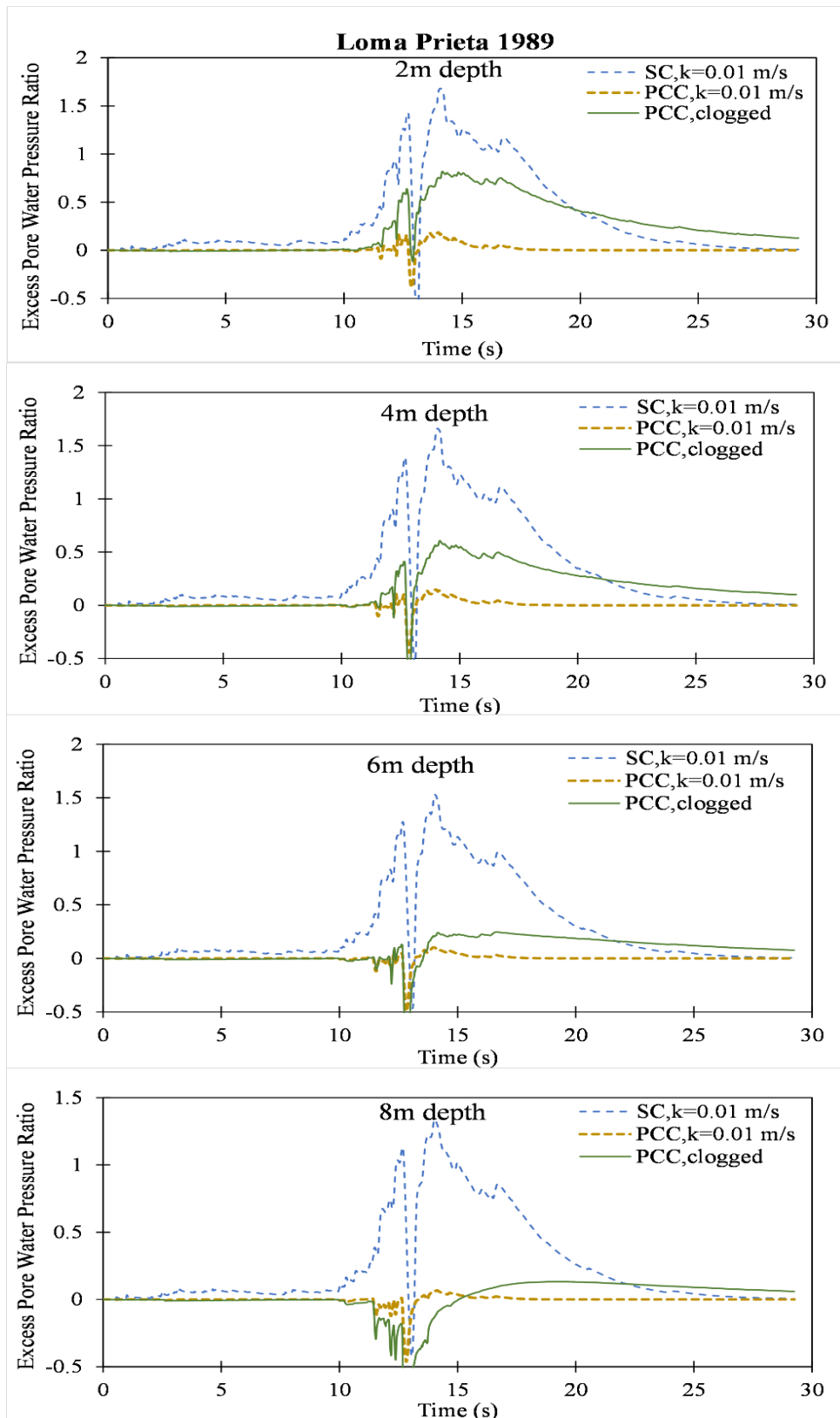
Figure 6.24 Effect of clogged PCC on excess pore water pressure ratio at depths of (a) 2 m (b) 4 m (c) 6 m and (d) 8 m from ground surface. (Diameter of column =1.0 m, AR=13%, End-bearing condition)

6.7.6 Efficacy of pervious concrete column in various soil strata

The efficacy of PCC on three types of soil strata were analyzed. The three soil types considered were loose sand, medium-dense sand and silt strata. The lateral displacement-time history plots of improved ground using SC and PCC remediation having column diameter of 0.6 m with an area ratio of 20% are presented in Fig.6.25 for all soil types considered. From Fig.6.25 it is clear that the lateral displacement reduction due to PCC remediation is nearly 90%, 82% and 75 % higher than that of SC improved ground for loose sand, medium-dense sand and silt strata respectively. The excess pore pressure-time history plots of unimproved ground, improved ground with SC and PCC are shown in Fig.6.26(a) and Fig.6.26(b) respectively for El-Centro and Loma Prieta excitations for three types of strata (loose sand, medium-dense sand and silt strata) considered. The excess pore water pressure at the center of finite element mesh (representing center of column) and edge of finite element mesh (representing surrounding soil) as shown in Fig.6.26(a) and Fig.6.26(b) show lower excess pore pressure generation for PCC improved ground.

The reduction in excess pore water pressure generation for PCC improved ground is also seen at the edge of finite element mesh representing farthest location from column inclusion than SC improved ground. However, for silt strata, the excess pore water pressure at farthest location is seemed to be similar with SC and PCC inclusion. This performance may be due to the very less permeability of silt strata.

The reduction in lateral displacement and lower excess pore water pressure generation due to PCC inclusion is observed in all the three types of soil strata studied. This reveals the better seismic performance and efficacy of PCC remediation when compared to SC improved ground.
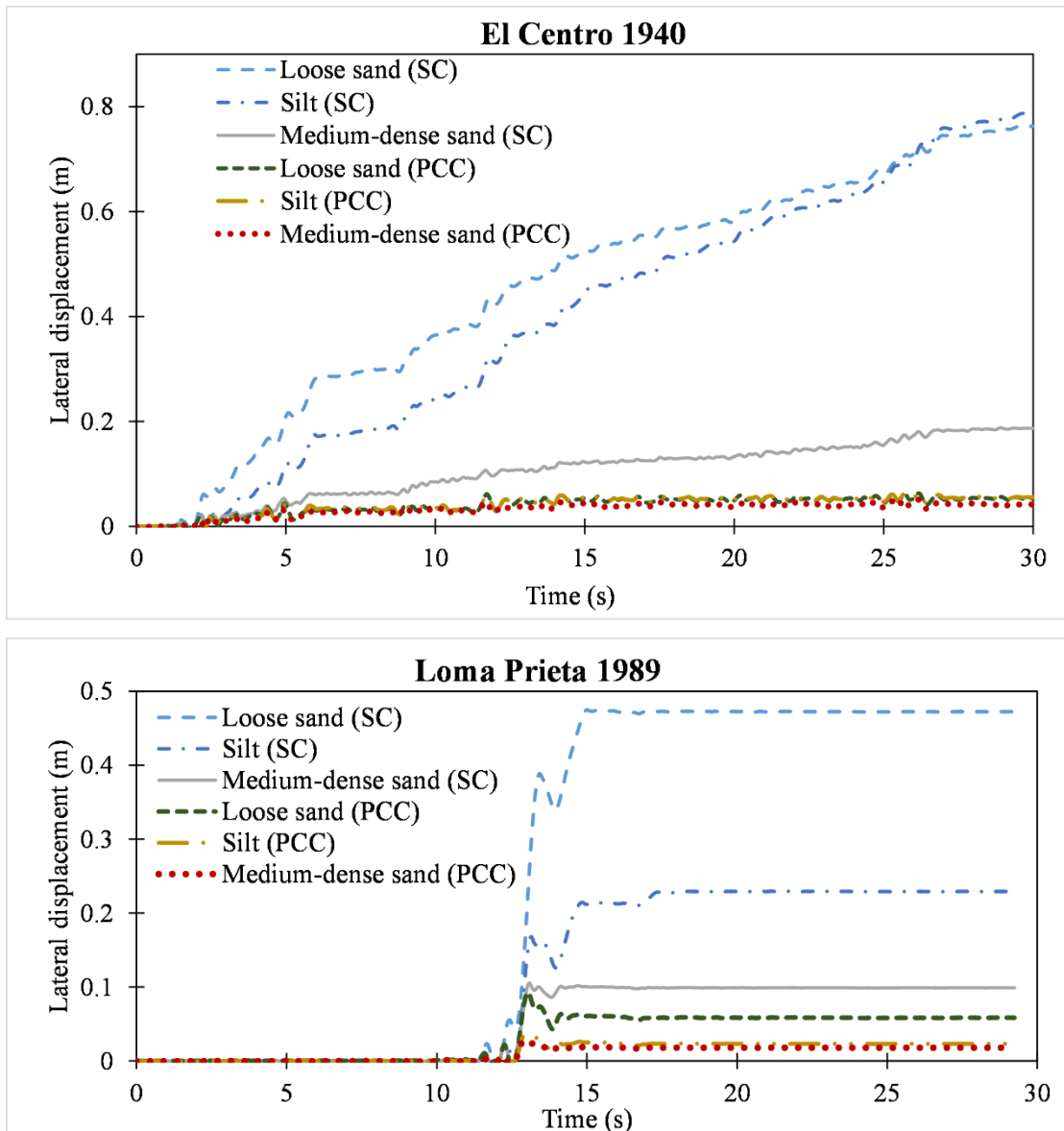
Figure 6.25 Efficacy of PCC on lateral displacement for loose sand, medium-dense sand and silt strata
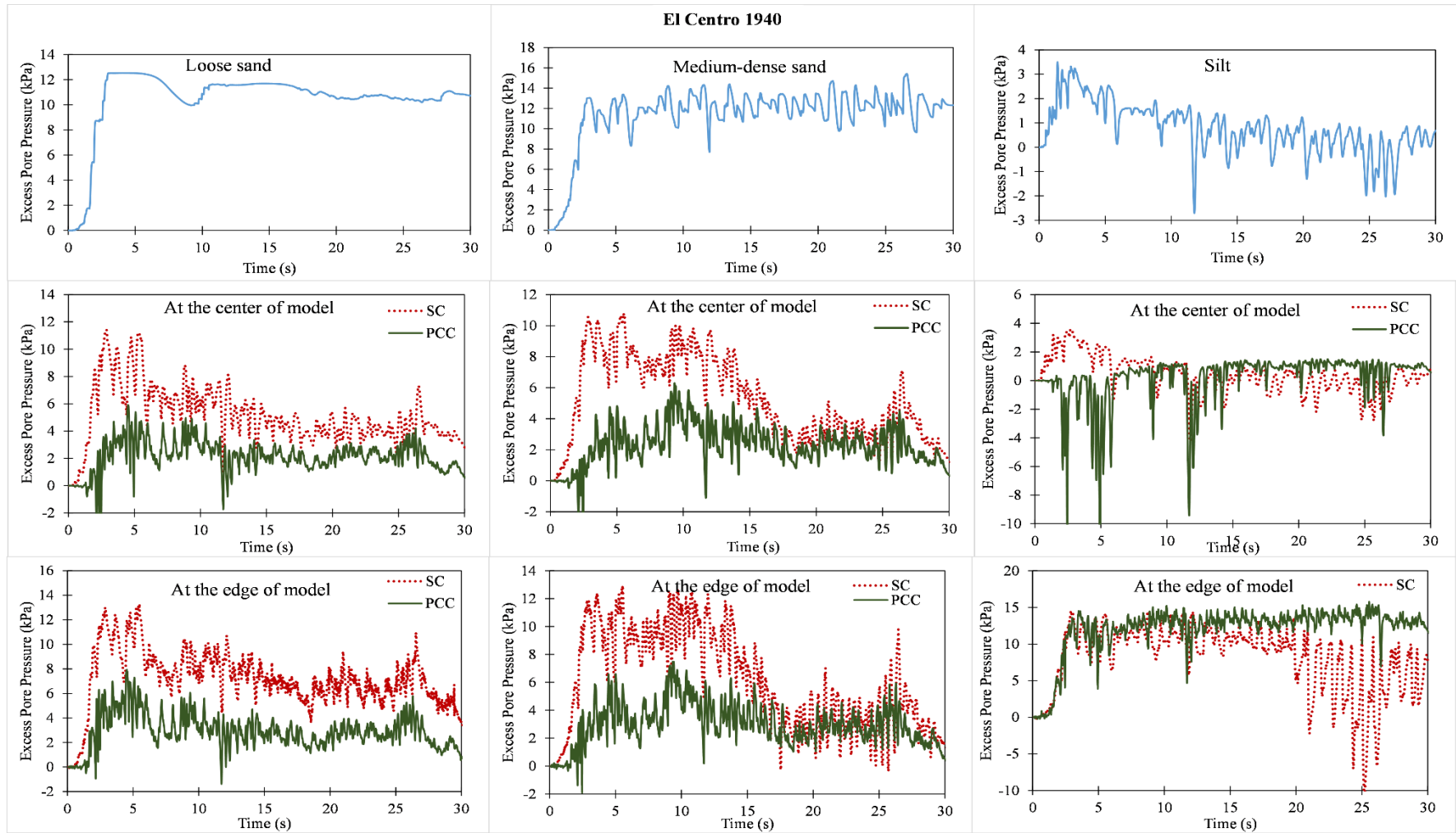
Figure 6.26(a) Excess pore pressure-time history plot at the center and edge of mesh for loose sand, medium-dense sand and silt strata subjected to El-Centro excitation
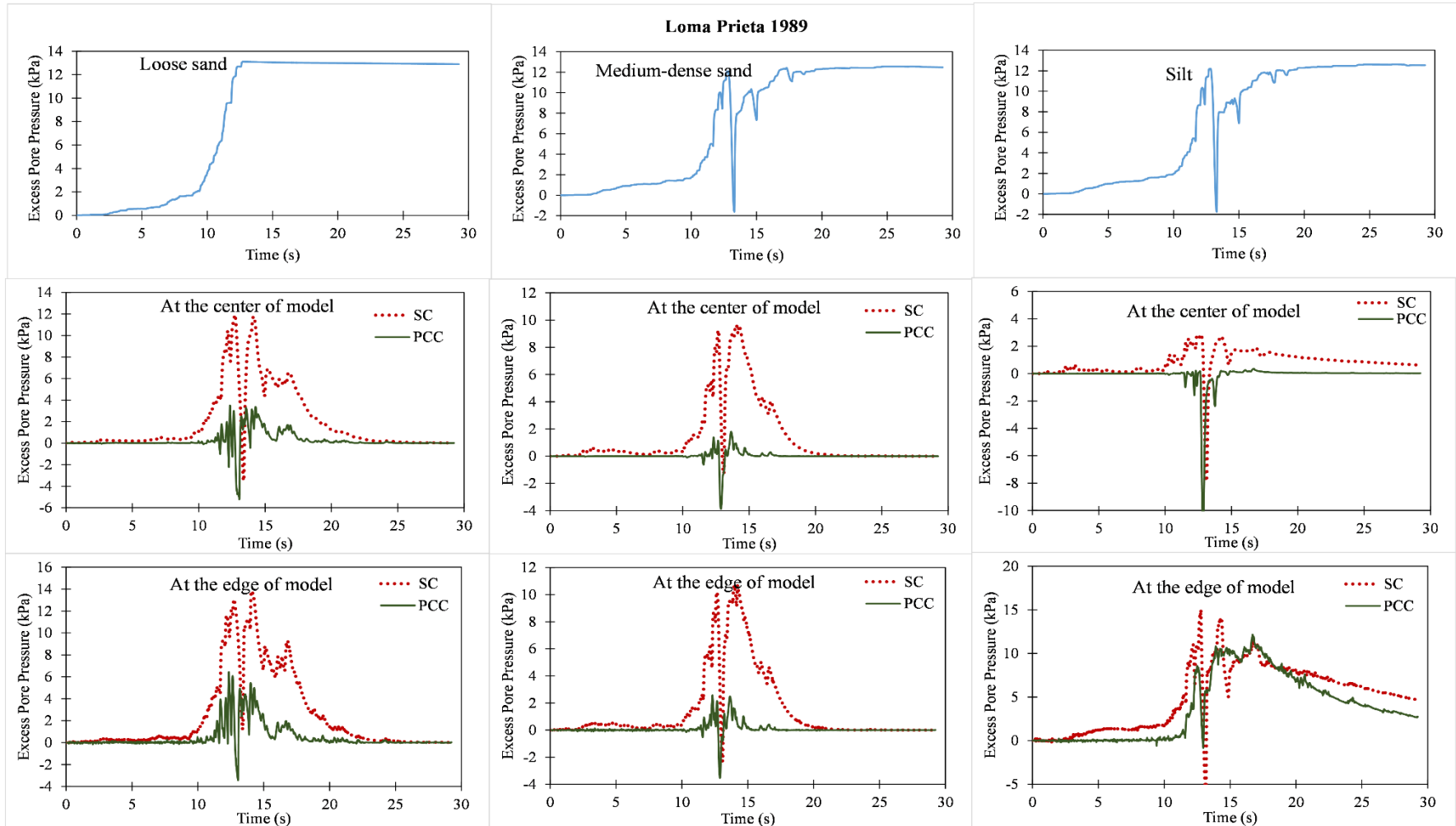
Figure 6.26(b) Excess pore pressure-time history plot at the center and edge of mesh for loose sand, medium-dense sand and silt strata subjected to Loma Prieta excitation

6.7.7 Influence of thickness of liquefiable soil

The influence of thickness of liquefiable soil on lateral displacement was studied on a soil model with varying thickness from 2 m to 8 m (Fig.6.6). The lateral displacement versus thickness of liquefiable soil plot is shown in Fig.6.27. The lateral deformation increased with increase in thickness of liquefiable soil for both SC and PCC remediation. However, lateral displacements were reduced while using PCC inclusion when compared to SC inclusion (Fig.6.27).
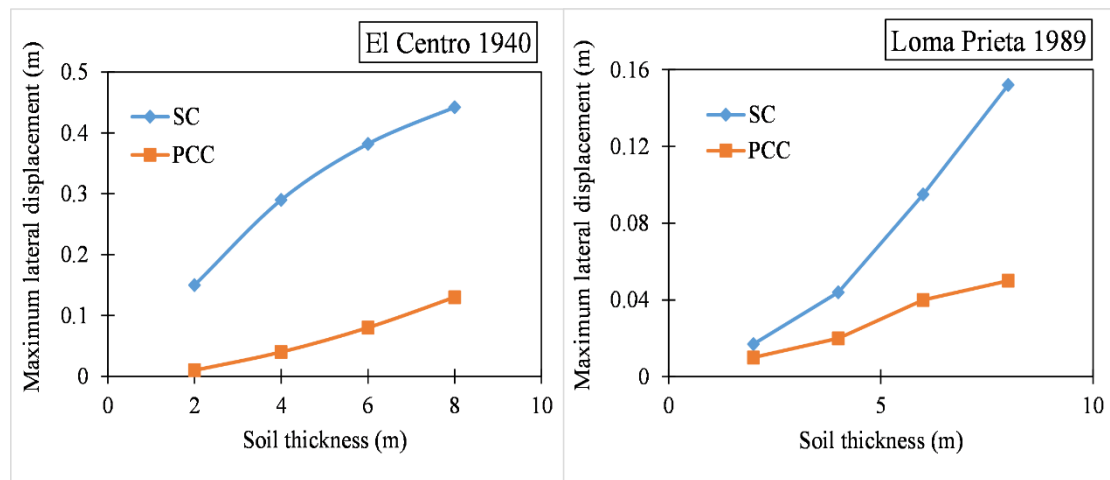
Figure 6.27 Effect of thickness of liquefiable soil on lateral displacement

When the thickness of liquefiable soil is 2m, SC remediation would be sufficient for preventing liquefaction induced lateral spreading. But for greater thickness of liquefiable soil (4m, 6m and 8m), PCC remediation is found to be suitable for reducing lateral spreading.

6.7.8 Influence of surrounding soil permeability

In order to understand the influence of soil permeability on lateral deformation, the soil permeability of medium-dense sand strata was replaced with soil permeability (Ks) ranging from 6.6×10^{-02} m/s to 6.6×10^{-04} m/s.

The results of maximum lateral displacement at the center of the finite element mesh for improved ground with SC and PCC of diameter 0.6 m for an area ratio of 20% is listed in Table 6.4. The results indicate that the maximum lateral displacement is dependent on the permeability of surrounding soil when the ground is remediated with stone columns. However, while using pervious concrete remediation, the maximum lateral displacement for all soil permeability considered are found to be similar. This

indicates that the lateral displacement of PCC improved ground is independent of surrounding soil permeability.

Table 6.4 Effect of surrounding soil permeability on lateral displacement

Permeability of soil(m/s)	Maximum ground lateral displacement (m)			
	El-Centro		Loma Prieta	
	SC	PCC	SC	PCC
6.60×10^{-02}	0.036	0.042	0.014	0.018
6.60×10^{-03}	0.048	0.042	0.03	0.018
6.60×10^{-04}	0.105	0.042	0.08	0.018
6.60×10^{-05}	0.187	0.04	0.09	0.018

The excess pore pressure-time history plots for SC and PCC improved ground at center and edge of finite element mesh representing column location and farther away from column inclusion (surrounding soil) are shown in Fig.6.28 for all soil permeability ranges. From Fig.6.28, it is seen that for all soil permeability range considered, PCC improved ground has lesser excess pore pressure generation than SC improved ground, indicating better excess pore water dissipation due to PCC inclusion than that of SC inclusion.
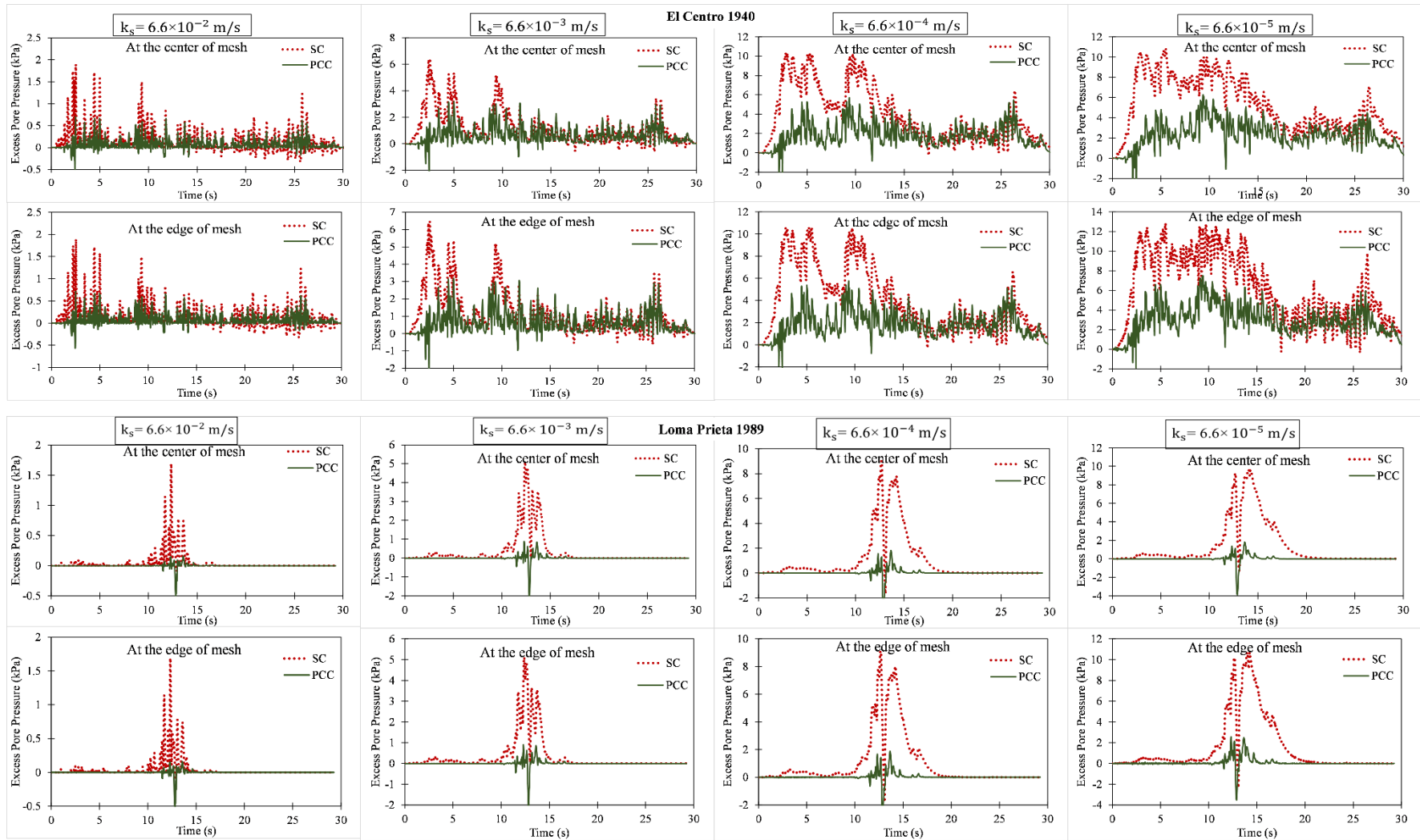
Figure 6.28 Effect of soil permeability on excess pore pressure at the center and edge of mesh

131

6.7.9 Influence of ground surface inclination

The influence of ground surface inclination on lateral spreading was studied by varying ground surface inclination from 0° to 8° for improved ground with SC as well as PCC inclusions of diameter 1m corresponding to an area ratio of 13%. The variation of maximum lateral displacement with ground surface inclination at the center of finite element mesh is shown in Fig.6.29. It is found that the lateral displacement increases with increase in ground surface inclination for both SC and PCC improved ground. This is due to the presence of higher static shear stresses due to gravity for higher slope angles.
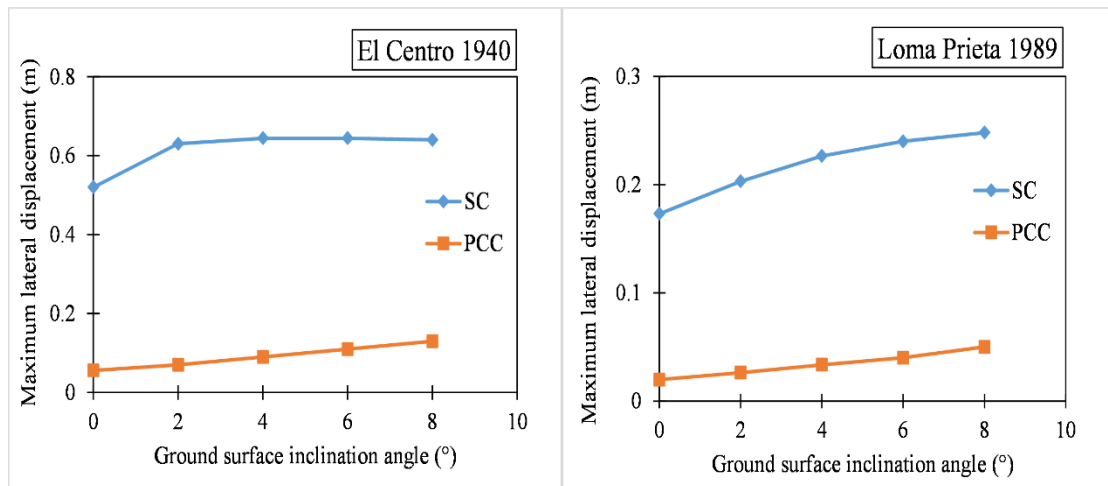
Figure 6.29 Influence of ground surface inclination on lateral displacement

6.7.10 Influence of peak ground acceleration

For studying the influence of peak ground acceleration on lateral displacement, the earthquake excitation applied at the base of the model was scaled to 0.1g, 0.2g, 0.4g, 0.6g and 0.8g. The model used corresponds to an area ratio of 20% with SC and PCC remediated ground. The diameter of column considered was 0.6 m. The variation of lateral displacement versus peak ground acceleration is shown in Fig.6.30. The lateral displacement is found to be increased with increase in peak ground acceleration. For SC remediated ground, lateral displacement is found to be high. The lateral displacement of PCC improved ground even for peak ground acceleration of 0.6g is found to be around 0.3 m and 0.22 m respectively for El-Centro and Loma Prieta excitations. Whereas for SC improved ground, for peak ground acceleration for 0.6g,

132

the lateral displacements are found to be 2.5 m and 0.5 m respectively for El-Centro and Loma Prieta excitations.
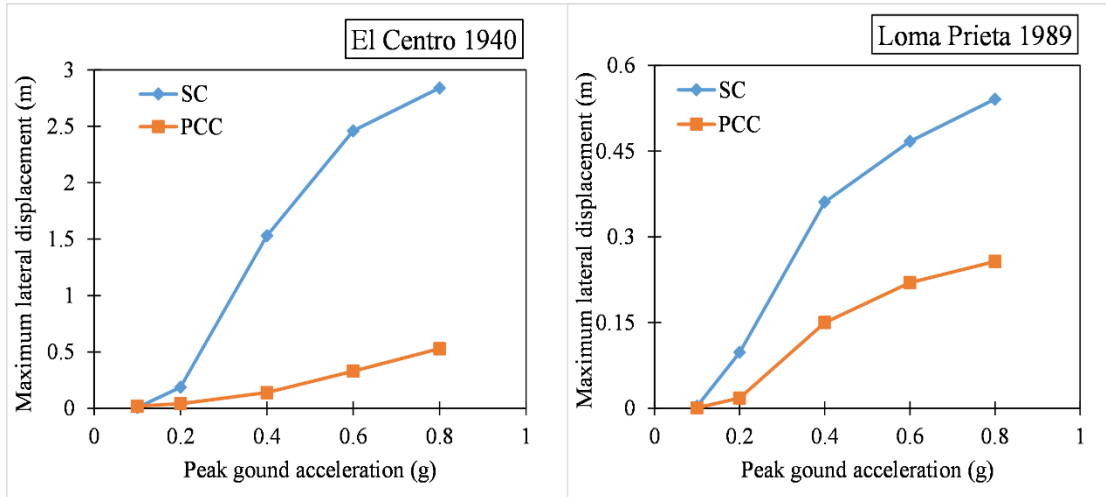
Figure 6.30 Effect of PGA on lateral displacement

Seismic induced lateral displacements at the ground surface are found to increase with increase in peak ground acceleration. The regions where higher peak acceleration is expected during seismic activity, PCC can be considered as a better alternative to stone columns in mitigating lateral spreading. The effect of PGA on excess pore pressure ratio at the center of mesh is shown in Fig.6.31. It is found that the excess pore pressure ratio (r_u) for PCC improved ground for all peak ground accelerations other than 0.8g are less than 0.6, which means the improved ground with PCC inclusion is non-liquefied (Jiaer et al.2004). But, for SC improved ground, r_u is found to be approximately between 1.0 and 3.0 for all peak ground accelerations studied (Fig.6.31). It is clear that the PCC dissipated pore water pressure representing reduction in excess pore pressure ratio for all peak ground accelerations (Fig.6.31).
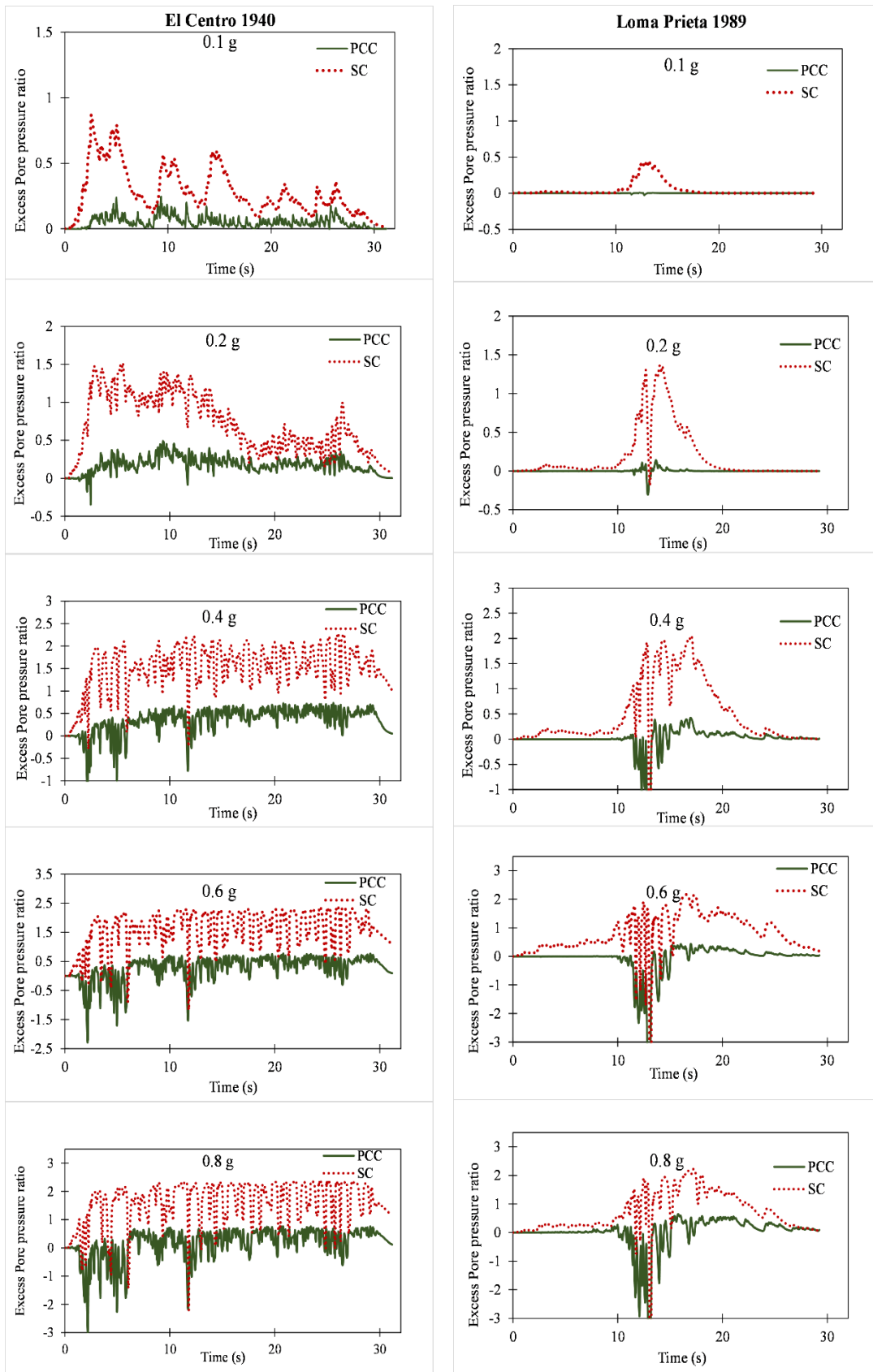
Figure 6.31 Effect of PGA on excess pore pressure at the center of mesh

6.7.11 Influence of surface load

To understand the influence of surface load on lateral displacement for improved ground with PCC inclusion and SC inclusion, surcharge on the ground surface was increased from 50 kPa to 200 kPa. The surcharge load was varied and applied to improved ground with an area ratio of 13% and column diameter of 1m.

Fig.6.32 shows the variation of lateral displacement of SC and PCC improved ground subjected to two different earthquake excitations with different surface loads. It is seen from Fig.6.32 that the ground lateral displacement drastically decreased with increase in surface surcharge for SC and PCC improved ground. This is due to the increase in effective confinement of soil with increase in surcharge load. The lateral displacement at ground surface is noted as approximately zero at the surcharge of 200 kPa for SC as well as PCC remediated ground. A surcharge of 150 kPa imposed a near zero lateral displacement for PCC improved ground and a surcharge of 200 kPa considerably reduced ground surface lateral deformation with SC remediation. That means, the ground lateral deformation may be reduced to near zero level for SC and PCC improved ground with a surcharge of 200 kPa and 150 kPa respectively.
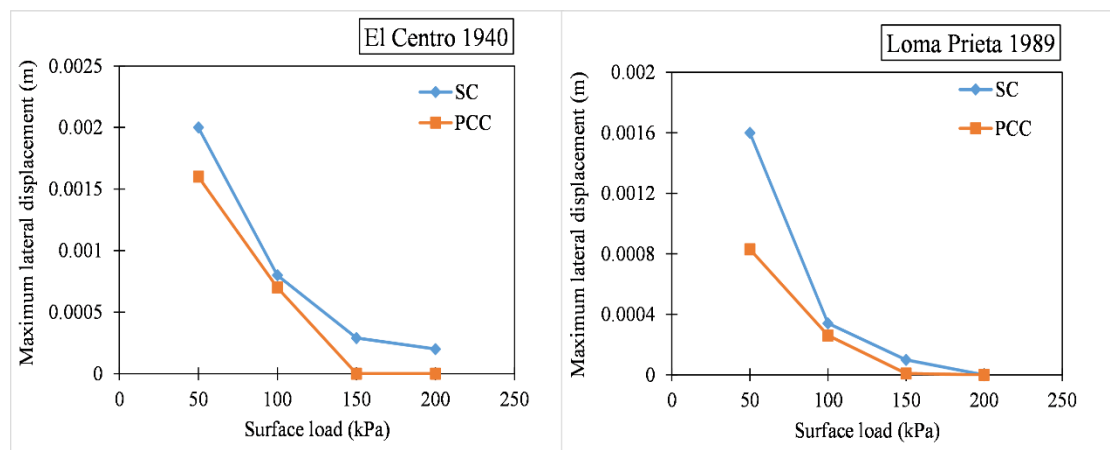
Figure 6.32 Effect of surface load on lateral displacement

6.7.12 Influence of earthquake characteristics

This section details the seismic performance of pervious concrete column improved ground in comparison with stone column improved ground subjected to ground motions with different earthquake characteristics. The diameter of column inclusion considered in improved case was 0.6 m with a wider center to center spacing of 3D, corresponding to an area ratio of 9%.

Figure 6.33 represents the lateral displacement-time history plot at the center of finite element model of three benchmark cases: unimproved sand strata (Free field), improved sand strata with stone column (SC) and pervious concrete column (PCC) shown along with arias intensity plot of each earthquake excitation. The lateral displacement response significantly correlates with arias intensity of seismic excitation. It is seen that the lateral displacement at the ground surface of PCC improved strata is less than 0.15 m, even for a wider spacing between columns of 3D subjected to two earthquake excitations. However, for SC improved ground, the lateral displacement is around 0.6 m and 0.2 m for El-Centro earthquake (relatively low frequency with longer significant duration) and Loma Prieta excitations (relatively high frequency with shorter significant duration) respectively. The lower lateral displacement of SC improved ground under Loma Prieta excitation is attributed to the lower significant duration of excitation. Relatively lower frequency earthquake with longer duration has increased lateral displacement of three benchmark cases (Free field, SC and PCC). However, irrespective of frequency content and duration of earthquake, PCC improved ground has lesser lateral displacement than SC improved ground.

Figure 6.34 shows the variation of excess pore pressure generation in the three benchmark cases at the center of model for various depths of 2 m, 4 m, 6 m and 8 m respectively subjected to El-Centro and Loma Prieta earthqakes.

The excess pore pressure is seen to increase during times of peak acceleration of ground excitation as shown in Fig.6.34. This increase in peak excess pore pressure is observed at around 2.0 s and 12 s for El-Centro earthquake and Loma Prieta respectively. In addition, the generation of excess pore pressure in the case of PCC is lesser than that of SC with similar permeability. This indicates that the PCC facilitated to quickly dissipate pore pressure through the column inclusion and limited excess pore pressure generation is observed for PCC improved ground when compared to SC improved ground as well as for unimproved sand strata for all the depths considered (Fig.6.34).
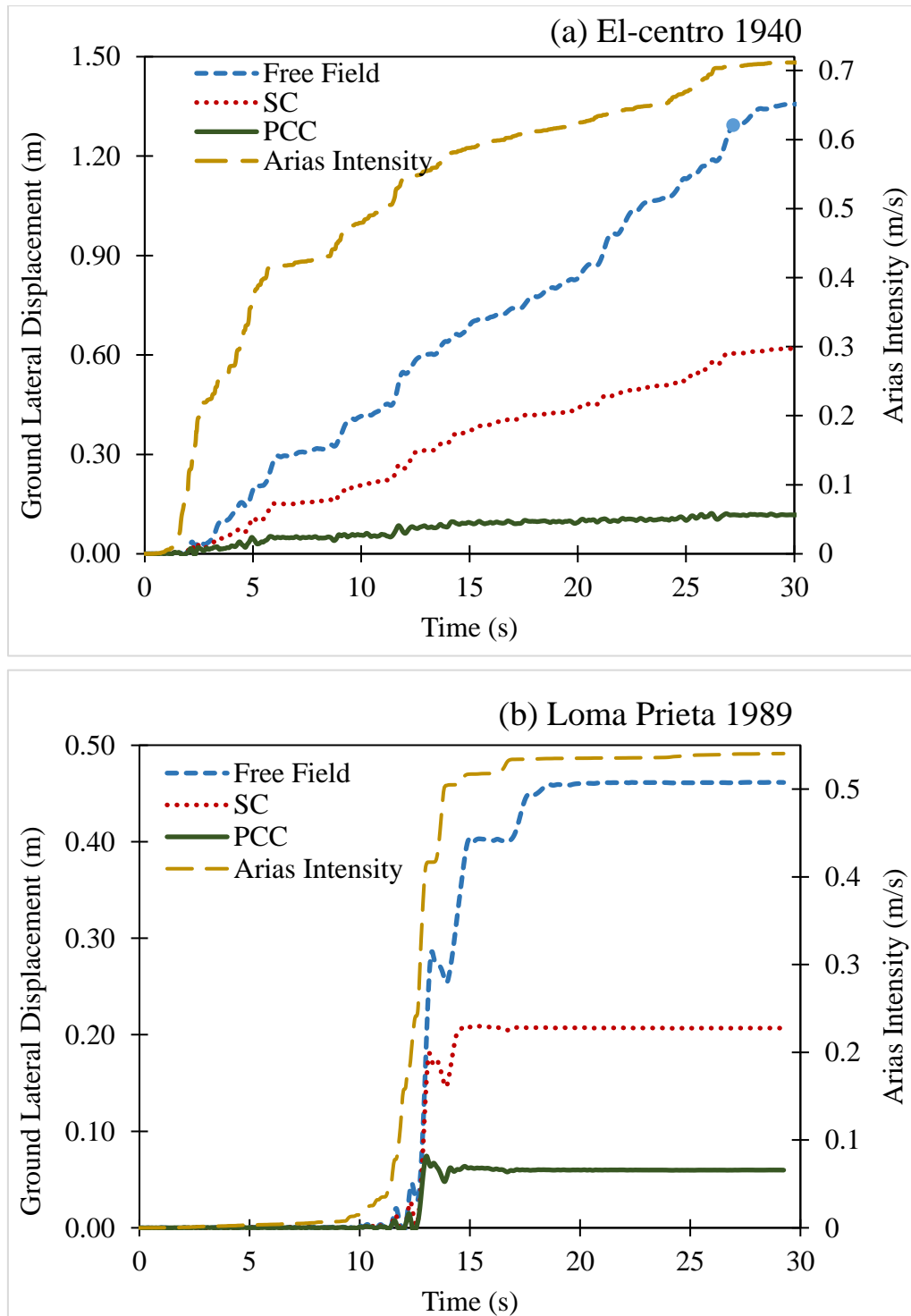
Figure 6.33 Lateral displacement-time history plot of three cases at the center of model subjected to (a) El-Centro and (b) Loma Prieta excitations
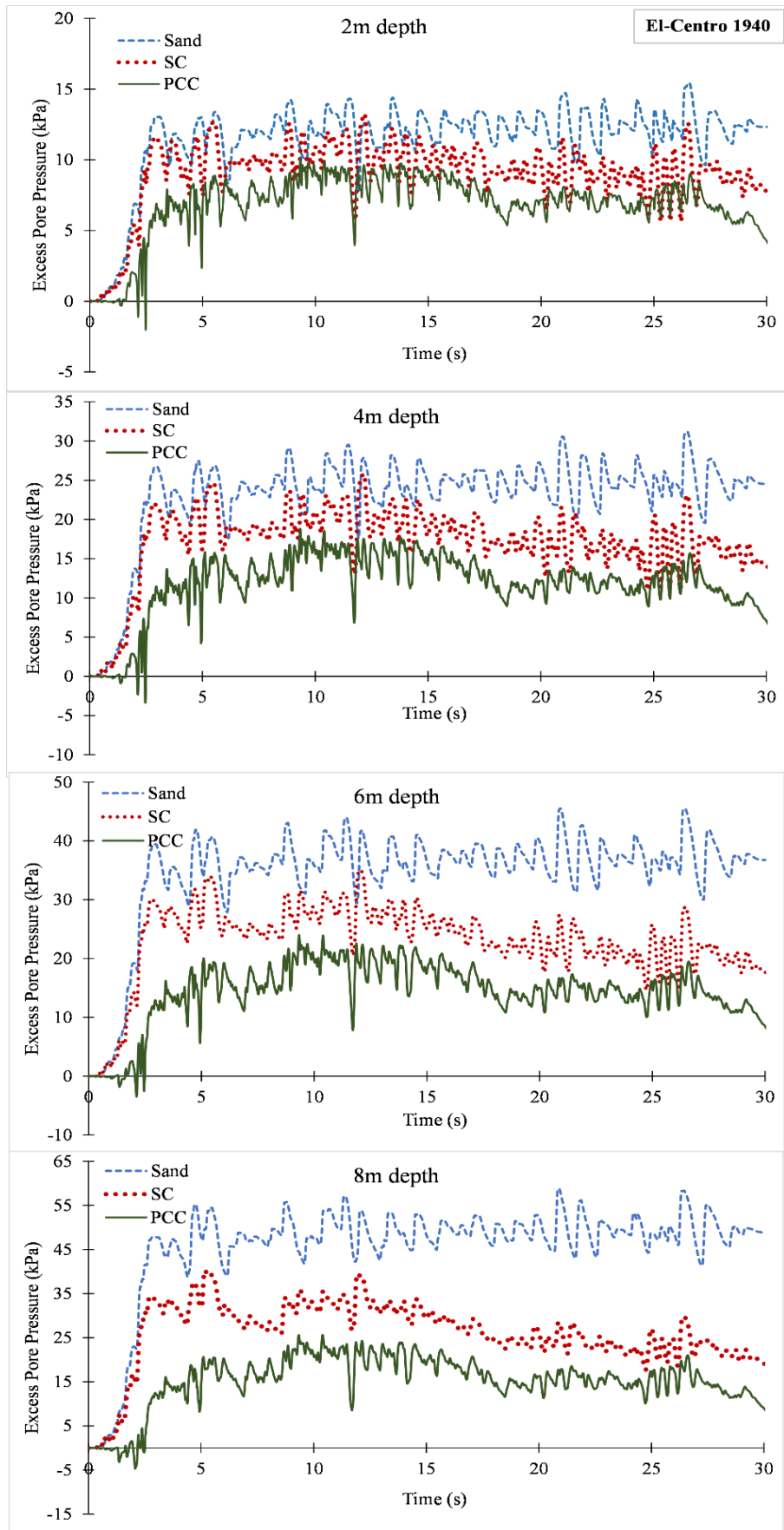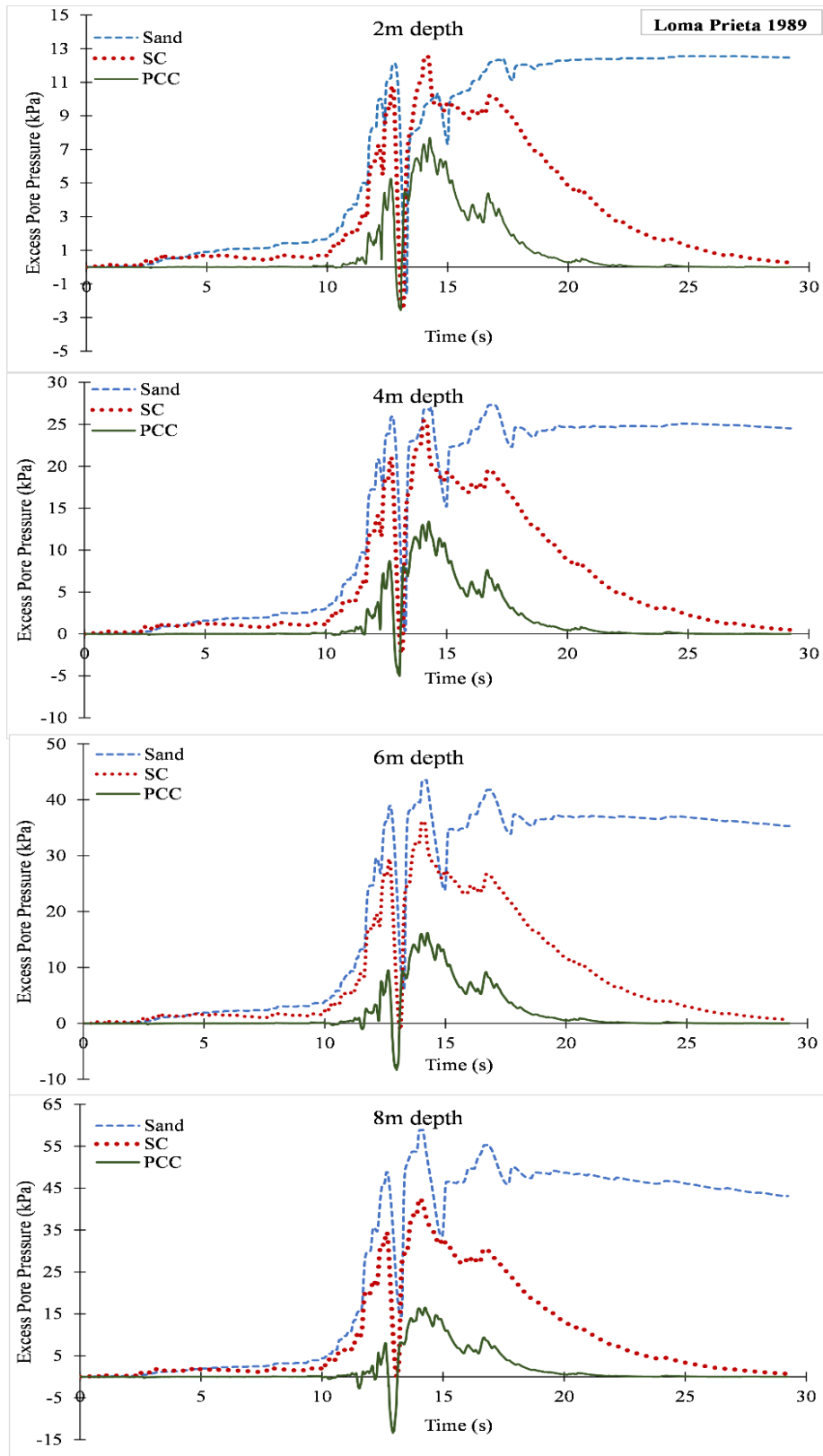
Figure 6.34 Excess pore pressure generation of benchmark cases at the model center for 2 m, 4 m, 6 m and 8 m depths under (a) El-Centro and (b) Loma Prieta excitations

When the value of r_u reaches above 0.6, initiation of liquefaction occurs and hence to find the permeability of PCC for which the excess pore pressure ratio, r_u approaches 0.6, seismic analysis of soil model with varying ranges of PCC permeability was performed. Also, the optimum value of PCC permeability to generate zero excess pore pressure condition was also found.

Figure 6.35 shows the time history plot of excess pore pressure ratio of soil model with PCC inclusions of various permeability values at depths of 2 m, 4 m, 6 m and 8 m when subjected to the two earthquakes. It is found that the excess pore pressure ratio reached 0.6, when the PCC permeability is nearly 0.08 m/s and 0.008 m/s for El-Centro and Loma Prieta earthquakes. In other words, if the permeability of PCC is less than 0.08 m/s and 0.008 m/s respectively at the incidence of El-Centro and Loma Prieta earthquakes, triggering of liquefaction could happen. It is also found that the zero excess pore pressure generation is seen for permeability of PCC above 0.3 m/s for both the earthquakes. So the optimum value of PCC permeability to fully dissipate excess pore pressure is 0.3 m/s irrespective of earthquake characteristics.
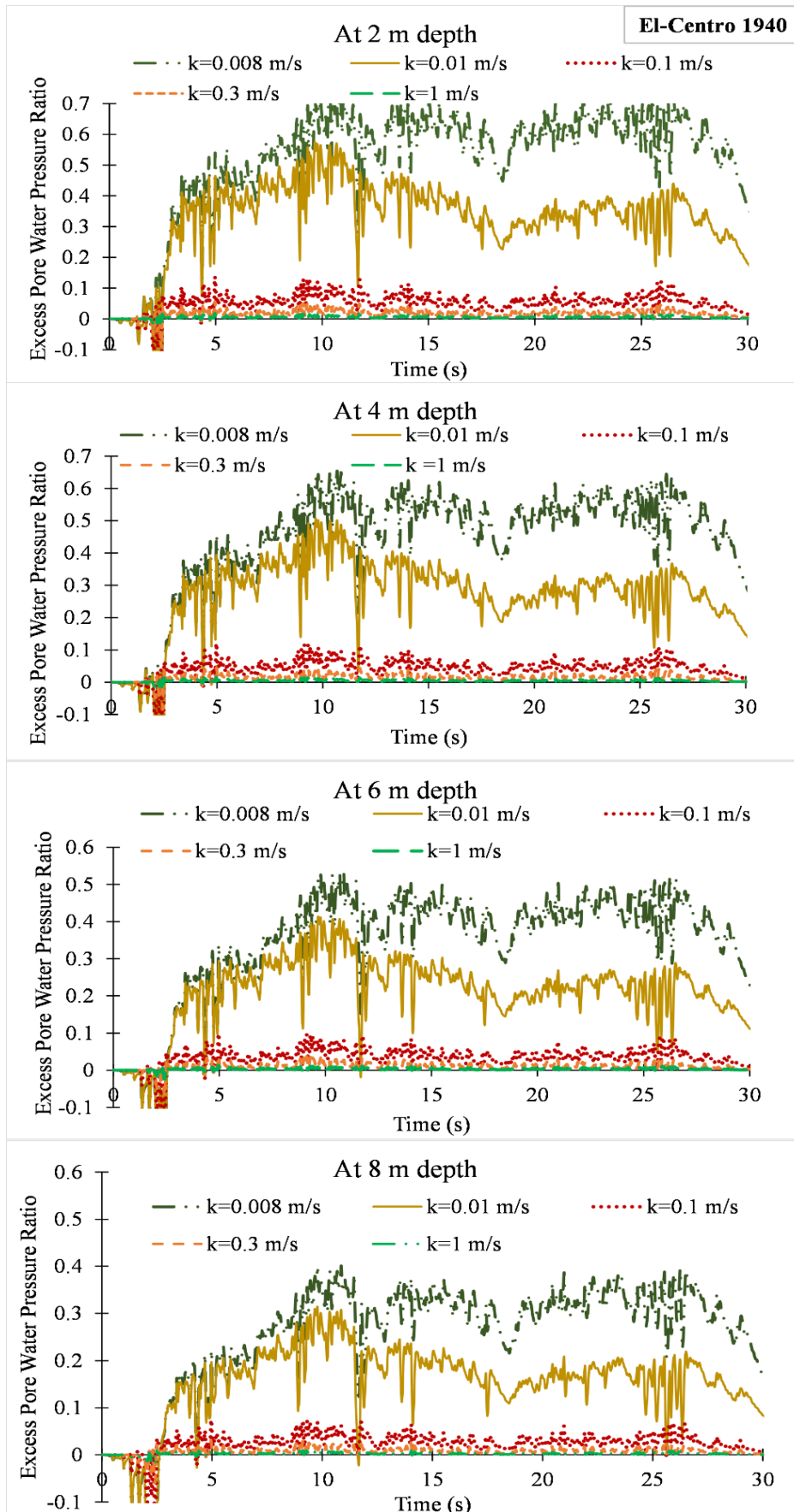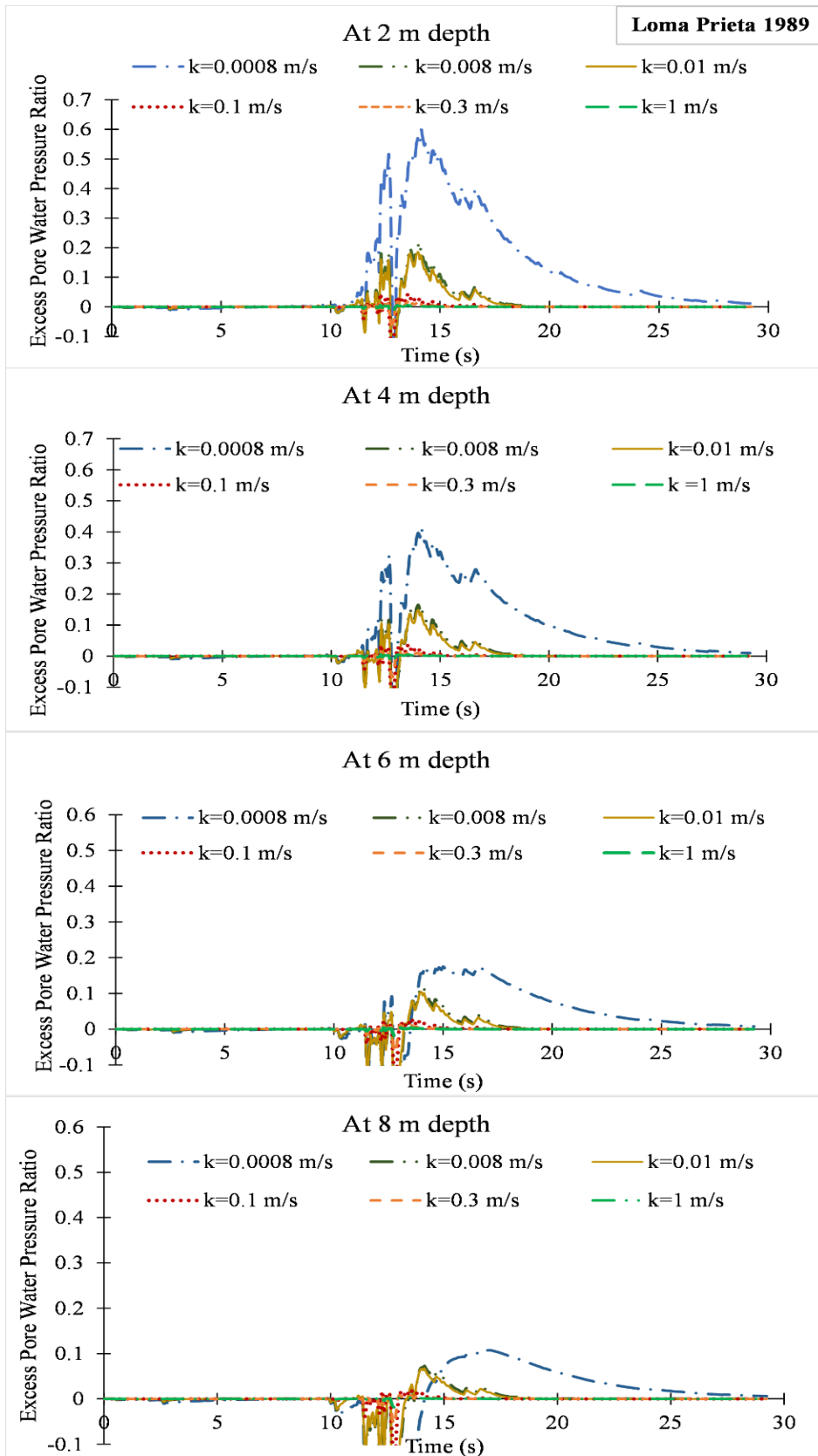
Figure 6.35 Time history of excess pore pressure ratio for various permeability of PCC under (a) El-Centro and (b) Loma Prieta excitations

The shear stress-strain behaviour of improved ground with PCC improved ground and SC improved ground at a distance of 0.7 m from the center of finite element mesh representing surrounding soil at various depths of 1.4 m, 3.4 m, 5.4 m and 7.4 m is shown in Fig.6.36. It is noted that for SC improved ground under El-Centro earthquake, at the depths of 1.4 m and 3.4m, shear stress reduction to zero with higher strain level indicates that the surrounding soil is liquefied, whereas for Loma Prieta earthquake, the surrounding soil is not liquefied. Stress reversal does not occur during less number of cycles and the SC improved ground did not liquefy due to degradation of strength when subjected to Loma Prieta earthquake. The difference in shear stress-strain behaviour at these depths for SC improved ground under two seismic events are attributed to the difference in the number of significant cycles. However, the PCC improved ground resisted the degradation of strength owing to its higher strength and stiffness similar to that of normal concrete even for El-Centro earthquake with more number of cycles. Therefore, it is concluded that, higher the number of significant cycles, the chances of SC improved ground to liquefy is high whereas for PCC improved ground, the soil has not shown any initiation of liquefaction even with higher number of significant cycles. The time history of shear stress developed at the center of the column location in improved ground and unimproved sand strata for various depths are shown in Fig.6.37. It is seen that the PCC resisted the seismic shaking well and the maximum shear stress values are observed at times of peak acceleration of ground excitation i.e., at around 2.0 s and 12 s for El-Centro and Loma Prieta events respectively. Thereafter the shear stress values are seen to be elevated up to the end of shaking. But, the shear stress at the center of SC is found to be similar to that of unimproved sand strata. The seismic shear resistance shown by PCC improved ground irrespective of earthquake characteristics is attributed to the shear strength and stiffness of pervious concrete column improved ground.
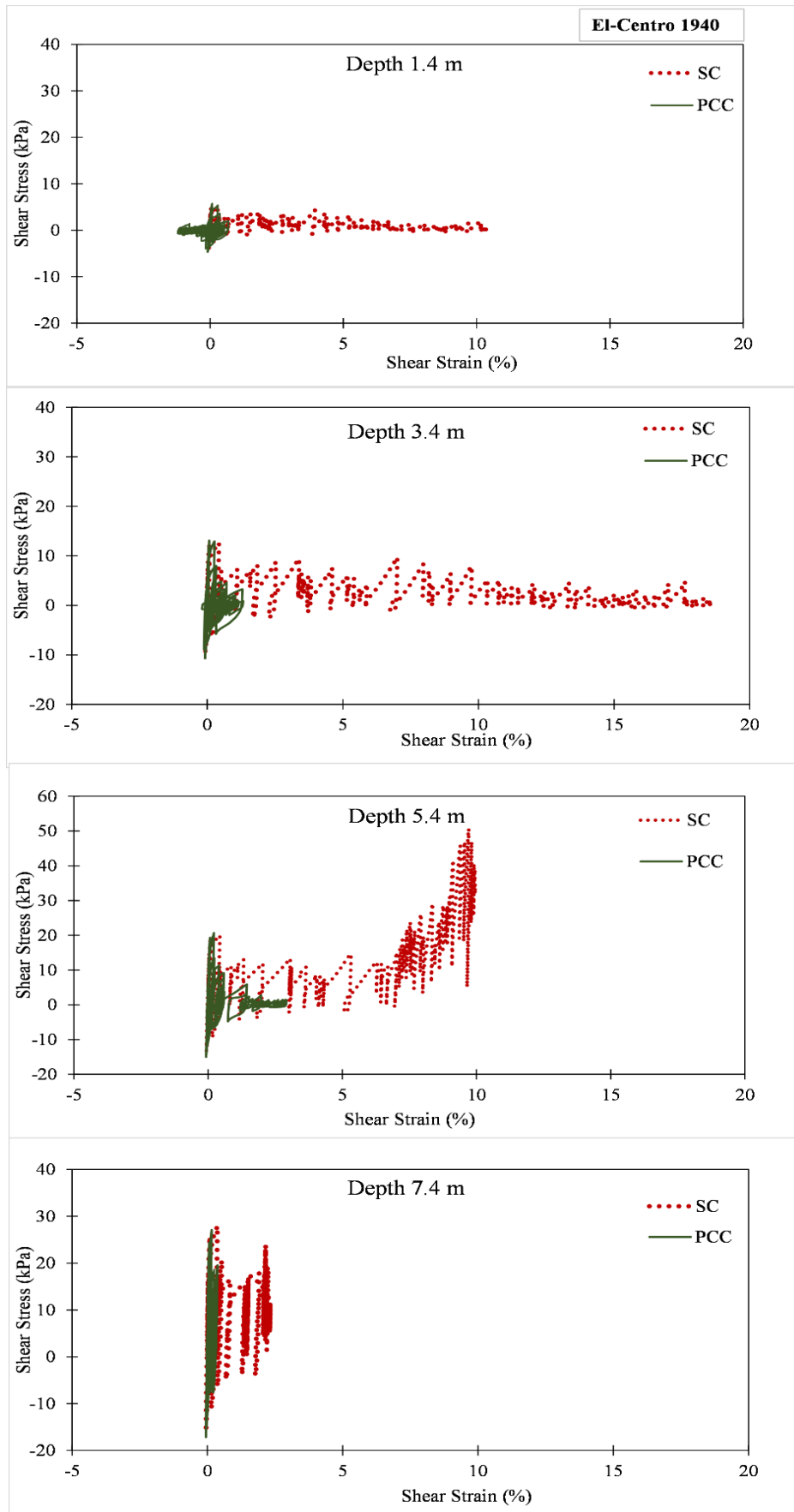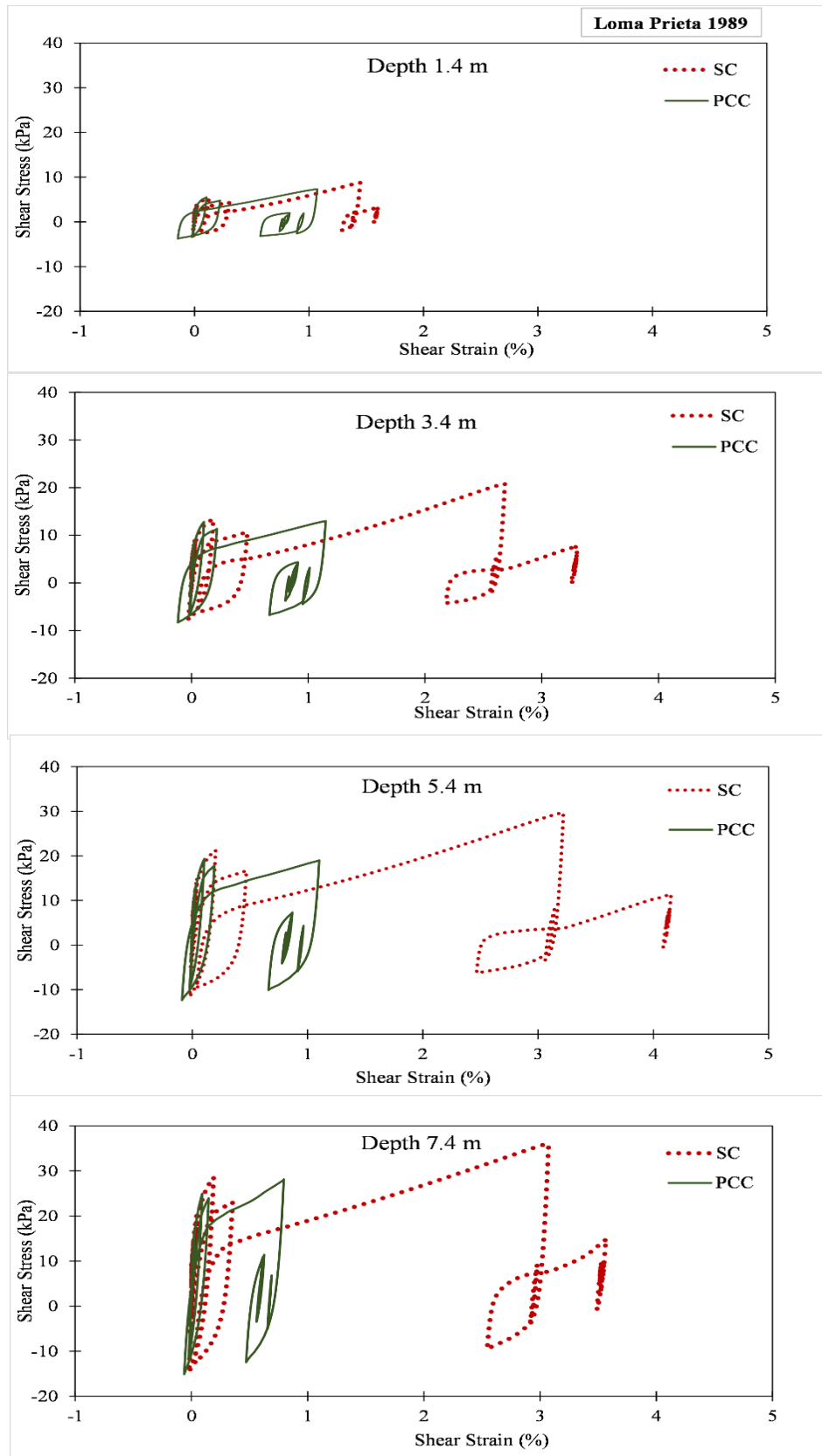
Figure 6.36 Shear stress strain behaviour of improved ground under (a) El-Centro and (b) Loma Prieta excitations

145
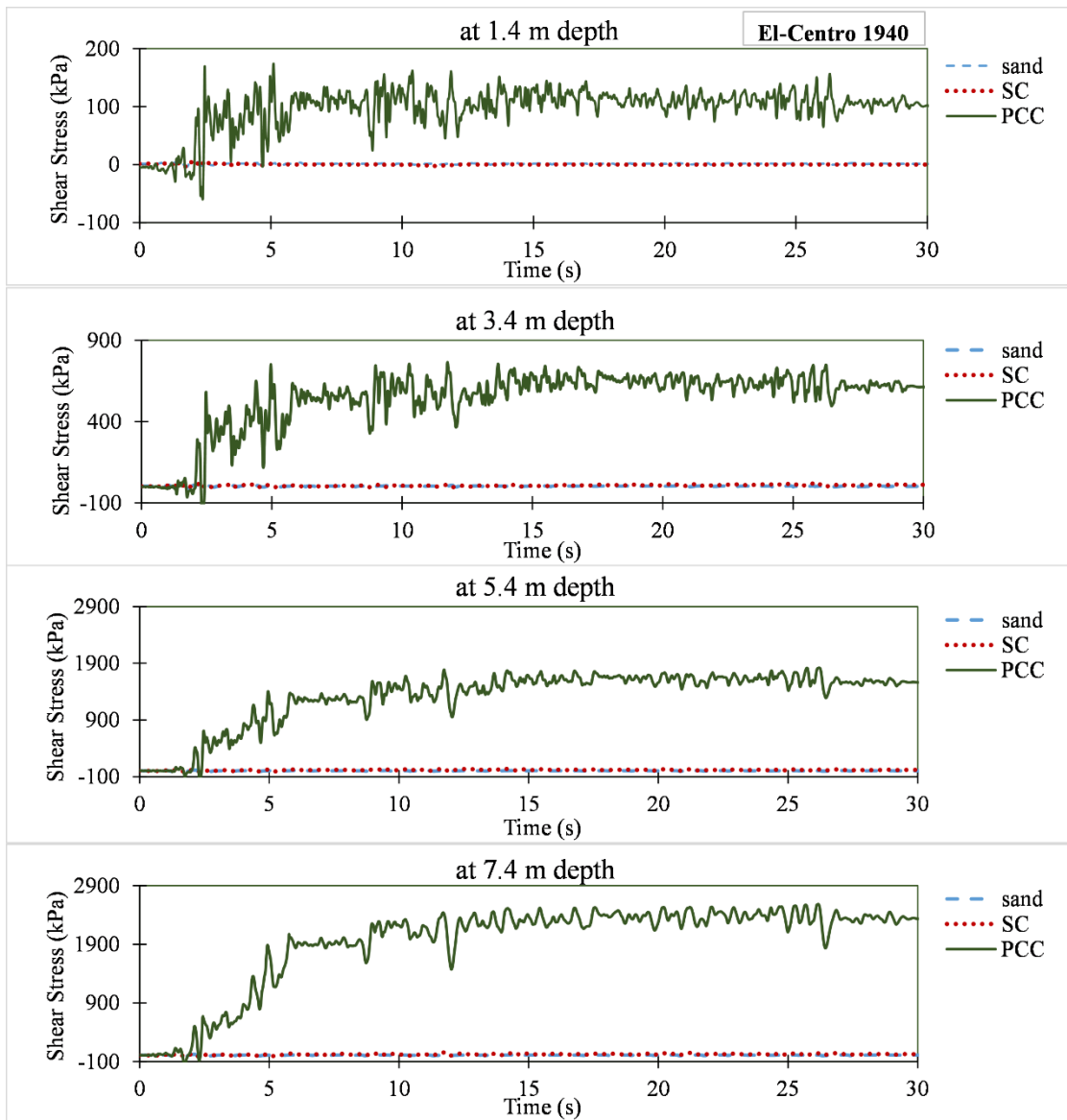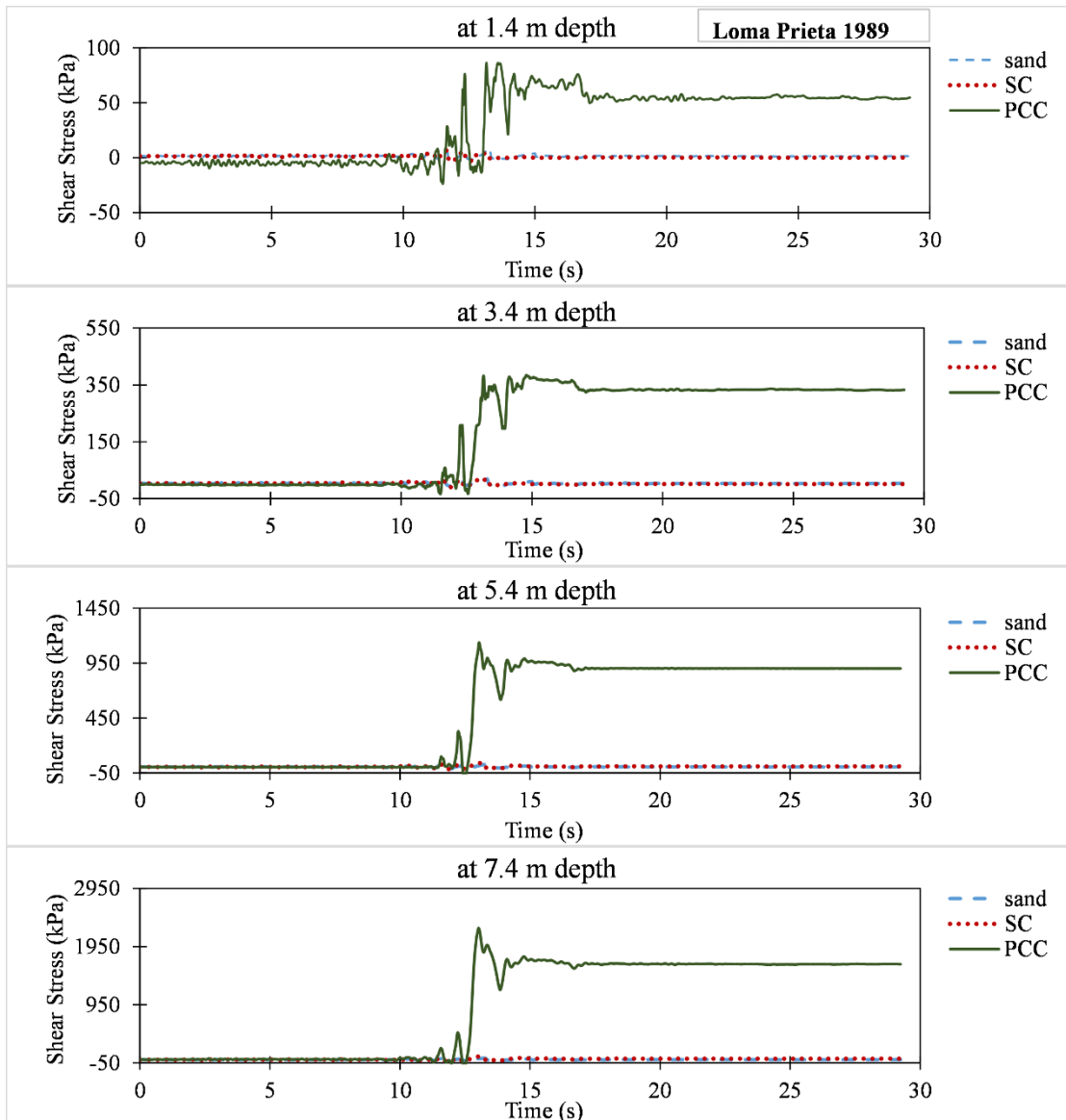
Figure 6.37 Time history plot of shear stress at the center of column under (a) El-Centro and (b) Loma Prieta excitations

Liquefaction is commonly observed in homogeneous saturated sand deposits and sandwiched liquefiable soil layer between non-liquefiable layers at top and bottom (Ishihara 2007). Therefore, the performance of pervious concrete column installed in a sandwiched liquefiable soil layer with varying thickness of liquefiable soil layer as shown in Fig.6.6 was considered. The thickness of sandwiched liquefiable soil layer were varied as 2m, 4m, 6m, and 8m as shown in Fig.6.6 and the seismic performance of PCC and SC inclusions were compared. The comparison of maximum responses along the depth for varying thickness of liquefiable soil layer subjected to El-Centro and Loma Prieta earthquake events are presented in Fig.6.38, Fig.6.39 and Fig.6.40

147

for lateral displacement, excess pore pressure ratio and shear stress at column location respectively.

The lateral displacement profile for SC is entirely different from that of PCC and pattern is seen similar under both earthquakes (Fig.6.38). The drastic reduction of lateral displacement with PCC inclusion for all varying thickness considered is attributed to the rigidity and stiffness of PCC.
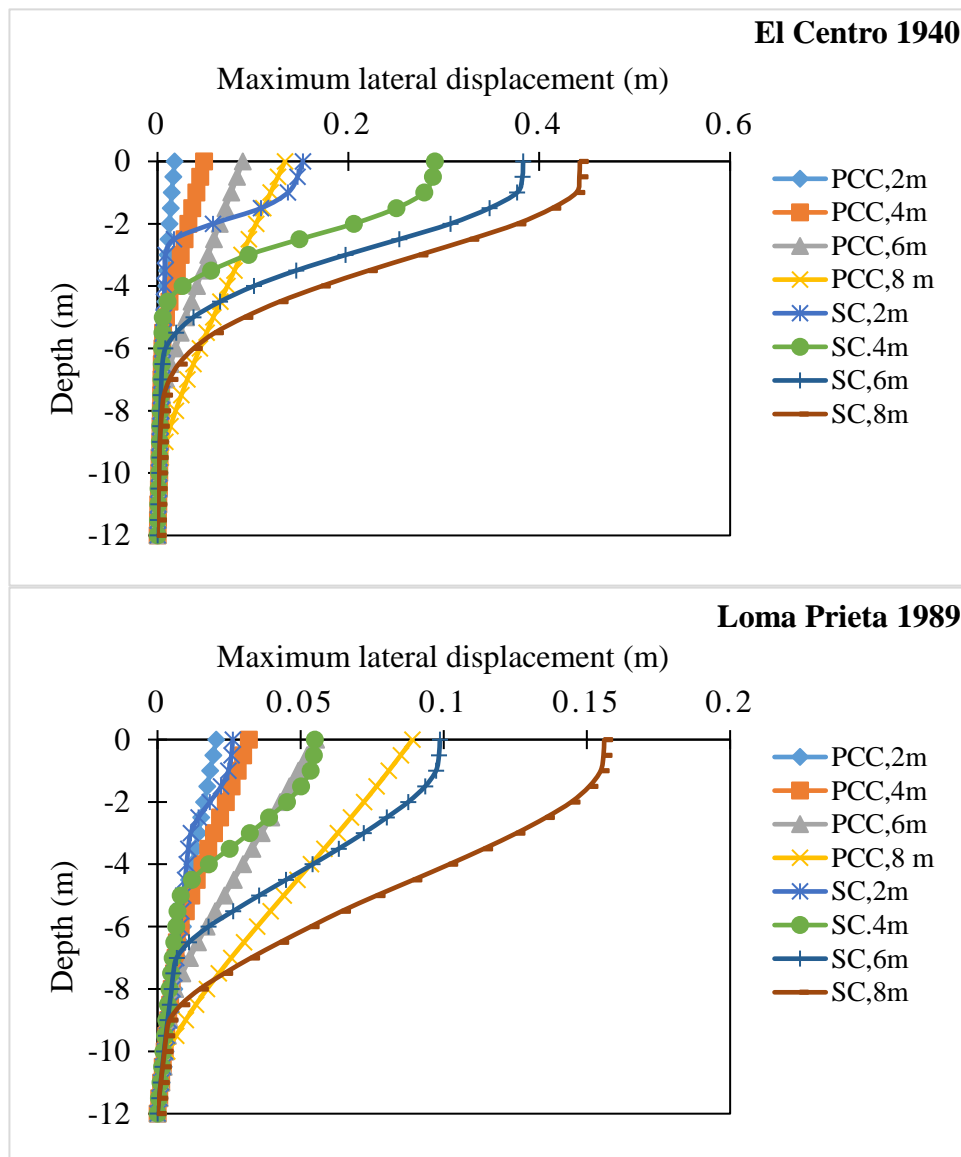
Figure 6.38 Comparison of maximum lateral displacement response along the depth for varying thickness of liquefiable soil layer subjected to (a) El-Centro (b) Loma Prieta excitations

Excess pore pressure ratio, r_u is found to be high for SC improved soil profile with r_u >1.0 for all thicknesses considered. For PCC improved soil profile, the excess pore pressure values, r_u is found to be less than 1 (r_u reaching 0.6) for El Centro and Loma Prieta earthquakes. i.e., r_u <1 except for 8m thick liquefiable layer subjected to Loma Prieta earthquake (Fig.6.39).
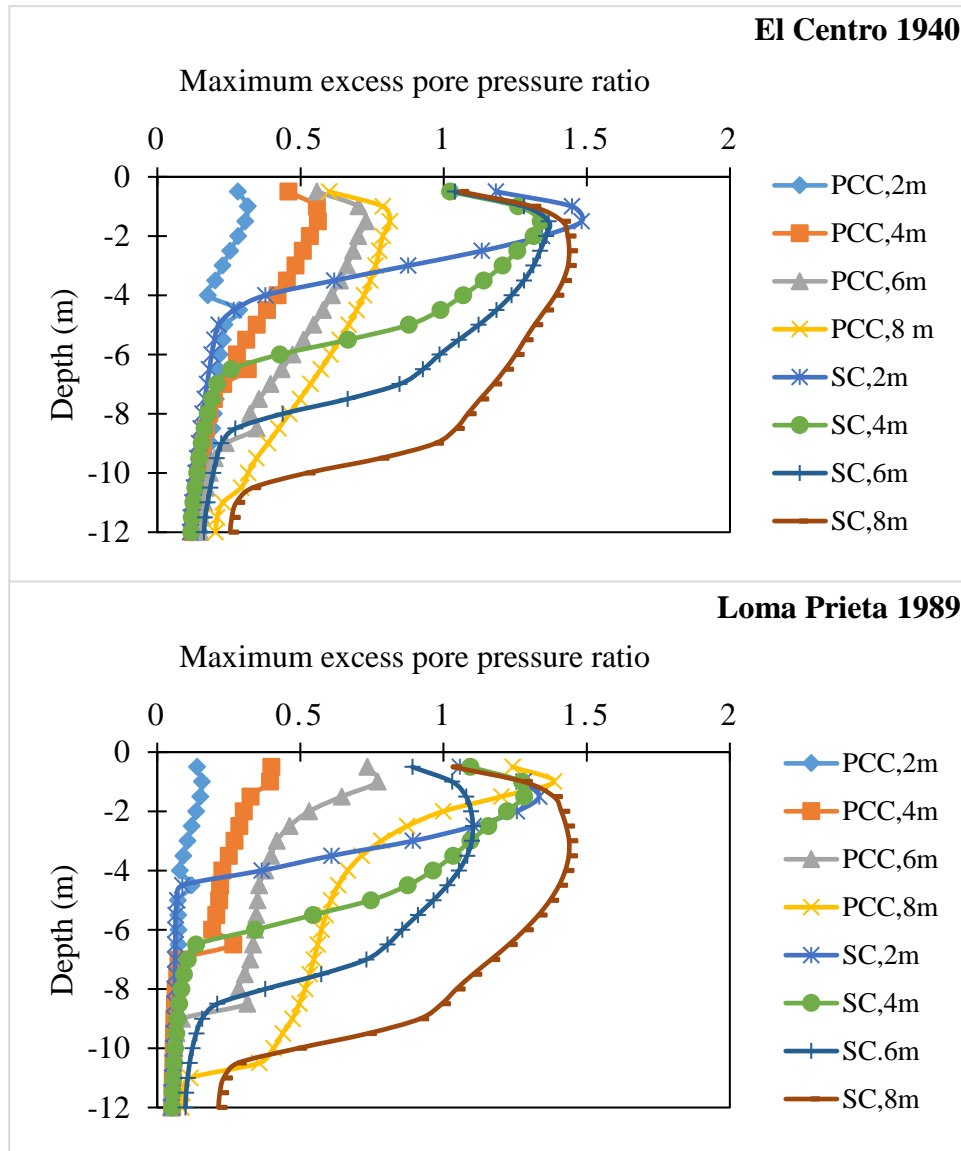
Figure 6.39 Comparison of maximum excess pore pressure ratio along the depth for varying thickness of liquefiable soil layer subjected to (a) El-Centro (b) Loma Prieta excitations

The maximum excess pore pressure values are observed within 4m from ground surface for all cases. It is also noted that the excess pore pressure value exceeded 1.0 when subjected to Loma Prieta earthquake for sandwiched liquefiable layer of thickness 8m.

However, excess pore pressure ratio exceeded for PCC improved ground is noted at a depth in between overlying non-liquefiable soil and liquefiable layer (Fig.6.39). Also, the performance is better than that of SC improved ground with the same circumstances. Thick liquefiable soil layer requires more time for dissipating excess pore pressures and is more susceptible to liquefaction (Ishihara 2007). However, for all thicknesses of sandwiched liquefiable soil, the performance of PCC is better than SC in terms of reduction in lateral displacement, limited pore pressure dissipation and improved shear strength due to rigid PCC inclusion.

The maximum shear stress pattern observed at the center of column along the depth of improved soil model for varying thickness of liquefiable soil layer subjected to El-Centro 1940 and Loma Prieta 1989 are different in formation (Fig.6.40). However, the shear strength is maximum for PCC improved ground than SC improved ground.
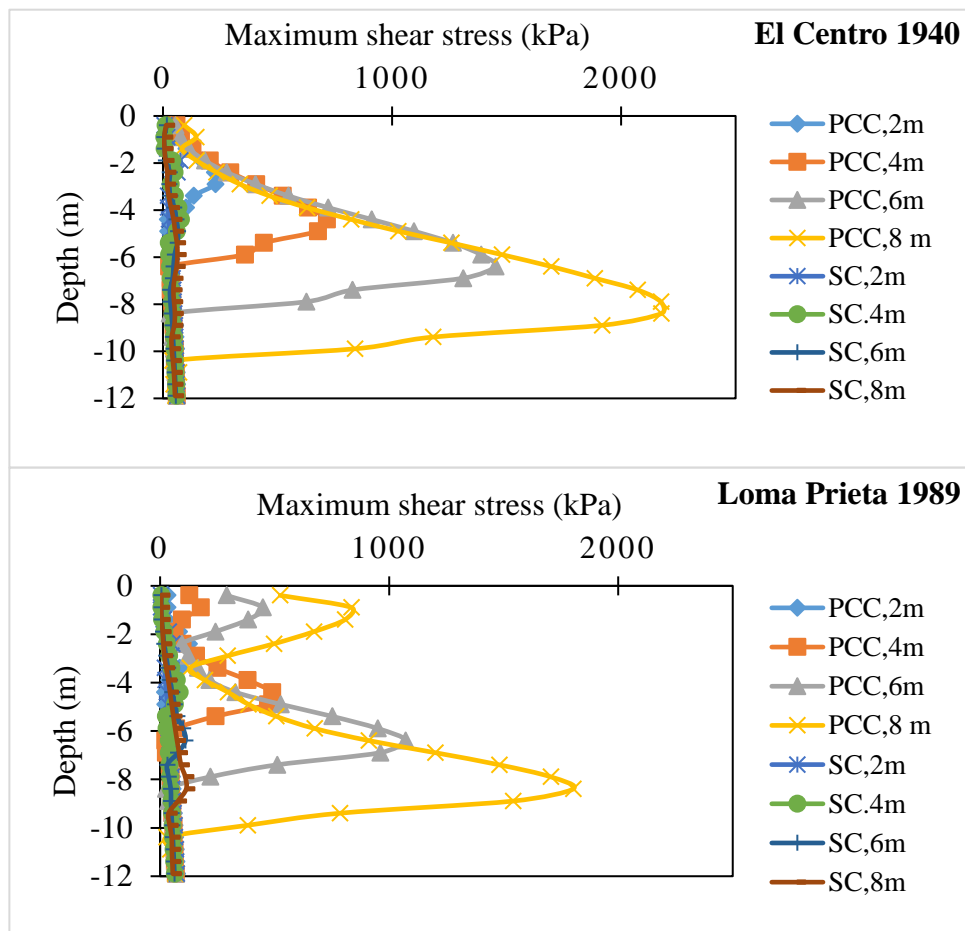
Figure 6.40 Comparison of maximum shear stress at center of column along the depth for varying thickness of liquefiable soil layer subjected to (a) El-Centro (b) Loma Prieta excitations

6.7.13 Total stress analysis versus effective stress analysis

Figure 6.41, Fig.6.42 and Fig.6.43 show the response profiles of maximum acceleration, maximum excess pore pressure ratio and maximum shear stress along the depth from total stress analysis (TSA) and effective stress analysis (ESA) for the benchmark cases of SC and PCC improved ground subjected to El-Centro and Loma Prieta earthquake excitation with peak ground acceleration scaled to 0.2g.

The maximum acceleration response from TSA is seen to increase monotonically from rock level to ground level for both seismic excitations. However, a different pattern is seen in the maximum acceleration profile from ESA (Fig.6.41). The improved soil model from TSA subjected to El Centro event has higher peak surface acceleration than from ESA. But the trend of peak surface acceleration of improved soil models from TSA and ESA is quite opposite when subjected to Loma Prieta earthquake. The maximum acceleration response profile along the depth is highly influenced by pore pressure build up. This is evident from the difference in maximum acceleration response from TSA and ESA (Dikmen and Ghaboussi 1984). However, for earthquake with longer duration and relatively lower frequency, maximum acceleration response is found to be higher from TSA than from ESA. And for earthquake with shorter duration and relatively high frequency, maximum acceleration response is found to be lesser from TSA than from that of ESA. That means for model ground with columnar inclusions, along with pore pressure build-up, the influencing factors in maximum acceleration response along the depth are significant duration and frequency of seismic excitation.
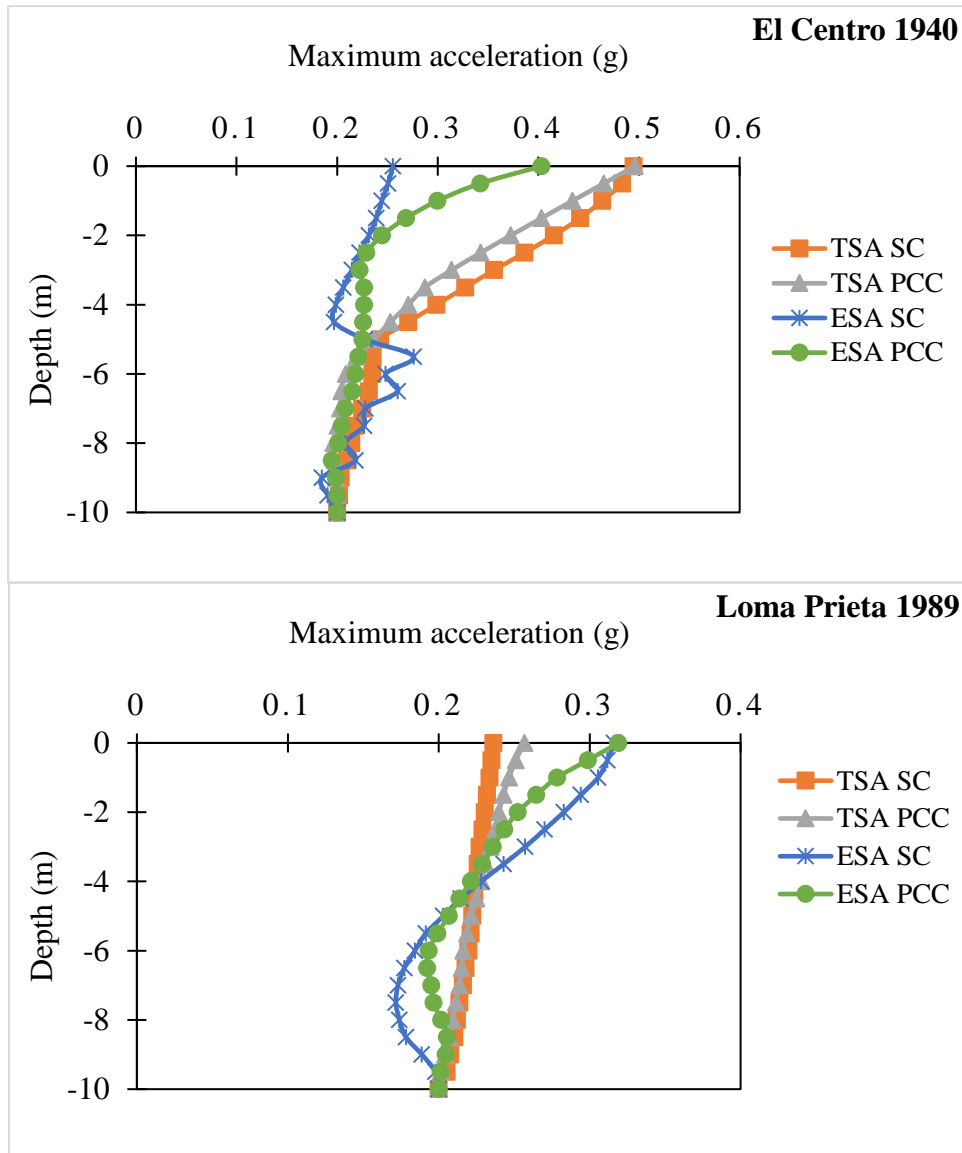
Figure 6.41 Comparison of maximum acceleration response along the depth from TSA and ESA for improved ground subjected to (a) El-Centro (b) Loma Prieta excitations

The excess pore pressure ratio, r_u is observed to be high within the depth of 4 m from ground level when subjected to seismic excitations (Fig.6.42). The excess pore pressure ratio, r_u at the center of PCC from ESA shows a value much lesser than that of SC, indicating the superior behaviour of PCC. The maximum shear stress at the center of column increased for PCC than SC for TSA as well as ESA (Fig.6.43). This demonstrates the enhanced shear resistance of PCC inclusions in place of stone columns.
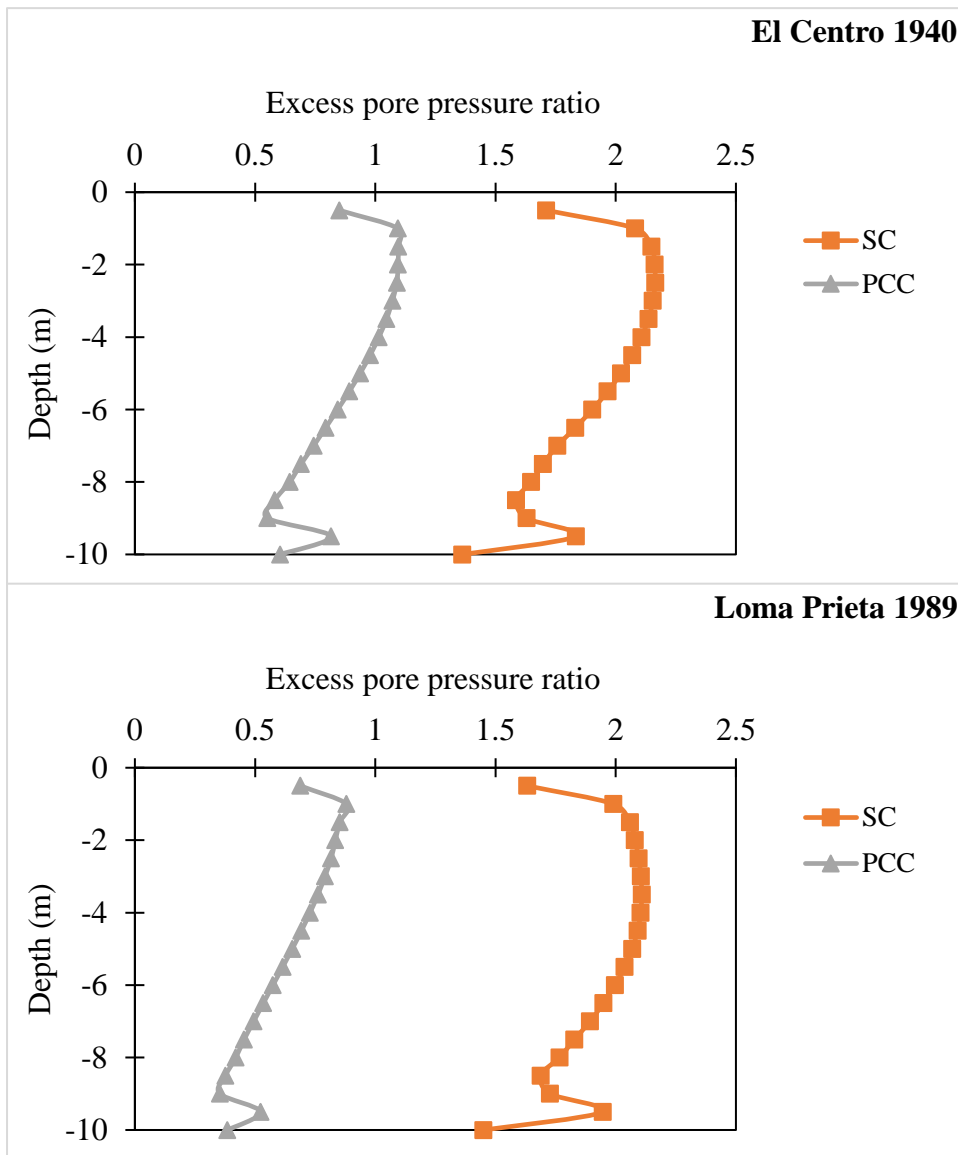
Figure 6.42 Comparison of maximum excess pore pressure ratio along the depth from ESA for improved ground subjected to (a) El-Centro (b) Loma Prieta excitations
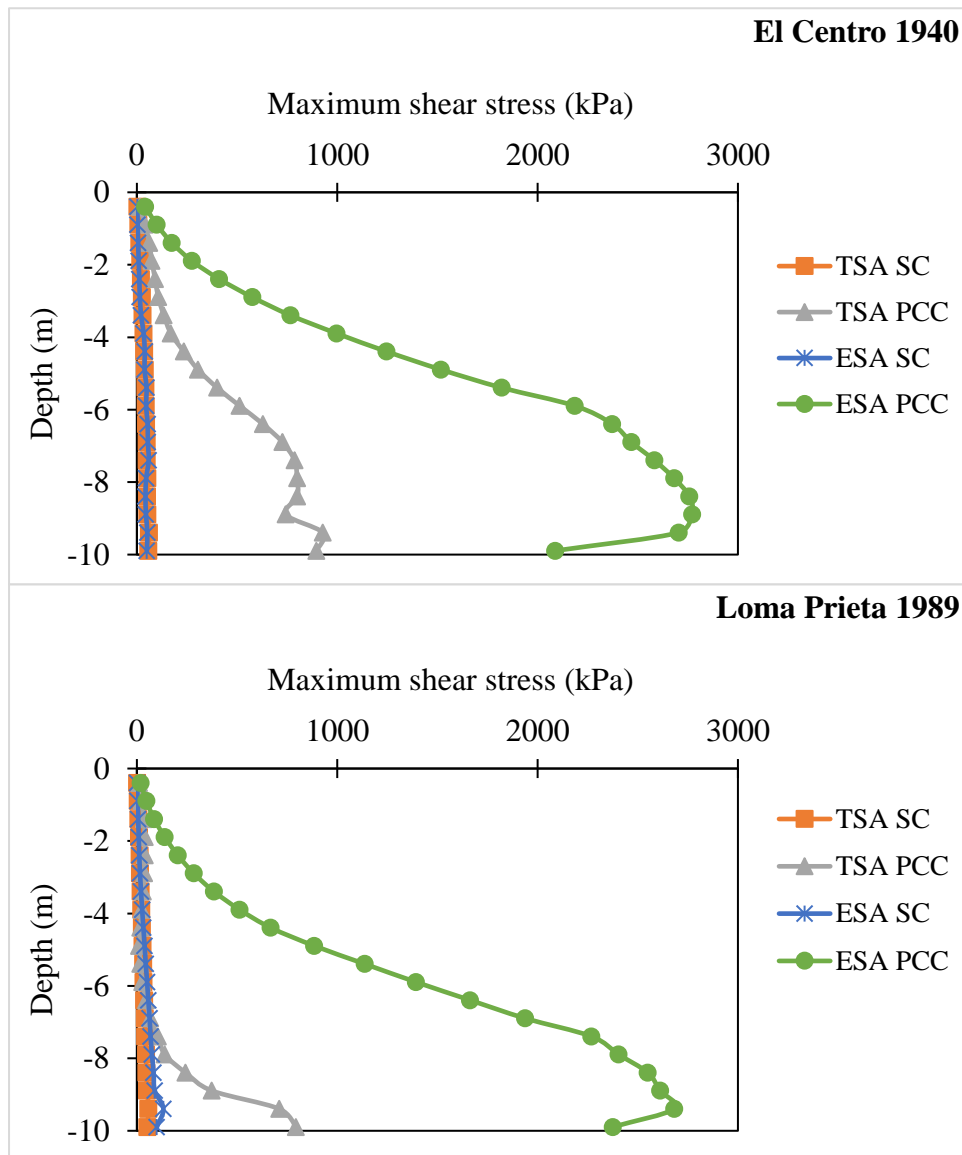
Figure 6.43 Comparison of maximum shear stress response along the depth from TSA and ESA for improved ground subjected to (a) El-Centro (b) Loma Prieta excitations

The various parameters influencing the seismic performance of column improved ground in terms of lateral displacement ratio are presented here. Lateral displacement ratio is a dimensionless factor defined as the ratio of lateral displacement of improved ground to the lateral displacement of unimproved sand strata. The influencing parameters versus lateral displacement ratio includes the area ratio, diameter, ground surface inclinations, peak ground acceleration, surface load, soil permeability and column permeability.

Figure 6.44 to Fig 6.50 shows the variation of influencing parameters such as area ratio, diameter, ground surface inclination, peak ground acceleration, surface load, soil permeability and column permeability with a dimensionless factor lateral displacement ratio. It is observed that the lateral displacement ratio decreases with increase in area ratio as well as diameter for stone column and pervious concrete column improved ground. This means that the liquefaction induced lateral spreading can be reduced with ground remediation, either by increasing the diameter of column inclusion or by reducing the center to center spacing between the column inclusions. The influence of ground surface inclination on lateral displacement ratio is found to be relatively insignificant. The lateral displacement ratio increased with increase in peak ground acceleration for stone column and pervious concrete column improved ground. However, pervious concrete column improved ground has much less lateral spreading than stone column improved ground when subjected to two different seismic excitations. The lateral displacement ratio is found to decrease with increase in ground surcharge. This is attributed to the enhanced confinement due to surface load. The lateral displacement ratio is found to be zero for pervious concrete column improved ground, when the surface load at the ground surface is around 150 kPa under two unique earthquake conditions. The lateral displacement ratio of stone column improved ground is observed to be highly dependent on the hydraulic conductivity of stone column and surrounding sand strata. However, the lateral displacement ratio of pervious concrete column improved ground is found to be independent of hydraulic conductivity of pervious concrete column as well as surrounding sand strata. The reduction in lateral displacement, independent of sand permeability makes pervious concrete column a better liquefaction mitigation measure in place of stone columns, for a wider range of liquefiable soil profiles with varying permeability ranges.
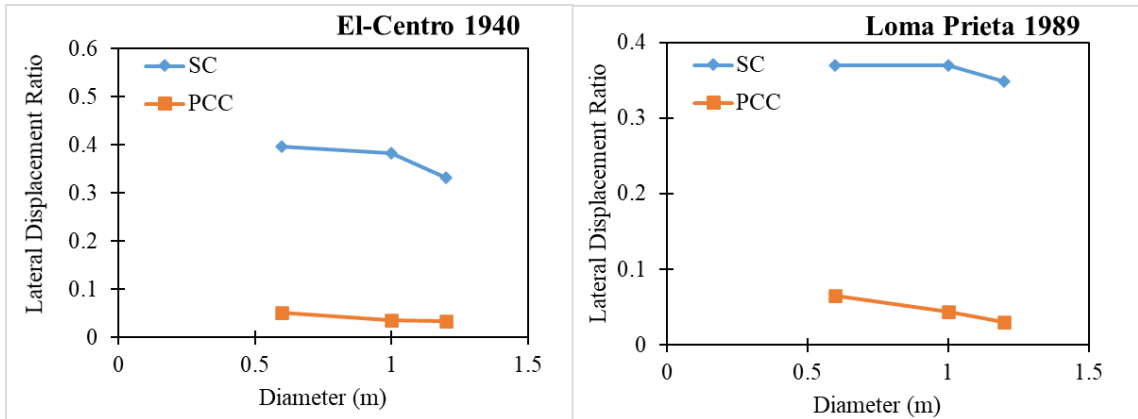
Figure 6.44 Diameter of column versus lateral displacement ratio
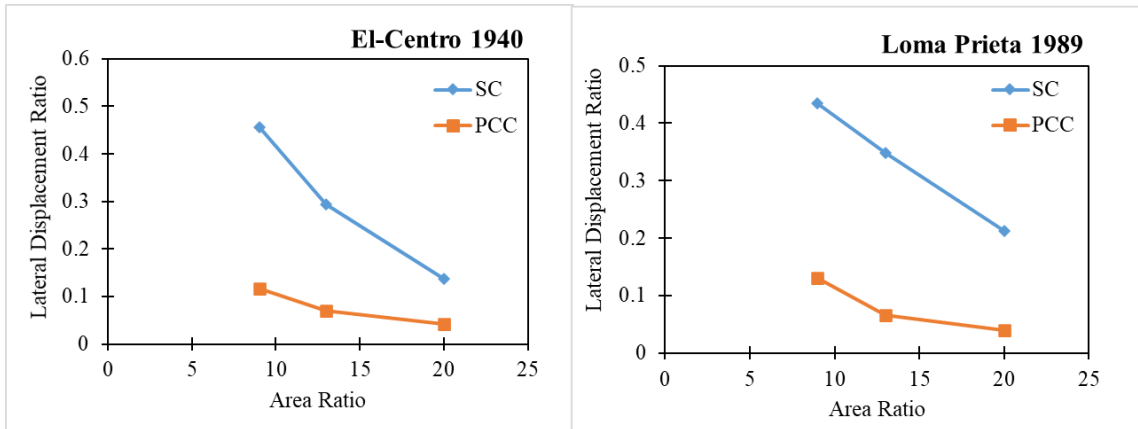
Figure 6.45 Area ratio versus lateral displacement ratio
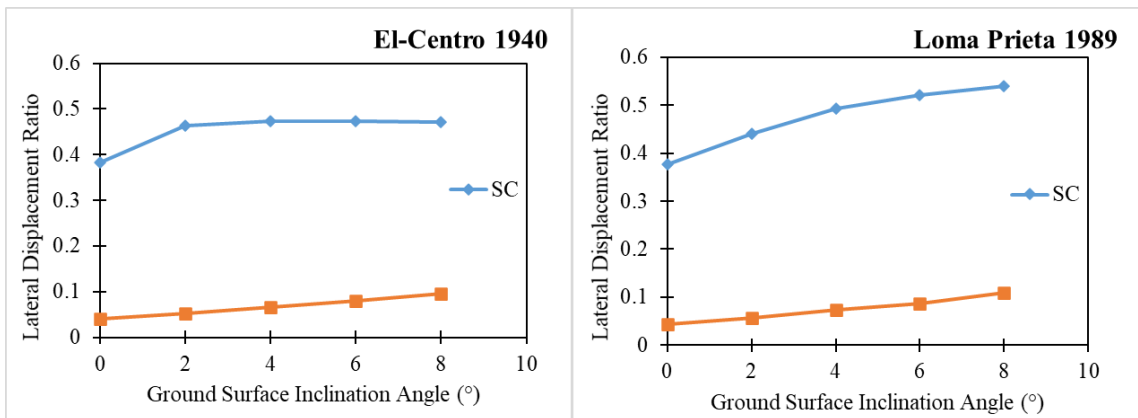
Figure 6.46 Ground surface inclination versus lateral displacement ratio

156
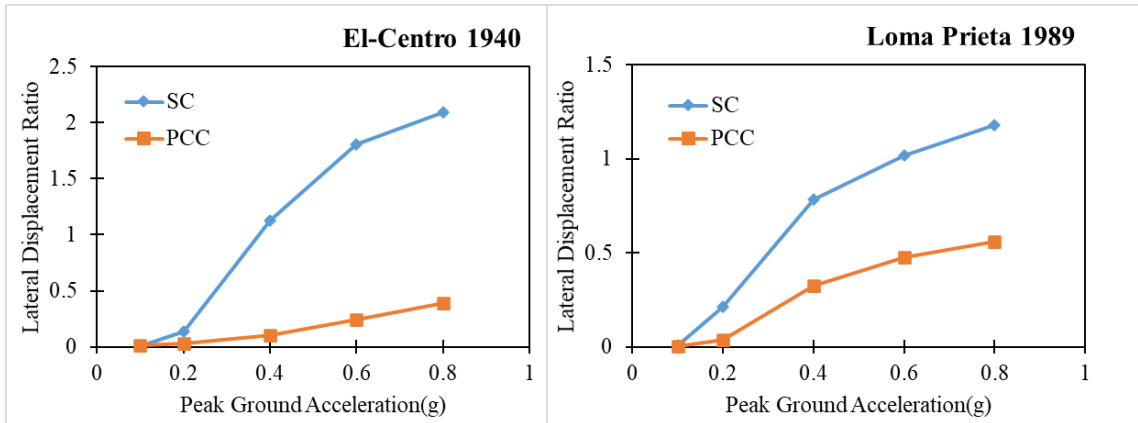
Figure 6.47 Peak ground acceleration versus lateral displacement ratio
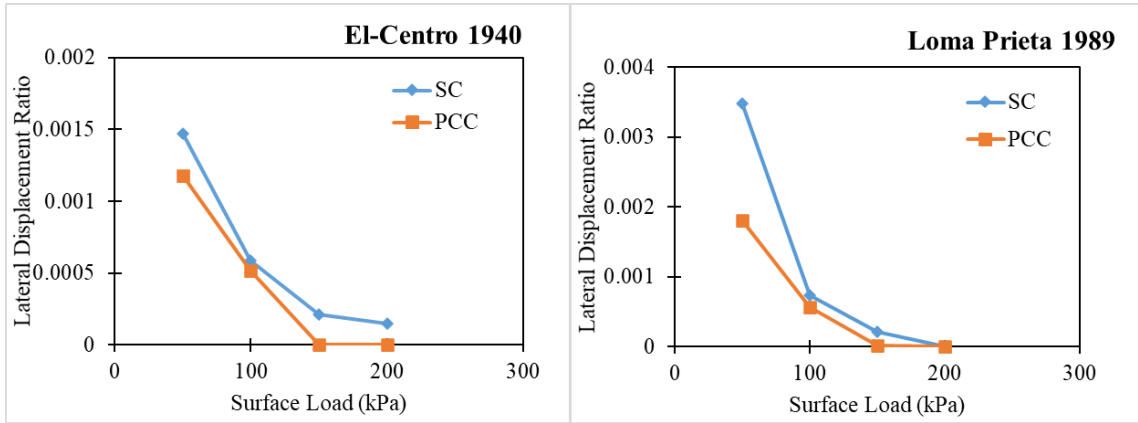
Figure 6.48 Surface load versus lateral displacement ratio
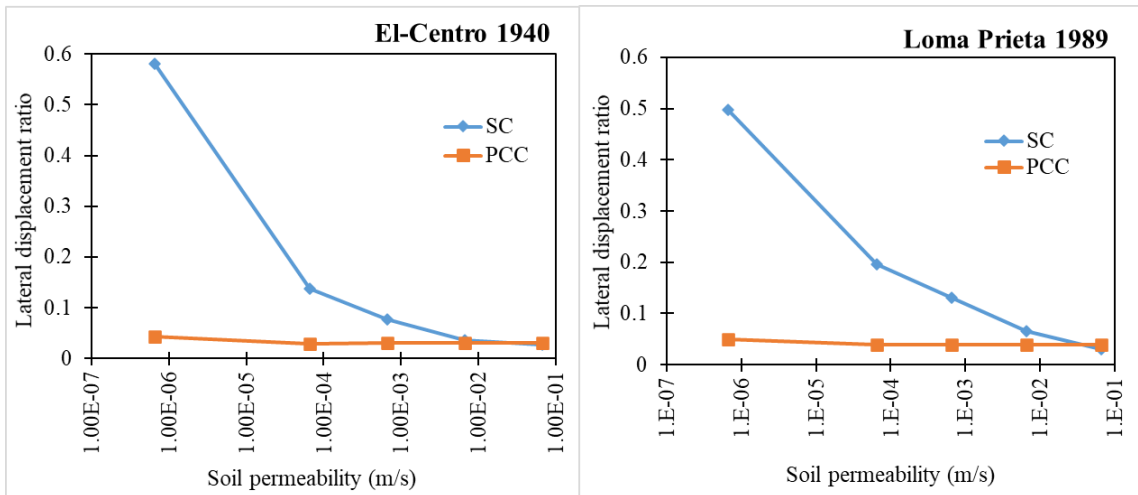
Figure 6.49 Soil permeability versus lateral displacement ratio

157
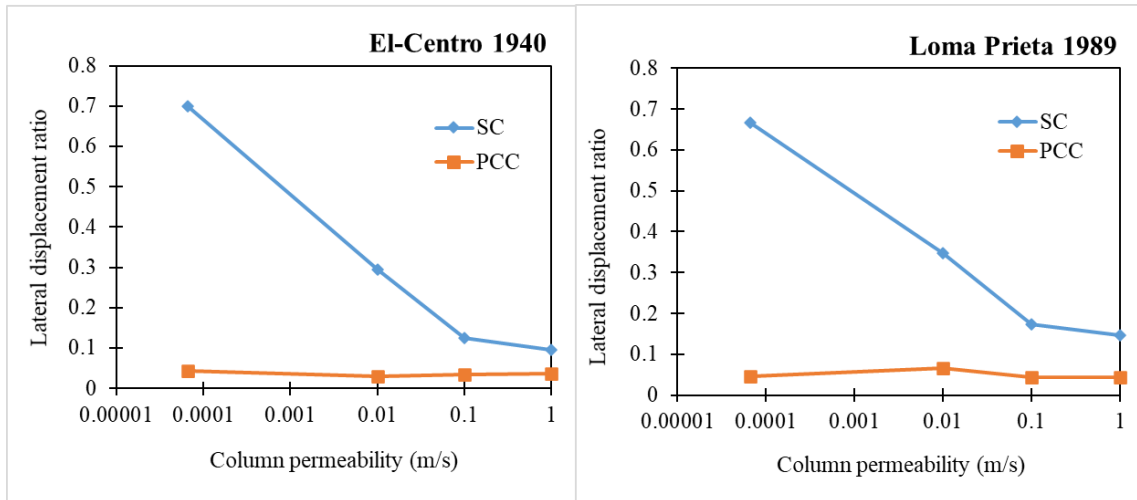
Figure 6.50 Column permeability versus lateral displacement ratio

6.8 SUMMARY

The seismic performance and liquefaction mitigation potential of improved ground using pervious concrete column is investigated in this chapter. It is found that the seismic resistance of pervious concrete column improved ground is better than conventional stone column improved ground. The lateral displacement response of pervious concrete column is similar to that of pile pinning case with almost zero displacement. The stone column is found to move along with surrounding soil during seismic excitations. The limited excess pore pressure generation indicates that the pervious concrete column drained the excess water though its pores to the surface better than stone column. The least deformation profile along with superior hydraulic functionality, makes PCC a better alternative to stone columns. It is strongly recommended to provide the pervious concrete column till the hard strata for minimizing lateral spreading during earthquakes.

In the case of SC improved ground, the dense gravel piles (stone column) get distorted during seismic loading due to shearing and causes dilation (increase in volume). The distorted gravel structure of stone column increases the length of drainage path thereby retarding the dissipation of excess pore water generated due to shaking. This causes reduction in effective stress and results in more lateral displacement. The PCC inclusion reduces the length of drainage path for excess pore water to dissipate quickly as the PCC structure is not distorted due to seismic shaking. Therefore, the seismic shear strains developed in the soil is very less. The limited excess pore pressure

generation and relatively higher effective confinement reduces the lateral displacement of PCC improved ground significantly.

The lateral displacement of pervious concrete column improved ground with area ratio of 9% is found to be lesser than stone column improved ground with an area ratio of 20%. From practical point of view, it would be a better field application to use pervious concrete column with wider spacing instead of conventional stone column with closer spacing. The seismic performance of pervious concrete column increases with increase in permeability of pervious concrete columns. The clogged pervious concrete column improved ground performed similar to that of unclogged stone column ground. The reduction in excess pore pressure shows significant reduction in shear stress-strain behaviour and relatively higher effective confinement. This confirms the higher liquefaction mitigation potential of pervious concrete columns.

The pervious concrete column remediation is also found to be effective than stone column remediation in loose sand, medium-dense sand and silt strata for reducing the lateral deformation induced due to earthquakes.The influence of thickness of liquefiable soil on lateral deformation is studied and results show that the pervious concrete column inclusion significantly reduces the lateral deformation even for liquefiable soil thickness of 8m. For less liquefiable soil thickness, stone column inclusion would perform well by reducing lateral deformation.

The lateral deformation of pervious concrete column improved ground is found to be independent of surrounding soil permeability which makes pervious concrete column a better alternative to stone column for different soil types with varying ranges of permeability. The lateral deformation of pervious concrete column and stone column improved ground increases with increase in ground surface inclination and peak ground acceleration. However, the seismic performance of pervious concrete column improved ground exhibits better performance than stone column improved ground even when subjected to a peak ground acceleration of 0.6g. This indicates that pervious concrete columns can be used in seismically active regions to mitigate liquefaction.

A zero-pore pressure generation condition occurs when the pervious concrete column permeability is greater than 0.3 m/s irrespective of earthquake characteristics. The stone column improved ground shows sudden shear stress reduction to zero along with high shear strain amplitude for earthquake with more number of cycles indicating

that the soil has liquefied whereas for earthquake with less number of significant cycles, the soil is not found to liquefy. However, the pervious concrete column improved ground did not show any liquefaction trigger when subjected to both the earthquakes considered. The comparison between response profiles of column improved ground from total stress analysis and effective stress analysis are observed to be influenced by significant duration and frequency of seismic excitations in addition to pore pressure build-up.

It is concluded that the pervious concrete columns can be considered as an economically and practically feasible alternative to conventional stone columns based on better performance in terms of pore pressure development, lateral deformation, shear stress-strain behaviour and effective confinement during ground motions. It is also found that the pervious concrete column improved ground efficiently mitigates seismically induced liquefaction.

CHAPTER 7

DESIGN EXAMPLE AND STABILITY ANALYSIS OF COLUMN SUPPORTED EMBANKMENT SYSTEM

In this chapter, design examples of embankment supported by ordinary stone columns and pervious concrete column are presented. In addition, two-dimensional slope stability analysis of an embankment system is evaluated by limit equilibrium method using PLAXIS LE.

7.1 DESIGN EXAMPLES

The design of stone column and pervious concrete column for a 5 m high embankment overlying 10 m thick weak clay with undrained cohesion of 10 kPa and a saturated density of 15 kN/m^3 is considered. The hard rock layer is assumed at the bottom of 10 m thick clay layer. The columns are assumed to be resting on this hard rock layer. A sample plan and cross-section of the column arrangement used in the design example is shown in Fig.7.1 and Fig.7.2 respectively. The water table is assumed at the ground level. The properties of clay, embankment fill, stones and pervious concrete are summarised in Table 7.1. The assumptions, detailed calculation steps and design of stone column and pervious concrete column for supporting 5 m high embankment is presented in Sections 7.1.1 and 7.1.2 respectively.

Table. 7.1 Material Properties

Material Properties	Clay	Embankment Fill	Stones	Pervious Concrete
Saturated Unit weight (kN/m^3)	15	18	19	19
Undrained Cohesion (kPa)	10	0	0	3000
Friction angle (°)	0	32	38	38
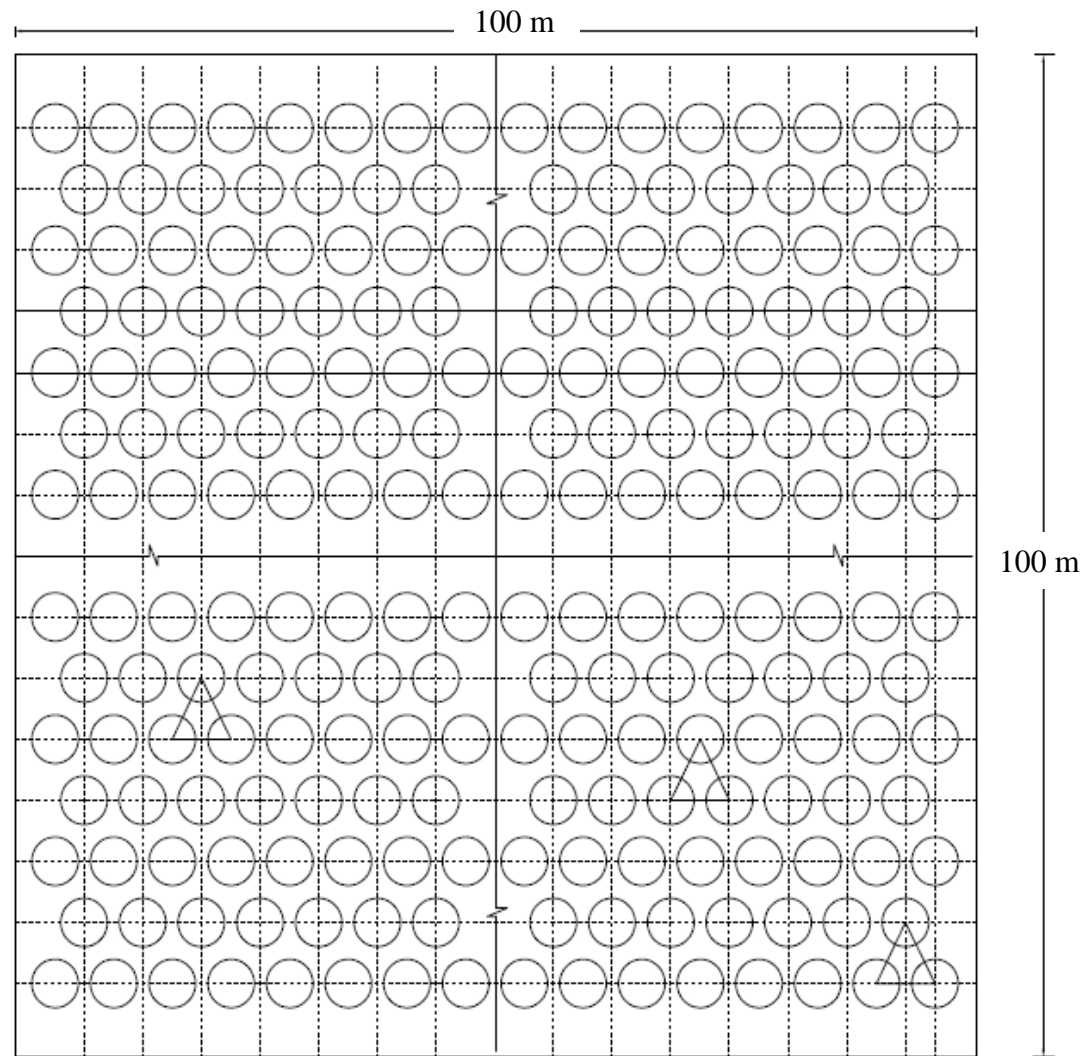
Figure 7.1 Plan showing triangular arrangement of columns
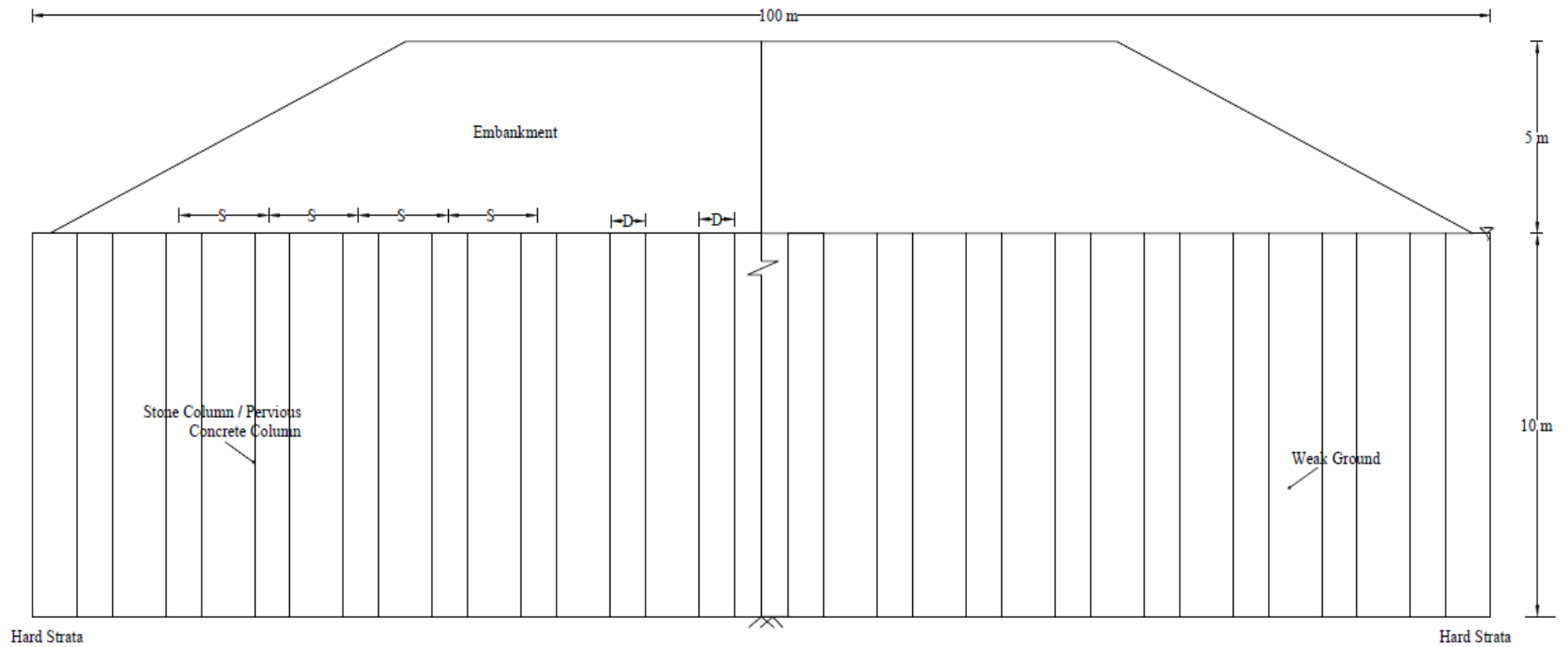
Figure 7.2 Elevation of column supported embankment system

7.1.1 Stone Column Supported embankment system

Design of stone column using material parameters as shown in the Table 7.1 for 5 m high embankment system is detailed in this section. The estimation of load carrying capacity of stone column is performed as per IS 15284.

Assume   Diameter of stone column, D = 1.0 m

Spacing between stone columns, S = 2D = 2.0 m

The load carrying capacity of stone column is estimated as the sum of capacity based on bulging of column, capacity based on surcharge effect and capacity based on bearing support by intervening soil. Therefore,

$$Q = Q_1 + Q_2 + Q_3 \tag{7.1}$$

where

Q : Total safe load on stone column and its tributary soil

$Q1$: Safe load on column alone due to bulging,

$Q2$: Safe load on column alone due to surcharge

$Q3$: Safe load taken by intervening soil between stone columns

(A) To find Q_1: Capacity based on bulging of stone column

Capacity based on bulging $= \sigma_v \frac{\pi}{4} D^2$

$$= \left[(\sigma_{r0} + 4c_u) k_{pcol} \right] \frac{\pi}{4} D^2$$

$$= \left[\left((k_0 \gamma'_c \, 2 \, D) + 4c_u \right) k_{pcol} \right] \frac{\pi}{4} D^2 \tag{7.2}$$

Where,

σ_v : Limiting axial stress in column given by $\sigma_v = \sigma_{rl} \, k_{pcol}$

σ_{rl} : Limiting radial stress given by $\sigma_{rl} = \left((\sigma_{r0} + 4c_u) k_{pcol} \right)$

σ_{r0} : Initial radial stress given by $\sigma_{r0} = k_0 \, \sigma_{v0}$

σ_{v0} : Initial effective stress given by $\sigma_{v0} = k_0 \, \gamma'_c \, 2 \, D$

In this example,

$k_{pcol} = tan^2 \left(45° + \frac{\emptyset sc}{2} \right) = tan^2 \left(45° + \frac{38}{2} \right) = 4.2$

$k_0 = 0.60$ (from IS 15284 part 1)

$D = 1$ m

$\gamma'_c = 15\text{-}10 = 5 \text{ kN/m}^3$

$c_u = 10 \text{ kPa}$

164

Now, From Eqn.7.2,

Capacity based on bulging = 151.74 kN

Safe load on column alone, Q1 = $\dfrac{151.74}{2}$ (FOS=2)

Q1 = 75.86 kN

B) To find Q2: Capacity based on surcharge effect

Safe capacity based on surcharge effect, $Q2 = k_{pcol} \dfrac{q_{safe}}{3}(1+2k_0)\dfrac{\pi}{4}D^2$ (7.3)

q_{safe} : safe bearing pressure of soil with FOS, $q_{safe} = \dfrac{c_u\,N_c}{2.0}$

Where, N_c= 5.14

From Eqn.7.3,

Safe capacity based on surcharge effect, Q2 = 33.893 kN

(C) To find Q3: Capacity based on bearing support by intervening soil between stone columns

$Q3 = \dfrac{c_u\,N_c}{2.0}(0.866\,S^2 - \dfrac{\pi}{4}D^2) = 68.85$ kN (7.4)

Hence total safe load = Q1 + Q2 + Q3

Q = 178.63 kN

Total stress for 5 m high Embankment = 5 *18 = 90 kN/m^2

Assume total area of ground improvement = 100 m x 100 m = 10000 m^2

Total load on the ground, Load T = 90 x 10000 = 900000 kN

To check the spacing of stone columns,

Number of stone columns = $\dfrac{\text{Load T}}{Q} = \dfrac{900000}{178.63} = 5038.3$

Therefore, area per column = $\dfrac{10000}{5038.3} = 1.984$ m^2

$0.866\,S^2 = 1.984$

S = 1.5 m

The assumed spacing is not matching with the final calculation. Hence, the assumed spacing is reduced and repeated calculations indicate the spacing of stone column as 1.5 m.

Design summary

Diameter of stone column, D = 1.00 m

Spacing, S = 1.5 m

Area ratio = $0.907\left(\dfrac{D}{S}\right)^2 = 40$ %

7.1.2 Pervious concrete Column Supported embankment system

Design of pervious concrete column using soil parameters as shown in the Table 7.1 for 5 m high embankment system is detailed in this section.

Assume   Diameter of pervious concrete column, D = 1.0 m

                    Spacing between pervious concrete columns, S = 2D = 2.0 m

Since the behaviour of the pervious concrete column is reported as similar to that of rigid pile, load carrying capacity of pervious concrete column is estimated as the sum of capacity based on axial capacity of rigid column and capacity based on bearing support by intervening soil. Therefore,

$$QP = QP1 + QP2 \tag{7.5}$$

where

QP : Total safe load on pervious concrete column and tributary soil

QP1 : Safe axial load on pervious concrete column

QP2 : Safe load on bearing support by intervening soil between pervious concrete columns

(A) To find QP1: Safe axial load on pervious concrete column column

Safe axial load on pervious concrete pile is calculated from load carrying capacity of rigid piles

Load carrying capacity (geotechnical capacity) of rigid piles,

$$Q_u = Q_{u1} + Q_{u2} = c_u N_c \frac{\pi}{4} D^2 + \alpha \, \bar{c} \, \pi \, D \, L \tag{7.6}$$

Where,

Q_{u1} = End-bearing resistance of pervious concrete column base given by $c_u N_c \frac{\pi}{4} D^2$

Q_{u2} = Skin resistance developed between clay and pervious concrete column given by $\alpha \, \bar{c} \, \pi \, D \, L$

N_c = 9 for piles

D = 1 m

c_u = 10 kPa

L = 10 m

$\alpha \, \bar{c}$ = 1.0 * 10 = 10 kPa

Safe axial load on column, $QP1 = \dfrac{Q_{u1}}{2} + \dfrac{Q_{u2}}{1.5}$

Considering FOS as 2 for end-bearing resistance and 1.5 for skin resistance,

$$QP1 = \frac{70.65}{2} + \frac{314}{1.5} = 244.65 \text{ kN}$$

Also, permissible structural load on column,

$$Qs1 = 0.25\, f_{ck}\, \frac{\pi}{4} D^2 \tag{7.7}$$

f_{ck} = Characteristic compressive strength of concrete =20 MPa

$Qs1 = 3925$ kN

Therefore, From QP1 and Qs1, minimum value is taken as load capacity of pervious concrete column = 244.65 kN

(B) To find QP2 : Capacity based on bearing support by intervening soil between pervious concrete columns

From Eqn.7.4,

$$QP2 = \frac{c_u\, N_c}{2.0}\, (0.866\, S^2 - \frac{\pi}{4} D^2)$$

$$= 120.55 \text{ kN}$$

Hence total safe load on pervious concrete column and tributary soil, QP = QP1 + QP2

QP = 365.213 kN

Total stress for 5 m high Embankment = 5 *18 = 90 kN/m^2

Assume total area of ground improvement = 100 m x 100 m = 10000 m^2

Total load on the ground Load T = 90 x 10000 = 900000 kN

To check the spacing of stone columns,

$$\text{Number of stone columns} = \frac{\text{Load T}}{Q} = \frac{900000}{365.213} = 2464.315$$

$$\text{Therefore, area per column} = \frac{10000}{2464.315} = 4.05 \text{ m}^2$$

$0.866\, s^2 = 4.05$

S = 2.16 m

The assumed spacing is matching with the final calculation. Hence, this design represents the optimum design of pervious concrete column.

Design summary

Diameter of pervious concrete column, D = 1.00 m

Spacing, S = 2.0 m

Area ratio $= 0.907 \left(\frac{D}{S}\right)^2 = 23$ %

7.2 SLOPE STABILITY ANALYSIS OF COLUMN SUPPORTED EMBANKMENT SYSTEM

The common failure envelope of stone column supported embankment system is reported as deep-seated failure envelope (Barksdale and Bachus 1983; Christoulas et al. 1997; Tan et al. 2008; Abusharar and Han 2011; Chen et al. 2015; Mohapatra and Rajagopal 2017). Moreover, for an embankment supported by granular/semi-rigid inclusions, it is reported that the failure surface is non continuous and non-circular (Han et al. 2004; Abusharar and Han 2011; Mohapatra et al. 2017; Mohapatra and Rajagopal 2017). Therefore, it is necessary to evaluate the performance of modified column improved ground supporting embankment system. Stability analysis of embankment supported on pervious concrete column improved ground is also limited in literature. Therefore, the FOS of pervious concrete column-embankment system is focussed and compared with that of stone column supported embankment system.

The stability analysis of column supported embankment system was conducted using PLAXIS LE 2D. The validation of model generated in PLAXIS LE was carried out by comparing the numerical results of stability analyses reported by Abusharar and Han (2011). The stability analysis of stone column supported embankment system used for validation is detailed as follows: The stone columns of diameter 1m were placed at a clear spacing of 3.2 m and was extended till sand strata of 2 m thick. The embankment was 5 m high with a crest width of 20 m and embankment slope was 2H:1V. Employing plane strain conditions and symmetry of system, half of the model was analysed using FLAC/Slope Version.5 software in their study. They used Mohr- Coulomb material properties and similar properties are used for validating the model generated in PLAXIS LE. The results of the model generated in PLAXIS LE as shown in Fig.7.3 is found to be following the trend and is in good agreement with the study by Abusharar and Han (2011).
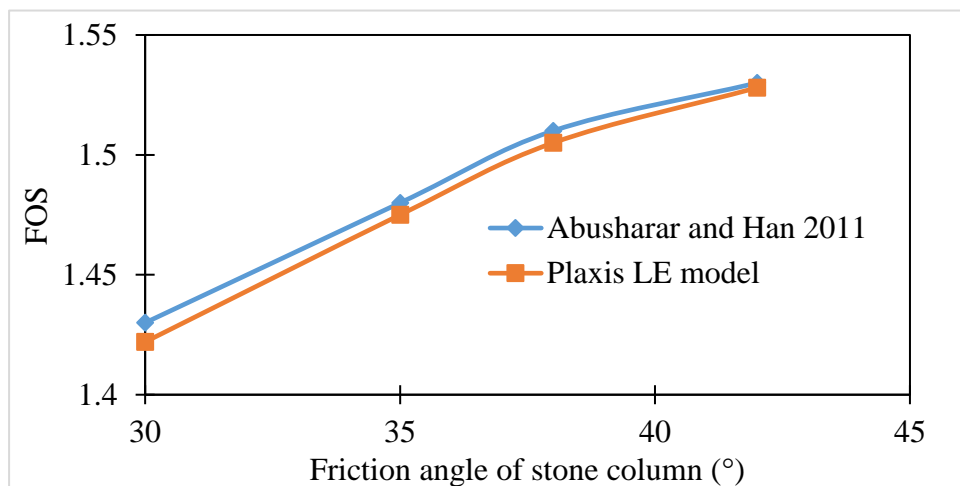
Figure 7.3 Validation of model generated in PLAXIS LE

7.2.1 Limit equilibrium slope stability Analysis

The embankment over the foundation soil of 10 m thick weak ground was considered as the unimproved system. The model dimensions used in this study are shown in Fig.7.4. The total width of embankment crest was 20 m. Half of the model was considered for the 2D Limit Equilibrium analysis. The embankment was 5 m high with a slope angle of 26.5°(1V:2H). The water table was assumed at the ground level, which is common for cohesive soils. The bottom boundary of clayey ground at 10 m below was assumed as the hard layer. The weak ground was further extended laterally to 20 m from the toe of the embankment such that the development of failure surfaces were not influenced by boundary effects (Abusharar and Han 2011). The lateral boundary was restricted for horizontal movements and due to symmetry, the center of the embankment was assumed with restraints in horizontal movement. The weak ground reinforced with stone columns of diameter 1.0 m placed at a center to center spacing of 2.5D (where D is the diameter of column) was considered as improved embankment case with ordinary stone columns. The dimension of pervious concrete column was kept similar to that of stone column for comparing the stability of embankment using both of these improvement methods. The General Limit Equilibrium (GLE) method was selected as the calculation method, available in PLAXIS LE. The GLE method uses moment equilibrium as well as force equilibrium, incorporating interslice forces (PLAXIS LE).

The failure of embankment on clayey soil is critical during construction and at the end of embankment construction. Hence short-term stability analysis was considered employing total stress method, which is applicable to situations where an embankment is constructed over saturated clays with no change in water content occurs in the subsoil prior to failure. Hence, undrained shear strength parameters are considered in the short-term stability analysis (IRC-75 2015). Therefore, the weak ground, embankment fill, stone column and pervious concrete were modelled with perfectly plastic and elastic Mohr-Coulomb model, which is commonly used. Additionally, for the short-term stability analysis of embankment system, undrained shear strength parameters are reported to be significant than elastic properties (Abusharar and Han 2011; Ho 2015; Mohapatra et al. 2017; Mohapatra and Rajagopal 2017; Zhang et al. 2020). Therefore, Mohr coulomb constitutive model was chosen for representing material properties as shown in Table.7.1. The unimproved ground was made up of weak clay and therefore cohesion value of 10 kPa was used. The ordinary stone column (OSC) was considered as gravel (cohesionless soil) with a friction angle of 38°. The pervious concrete column (PCC) was modelled with shear strength parameters similar to that of normal concrete. The performance of pervious concrete is reported as similar to that of concrete pile under static shear loading

conditions (Rashma et al. 2020, 2021). Therefore, the cohesion and friction angle of pervious concrete was selected as 3000 kPa and 38° respectively. The boundary conditions already implemented in the PLAXIS LE software were used.

The stability of embankment supported by pervious concrete column and conventional stone column was compared with the natural weak ground supported embankment system. The benchmark improved cases with stone column and pervious concrete column considered have columns of diameter 1.0 m placed at a center to center spacing of 2.5 D. The failure surface for an embankment supported by homogeneous weak ground is generally of circular envelope. However, for an embankment supported by granular/semi-rigid inclusions, it is reported that the failure surface is non continuous and non-circular (Han et al. 2004; Abusharar and Han 2011; Mohapatra et al. 2017; Mohapatra and Rajagopal 2017). Therefore, a comparison of failure envelope considering circular and non-circular envelope for improved benchmark cases is presented in Fig.7.5 and Fig.7.6 for stone column and pervious concrete column improved embankment system respectively. From the comparison, it is seen that the values of factor of safety are nearly same.
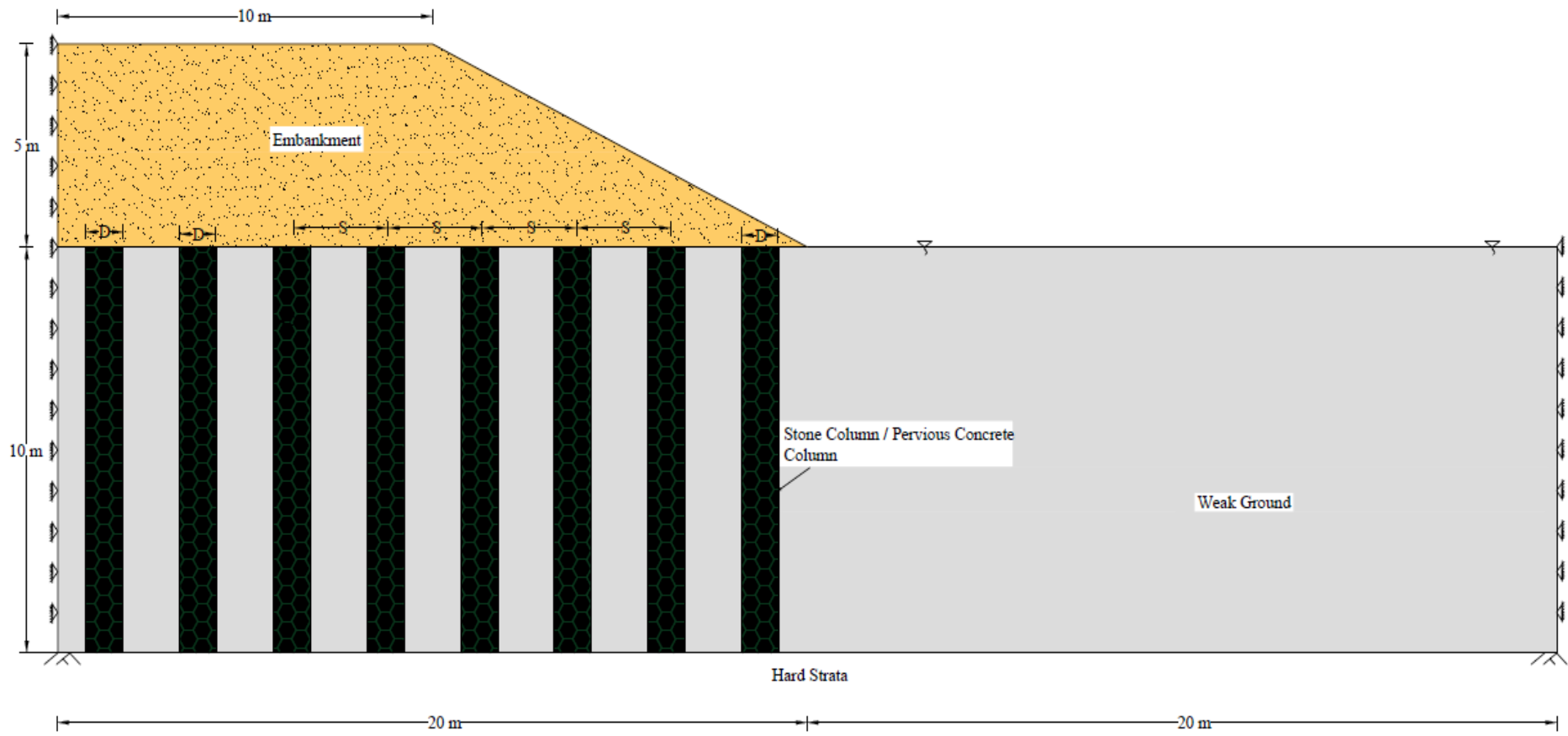
Figure 7.4 Column supported embankment system
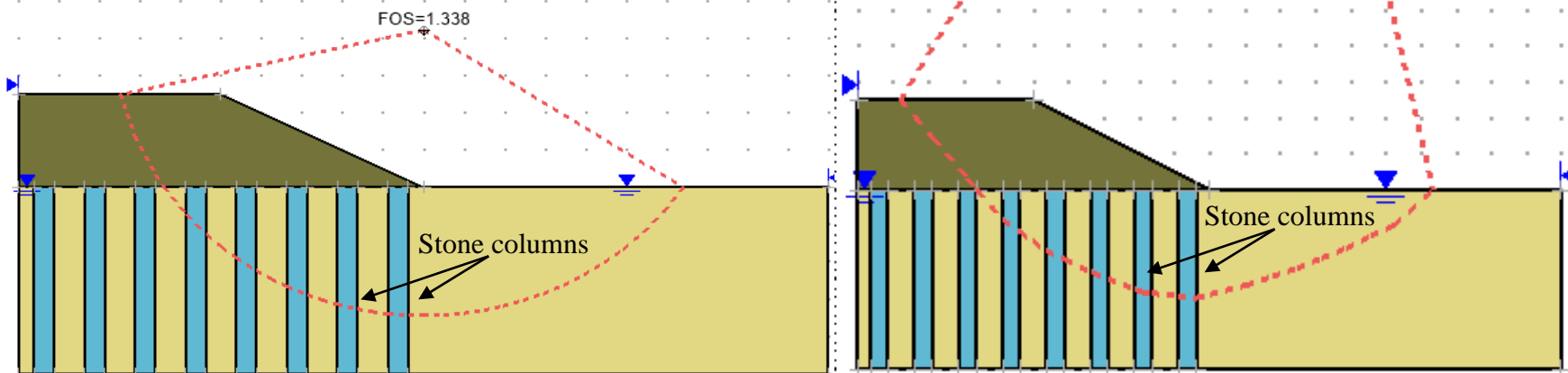
Figure 7.5 Critical slip surface of stone column supported embankment system(a) Circular envelope (b) Non-Circular envelope

(a) Circular slip Surface

FOS=1.532

(b) Non-Circular slip Surface

FOS=1.554

Pervious concrete columns
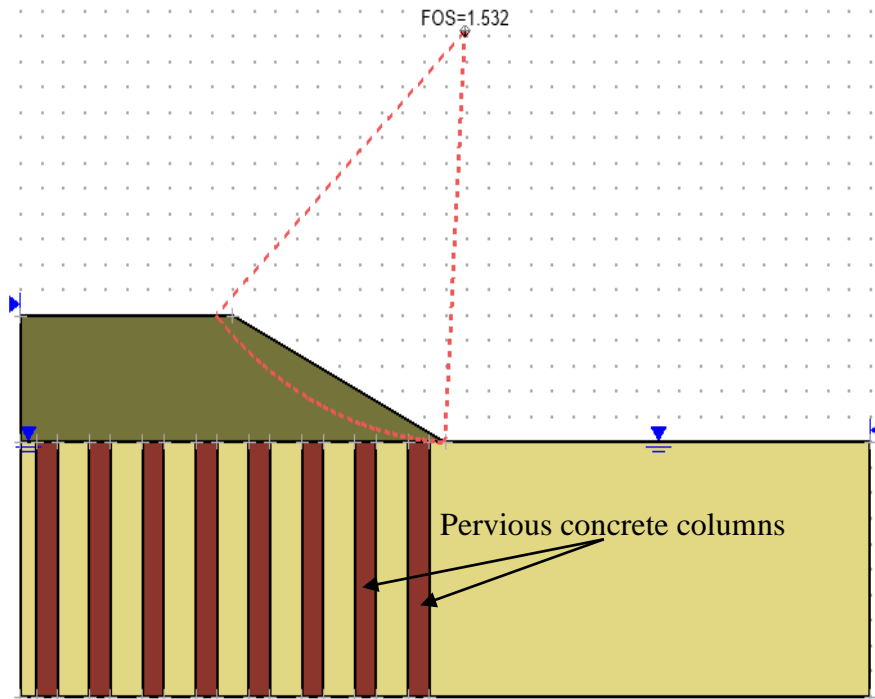
Pervious concrete columns
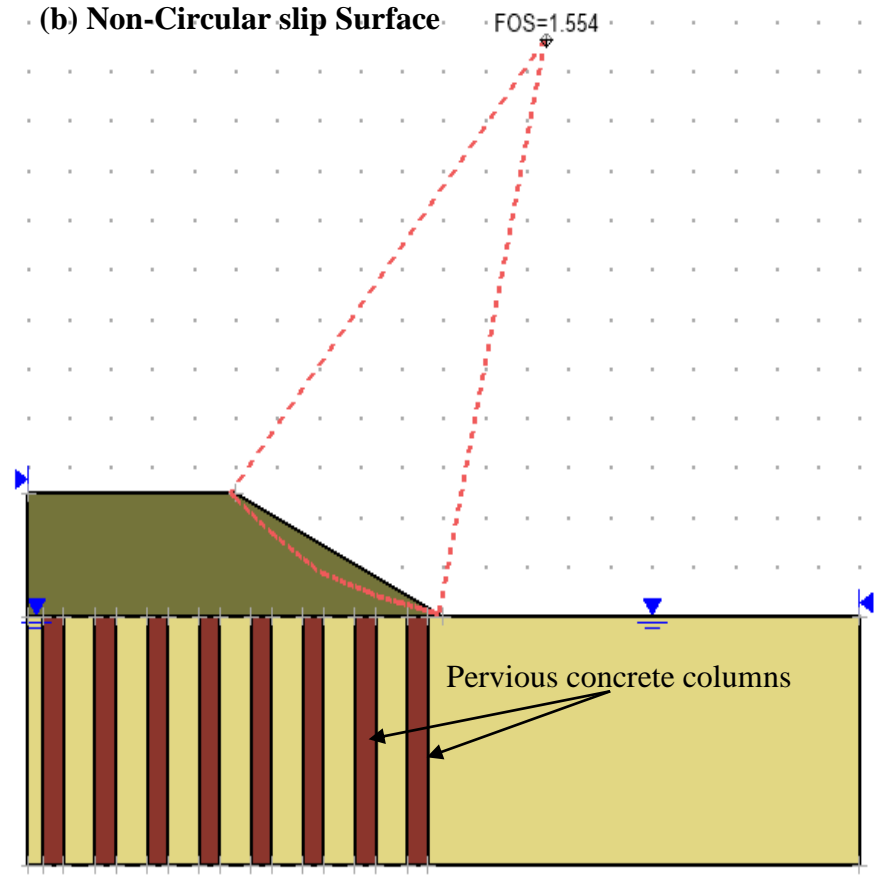
Figure 7.6 Critical slip surface of pervious concrete column supported embankment system(a) Circular envelope (b) Non-Circular envelope

The factor of safety of embankment without any ground improvement is 0.778. The improvement of stability for stone column and pervious concrete column supported embankment system is found to be 72 % and 100 % when compared to unimproved ground. Also, the critical failure slip surface of stone column-embankment system is observed to be of deep-seated failure envelope whereas the failure envelope of pervious concrete column-embankment system is observed to be of toe failure surface. Therefore, from the critical failure envelope and improvement in factor of safety values, it can be concluded that pervious concrete column supported embankment system has better stability than conventional stone column-embankment system.

7.3 SUMMARY

From the design of column supported embankment, it is observed that the area ratio required is 40% for OSC whereas for PCC, the area ratio is found to be 23%. This indicates that the spacing between pervious concrete columns could be more than the spacing between stone columns for the same design requirement and this could reduce the cost of construction using PCC. Considering the lower quantity of fine aggregate required, use of existing methods for construction of pervious concrete columns and more spacing between columns could result in an economical design and construction of pervious concrete column ground with improved performance. Additionally, the improvement of stability for stone column and pervious concrete column supported embankment system is found to be 72% and 100% when compared to unimproved ground. The critical failure envelope of pervious concrete column supported embankment system is observed to be of toe failure whereas the failure envelope of stone column supported embankment system is generally of deep-seated nature.

CHAPTER 8
CONCLUSIONS

An attempt has been made to evaluate the performance of pervious concrete column improved ground as an alternative to conventional stone column improved ground in terms of shear resistance and seismic performance. Numerical analysis of direct shear test and large shear test models were carried out to quantify the shear performance of pervious concrete column improved ground. The seismic performance of pervious concrete column improved ground is compared to stone column improved ground in terms of lateral displacement, excess pore water pressure generation, shear stress-strain behaviour along with effective confinement stress criteria. The various parameters influencing seismic performance are analyzed and the seismic performance of pervious concrete column improved ground is compared with that of conventional stone column improved ground.

From static shear and seismic analysis, the following conclusions are drawn:

8.1 STATIC SHEAR ANALYSIS

(i) The pervious concrete column for improving weak ground is found to offer higher shear resistance (52%) than conventional stone column. It is also observed that the shear resistance of conventional stone column improved ground is almost zero.

(ii) The shear strength of pervious concrete column improved ground with zero normal pressure is significantly (87%) higher than stone column improved ground. Placing pervious concrete columns beneath the toe of the embankment could be implemented for a better shear performance of column supported embankment systems.

(iii) The shear strength of positive slope increases with increase in slope angle, whereas for improved ground with negative slope, shear strength decreases with increase in slope angle. It is also recommended to consider the slope effect while determining shear strength.

(iv) From large shear test tank analyses, pervious concrete column in place of conventional stone column is found to offer higher shear resistance for improving weak ground.

(v) The pervious concrete column with end-bearing condition exhibits significant shear resistance than floating conditions. Therefore, it is recommended to provide pervious concrete columns till the hard bearing strata for optimum shear performance.

(vi) Pervious concrete columns show significantly lesser lateral displacements compared to ordinary stone columns. Also, the profile of lateral displacements obtained with pervious concrete columns and ordinary stone columns are entirely different. Peak lateral displacements in case of pervious concrete column are at the surface and the deflected profile of the column is very much like that of a rigid pile with a free or unrestrained head condition. In the case of ordinary stone columns, the peak lateral displacements occurred at some depth beneath the ground surface. Stone columns placed beneath the toe of the embankment are liable to undergo shear failure and are seen to move along with the soil.

8.2 SEISMIC ANALYSIS

(i) The pervious concrete column inclusion shortens the drainage path for excess pore water to dissipate quickly as the pervious concrete column structure is not distorted due to seismic shaking. Therefore, the seismic shear strains developed in the soil is very less. The limited excess pore pressure generation and relatively higher effective confinement reduces the lateral displacement of pervious concrete column improved ground significantly. The stone column gets distorted during seismic loading due to shearing and causes dilation. The distorted gravel structure of stone column lengthens the drainage path thereby retarding the dissipation of excess pore water generated due to shaking. This causes reduction in effective stress and results in more lateral displacement.

(ii) The lateral displacement response of pervious concrete column is similar to that of pile pinning case with almost zero displacement. The stone column is found to move along with surrounding soil during seismic excitations. The limited excess pore pressure generation demonstrates that the pervious concrete column

176

drained the excess water through its pores to the surface better than stone columns. The least deformation profile along with superior hydraulic functionality, makes pervious concrete column a better alternative to stone columns.

(iii) The end bearing pervious concrete column has better performance than floating pervious concrete columns. It is strongly recommended to provide the pervious concrete column till the hard strata for minimizing lateral spreading during earthquakes.

(iv) The lateral displacement of pervious concrete column improved ground with area ratio of 9% is found to be lesser than stone column improved ground with an area ratio of 20%. From practical point of view, it would be a better field application to provide pervious concrete columns with wider spacing instead of conventional stone columns with closer spacing. The lateral spreading of improved ground with stone column and pervious concrete column inclusion is found to decrease with increase in diameter as well as area ratio.

(v) The seismic performance of pervious concrete column increases with increase in permeability of pervious concrete column. The clogged pervious concrete column improved ground performed similar to that of unclogged stone column ground. The reduction in excess pore pressure demonstrates significant reduction in shear stress-strain behaviour and relatively higher effective confinement. This indicates the higher liquefaction mitigation potential of pervious concrete column improved ground.

(vi) It is concluded based on better performance in terms of pore pressure development, lateral deformation, shear stress-strain behaviour and effective confinement during ground motions, the pervious concrete columns can be considered as an economically and practically feasible alternative to conventional stone columns. It is also found that the pervious concrete column improved ground efficiently mitigates seismically induced liquefaction.

(vii) The pervious concrete column remediation is found to be effective than stone column remediation in loose sand, medium-dense sand and silt strata for mitigating lateral deformation induced due to earthquakes.

177

(viii) The effect of liquefiable soil thickness on lateral deformation indicates that the pervious concrete column inclusion has significantly reduced lateral deformation even for liquefiable soil thickness of 8 m. For less liquefiable soil thickness, stone column inclusion would perform well by reducing lateral deformation.

(ix) The lateral deformation of pervious concrete column improved ground is independent of surrounding soil permeability which makes pervious concrete column a better alternative to stone column for different soil types with varying ranges of permeability.

(x) The lateral deformation of pervious concrete column and stone column improved ground increases with increase in ground surface inclination and peak ground acceleration. However, seismic performance of pervious concrete column improved ground is significantly better even when subjected to a peak ground acceleration of 0.6g. This indicates that pervious concrete columns can be used in seismically active regions to mitigate liquefaction.

(xi) The lateral deformation of stone columns and pervious concrete column improved ground decreases with increase in surcharge load, indicating that the surcharge on the ground surface increases soil confinement and thus reduces lateral deformation.

(xii) The lateral displacement of pervious concrete column improved ground subjected to a ground motion having longer significant duration with relatively lower frequency content is higher than the excitation with shorter significant duration and with relatively high frequency content.

(xiii) The excess pore pressure generation is maximum at the instant of peak acceleration under both earthquakes. It is found that the generation of excess pore pressure reaches near zero values when the pervious concrete column permeability is greater than 0.3 m/s irrespective of different earthquake characteristics.

(xiv) The stone column improved ground undergoes sudden shear stress reduction to zero along with high shear strain amplitude for earthquake with more number of cycles indicating that the soil has liquefied whereas for earthquake with less number of significant cycles, the soil is not found to liquefy. However, the

pervious concrete column improved ground did not show any liquefaction trigger when subjected to both earthquakes considered.

(xv) The response profiles of column improved ground based on total stress analysis and effective stress analysis are highly influenced by significant duration and frequency of seismic excitation in addition to pore pressure build up.

The shear and seismic performance of pervious concrete column inclusions in weak ground/liquefiable ground is found to be significantly higher than stone column inclusions. The superior performance of pervious concrete columns, independent of surrounding soil properties, similar to piles in very soft clays/weak ground along with hydraulic functionality is essential for present-day situations due to non-availability of resilient grounds. The study also confirms the limitations of conventional stone columns in resisting shear movements. It is also inferred from the study that the stone column structure distorts due to seismic shaking without adequate confinement. This alarms a need for improving conventional stone columns internally or externally for better performance. Pervious concrete is made with less quantities of fine aggregate, which also make it an environmental-friendly sustainable alternative to stone columns. Pervious concrete columns can be installed in the site with existing installation methods, is an additional advantage. Therefore, the study recommends the use of pervious concrete columns for better shear and seismic performance and also for mitigating liquefaction in different types of soil strata competently.

The present study reports the major parameters influencing the performance of pervious concrete column improved ground under static shear and seismic loading conditions. Therefore, the identification of these parameters serves as a pilot study in the development of possible application of pervious concrete columns for improving weak grounds and to mitigate liquefaction and the associated disasters.

8.3 RECOMMENDATIONS FOR FIELD APPLICATIONS

Some recommendations for field applications from the findings of the present study are as follows:

(i) The study recommends the use of pervious concrete columns for supporting huge embankments over weak ground. This ground improvement practice

increases the shear resistance of improved ground along with hydraulic functionality similar to stone columns and increased vertical load carrying capacity than conventional stone columns.

(ii) The lateral deformation of pervious concrete column is similar to that of a rigid pile and the pervious concrete columns can be employed in the site with existing installation methods used for stone column construction is a benefit. The lower requirement of fine aggregate for constructing pervious concrete column is an added economical advantage and a sustainable solution.

(iii) Results suggest that the pervious concrete columns at wider spacing can also be implemented as the pervious concrete column improved ground with an area ratio of 9% has shown significant seismic performance.

(iv) Ground improvement using pervious concrete columns is highly recommended for mitigating liquefaction in seismically active regions. Pervious concrete columns can be effectively used in different types of liquefiable soil strata.

8.4 LIMITATIONS OF THE STUDY

i) The installation effects of stone column and pervious concrete column is not considered in this study.

ii) In seismic analysis, the interface between column-surrounding strata is assumed as perfect bonding. Therefore, the soil-structure interaction can be considered for further analysis.

iii) Settlement of ground due to liquefaction is not considered.

8.5 SCOPE OF FUTURE RESEARCH

This work can be extended in the following ways:

(i) Experimental and field investigations can be conducted on group of pervious concrete columns.

(ii) Post liquefaction settlement behaviour of pervious concrete column remediated ground can be conducted.

(iii) Three-Dimensional Stability analysis and seismic analysis of group of pervious concrete column can be carried out.

(iv) Studies on pervious concrete column improved ground incorporating installation effects of columns along with densification of surrounding soil during installation can be investigated.

APPENDIX I: SHEAR STRESS RATIO

Table AI-1 Shear stress ratio of improved ground with 50 mm, 70 mm and 90 mm diameter columns when subjected to varying normal pressures ranging from 15 kPa to 75 kPa

Normal Pressure(kPa)	Diameter(mm)	Shear stress ratio		
		Clay	OSC	PCC
15	50	0.357	0.398	0.579
	70		0.4176	0.786
	90		0.45	0.945
30	50	0.3351	0.339	0.502
	70		0.3545	0.6268
	90		0.3588	0.749
45	50	0.266	0.306	0.46308
	70		0.31	0.5635
	90		0.317	0.66187
60	50	0.2787	0.272	0.436
	70		0.284	0.518
	90		0.2808	0.599
75	50	0.27	0.267	0.414
	70		0.269	0.485
	90		0.269	0.555

Table AI-2 Shear stress ratio of improved ground with 50 mm diameter column for varying inclination of shear surfaces ranging from P 20° to N 20°

Normal Pressure(kPa)	Slope Angle (Degree)	Shear stress ratio		
		Clay	OSC	PCC
15	P 20	0.7995	0.817	2.5
	P 15	0.679	0.702	2.34
	P 10	0.57	0.601	1.847
	P 5	0.458	0.549	1.46
	0	0.357	0.45	0.945
	N 5	0.265	0.371	0.809
	N 10	0.174	0.286	0.899
	N 15	0.077	0.216	0.8918
	N 20	0	0.1767	0.864

	P 20	0.6938	0.695	1.97
	P 15	0.594	0.591	1.8
	P 10	0.51	0.519	1.316
	P 5	0.421	0.44	1.042
30	0	0.335	0.359	0.749
	N 5	0.2465	0.29	0.698
	N 10	0.161	0.21	0.701
	N 15	0.073	0.14	0.774
	N 20	0	0.09	0.736
	P 20	0.64	0.628	1.6
	P 15	0.537	0.527	1.47
	P 10	0.46	0.458	1.107
	P 5	0.37	0.38	0.898
45	0	0.302	0.318	0.6618
	N 5	0.219	0.241	0.625
	N 10	0.144	0.174	0.598
	N 15	0.064	0.11	0.645
	N 20	0	0.06	0.523
	P 20	0.597	0.58	1.39
	P 15	0.498	0.485	1.278
	P 10	0.42	0.411	0.982
	P 5	0.34	0.342	0.804
60	0	0.278	0.28	0.599
	N 5	0.198	0.218	0.572
	N 10	0.136	0.156	0.533
	N 15	0.0609	0.0967	0.566
	N 20	0	0.05	0.526
	P 20	0.5789	0.551	1.24
	P 15	0.483	0.462	1.129
	P 10	0.408	0.4001	0.887
	P 5	0.33	0.332	0.73
75	0	0.27	0.268	0.555
	N 5	0.191	0.206	0.53
	N 10	0.131	0.149	0.487
	N 15	0.0602	0.09	0.512
	N 20	0	0.049	0.475

Table AI-3 Shear stress ratio of improved ground with 70 mm diameter column for varying inclination of shear surfaces ranging from P 20° to N 20°

Normal Pressure(kPa)	Slope Angle (Degree)	Shear stress ratio		
		Clay	OSC	PCC
15	P 20	0.7995	0.795	1.89
	P 15	0.679	0.69	1.65
	P 10	0.57	0.58	1.53
	P 5	0.458	0.5	1.22
	0	0.357	0.41	0.79
	N 5	0.265	0.32	0.704
	N 10	0.174	0.23	0.69
	N 15	0.077	0.15	0.63
	N 20	0	0.06	0.7
30	P 20	0.6938	0.69	1.58
	P 15	0.594	0.598	1.25
	P 10	0.51	0.51	1.1
	P 5	0.421	0.43	0.9
	0	0.335	0.35	0.62
	N 5	0.2465	0.268	0.58
	N 10	0.161	0.19	0.53
	N 15	0.073	0.113	0.5
	N 20	0	0.032	0.54
45	P 20	0.64	0.628	1.31
	P 15	0.537	0.54	1.08
	P 10	0.46	0.45	0.92
	P 5	0.37	0.38	0.78
	0	0.302	0.31	0.56
	N 5	0.219	0.233	0.52
	N 10	0.144	0.164	0.48
	N 15	0.064	0.09	0.41
	N 20	0	0.03	0.45
60	P 20	0.597	0.58	1.16
	P 15	0.498	0.494	0.96
	P 10	0.42	0.415	0.83
	P 5	0.34	0.34	0.71
	0	0.278	0.28	0.52
	N 5	0.198	0.21	0.48
	N 10	0.136	0.148	0.44
	N 15	0.0609	0.08	0.36
	N20	0	0.006	0.39
75	P 20	0.5789	0.55	1.04
	P 15	0.483	0.464	0.87

	P 10	0.408	0.39	0.75
	P 5	0.33	0.326	0.65
	0	0.27	0.26	0.49
	N 5	0.191	0.19	0.44
	N 10	0.131	0.14	0.406
	N 15	0.0602	0.077	0.33
	N 20	0	0.006	0.3356

Table AI-4 Shear stress ratio of improved ground with 90 mm diameter column for varying inclination of shear surfaces ranging from P 20° to N 20°

Normal Pressure(kPa)	Slope Angle (Degree)	Shear stress ratio		
		Clay	OSC	PCC
15	P 20	0.7995	0.787	1.6
	P 15	0.679	0.677	1.37
	P 10	0.57	0.56	1.09
	P 5	0.458	0.48	0.82
	0	0.357	0.39	0.58
	N 5	0.265	0.3	0.6
	N 10	0.174	0.21	0.59
	N 15	0.077	0.124	0.55
	N 20	0	0.035	0.51
30	P 20	0.6938	0.68	1.1
	P 15	0.594	0.59	0.93
	P 10	0.51	0.49	0.8
	P 5	0.421	0.42	0.66
	0	0.335	0.34	0.5
	N 5	0.2465	0.26	0.47
	N 10	0.161	0.18	0.42
	N 15	0.073	0.099	0.369
	N 20	0	0.014	0.37
45	P 20	0.64	0.63	0.95
	P 15	0.537	0.54	0.83
	P 10	0.46	0.44	0.72
	P 5	0.37	0.37	0.6
	0	0.302	0.31	0.46
	N 5	0.219	0.224	0.43
	N 10	0.144	0.15	0.37
	N 15	0.064	0.08	0.33
	N 20	0	0	0.296
60	P 20	0.597	0.58	0.85
	P 15	0.498	0.49	0.75

	P 10	0.42	0.4	0.65
	P 5	0.34	0.338	0.56
	0	0.278	0.27	0.44
	N 5	0.198	0.2	0.4
	N 10	0.136	0.136	0.35
	N 15	0.0609	0.071	0.3
	N 20	0	0	0.27
	P 20	0.5789	0.56	0.78
	P 15	0.483	0.465	0.69
	P 10	0.408	0.38	0.61
	P 5	0.33	0.327	0.53
75	0	0.27	0.266	0.42
	N 5	0.191	0.19	0.38
	N 10	0.131	0.131	0.32
	N 15	0.0602	0.06	0.27
	N 20	0	0	0.24

APPENDIX II: DETAILED STRESS PATH

Figure AII-1 Detailed stress path of (a) Sand (Free-field) (b) SC and (c) PCC cases under El-Centro ground motions

Figure AII-2 Detailed stress path of (a) Sand (Free-field) (b) SC and (c) PCC cases under Loma Prieta ground motions

REFERENCES

ABAQUS/CAE 6.16 Documentation. Dassault Systèmes Simulia. (2016). Providence, RI, USA.

Abusharar, S.W. and Han, J (2011) "Two-dimensional deep-seated slope stability analysis of embankments over stone column-improved soft clay." *Engineering Geology* 120:103–110. https://doi.org/10.1016/j.enggeo.2011.04.002

Adalier, K., Elgamal, A., Meneses, J., and Baez, J. I. (2003). "Stone columns as liquefaction countermeasure in non-plastic silty soils." *Soil Dynamics and Earthquake Engineering*, 23(7), 571–584.

Ali, K., Shahu, J. T., and Sharma, K. G. (2014). "Model Tests on Stone Columns Reinforced with Lateral Circular Discs." *International Journal of Civil Engineering Research*, 5(2), 97–104.

Almeida, M. S. S., Hosseinpour, I., and Riccio, M. (2013). "Performance of a geosynthetic-encased column (GEC) in soft ground: Numerical and analytical studies." *Geosynthetics International*, 20(4), 252–262.

Ambily, A. P., and Gandhi, S. R. (2007). "Behavior of Stone Columns Based on Experimental and FEM Analysis." *Journal of Geotechnical and Geoenvironmental Engineering*, 133(4), 405–415.

Asgari, A., Oliaei, M., and Bagheri, M. (2013). "Numerical simulation of improvement of a liquefiable soil layer using stone column and pile-pinning techniques." *Soil Dynamics and Earthquake Engineering*, 51, 77–96.

Ashford, S. A., Rollins, K. M., Case Bradford, V. S., Weaver, T. J., and Baez, J. I. (2000). "Liquefaction mitigation using stone columns around deep foundations: Full-scale test results." *Transportation Research Record*, (1736), 110–118.

ASTM-D3080. (1998). *Standard Test Method for Direct Shear Test of Soils Under Consolidated Drained*. *Annual book of ASTM standards*.

Aziz, N., Majoor, D., and Mirzaghorbanali, A. (2017). "Strength Properties of Grout for Strata Reinforcement." *Procedia Engineering*, 191, 1178–1184.

Baez, J. I. (1995). "A Design Model for the Reduction of Soil Liquefaction by Vibro-Stone Columns,PhD dissertation." *University of Southern California Digital Library*, University of Southern California Digital Library.

Barksdale, R. D., and Bachus, R. C. (1983). "Design and constrcution of stone columns volume 1, FHWA-RD-83-026 Final Report." *Federal Highway Administration*, (December).

Beaty, M. H. and Peter M. Byrne. (1998). "Liquefaction and Deformation Analyses Using a Total Stress Approach." *Journal of Geotechnical and Geoenvironmental Engineering*, 124(6), 551–555.

Ben Salem, Z., Frikha, W., and Bouassida, M. (2016). "Effect of granular-column installation on excess pore pressure variation during soil liquefaction." *International Journal of Geomechanics*, 16(2).

Bergado, D. T., Shivashankar, R., Sampaco, C. L., Alfaro, M. C., and Anderson, L. R. (1991). "Behavior of a welded wire wall with poor quality, cohesive-friction backfills on soft Bangkok clay: a case study." *Canadian Geotechnical Journal*, 28(6), 860–880.

Black, J. A., Sivakumar, V., Madhav, M. R., and Hamill, G. A. (2007). "Reinforced stone columns in weak deposits: Laboratory model study." *Journal of Geotechnical and Geoenvironmental Engineering*, 133(9), 1154–1161.

Boulanger, R. W. W., Stewart, D. P., Idriss, I. M. M., Hashash, Y., and Schmidt, B. (1997). *Ground Improvement Issues for the Posey & Webster St.Tubes Seismic Retrofit Project: Lessons from Case Histories*.

Boulanger, RW and Idriss, I. M. (2010). "CPT and SPT Based Liquefaction Triggering Procedures." *Center for Geotechnical Modeling*, (10–02), 134.

Castro, J. (2017). "Groups of encased stone columns: Influence of column length and arrangement." *Geotextiles and Geomembranes*, 45(2), 68–80.

Chen, J.-F., Li, L.-Y., Xue, J.-F., and Feng, S.-Z. (2015). "Failure mechanism of geosynthetic-encased stone columns in soft soils under embankment." *Geotextiles and Geomembranes*, 43(5), 424–431.

Chen, S. E., and Ong, C. K. (2012). "Spectral analysis of surface wave for empirical elastic design of anchored foundations." *Advances in Civil Engineering*, 2012(February 2012).

Chopra, A. (2013). *Dynamics of Structures Theory and Applications to Earthquake Engineering*. *Pearson Prentice Hall*.

Chowdhury, I., and Dasgupta, S. P. (2019). *Soil dynamics and earthquake engineering. GeoPlanet: Earth and Planetary Sciences*.

Christoulas, S., Giannaros, C., and Tsiambaos, G. (1997). "Stabilization of embankment foundations by using stone columns." *Geotech. Geol. Eng.*, 15(3), 247–258.

Chu, D., and Truman, K. Z. (2004). "Effects of Pile Foundation Configurations in Seismic Soil-Pile-Structure Interaction." *13th World Conference on Earthquake Engineering*, (1551), Paper No. 1551.

Daniel Kraus. (2020). *Data analysis and visualization was aided by Daniel's XL Toolbox addin for Excel*. Würzburg, Germany.

Deb, K., Basudhar, P. K., and Chandra, S. (2007). "Generalized model for geosynthetic-reinforced granular fill-soft soil with stone columns." *International Journal of Geomechanics*, 7(4), 266–276.

Deb, K., Chandra, S., and Basudhar, P. K. (2008). "Response of multilayer geosynthetic-reinforced bed resting on soft soil with stone columns." *Computers and Geotechnics*, 35(3), 323–330.

Demir, S., and Özener, P. (2019). "Numerical investigation of seismic performance of high modulus columns under earthquake loading." *Earthquake Engineering and Engineering Vibration*, 18(4), 811–822.

Dheerendra Babu, M. R., Nayak, S., and Shivashankar, R. (2013). "A Critical Review of Construction, Analysis and Behaviour of Stone Columns." *Geotechnical and Geological Engineering*, 31(1), 1–22.

Dikmen, S. U., and Ghaboussi, J. (1984). "Effective stress analysis of seismic response and liquefaction: Case studies." *Journal of Geotechnical Engineering*, 110(5), 645–658.

Dobry, R., and Abdoun, T. (2017). "Recent Findings on Liquefaction Triggering in Clean and Silty Sands during Earthquakes." *Journal of Geotechnical and Geoenvironmental Engineering*, 143(10), 04017077.

Doherty, J., and Fahey, M. (2011). "Three-dimensional finite element analysis of the direct simple shear test." *Computers and Geotechnics*, 38(7), 917–924.

Elgamal, A., Lu, J., and Forcellini, D. (2009). "Mitigation of liquefaction-induced lateral deformation in a sloping stratum: Three-dimensional numerical simulation." *Journal of Geotechnical and Geoenvironmental Engineering*, 135(11), 1672–1682.

Elgamal, A., Yang, Z., Parra, E., and Ragheb, A. (2003). "Modeling of cyclic mobility in saturated cohesionless soils." *International Journal of Plasticity*, 19(6), 883–905.

Elgamal, A.-W., Dobry, R., Parra, E., and Zhaohui, Y. (1998). "Soil Dilation and Shear Deformations During Liquefaction." *4th International Conference on Case Histories in Geotechnical Engineering*, 10, 1238–1259.

Esmaeil, M., Khajehei, H., and Astaraki, F. (2017). "The Effectiveness of Deep Soil Mixing on Enhanced Bearing Capacity and Reduction of Settlement on Loose Sandy Soils." *International Journal of Railway Research*, 4(2), 33–39.

Fan, J., Wang, D., and Qian, D. (2018). "Soil-cement mixture properties and design considerations for reinforced excavation." *Journal of Rock Mechanics and Geotechnical Engineering*, 10(4), 791–797.

Fattah, M. Y. and Quitaba G Majeed. (2012). "Finite element analysis of Geogrid encased stone columns." *Geotechnical and Geological Engineering*, 30(4), 713–726.

FEMA 450. (2003). *NEHRP Recommended Provisions for Seismic Regulations for New Buildings and Other Structures Part 1: Provisions*. The, Building Seismic Safety Council for Agency, Federal Emergency Management.

Forcellini, D., and Tarantino, A. M. (2014). "Assessment of stone columns as a mitigation technique of liquefaction-induced effects during Italian Earthquakes (May 2012)." *The Scientific World Journal*, 2014.

Geng, L., Tang, L., Cong, S. Y., Ling, X. Z., and Lu, J. (2017). "Three-dimensional analysis of geosynthetic-encased granular columns for liquefaction mitigation." *Geosynthetics International*, 24(1), 45–59.

Ghasemi-Fare, O., and Pak, A. (2016). "Numerical investigation of the effects of geometric and seismic parameters on liquefaction-induced lateral spreading." *Soil Dynamics and Earthquake Engineering*, 89(April 2018), 233–247.

Gniel, J., and Bouazza, A. (2009). "Improvement of soft soils using geogrid encased stone columns." *Geotextiles and Geomembranes*, 27(3), 167–175.

Han J, Chai J-C, Leshchinsky D, Shen S-L (2004) "Evaluation of Deep-Seated Slope Stability of Embankments over Deep Mixed Foundations." *American Society of Civil Engineers, pp 945–954*

Han, J. (2014). "Development of Ground Column Technologies." *Proceedings of the Institution of Civil Engineers - Ground Improvement 1-19. http://dx.doi.org/10.1680/grim.13.00016*, 168.

Helwany, S. (2007). *Applied Soil Mechanics: With ABAQUS Applications. John Wiley & Sons, Inc.*

Ho I-H (2015) "Numerical Study of Slope-Stabilizing Piles in Undrained Clayey Slopes with a Weak Thin Layer." *International Journal of Geomechanics* 15:06014025. https://doi.org/10.1061/(asce)gm.1943-5622.0000445

Hong, Y.-S., Wu, C.-S., Kou, C.-M., and Chang, C.-H. (2017). "A numerical analysis of a fully penetrated encased granular column." *Geotextiles and Geomembranes*, 45(5), 391–405.

Huang, D., Wang, G., and Jin, F. (2020). "Effectiveness of Pile Reinforcement in Liquefied Ground." *Journal of Earthquake Engineering*, 24(8), 1222–1244.

IRC-75. (2015). *IRC Guidelines for the design of high embankments*. Indian Roads Congress.

IS 15284 (part 1). (2003) (Reaffirmed Year: 2018). *Design and construction for ground improvement-Guidelines. Bureau of Indian Standards, New Delhi*.

Ishihara, K. (1997). *Soil behaviour in earthquake geotechnics. Choice Reviews Online*.

Ishihara, K. (2007). "Material: Liquefaction of Subsurface Soils During Earthquakes."

Jiaer Wu, Kammerer, A. M., Riemer, M. F., Seed, R. B., and J.M., P. (2004). "Laboratory Study of Liquefaction Triggering Criteria." *13 th World Conference on Earthquake Engineering*, 74–76.

Kempfert, H. G. (2003). "Ground improvement methods with special emphasis on column-type techniques." *Int. Workshop on Geotechnics of Soft Soils-Theory and Practice*, 101–112.

Kia, A., Wong, H. S., and Cheeseman, C. R. (2017a). "Clogging in permeable concrete: A review." *Journal of Environmental Management*, 193(May), 221–233.

Kia, A., Wong, H. S., and Cheeseman, C. R. (2017b). "Development of clogging resistant permeable concrete." (June).

Kia, A., Wong, H. S., and Cheeseman, C. R. (2019). "High-strength clogging resistant permeable pavement." *International Journal of Pavement Engineering*, 0(0), 1–12.

Kiku, H., and Tsujino, S. (1996). *Post liquefaction characteristic of sand. 11th World Conference on Earthquake Engineering*.

Kitazume, M., and Maruyama, K. (2007). "Internal Stability of Group Column Type Deep Mixing Improved Ground Under Embankment Loading." *Soils and Foundations*, 47(3), 437–455.

Kolekar, Y. A., Mir, O. S., and S.Murty, D. (2011). "Behaviour of Stone Column Reinforced Marine Clay under Static and Cyclic Loading." *Proceedings of Indian Geotechnical Conference, December 15-17*, 429–432.

Kramer, S.L., (1997). *Geotechnical Earthquake Engineering*. Prentice-Hall International Series in Civil Engineering and Engineering Mechanics.

Kramer, S. L., and Elgamal, A. W. (2001). *Modeling Soil Liquefaction Hazards for Performance Based Earthquake Engineering. University of California*.

Krishna, A. M. (2011). "Mitigation of liquefaction hazard using granular piles." *International Journal of Geotechnical Earthquake Engineering*, 2(1), 44–66.

Law, H. K., and Lam, I. P. (2001). "Application of Periodic Boundary for Large Pile Group." *Journal of Geotechnical and Geoenvironmental Engineering*, 127(10), 889–891.

Lees, A. (2016). *Geotechnical Finite Element Analysis. Geotechnical Finite Element Analysis*.

Lo, S. R., Zhang, R., and Mak, J. (2010). "Geosynthetic-encased stone columns in soft clay: A numerical study." *Geotextiles and Geomembranes*, 28(3), 292–302.

Lu, J., Elgamal, A., Yan, L., Law, K. H., and Conte, J. P. (2012). "Large-scale numerical modeling in geotechnical earthquake engineering." *International Journal of Geomechanics*, 11(6), 490–503.

Lu, J., Kamatchi, P., and Elgamal, A. (2019). "Using Stone Columns to Mitigate Lateral Deformation in Uniform and Stratified Liquefiable Soil Strata." *International Journal of Geomechanics*, 19(5), 04019026.

Lu, J., Peng, J., Elgamal, A., Yang, Z., and Law, K. H. (2004). "Parallel finite element modeling of earthquake ground response and liquefaction." *Earthquake Engineering and Engineering Vibration*, 3(1), 23–37.

Luco, N., Valley, M., and Crouse, C. B. (2011). "FEMA P-751: Chapter 3: Earthquake Ground Motion." *NEHRP Recommended Provisions: Design Examples*, 1–28.

Malarvizhi, S. N., and Ilamparuthi, K. (2004). "Load versus settlement of claybed stabilized with stone & reinforced stone columns." *Proceedings of the 3 rdAsian Regional Conference on Geosynthetics, GEOASIA*, (1993), 322–329.

Marko, J., Thambiratnam, D., and Perera, N. (2006). "Study of viscoelastic and friction damper configurations in the seismic mitigation of medium-rise structures." *Journal of Mechanics of Materials and Structures*, 1(6), 1001–1039.

Martin, J. R., Guney Olgun, C., Mitchell, J. K., and Turan Durgunoglu, H. (2004). "High-modulus columns for liquefaction mitigation." *Journal of Geotechnical and Geoenvironmental Engineering*, 130(6), 561–571.

Martin, J. R., Olgun, C. G., Mitchell, J. K., and Durguno, H. T. (2006). "Discussion of "High-Modulus Columns for Liquefaction." (July), 946–961.

Marto, A., Moradi, R., Helmi, F., Latifi, N., and Oghabi, M. (2013). "Performance analysis of reinforced stone columns using finite element method." *Electronic Journal of Geotechnical Engineering*, 18 B, 315–323.

Mazzoni, S., McKenna, F., Scott, M. H., and Fenves, G. L. (2006). *Open System for Earthquake Engineering Simulation (OpenSEES) user command-language manual*. *Pacific Earthquake Engineering Research Center*, 465.

Meshkinghalam, H., Hajialilue-Bonab, M., and Khoshravan Azar, A. (2017). "Numerical investigation of stone columns system for liquefaction and settlement diminution potential." *International Journal of Geo-Engineering*, 8(1).

Mitchell J. (1981). "Soil Improvement — State of the Art Report." *International Society for Soil Mechanics and Geotechnical Engineering (ISSMGE)*, 536–537.

Mitchell, J. K., and Huber, T. R. (1985). "Performance of a stone column foundation." *Journal of Geotechnical Engineering*, 111(2), 205–223.

Mohapatra, S. R., Mishra, S. R., Nithin, S., Rajagopal, K., and Sharma, J. (2018). "Effect of Box Size on Dilative Behaviour of Sand in Direct Shear Test." *Lecture Notes in Civil Engineering*, Springer Singapore, 111–118.

Mohapatra, S. R., and Rajagopal, K. (2015). "Mode of failure of granular column subjected to lateral loading." *6th International Geotechnical Symposium on Disaster Mitigation in Special Geoenvironmental Conditions*.

Mohapatra, S. R., and Rajagopal, K. (2016). "Experimental and numerical modelling of geosynthetic encased stone columns subjected to shear loading." *Japanese Geotechnical Society Special Publication*, 2(67), 2292–2295.

Mohapatra, S. R., and Rajagopal, K. (2017). "Undrained stability analysis of embankments supported on geosynthetic encased granular columns." *Geosynthetics International*, 24(5), 465–479.

Mohapatra, S. R., Rajagopal, K., and Sharma, J. (2016). "Direct shear tests on geosynthetic-encased granular columns." *Geotextiles and Geomembranes*, 44(3), 396–405.

Mohapatra, S. R., Rajagopal, K., and Sharma, J. (2017). "3-Dimensional numerical modeling of geosynthetic-encased granular columns." *Geotextiles and Geomembranes*, 45(3), 131–141.

Mohapatra, S. R., Rajagopal, K., and Sharma, J. S. (2014). "Analysis of geotextile-reinforced stone columns subjected to lateral loading." *10th International Conference on Geosynthetics, ICG 2014*.

Mohraz, B., and Elghadarnsi, F. E. (1989). *Earthquake Ground Motion and Response Spectra. The Seismic Design Handbook*, 32–80.

Murali Krishna, A., Madhav, M. R., Kumar, K. (2014). "Ground Engineering with Granular Inclusions for Loose Saturated Sands Subjected to Seismic Loadings." *Indian Geotechnical Journal*, 44(2), 205–217.

Murugesan, S., and Rajagopal, K. (2006). "Geosynthetic-encased stone columns: Numerical evaluation." *Geotextiles and Geomembranes*, 24(6), 349–358.

Murugesan, S., and Rajagopal, K. (2008). "Performance of encased stone columns and design guidelines for construction on soft clay soils." *Geosynthetics in Civil and Environmental Engineering - Geosynthetics Asia 2008: Proceedings of the 4th Asian Regional Conference on Geosynthetics*, 729–734.

Murugesan, S., and Rajagopal, K. (2009). "Shear load tests on stone columns with and without geosynthetic encasement." *Geotechnical Testing Journal*, 32(1), 76–85.

Nguyen, B., Takeyama, T., and Kitazume, M. (2016). "Internal Failure of Deep Mixing Columns Reinforced by a Shallow Stabilized Soil Beneath an Embankment." *International Journal of Geosynthetics and Ground Engineering*, 2(4).

Ni, L. (2014). "Pervious Concrete Piles : Development and Investigation of an Innovative Ground Improvement System, PhD Dissertation." Lehigh University.

Ni, L., Suleiman, M. T., and Raich, A. (2016). "Behavior and Soil-Structure Interaction of Pervious Concrete Ground-Improvement Piles under Lateral Loading." *Journal of Geotechnical and Geoenvironmental Engineering*, 142(2), 4015071.

Noorzad, A., Poorooshasb, H. B., and Madhav, M. R. (2007). "Performance of partially penetrating stone columns during an earthquake." *Proceedings of the 10th International Symposium on Numerical Models in Geomechanics NUMOG 10 - Numerical Models in Geomechanics NUMOG 10*, 503–508.

OpenSeesPL *Three-Dimensional Lateral Pile-Ground Interaction, User's Manual, Version 1.00*.(2011)

Pal, S., and Deb, K. (2019). "Effect of clogging of stone column on drainage capacity during soil liquefaction." *Soils and Foundations*, 59(1), 196–207.

Palmeria, E. M., and Milligan, G. W. E. (1989). "Large scale direct shear tests on reinforced soil." *Soils and Foundations*, 29(1), 18–30.

Pecker, A., Chatzigogos, C. T., and Salençon, J. (2009). *A Dynamic Macro-Element for Performance-Based Design of Foundations. Geotechnical, Geological and Earthquake Engineering*.

Peiris, T., Thambiratnam, D., Perera, N., and Gallage, C. (2014). "Soil-Pile interaction of pile embedded in Deep-Layered marine sediment under seismic excitation." *Structural Engineering International: Journal of the International Association for Bridge and Structural Engineering (IABSE)*.

Phatak, D. R., and Pathak, S. R. (1999). "Assessment of Liquefaction Potential during Earthquakes by Arias Intensity." *Journal of Geotechnical and Geoenvironmental Engineering*, 125(7), 626–628.

PLAXIS LE 2D Limit Equilibrium Slope Stability Analysis Theory Manual, The Benteley Systems (2020).

Potts, D. M., Dounias, G. T., and Vaughan, P. R. (1987). "Finite element analysis of the direct shear box test." *Geotechnique*, 37(1), 11–23.

Prasad Bharat Bhushan. (2013). *Fundamentals of Soil Dynamics and Earthquake Engineering*.

Pul, S., Ghaffari, A., Oztekin, E., Hüsem, M., and Demir, S. (2017). "Experimental Determination of Cohesion and Internal Friction Angle on Conventional Concretes." *ACI Materials Journal*, 114(3).

Rahmani, A., Ghasemi Fare, O., and Pak, A. (2012). "Investigation of the influence of permeability coefficient on the numerical modeling of the liquefaction phenomenon." *Scientia Iranica*, 19(2), 179–187.

Rajagopal, K., and Mohapatra, S. R. (2016). "Behaviour of geosynthetic encased granular columns under vertical and lateral loading." *GA 2016 - 6th Asian Regional Conference on Geosynthetics: Geosynthetics for Infrastructure Development, Proceedings*, KN83—-KN99.

Raju, K. V. S. B., Govinda, L., and Chandrashekhar, A. S. (2013). "Cyclic Response of Stone Columns." *International Journal of Scientific & Engineering Research*, 4(5), 29–32.

Rayamajhi, D. (2014). "Shear Reinforcement Effects of Discrete Columns in Liquefiable Soils, PhD Dissertation." Oregon State University.

Rayamajhi, D., Nguyen, T. V., Ashford, S. A., Boulanger, R. W., Lu, J., Elgamal, A., and Shao, L. (2014). "Numerical Study of Shear Stress Distribution for Discrete Columns in Liquefiable Soils." *Journal of Geotechnical and Geoenvironmental Engineering*, 140(3).

Rayamajhi, D., Ashford, S. A., Boulanger, R. W., and Elgamal, A. (2016a). "Dense granular columns in liquefiable ground. I: Shear reinforcement and cyclic stress ratio reduction." *Journal of Geotechnical and Geoenvironmental Engineering*, 142(7), 1–11.

Rayamajhi, D., Boulanger, R. W., Ashford, S. A., and Elgamal, A. (2016b). "Dense granular columns in liquefiable ground. II: Effects on deformations." *Journal of Geotechnical and Geoenvironmental Engineering*, 142(7), 1–10.

Robert W. Day. (2002). *Earthquake engineering handbook. McGRAW-HILL*.

Rohatgi, A. (2020). *WebPlotDigitizer*. California, USA.

Rostami, R., Bhattacharya, S., Hytiris, N., and Mickovski, S. B. (2018). "Seismic risk management of piles in liquefiable soils stabilised with cementation or lattice structures." *Geotechnical Research*, 6(2), 130–143.

Royo, J., and Melentijevic, S. (2014). "Comparison of laboratory direct shear test results with the numerical analysis." *Numerical Methods in Geotechnical Engineering*, CRC Press, 199–204.

Ryu, J. H., and Kim, J. M. (2013). "Seismic performance of stone-column-reinforced marine soft soil." *Electronic Journal of Geotechnical Engineering*, 18 C, 497–508.

Şahinkaya, F., Vekli, M., and Çadır, C. C. (2017). "Numerical analysis under seismic loads of soils improvement with floating stone columns." *Natural Hazards*, 88(2), 891–917.

Samadhiya, N. ., Priti, M., Partha, B., and Bhushan, K. M. (2008). "Load - Settlement Characteristics of Granular Piles with Randomly Mixed Fibres." *Indian Geotech. Journal*, 38(3), 335–344.

Santucci de Magistris, F., Lanzano, G., Forte, G., and Fabbrocino, G. (2014). "A peak acceleration threshold for soil liquefaction: lessons learned from the 2012 Emilia earthquake (Italy)." *Natural Hazards*, 74(2), 1069–1094.

Seed, B. H. B., Asce, F., Wong, R. T., Asce, M., Idriss, I. M., Asce, M., and Tokimatsu, K. (1987). "Moduli and damping factors for dynamic analyses of cohesionless soils." *Journal of Geotechnical and Geoenvironmental Engineering*, 112(11), 1016–1032.

Seed, H. B., and Idriss, I. M. (1970). *Soil Moduli and Damping Factors for Dynamic Response Analyses [Report No. EERC 70-10]*. 41.

Seed, H., and Booker, J. (1978). *Stabilization of Potential Liquefiable Sand Deposits Using Gravel Drains*. *Journal of Geotechnical and Geoenvironmental Engineering*.

Seismosoft. (2020). *SeismoSignal - A computer program for signal processing of time-histories*.

Serbulea, M.-S. (1962). *Abaqus for Geotechnical Engineering*.

Shahu, J. T., and Reddy, Y. R. (2011). "Clayey Soil Reinforced with Stone Column Group: Model Tests and Analyses." *Journal of Geotechnical and Geoenvironmental Engineering*, 137(12), 1265–1274.

Shenthan, T., Nashed, R., Thevanayagam, S., and Martin, G. R. (2004). "Liquefaction mitigation in silty soils using composite stone columns and dynamic compaction." *Earthquake Engineering and Engineering Vibration*, 3(1), 39–50.

Shivashankar, R., Dheerendra Babu, M. R., Nayak, S., and Manjunath, R. (2010). "Stone Columns with Vertical Circumferential Nails: Laboratory Model Study." *Geotechnical and Geological Engineering*, 28(5), 695–706.

Shrestha, S., Chai, J. C., Bergado, D. T., Hino, T., and Kamo, Y. (2015). "3D FEM investigation on Bending failure mechanism of column inclusion under embankment load." *Lowland Technology International*, 17(3), 157–166.

Stewart, D., and Knox, R. (1995). "What is the Maximum Depth Liquefaction Can Occur?" *Third International Conference on Recent Advances in Geotechnical Earthquake Engineering & Soil Dynamics*.

Suleiman, M. T., Ni, L., and Raich, A. (2014). "Development of Pervious Concrete Pile Ground-Improvement Alternative and Behavior under Vertical Loading." *Journal of Geotechnical and Geoenvironmental Engineering*, 140(7), 4014035.

Surendra, C., and Mohanty, S. (2017). "Parametric Study on Seismic Behavior of Black Cotton Soil Reinforced With Granular Column." 14–17.

Taboada, V. M., Dantal, V., Roque, D. C., Lopez, F. F., and Nabor, P. B. (2016). "Normalized modulus reduction and material damping ratio curves for Bay of Campeche sand." *Proceedings of the Annual Offshore Technology Conference*, 125–147.

Taiebat, M., and Pak, A. (2004). "A Fully Coupled Dynamic Analysis of Velacs Experiment No . 1 , Using a Critical State Two-Surface Plasticity." *13th World Conference on Earthquake Engineering*, (2239), Paper No. 2239.

Tan SA, Tjahyono ; S., Oo KK (2008) Simplified Plane-Strain Modeling of Stone-Column Reinforced Ground. https://doi.org/10.1061/ASCE1090-02412008134:2185

Tang, L., Cong, S., Ling, X., Lu, J., and Elgamal, A. (2015). "Numerical study on ground improvement for liquefaction mitigation using stone columns encased with geosynthetics." *Geotextiles and Geomembranes*, 43(2), 190–195.

Tang, L., Zhang, X., and Ling, X. (2016). "Numerical simulation of centrifuge experiments on liquefaction mitigation of silty soils using stone columns." *KSCE Journal of Civil Engineering*, 20(2), 631–638.

Taboada-Urtuzuastegui Victor M., and Dobry, R. (1998). "Centrifuge modeling of earthquake-induced lateral spreading in sand." *Journal of Geotechnical and Geoenvironmental Engineering*, (December), 1195–1206.

Wang, G. (2010). "Consolidation of soft clay foundations reinforced by stone columns under time-dependent loadings." *Journal of Geotechnical and Geoenvironmental Engineering*, 135(12), 1922–1931.

Wissmann, K. J., Ballegooy, S. V., Metcalfe, B. C., Dismuke, J. N., and Anderson, C. K. (2015). "Rammed Aggregate Pier Ground Improvement as a Liquefaction Mitigation Method in Sandy and Silty Soils." *The 6th International Conference on Earthquake Geotechnical Engineering*, (November), 1–8.

Wu, C. S., and Hong, Y. S. (2009). "Laboratory tests on geosynthetic-encapsulated sand columns." *Geotextiles and Geomembranes*, 27(2), 107–120.

Wu, C. S., Hong, Y. S., and Lin, H. C. (2009). "Axial stress-strain relation of encapsulated granular column." *Computers and Geotechnics*, 36(1–2), 226–240.

Wu, W., and Borja, R. I. (2008). *Features of liquefaction-induced damages*. *Springer Series in Geomechanics and Geoengineering*.

Yang, Z., Lu, J., and Elgamal, A. (2008). *OpenSees soil models and solid-fluid fully coupled elements: user's manual, Version 1*. *San Diego: University of California*.

Youd, T. L. (1984). "Geologic effects—Liquefaction and associated ground failure." Proc., Geologic and Hydrologic Hazards Training Program, U.S. Geological Survey, Washington, DC, 210–232.

Youd, T. L. (2018). "Application of MLR Procedure for Prediction of Liquefaction-Induced Lateral Spread Displacement." *Journal of Geotechnical and Geoenvironmental Engineering*, 144(6), 04018033.

Yu, C., Yin, Z., and Zhang, D. (2014). "Micromechanical modelling of phase transformation behaviour of a transitional soil." *Acta Mechanica Solida Sinica*, 27(3), 259–275.

Zarnani, S., and Bathurst, R. J. (2009). "Numerical parametric study of expanded polystyrene (EPS) geofoam seismic buffers." *Canadian Geotechnical Journal*, 46(3), 318–338.

Zhan, Y. G., Wang, H., and Liu, F. C. (2012). "Modeling vertical bearing capacity of pile foundation by using ABAQUS." *Electronic Journal of Geotechnical Engineering*, 17 M, 1855–1865.

Zhan, Y., Jiang, G., and Yao, H. (2014). "Dynamic Characteristics of Saturated Silty Soil Ground Treated by Stone Column Composite Foundation." *Advances in Materials Science and Engineering*.

Zhang, Y., and Zhang, X. (2011). "Dynamic response analysis of liquefaction foundation treated by stone columns." *2011 International Conference on Electric Technology and Civil Engineering, ICETCE 2011 - Proceedings*, 254–257.

Zhang, J., Cui, X., Huang, D., Jin, Q., Lou, J., and Tang, W. (2016). "Numerical Simulation of Consolidation Settlement of Pervious Concrete Pile Composite Foundation under Road Embankment." *International Journal of Geomechanics*, 16(1), 1–10.

Zhang, J., Cui, X., Lan, R., Zhao, Y., Lv, H., Xue, Q., and Chang, C. (2017). "Dynamic Performance Characteristics of Pervious Concrete Pile Composite Foundations under Earthquake Loads." *Journal of Performance of Constructed Facilities*, 31(5), 04017064.

Zhang Z, Xiao Y, Han J, et al (2020) Modified Equivalent-Area Method for Calculating Factors of Safety against Deep-Seated Failure of Embankments over Deep-Mixed Foundations. International Journal of Geomechanics 20:04019196. https://doi.org/10.1061/(asce)gm.1943-5622.0001592

Zhaohui, Y., and Ahmed, E. (1979). "Influence of Permeability on Liquefaction-Induced Shear deformation." *Journal of Engineering Mechanics*, 128(7), 720–729.

PUBLICATIONS

JOURNAL ARTICLES

1) Rashma, R.S.V., Shivashankar, R. & Jayalekshmi, B.R. Shear Response of Pervious Concrete Column Improved Ground. Indian Geotech J (2020). https://doi.org/10.1007/s40098-020-00473-9 (SCOPUS Indexed)

2) Rashma, R.S.V., Jayalekshmi, B.R. & Shivashankar, R. Liquefaction Mitigation Potential of Improved Ground Using Pervious Concrete Columns. Indian Geotech J (2021). https://doi.org/10.1007/s40098-021-00536-5 (SCOPUS Indexed)

3) Rashma, R.S.V., Jayalekshmi, B.R. & Shivashankar, R. (2021) "Shear Strength Behavior of Pervious concrete column improved soft clay bed: A Numerical Study", Transportation Infrastructure Geotechnology, Springer. https://doi.org/10.1007/s40515-021-00179-2 (SCOPUS Indexed)

4) Rashma R.S.V, Shivashankar R &. Jayalekshmi B.R, (2018) "Behavior of Pervious concrete columns Subjected to Static shear Loading Conditions", 7(4), 6928-6933, International Journal of Engineering and Technology (UAE), Science Publishing Corporation. https://www.sciencepubco.com/index.php/ijet/article/view/27587

5) Rashma, R.S.V., Jayalekshmi, B.R. & Shivashankar, R. "Influence of earthquake characteristics on the performance of pervious concrete column improved ground", Geotechnical and Geological Engineering, Springer Netherlands, 2021 (Revision Under Review)

6) Rashma, R.S.V., Jayalekshmi, B.R. & Shivashankar, R. "Liquefaction-induced Lateral Spreading mitigation using Pervious Concrete Column Inclusion on Sloping Strata", Journal of Earthquake Engineering, TandF Online, 2021 (Under Review)

7) Rashma, R.S.V., Jayalekshmi, B.R. & Shivashankar, R., "A critical review on the performance of column improved ground under shear and seismic loading" Ground Improvement Proceedings of the ICE, 2021 (Under Review)

8) Rashma, R.S.V., Jayalekshmi, B.R. & Shivashankar, R. "A numerical study on the shear strength of pervious concrete column in weak ground" Acta Geotechnica Slovenica. (Under Review)

9) Rashma, R.S.V., Jayalekshmi, B.R. & Shivashankar, R., "Limit Equilibrium Slope Stability Analysis of Column Supported Embankment on weak ground" Special

issue: Soft ground Improvement, International Journal of Geosynthetics and Ground Engineering (Under Review)

CONFERENCE PROCEEDING

10) Rashma R.S.V, Jayalekshmi B.R and Shivashankar R, "Seismic Performance of Pervious Concrete Column Improved Ground in Mitigating Liquefaction", IOP Conf. Ser.: Mater. Sci. Eng. 1114 012015 (2021). https://doi.org/10.1088/1757-899X/1114/1/012015 (Conference Proceedings Citation Index—Science (CPCI-S) (Clarivate, Web of Science))

BOOK CHAPTER

11) Rashma, R.S.V., Jayalekshmi, B.R. & Shivashankar, R. "Efficacy of pervious concrete columns vis-a-vis stone columns in sandy strata in mitigating liquefaction", Geohazard Mitigation. Lecture notes in Civil Engineering, Springer Singapore 2021. DOI: 10.1007/978-981-16-6140-2 (SCOPUS Indexed-In Press)

PAPERS PRESENTED IN INTERNATIONAL CONFERENCES

1) Rashma R.S.V, Jayalekshmi B.R and Shivashankar R, "Seismic Performance of Pervious Concrete Column Improved Ground in Mitigating Liquefaction", Presented by first author on 19/12/2020 to International Conference on Civil engineering Advances for Sustainable Infrastructure Development & Environment (CEASIDE 2020)-Track 1 of sixth edition of the biennial International Conference on Emerging Trends in Engineering, Science and Technology, ICETEST 2020 Organized by Government Engineering College Thrissur,Kerala- India

2) Rashma R.S.V, Jayalekshmi B.R and Shivashankar R, "Efficacy of pervious concrete columns vis-a-vis stone columns in sandy strata in mitigating liquefaction", Presented by first author on 19/03/2021 to Virtual Conference on Disaster Risk Reduction-Civil Engineering for a Disaster Resilient Society (VCDRR) jointly organized by National Institute of Technology Karnataka (NITK), Asian Disaster Reduction and Response Network (ADRRN), and Institute of Himalayan Risk Reduction (IHRR) Nepal supported by several other organizations and societies during 15-20 March 2021.

BIODATA

<u>**Personal Profile**</u>

Name	:	Rashma R S V
Permanent Address	:	Anugraha, T.C.19/1201(1), LVRA-59, Poojappura P.O, Trivandrum-12 Kerala.
Email	:	rashmarsv@gmail.com
Contact Number	:	+971-50-7131236

<u>**Educational Qualification**</u>

Degree/Major/Institution	Percentage of Marks	Year of Graduation
Doctor of Philosophy, Ph.D in Civil Engineering National Institute of Technology, Karnataka, Surathkal, India.	CGPA: 10 (for coursework)	Pursuing
Master of Technology, M.Tech Geotechnical Engineering, National Institute of Technology Karnataka, Surathkal, India.	CGPA: 10	2011
Bachelor of Technology, B.Tech Civil Engineering, TKM College of Engineering, Kerala, India. University of Kerala	83.50%	2009

<u>**Publications**</u>

International Journals   : 05
Book Chapter   : 01

<u>**Academic Experience**</u>

Sl.No	Institution	Designation	Tenure
1	Mohandas College of Engineering and Technology, Trivandrum, India	Assistant Professor	June 2011 to May 2013
2	Manipal University, Dubai Campus	Assistant Professor	August 2013 to July 2017